

**PHYSIOLOGICAL RESPONSES OF A  
SOUTH AFRICAN HIGH-LATITUDE CORAL  
COMMUNITY TO GLOBAL WARMING**

TANJA HANEKOM

218 086 935

Submitted in fulfilment of the academic requirements for the degree of  
MASTER OF SCIENCE

In the Oceanographic Research Institute of the School of Life Sciences  
Faculty of Science and Agriculture  
University of KwaZulu-Natal  
Durban

June 2021

## **Preface**

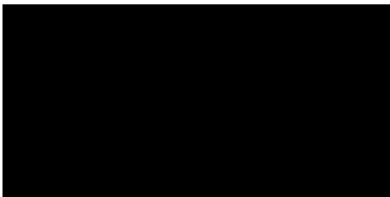
The work described in this thesis was carried out at the Oceanographic Research Institute (ORI), South African Association for Marine Biological Research (SAAMBR), which is affiliated with the School of Life Sciences at the University of KwaZulu-Natal (UKZN), Westville, South Africa. The field and experimental work was conducted at Sodwana Bay, South Africa and at the ORI Research Aquarium, respectively, from 2018 to 2019, under the supervision of Doctor Sean Nixon Porter and Professor Michael Henry Schleyer. This thesis represents original work by the author and has not otherwise been submitted in any form for any degree or diploma to any tertiary institute. Where use has been made of the work of others, it is duly acknowledged throughout the text.

I certify that the above statement is correct, and that this thesis/dissertation has been approved for submission by both supervisors:



---

Tanja Hanekom (Candidate) | 22 June 2021



---

Dr Sean N Porter (Supervisor) | 30 June 2021



---

Prof. Michael H Schleyer (Co-supervisor) | 30 June 2021

## **Declaration 1 – Plagiarism**

I, Tanja Hanekom, declare that:

1. The research reported in this thesis, except where otherwise indicated, is my original research.
2. The thesis has not been submitted for any degree or examination at any other university.
3. This thesis does not contain other persons' data, pictures, graphs or other information, unless specifically acknowledged as being sourced from other persons.
4. This thesis does not contain other persons' writing, unless specifically acknowledged as being sourced from other researchers. Where other written sources have been quoted:
  - a) Their words have been re-written, but the general information attributed to them has been referenced.
  - b) Their exact words have been used, then their writing has been placed in italics and inside quotation marks and referenced.
5. This thesis does not contain text, graphics, or tables copied and pasted from the internet, unless specifically acknowledged. The source is detailed in the thesis and in the reference sections.



Tanja Hanekom | 22 June 2021

## Abstract

The health of the world's coral reefs is deteriorating rapidly due to global climate change and increasing localised anthropogenic stressors. The substantial benefits resulting from coral reef ecosystems, economically and ecologically, requires that research be conducted on their responses to rising sea temperatures driven by climate change. Millions of people depend on the natural resources that coral reefs provide, whether for food or eco-tourism, trade and other indirect sources of income. Although South African coral reef communities lie within a long-established marine protected area, the iSimangaliso Wetland Park World Heritage Site, this status does not preclude them from being affected by the potential effects of global warming. Therefore, the objective of this study was to quantify several physiological parameters, including net community calcification (total alkalinity), growth (dimension and weight) and photosynthetic efficiency in the hard coral *Acropora appressa*, the soft coral *Sinularia brassica* and 'live rock' under local historical-average (24.4°C), future (26.9°C) and bleaching-threshold (28.8°C) temperatures indicative of climate change conditions projected at Sodwana Bay.

Corals and live rock were exposed to the three different temperature treatments during a 10-week long mesocosm experiment that consisted of three phases: the initial phase during which temperatures were increased from 24.4°C over four weeks to reach setpoints of 26.9°C (future) and 28.8°C (bleaching threshold), respectively; the middle phase during which temperatures were held stable at each treatment's setpoint for the proceeding four weeks; and the final phase during which a further 1°C increase was done over two weeks in the bleaching-threshold treatment to simulate an extreme warming scenario.

An initial increase in size was evident in both coral species exposed to the historical-average control temperature and the future temperature projected for Sodwana Bay in 2100 by the representative concentration pathway (RCP) 4.5 climate change scenario. Although the growth trends of both species persisted in the control treatment, the overall linear growth of *A. appressa* was lower under the RCP 4.5 climate change temperature scenario and bleaching-threshold temperature relative to the control temperature. While no significant treatment effects were found, a decrease in the linear extension of *A. appressa* was evident at the end of the experiment at the bleaching-threshold temperature relative to the control temperature. Continuous growth trends were evident in the control and RCP 4.5 climate change scenario for *S. brassica*, however a reduction in diameter after 5 weeks was apparent in the bleaching-threshold treatment.

A gradual increase in buoyant weight of *A. appressa* was evident across all treatments and experimental phases, with a slower growth rate only apparent towards the end of the experiment

in the bleaching-threshold treatment. The buoyant weight of *S. brassica* decreased up until the start of the middle phase in the control treatment and RCP 4.5 treatment. However, an increasing trend in the weight of *S. brassica* was measured in the same two treatments from the end of the middle phase until the experiment concluded. Contrastingly, the weight of *S. brassica* in the bleaching-threshold treatment continued to decrease throughout the course of the experiment.

Pulse-amplitude modulated fluorometry measurements of the photosynthetic efficiency of both *A. appressa* and *S. brassica* were lower under the temperature conditions projected by the RCP 4.5 scenario and by the bleaching-threshold temperature, relative to the historical-average control temperature. Contrastingly, live rock showed no significant differences in photosynthetic efficiency among the different temperature treatments. On average, total alkalinity levels were higher under future temperature conditions projected by the RCP 4.5 temperature scenario and by the bleaching-threshold temperature, relative to the control temperature, indicating suppressed net community calcification. Suppressed net community calcification was particularly evident during (week 6) and at the end (week 8) of the middle phase of the experiment.

The experiment revealed that exposure to temperatures equivalent to those projected by the RCP 4.5 climate change scenario in 2100 and the local bleaching threshold are likely to be deleterious to high-latitude corals and coral reef communities in South Africa: buoyant weight and dimension, as well as photosynthetic efficiency were negatively affected in both species of coral and net community calcification was suppressed under the two future climate scenarios of warming. Due to the location of Sodwana Bay reefs, the results indicate that calcification processes will be an essential physiological response to consider under global warming conditions. However, as high-latitude reef areas generally fared better during recent bleaching conditions, these reefs can be utilised to improve climate-change projection models. Such model improvements can guide climate policymakers in enhanced conservation efforts that will further stakeholder engagement and outreach. Accordingly, urgent action is needed to reduce greenhouse gas emissions to minimise the effects of global warming on coral reef communities as much as possible. Such efforts will further help to attain the 2°C Paris Climate Agreement and improve socioeconomic development for the management of reefs.

## **Key Words**

Climate change | anthropogenic impacts | marginal coral reefs | growth | photosynthetic efficiency | net community calcification | socioeconomic development

## **Acknowledgements**

I wish to thank a great, dynamic group of people I had the privilege to work with during the thesis. Thank you to some of the most marine ecologically-minded and patient supervisors, Dr Sean Porter and Prof. Michael Schleyer. The support I received from both of you throughout some crazy design ideas, unexpected load reduction of water and electricity, going back to the drawing board to try again, and additional university challenges we had to face were boundless and highly valued. I can continue my ocean science journey with enriched knowledge on reef environments, marine protected areas and how to go forward with improved management protocols. Thank you for introducing me to a global coral research community and for having faith in me to lead an efficacious experiment in the Research Aquarium of the Oceanographic Research Institute (ORI).

I am grateful for the generous help and expertise offered by the various SeaWorld departments, especially when it came to installing all the equipment for the experiments. A special thanks to Mr Kerwyn L Randall, Mr Cornelius Koekemoer and Mr John Ballard, who provided me with invaluable guidance, including the hands-on knowledge on specialised equipment and techniques in the workshop. I had the opportunity to work with power tools and machinery, which was not only enjoyable but also a fantastic learning curve. I also appreciated the Durban Marine Theme Park (DMTP) security team when I had to complete readings during those “what-felt-to-be endless” nightshifts. Further research work, which exceeded the scope of this thesis, was conducted in the genetics laboratory with Dr David Pearton. I want to thank him for his time and genetics expertise that allowed me to enter the fascinating world of genetics, as well as providing me with prospective RNA work that can be analysed to determine individual genotypes among the coral colonies.

When the statistical design became a bit of a brainteaser, thank you to Prof. Marti J Anderson for advising and brainstorming with us to analyse the data appropriately. For guidance on coral husbandry, I want to thank the aquarium industry professional Mr Anthony R Calfo, who advised us on propagation techniques of sensitive species rarely or never been propagated before. It resulted in the initiation of creative thinking and has led to what may be a novel propagation technique for buoyant weighing of soft corals.

The past two years have been of the more challenging scientific journeys I have endeavoured. Hence, I cannot say thank you or show my appreciation enough to my family, friends, partner and work colleagues (that are now my new science family). Your endless encouragement and feedback throughout kept me going and pushing for a successful product. All the “care packages”

sent from Cape Town to Durban, especially from my loving parents, were appreciated immensely and always came in handy when it was needed the most.

The research work would not have been possible without the funding provided by the National Research Foundation (NRF) of South Africa (Grant Number: 111730 awarded to Dr Sean N. Porter) and the South African Association for Marine Biological Research (SAAMBR). I acknowledge that any opinions, findings and conclusions or recommendations expressed in the thesis are that of my own and that the NRF accepts no liability whatsoever in this regard. The iSimangaliso Wetland Park Authority and Ezemvelo KwaZulu-Natal Wildlife are thanked for supporting my research in the marine protected area. Further thanks go out to the Western Indian Ocean Marine Science Association (WIOMSA) for funding me to participate in the 11<sup>th</sup> WIOMSA Scientific Symposium, which was held at the University of Mauritius, Port Louis where I presented my thesis work internationally for the first time.

# Contents

Preface.....	i
Declaration 1 – Plagiarism .....	ii
Abstract .....	iii
Acknowledgements .....	v
List of Figures .....	x
List of Tables.....	xiii
List of Abbreviations.....	xviii
CHAPTER 1   INTRODUCTION.....	1
1.1 Thematic context of the study .....	1
1.2 What are coral reefs?.....	3
1.3 The importance of coral reefs.....	5
1.4 Climate change and global warming .....	7
1.5 South African high-latitude coral reefs and global warming .....	11
1.6 Mesocosm experiments and their importance in coral reef studies.....	14
1.7 Physiological responses to global warming .....	15
1.7.1 Coral growth according to size and buoyant weight .....	15
1.7.2 Photosynthetic efficiency .....	17
1.7.3 Net community calcification .....	19
1.8 Aims, objectives and hypotheses .....	21
CHAPTER 2   METHODS .....	23
2.1 Collection site.....	23
2.2 Study species, their collection and preparation .....	26
2.3 Experimental design.....	28
2.4 Water temperature selection.....	34
2.5 Coral feeding and general maintenance .....	36

2.6	Data collection.....	36
2.6.1	Growth.....	37
2.6.2	Photosynthetic efficiency .....	38
2.6.3	Net community calcification .....	40
2.7	Data analysis .....	44
2.7.1	Temperature .....	45
2.7.2	Growth.....	45
2.7.3	Photosynthetic efficiency .....	46
2.7.4	Net community calcification .....	47
CHAPTER 3   RESULTS .....		48
3.1	Water temperature .....	48
3.2	Buoyant weights of marbles at different temperatures.....	50
3.3	Physiological responses.....	50
3.3.1	Growth.....	50
3.3.1.1	Growth according to size (linear extension and diameter increase).....	50
3.3.1.2	Growth according to buoyant weight .....	57
3.3.2	Photosynthetic efficiency .....	64
3.3.3	Net community calcification .....	81
CHAPTER 4   DISCUSSION .....		90
4.1	Overview .....	90
4.2	Water temperatures simulated in experiments .....	92
4.3	Buoyant weights of marbles at different temperatures.....	95
4.4	Physiological responses.....	95
4.4.1	Coral growth according to size and buoyant weight .....	96
4.4.2	Photosynthetic Efficiency .....	101
4.4.3	Net community calcification .....	104
4.5	Conclusions .....	107

4.5.1	Concluding Remarks .....	107
4.5.2	Future recommendations .....	109
	References .....	111

## List of Figures

- Figure 1.4.1** Confidence levels of climate change affecting the marine environment based on evidence and consensus. The increased levels of evidence and degrees of agreement are associated with increasing confidence, as indicated by the increasing strength of shading in the confidence scale (adapted from IPCC 2013). ..... 8
- Figure 1.4.2** A risk level criterion of the impacts of climate change concerning ocean warming and acidification on calcifying marine species (with a focus on corals and reefs). The risk level criterion is consistent with the confidence levels that are further based on evidence and the degree of scientific agreement (see Fig 1.4.1). Accordingly, the level of additional risk is indicated by the colour bar (adapted from IPCC 2014). ..... 9
- Figure 1.4.3** Projected trajectories of the four Representative Concentration Pathways (RCPs) to the year 2100 based on accumulative atmospheric greenhouse gases (i.e. CO<sub>2</sub>-equivalent concentrations) outlined by the fifth IPCC Assessment Report (adapted from van Vuuren *et al.* 2011). ..... 10
- Figure 2.1** Collection site on Two-mile Reef situated in Sodwana Bay, KwaZulu-Natal, South Africa where biological material was collected for mesocosm experiments. .... 24
- Figure 2.2** The study species *Acropora appressa* (A), *Sinularia brassica* (B) and live rock (C), collected from Two-mile Reef, Sodwana Bay, South Africa and used in mesocosm experiments. .... 26
- Figure 2.3.1** A schematic representation of the experimental setup. The top part of the figure shows the incoming seawater and the three header tanks for each treatment. Water flows from each header tank that is pseudo-replicated into triplicate mesocosms (M<sub>1</sub> to M<sub>9</sub>) located in their respective water baths. A photograph of a typical mesocosm is provided at the bottom-left corner of the figure. .... 30
- Figure 2.3.2** The research aquarium at the Oceanographic Research Institute showing the experimental system built to test the effects of global warming on coral communities, including header tanks, water baths, mesocosms and various electronic peripheral equipment. .... 31
- Figure 2.3.3** Photographs of the representative coral communities in the different temperature treatments. Each of the three colonies of both *Acropora appressa* and *Sinularia brassica* were

split and randomly assigned per treatment (historical-average (24.4°C), RCP 4.5 year-2100 (26.9°C) and bleaching-threshold (28.8°C) scenarios). Each photograph, taken during week 8 of the experiment, represented a mesocosm that was pseudo-replicated per treatment with the respective hard coral control mount (top-left corner) and soft coral control mount (bottom-left corner)..... 33

**Figure 3.1** Hourly temperature time series over the 10-week experiment for each replicate mesocosm according to each temperature treatment and their associated climate scenarios. Solid grey vertical lines denote the three different phases of temperature change during the experiment and dotted lines indicate the setpoint temperatures (also in brackets) for each treatment including the extended final phase when temperatures were increased by 1°C to 29.8°C in the warmest treatment (28.8°C)..... 48

**Figure 3.2** Raw marble buoyant weight (g) comparisons measured at each of the three setpoint temperature treatments (24.4°C, 26.9°C and 28.8°C) with maximum (max.) ranges and standard deviations (SD) according to each marble across the three different temperatures. Values inside the bars indicate the instantaneous temperature a marble was measured at..... 50

**Figure 3.3.1** Average ± standard deviation (SD) linear extension (mm) of *Acropora appressa* fragments measured at weekly intervals plotted according to three temperature treatments associated with different climate change scenarios..... 51

**Figure 3.3.2** Average ± standard deviation (SD) change in diameter (mm) of *Sinularia brassica* discs measured at weekly intervals plotted according to three temperature treatments associated with different climate change scenarios..... 52

**Figure 3.3.3** Average ± standard deviation (SD) growth (g) of *Acropora appressa* throughout the experiment based on weekly buoyant weight measurements plotted according to each temperature treatment. Solid lines indicate a change in coral growth and dotted lines indicate a change in the control mounts. .... 57

**Figure 3.3.4** Average ± standard deviation (SD) growth (g) of *Sinularia brassica* throughout the experiment based on weekly buoyant weight measurements plotted according to each temperature treatment. Solid lines indicate a change in coral growth and dotted lines indicate a change in the control mounts..... 58

**Figure 3.3.5** Average ± standard deviation (SD) photosynthetic efficiency ( $F_v/F_M$ ) of the hard coral *Acropora appressa* throughout the experiment..... 64

<b>Figure 3.3.6</b> Average $\pm$ standard deviation (SD) photosynthetic efficiency ( $F_V/F_M$ ) of the soft coral <i>Sinularia brassica</i> throughout the experiment. ....	65
<b>Figure 3.3.7</b> Average $\pm$ standard deviation (SD) photosynthetic efficiency ( $F_V/F_M$ ) of live rock throughout the experiment. ....	66
<b>Figure 3.3.8</b> Average $\pm$ standard error (SE) net community calcification (NCC) according to the calcium carbonate concentration ( $\mu\text{mol CaCO}_3 \text{ kg}^{-1}$ ) averaged across the three diel periods at the end of the fourth, sixth and eighth week of the experiment, for each temperature treatment. The bar at the bottom indicates night-time (black) and daytime (white) measurements.....	82
<b>Figure 3.3.9</b> Average $\pm$ standard deviation (SD) net community calcification (NCC) according to the calcium carbonate concentration ( $\mu\text{mol CaCO}_3 \text{ kg}^{-1}$ ) during diel period 1 at the end of the initial phase (week 4) of the experiment according to each temperature treatment. The bar at the bottom indicates night-time (black) and daytime (white) measurements. ....	84
<b>Figure 3.3.10</b> Average $\pm$ standard deviation (SD) net community calcification (NCC) according to the calcium carbonate concentration ( $\mu\text{mol CaCO}_3 \text{ kg}^{-1}$ ) at diel period 2 (week 6) during the middle phase of the experiment according to each temperature treatment. The bar at the bottom indicates night-time (black) and daytime (white) measurements.....	85
<b>Figure 3.3.11</b> Average $\pm$ standard deviation (SD) net community calcification (NCC) according to the calcium carbonate concentration ( $\mu\text{mol CaCO}_3 \text{ kg}^{-1}$ ) during diel period 3 (week 8) at the end of the middle phase of the experiment according to each temperature treatment. The bar at the bottom indicates night-time (black) and daytime (white) measurements.....	85
<b>Figure 4.1</b> Summary of the results of the experiments based on permANOVA analyses conducted on each physiological parameter including coral size, buoyant weight, photosynthetic efficiency and net community calcification for the three functional groups (hard coral, soft coral and live rock) and the coral community. The summary indicates the status of statistical significance and the direction of change in each physiological parameter relative to the control treatment for the various factors (fixed effects) and their interactions. This was achieved by comparing the different physiological responses derived from the year-2100 (RCP 4.5) and bleaching-threshold scenarios with the historical-average scenario or control treatment. The cells were merged when the <i>a priori</i> tests on each physiological parameter indicated a non-significant difference ( $\alpha = 0.05$ ), obviating the need for <i>post hoc</i> comparisons, but the direction of the non-significant change was still indicated. NA = not applicable.....	93

## List of Tables

<b>Table 3.1</b> Temperature (°C) summary statistics based on hourly measurements obtained for all three temperature treatments during each of the three phases of the experiment. The target rate of increase (°C.d <sup>-1</sup> ) for the initial phase as well as setpoint temperatures for the other phases are also provided. RCP = Representative concentration pathway. SD = standard deviation. Min. = minimum. Max. = maximum.....	49
<b>Table 3.3.1</b> Permutational ANOVA (permANOVA) and permutational analyses of dispersion (permDISP) investigating variation in the change in size of hard and soft corals exposed to three different temperature treatments, based on weekly measurements of their linear extension and diameter, respectively. Significant differences are indicated in bold ( $\alpha \leq 0.05$ ).....	53
<b>Table 3.3.2</b> <i>Post hoc</i> pairwise permutational ANOVA (permANOVA) and permutational analyses of dispersion (permDISP) comparisons of growth between all phases (initial, middle and final) of the experiment for hard and soft corals combined. Significant differences are indicated in bold ( $\alpha \leq 0.05$ ).....	53
<b>Table 3.3.3</b> <i>Post hoc</i> pairwise permutational ANOVA (permANOVA) and permutational analysis of dispersion (permDISP) comparisons of the variation in growth between weeks for each phase of the experiment for hard and soft corals combined. Significant differences are indicated in bold ( $\alpha \leq 0.05$ ).....	54
<b>Table 3.3.4</b> <i>Post hoc</i> pairwise permutational ANOVA (permANOVA) and permutational analysis of dispersion (permDISP) comparisons investigating the variation in growth between hard and soft coral for the different weeks within each phase of the experiment. Significant differences are indicated in bold ( $\alpha \leq 0.05$ ). .....	55
<b>Table 3.3.5</b> <i>Post hoc</i> pairwise permutational ANOVA (permANOVA) and permutational analyses of dispersion (permDISP) comparisons investigating the variation in growth between the different weeks of each experimental phase for hard and soft coral. Significant differences are indicated in bold ( $\alpha \leq 0.05$ ).....	56
<b>Table 3.3.6</b> Permutational ANOVA (permANOVA) and permutational analysis of dispersion (permDISP) investigating variation in the growth (change in weekly buoyant weight) of hard and soft corals exposed to three different temperature treatments. The relevant <i>a priori</i> pairwise	

contrasts for species (i.e. hard or soft corals and their controls) have been included and are indicated in italics. Significant differences are indicated in bold ( $\alpha \leq 0.05$ ). ..... 59

**Table 3.3.7** *Post hoc* pairwise permutational ANOVA (permANOVA) and permutational analysis of dispersion (permDISP) comparisons investigating variation in the growth of hard and soft corals between the different temperature treatments for each phase of the experiment. Significant differences are indicated in bold ( $\alpha \leq 0.05$ ). \*Temperatures were increased to 29.8°C during the final phase of the bleaching-threshold treatment. .... 61

**Table 3.3.8** *Post hoc* pairwise permutational ANOVA and permutational analysis of dispersion (permDISP) comparisons investigating variation in the growth of hard and soft corals between different phases of the experiment for each temperature treatment. Significant differences are indicated in bold ( $\alpha \leq 0.05$ ). \*Temperatures were spiked to 29.8°C during the final phase of the bleaching-threshold treatment. .... 61

**Table 3.3.9** *Post hoc* pairwise permutational ANOVA and permutational analysis of dispersion (permDISP) comparisons investigating variation in growth between hard coral and its control for each experimental phase during the different corresponding weeks. Significant differences are indicated in bold ( $\alpha \leq 0.05$ ). ..... 62

**Table 3.3.10** *Post hoc* pairwise permutational ANOVA and permutational analysis of dispersion (permDISP) comparisons investigating variation in growth between hard coral and its control for each temperature treatment during the different experimental phases and their corresponding weeks. Significant differences are indicated in bold ( $\alpha \leq 0.05$ ). ..... 63

**Table 3.3.11** Permutational ANOVA (permANOVA) and permutational analysis of dispersion (permDISP) investigating variation in photosynthetic efficiency among hard and soft coral, as well as live rock, exposed to different temperature treatments. *A priori* pairwise contrasts between species are given in italics. Significant differences are indicated in bold ( $\alpha \leq 0.05$ ). ..... 67

**Table 3.3.12** *Post hoc* pairwise permutational ANOVA (permANOVA) and permutational analysis of dispersion (permDISP) comparisons of photosynthetic efficiency of hard and soft coral, as well as live rock, between different phases of the experiment. Significant differences are indicated in bold ( $\alpha \leq 0.05$ ). ..... 68

**Table 3.3.13** *Post hoc* pairwise permutational ANOVA (permANOVA) and permutational analysis of dispersion (permDISP) comparisons of photosynthetic efficiency between weeks for each phase of the experiment. Significant differences are indicated in bold ( $\alpha \leq 0.05$ ). ..... 69

**Table 3.3.14** *Post hoc* pairwise permutational ANOVA (permANOVA) and permutational analysis of dispersion (permDISP) comparisons of photosynthetic efficiency between different temperature treatments for the initial, middle and final phases of the experiment. Significant differences are indicated in bold ( $\alpha \leq 0.05$ ). \*Temperatures were spiked to 29.8°C during the final phase of the bleaching-threshold treatment..... 70

**Table 3.3.15** *Post hoc* pairwise permutational ANOVA (permANOVA) and permutational analysis of dispersion (permDISP) comparisons of photosynthetic efficiency between different phases of the experiment for each temperature treatment. Significant differences are indicated in bold ( $\alpha \leq 0.05$ ). \*Temperatures were increased to 29.8°C during the final phase of the bleaching-threshold treatment..... 71

**Table 3.3.16** *Post hoc* pairwise permutational ANOVA (permANOVA) and permutational analysis of dispersion (permDISP) comparisons of photosynthetic efficiency between each temperature treatment, for each week, according to the three phases of the experiment. Significant differences are indicated in bold ( $\alpha \leq 0.05$ ). \*Temperatures were increased to 29.8°C during the final phase of the bleaching-threshold treatment. .... 72

**Table 3.3.17** *Post hoc* pairwise permutational ANOVA (permANOVA) and permutational analysis of dispersion (permDISP) comparisons of photosynthetic efficiency between different weeks during each experimental phase of the experiment for different temperature treatments. Significant differences are indicated in bold ( $\alpha \leq 0.05$ ). \*Temperatures were increased to 29.8°C during the final phase of the bleaching-threshold treatment. .... 73

**Table 3.3.18** *Post hoc* pairwise permutational ANOVA (permANOVA) and permutational analysis of dispersion (permDISP) comparisons of photosynthetic efficiency between different weeks during each of the experimental phases for hard and soft coral, as well as live rock. Significant differences are indicated in bold ( $\alpha \leq 0.05$ )...... 75

**Table 3.3.19** *Post hoc* pairwise permutational ANOVA (permANOVA) and permutational analysis of dispersion (permDISP) comparisons investigating variation in photosynthetic efficiency between temperature treatments for hard and soft coral, as well as live rock, during each of the experimental phases. Significant differences are indicated in bold ( $\alpha \leq 0.05$ ). \*Temperatures were increased to 29.8°C during the final phase of the bleaching-threshold treatment..... 77

**Table 3.3.20** *Post hoc* pairwise permutational ANOVA (permANOVA) and permutational analysis of dispersion (permDISP) comparisons investigating variation in photosynthetic efficiency of hard and soft coral, as well as live rock, between different experimental phases for each temperature treatment. Significant differences are indicated in bold ( $\alpha \leq 0.05$ ). \*Temperatures were increased to 29.8°C during the final phase of the bleaching-threshold treatment..... 79

**Table 3.3.21** *Post hoc* pairwise permutational ANOVA (permANOVA) and permutational analysis of dispersion (permDISP) comparisons investigating variation in photosynthetic efficiency between hard coral and live rock for each temperature treatment during the different experimental phases and their corresponding weeks. Significant differences are indicated in bold ( $\alpha \leq 0.05$ )..... 80

**Table 3.3.22** Permutational ANOVA (permANOVA) and permutational analysis of dispersion (permDISP) investigating variation in net community calcification (NCC) according to the concentration of calcium carbonate (CaCO<sub>3</sub>) in water containing reef communities exposed to different temperature treatments based on total alkalinity concentrations measured at 6-hour intervals within a diel period at the end of weeks 4, 6 and 8 of the experiment. Significant differences are indicated in bold ( $\alpha \leq 0.05$ ). ..... 83

**Table 3.3.23** *Post hoc* pairwise permutational ANOVA (permANOVA) and permutational analysis of dispersion (permDISP) comparisons investigating variation in net community calcification (NCC) according to the concentration of CaCO<sub>3</sub>, in water containing reef communities, between different diel periods during the experiment. Significant differences are indicated in bold ( $\alpha \leq 0.05$ ). ..... 83

**Table 3.3.24** *Post hoc* pairwise permutational ANOVA (permANOVA) and permutational analyses of dispersion (permDISP) investigating variation in net community calcification (NCC) according to the CaCO<sub>3</sub> concentration, in water containing reef communities, between different 6-hour intervals (1-5) measured within a diel period during weeks 4, 6 and 8 of the experiment. Intervals, when samples were taken at night-time, are given in bold. Significant differences are indicated in bold ( $\alpha \leq 0.05$ ). ..... 86

**Table 3.3.25** *Post hoc* pairwise permutational ANOVA (permANOVA) and permutational analysis of dispersion (permDISP) investigating variation in net community calcification (NCC) according to CaCO<sub>3</sub> concentration, in water containing reef communities, between different

temperature treatments during each diel period. Significant differences are indicated in bold ( $\alpha \leq 0.05$ ). ..... 88

**Table 3.3.26** *Post hoc* pairwise permutational ANOVA (permANOVA) and permutational analysis of dispersion (permDISP) investigating variation in net community calcification (NCC) according to CaCO<sub>3</sub> concentration, in water containing reef communities, between different diel periods during the experiment for each temperature treatment. Significant differences are indicated in bold ( $\alpha \leq 0.05$ ). ..... 89

## List of Abbreviations

AAT	Alkalinity anomaly technique
C	Carbon
Ca	Calcium
CaCO <sub>3</sub>	Calcium carbonate
CCA	Crustose coralline algae
HCO <sub>3</sub> <sup>-</sup>	Bicarbonate
CO <sub>2</sub>	Carbon dioxide
CO <sub>3</sub> <sup>-2</sup>	Carbonate
D <sub>w</sub>	Density of buoyant fluid used in the weighing process
ENSO	El Niño-Southern Oscillation
F'	Fluorescence yield shortly before onset of a strong light pulse
F <sub>0</sub>	Basic fluorescence yield in the dark-adapted state
F <sub>0</sub> '	Minimum chlorophyll fluorescence yield in the light-adapted state
F <sub>M</sub>	Maximal chlorophyll fluorescence yield in the dark-adapted state
F <sub>M</sub> '	Maximal chlorophyll fluorescence yield in the light-adapted state
F <sub>V</sub>	Difference between maximum and minimum fluorescence yield
F <sub>V</sub> /F <sub>M</sub>	Maximum photochemical quantum yield
GBR	Great Barrier Reef
GHG	Greenhouse gas
GIS	Geographic information system
H <sub>2</sub> O	Water
HCl	Hydrochloric acid
HgCl <sub>2</sub>	Mercuric chloride
IOD	Indian Ocean Dipole
IPCC	Intergovernmental Panel on Climate Change
JR-PAM	Junior Pulse-Amplitude-Modulated (i.e. chlorophyll fluorometer)
KZN	KwaZulu-Natal
LED	Light-emitting diode
MHW	Marine heatwaves
NCC	Net community calcification
NRC	National Research Council
O <sub>2</sub>	Oxygen
OA	Ocean acidification

PAB	ProfiLux Aquatic Bus
PAR	Photosynthetically active radiation ( $\mu\text{mol photons m}^{-2} \text{s}^{-1}$ )
PermANOVA	Permutational analysis of variance
PERMANOVA	Permutational multivariate analysis of variance
PermDISP	Permutational analysis of dispersion
PRIMER	Plymouth Routine in Multivariate Ecological Research
PS II	Photosystem two
PVC	Polyvinyl chloride
RCP	Representative Concentration Pathway
rETR	Relative electron transport rate
RLC	Rapid light curve
RNA	Ribonucleic acid
ROS	Reactive oxygen species
SCUBA	Self Contained Underwater Breathing Apparatus
SD	Standard deviation
SE	Standard error
SLP	Saturating light pulse
SRES	Special Report on Emissions Scenarios
SST	Sea surface temperature
TA	Total alkalinity
UNEP	United Nations Environment Programme
UNESCO	United Nations Educational, Scientific and Cultural Organisation
$V_a$	Volume of skeletal material in the specimen
$W_a$	Total dry weight of skeletal material
WIO	Western Indian Ocean
$W_w$	Measured buoyant weight of the specimen
WWF	Worldwide Foundation
Y(II)	Photochemical quantum yield of PS II
$\alpha$	Alpha (i.e. significance level)
$\Phi\text{PS II}$	Effective quantum yield of PS II photochemistry
$\Omega_{\text{aragonite}}$	Degree of aragonite saturation

# CHAPTER 1 | INTRODUCTION

## 1.1 Thematic context of the study

The intricate and interwoven relationship between coral reefs and humans has been present for thousands of years. Along with the myriad benefits coral reefs generate, these marine ecosystems also bear the increasing strain of local communities' economic dependence. The impacts of local anthropogenic pressures are further exacerbated by global environmental pressures (Burke *et al.* 2011; Hoegh-Guldberg *et al.* 2019). The rapid pace at which climate change prevails potentially limits corals and reef communities' abilities to adapt (Hughes *et al.* 2017). The research conducted in this thesis thus focuses on marginal coral reef communities and how they may respond to different climate change scenarios attributable to global warming, based on a series of questions related to coral physiological responses. The responses of a typical high-latitude coral community from Sodwana Bay, comprised of hard coral, soft coral and 'live rock', are investigated relative to different global warming scenarios. The results reveal valuable insights into how coral reefs in the region are likely to respond to global warming and how the responses of the hard coral *Acropora appressa* differ from those of the soft coral *Sinularia brassica*, both representative corals on the reefs in question. The work involved undertaking replicated mesocosm experiments and quantifying several physiological parameters of individual corals and coral reef communities. Specifically, the experiments exposed coral communities to historical-average, future (year-2100; Moss *et al.* 2010) and bleaching-threshold temperatures at Sodwana Bay, South Africa.

Coral reefs worldwide are susceptible to the intensifying effects of global warming, increased nutrient enrichment and other anthropogenic influences (Hoegh-Guldberg 1999; Carpenter *et al.* 2008; Veron *et al.* 2009). The consensus is that the ocean has been warming since the start of the 20<sup>th</sup> century (Hoegh-Guldberg *et al.* 2014). Climate-change-driven effects such as increasing ocean temperatures, sea-level rise, and ocean acidification are occurring faster than many marine organisms' adaptive capacities (Bopp *et al.* 2013). Thus, there is concern about the ability of marine species to adapt and endure environmental changes associated with climate change (Hughes *et al.* 2003). Consequently, understanding the physiological responses of coral reef organisms to different climate change scenarios will help determine the potential for marginal coral reefs to acclimatise and adapt to increases in ocean temperature and related physical parameters. Research will provide an insight into how vulnerable these corals are to climate change and may aid in developing improved reef protection and conservation management strategies.

The scientific community's understanding of how climate change may affect marine ecosystems, specifically the increase of ocean temperatures, is inadequate. The lack of knowledge is partly due to the size and complexity of the ocean, as well as the relative difficulty of obtaining measurements in the marine environment (Rosenzweig *et al.* 2008). Given the overwhelming significance of the ocean to all life on earth, the potential effects of global warming accentuate the urgency with which humanity must act to lower atmospheric greenhouse gas (GHG) emissions and concurrently reduce the associated risks (Hoegh-Guldberg & Bruno 2010). Efforts to preserve and enhance the health of coral reef ecosystems must be considered within the long-term context of global climate change (UN Environment *et al.* 2018). Such efforts can only be achieved with further research, focusing on how coral reefs respond as a community and not only as their component parts, if disruption of the carbon cycle's impact on these vital ecosystems is to be understood. Further research based on the potential effects of climate change on coral reef ecosystems will help project and quantify global warming effects and influences (Murillo *et al.* 2014).

One way of addressing the potential future impacts of climate change on coral reefs is with mesocosm experiments that test the effects of different climate scenarios. The current effects of increasing ocean temperatures on corals and coral communities are already well recognised globally (Brown 1997) and in the western Indian Ocean (WIO) (McClanahan *et al.* 2007). Previous research conducted on this subject has been based on field observations and experimental mesocosm studies (Glynn & D'Croz 1990). However, there are relatively few studies on coral reef community-level responses to current and future climate conditions based on mesocosm experiments. There is no literature available on the subject of South African or south-west Indian Ocean coral reef communities and climate responses; to date such investigations have only been undertaken on kelp and crustose coralline algal communities (see Martin & Gattuso 2009; Connell & Russell 2010).

From the in-depth analyses of 255 coral heat-stress experimental studies, McLachlan *et al.* (2020) found that coral species in the WIO are profoundly understudied and were primarily excluded from heat-stress experiments. Globally, coral reef responses to future climate change scenarios are not yet well understood. The same is true for potential responses of South African high-latitude coral reef communities to projected climatic changes. This study seeks to understand the likely responses of high-latitude coral reef organisms and communities to climate change, using species representative of Sodwana Bay.

## 1.2 What are coral reefs?

Coral reefs are diverse habitats, supporting more than 25% of marine biodiversity globally, despite only covering approximately 0.2% of the ocean's surface area (Reaka-Kudla 1997; Knowlton *et al.* 2010). Coral reefs comprise colonial marine invertebrates called corals, which are individually composed of polyps. The polyps live in calcium carbonate ( $\text{CaCO}_3$ ) exoskeletons, cumulatively adding to the robust three-dimensional reef framework. The intricate relationships formed among the diverse organisms in reef ecosystems, as well as the ancient symbiosis between corals and zooxanthellae, enable coral species to be some of the most productive organisms on earth (Muscatine & Porter 1977; Stanley 2003; Wild *et al.* 2004). Reef systems mainly comprise scleractinian corals that have a symbiotic relationship with microscopic algae called zooxanthellae, generally from the dinoflagellate genus *Symbiodinium*.

*Symbiodinium* cells are unicellular microalgae found within the endodermal tissue of the coral polyp's body, providing the tissue with photosynthetic products whilst receiving limited organic nutrients from the host (Muscatine & Cernichiaro 1969; Stanley 2003). Approximately 60 to 85% of the nutritional products received by the host are derived from these symbionts (Muscatine *et al.* 1981). Other sources of nutrients that sustain coral reefs, such as particulate organic matter and detritus, come from exogenous sources such as plankton, or from endogenous sources such as 'live rock'. Live rock is dead coral or rock consisting of aragonite skeletons encrusted with coralline algae and other organisms that provide the foundation for most coral reefs in the ocean (Hauter & Hauter 2019). Live rock hosts numerous micro- and macroscopic marine forms of life that inhabit both the inside and outside of the rock. Consequently, live rock functions as a biological filter, hosting aerobic and anaerobic nitrifying bacteria, algae and marine invertebrates (ARC Reef 2016). Live rock also harbors many worm, crustacean, microbe and algae species that feed grazers and predators on the reef or add food particles directly to the water column as larvae and gametes (Hatcher 1997; Wild *et al.* 2004). Symbionts and live rock, in turn, assist with the survival and optimal functioning of coral reefs in oligotrophic tropical waters (Wild *et al.* 2004).

Broadly, coral reefs are generally distributed in the tropics between 30°N and 30°S of the equator (Kleypas *et al.* 1999). Coral reef ecosystems consist of diverse hard and soft corals, micro- and macro-organisms, including numerous marine invertebrate and vertebrate species. The reef-building corals are known as hermatypic (i.e. hard or stony corals), comprising the majority of the order Scleractinia, as they extract calcium ( $\text{Ca}^{2+}$ ) from the surrounding seawater. The  $\text{Ca}^{2+}$  combines with carbon (C) and oxygen ( $\text{O}_2$ ) to form aragonite, an isomer of  $\text{CaCO}_3$ , producing the coral's rigid exoskeleton (Stanley 2003). The exoskeleton, in turn, protects the coral's soft, sac-like polyp bodies and tissue cells. Contrastingly, the order Alcyonacea that comprises soft coral

species does not produce  $\text{CaCO}_3$  skeletons. Instead, soft corals contain numerous calcareous sclerites comprised of calcite, another isomer of  $\text{CaCO}_3$ , that are embedded within their tissues (known as the coenenchyme) to support their much softer bodies (Fabricius & Alderslade 2001).

Although corals generally live in oligotrophic tropical waters, high productivity among these ecosystems accentuates their importance in tropical oceans and their role in the marine environment globally (Hoegh-Guldberg, 1999). Corals that exist in subtropical and tropical waters are dependent on the ocean surface's physical and chemical interactions (Eakin *et al.* 2010), which restricts their growth to depths of approximately 60 m and optimal temperature conditions between 24 and 27°C. Only a few species of subtropical corals are found in water temperatures below 18°C (Kleypas *et al.* 1999). Other types of coral, such as deep-sea or cold-water corals, are often located at much greater depths below 100 m and at water temperatures of between 4 and 12°C (Roberts *et al.* 2006). Hence, cold-water coral distributions extend all over the world, allowing them to interact with a broader range of biogeochemical changes in the ocean (Freiwald *et al.* 2004; Eakin *et al.* 2010).

The type and response of coral species will depend on the rate at which natural and anthropogenic changes occur. Coral reef responses to natural and anthropogenic changes, whether on a micro- or macro-scale, translate into various trajectories that can be used to project and monitor coral reefs (Hubbard 2015). Long-term monitoring data and representative concentration pathways (RCPs) produced by climate models may be coupled to provide an insight into the future trajectories of different coral reefs. Such trajectories are essential in short- and long-term projections of the effects of global warming on coral reefs (Hubbard 2015; IPCC 2018). Four plausible scenarios of greenhouse gas concentration trajectories (also referred to as pathways) include the RCP 2.6, 4.5, 6.0 and 8.5 (further discussed in section 1.2.3; IPCC 2018). Considering what natural and anthropogenic changes may occur as a result of each potential trajectory is critical to understanding potential shifts in reef community structure. The changes observed on various reefs have generally been more obvious on low-latitude reefs compared to high-latitude reef systems, especially when one considers global warming and coral bleaching. Hence, varying environmental conditions that may occur are likely to have an influence on reef community structures (Edmunds & Leichter 2016).

### 1.3 The importance of coral reefs

Coral reef ecosystems are of incredible biodiversity and aesthetic value, placing them amongst the most unique marine ecosystems globally (Reaka-Kulda 1997). Due to the robust framework coral reefs create, they provide essential biogenic substrates and habitats for reef-associated organisms. Their framework thus functions as a food source and as a shelter (Cole *et al.* 2008). Reefs also provide a wealth of financial, cultural and ecosystem services that support livelihoods (Jiddawi 1997; Moffat *et al.* 1998), eco-tourism (Cesar *et al.* 2003) and provide coastal protection for millions of people worldwide (Richmond 1993; Reaka-Kulda 1997). Likewise, live rock that forms part of reefs provides a vital income source for people worldwide. For example, the live rock trade for mariculture and marine aquarium facilities has grown between 12 and 30% per annum since the 1990s (WWF 2004) and costs between US\$ 4 and US\$ 10 a kilogram, equivalent to an annual worth of between US\$ 44 and US\$ 121 million (Parks *et al.* 2003; WWF 2004). Nearly 90% of live rock is exported globally, with the United States of America being the largest consumer of both coral and live rock specimens. It is further estimated that the live rock trading sector is worth approximately US\$ 1.1 billion annually, with an estimated 15% global annual growth in market demand (Falls *et al.* 2003). Consequently, excessive anthropogenic pressures are experienced due to live rock extraction.

The importance of healthy coral communities hosting a diverse and high abundance of fish is evident from the revenue they create for national and international fishing fleets (Ferse *et al.* 2010). Diverse and healthy coral reefs also provide great nutritional sustenance to local communities primarily dependent on fish stocks (Spurgeon 1992). The abundance of fish stocks is mainly attributable to corals regulating competition and predation interactions among reef fishes by providing refuge spaces and specific niches (e.g. feeding) among coral colonies (Webster & Hixon 2000). For example, fish that live directly above the reef are more abundant than those that live among the coral colonies. The varied scleractinian corals greatly enhance fish species' survival and existence by providing supplementary shelter and moderating key ecosystem processes (Kerry & Bellwood 2012). That said, more than 25% of marine fish species are associated with coral reefs (Spalding *et al.* 2001; Allen 2008), even though not all species are entirely reliant on coral reef ecosystems (e.g. Cinner *et al.* 2009). Nevertheless, the highest fish abundances are found in areas with high coral cover (Jones *et al.* 2004; Pratchett *et al.* 2008).

Coral reefs also function as natural barriers against wave action and storms by controlling wave energy build-up through reflecting, dissipating, and shoaling waves. This barrier action thus protects the land, which supports approximately half a billion people residing within 100 km of reefs, by reducing coastal erosion processes (Harris *et al.* 2018). Live rock contributes to this

barrier function and acts as a habitat for marine life (ARC Reef 2016). Hence, the removal of live rock results in the destruction of critical reef habitats for fish and marine invertebrates, undermining coral reef structures and increasing underwater erosion (WWF 2004). Large coastal communities living near reef environments have also realised the dive tourism potential of these biodiverse ecosystems. Accordingly, coral reefs have become major tourist attractions, capable of generating over US\$ 29.9 billion annually from people visiting coral-reef regions (Cesar *et al.* 2003) through activities such as recreational SCUBA diving and snorkelling, boating and fishing trips, as well as visiting nearby hotels, restaurants and other businesses (Henkel 2012). Likewise, increased exploration of coral reefs has created an interest in bioprospecting research – the medicinal potential plant and animal species may have for new pharmaceuticals (Robert 2001). It has been found that coral reefs contribute to essential medicines that assist with cancer treatment, arthritis, asthma, ulcers, bacterial infections, heart diseases, viruses, and other types of diseases. Additionally, these pharmaceuticals provide sources of nutritional supplements, enzymes and cosmetics (Moberg & Folke 1999; Bruckner 2002; Demunshi & Chugh 2010).

Despite the immense importance of reef ecosystems for both the marine environment and society, they face an extensive list of threats and are documented to be in rapid decline across most regions (De'ath *et al.* 2012; Obura *et al.* 2017; Moritz *et al.* 2018). As coral reefs create numerous opportunities across various sectors of the economy, they may become exposed to a myriad of stressors. Such stressors include, but are not limited to, destructive fishing and diving practices, pollution, invasive species and ocean acidification (Henkel 2012; UN Environment *et al.* 2018). It is estimated that almost 90% of all coral reefs could be lost by the year 2050 due to growing impacts from human- and climate-induced stressors (van Hooidonk *et al.* 2016; IPCC 2018).

Even though little information is available on the response of live rock to global warming, research has revealed that crustose coralline algae (CCA) and other fauna on live rock are influenced by warming ocean temperatures (Martone *et al.* 2010). The encrusting CCA found on live rock is part of the order Corallinales, which photosynthesises. Live rock may also have a veneer of more fleshy organic matter, such as algal turf, around it and provides a refuge for other organisms such as crabs, numerous fish species, nudibranchs, molluscs and shrimp (WWF 2004; ARC Reef 2016). Hence, warming ocean temperatures may potentially cause bleaching and eventual necrosis of CCA (Martone *et al.* 2010). If bleached or necrotic, live rock has minimal nutritional value for fauna living in or around it, leading to a loss in biodiversity. Hence, the urgency for expanding research capabilities to better determine climate-induced impacts is essential to avoid global-scale reef degradation and the loss of financial returns that reef systems generate (UN Environment *et al.* 2018).

## 1.4 Climate change and global warming

While climate change and global warming are related, these two physical phenomena do differ. Greenhouse gases (GHGs), such as those emitted by human activities, cause anthropogenically-induced global warming, which in turn causes climate change (Broecker 1975; Weart 2008). The 2018 Special Report of the United Nations Intergovernmental Panel on Climate Change (IPCC) stated that anthropogenic activities have already caused an approximate 1.0°C increase above pre-industrial levels in Earth's global temperature. The consequences of this are already becoming evident through more extreme weather events, an overall rise in sea levels, marine heatwaves and diminishing Arctic ice sheets, among other changes (Hoegh-Guldberg *et al.* 2018; IPCC 2018).

The IPCC Representative Concentration Pathways (RCPs) developed in 2010 (Moss *et al.* 2010) from the Special Report on Emissions Scenarios of 2000 (SRES; Nakicenovic *et al.* 2000) present four different 21<sup>st</sup>-century outcomes. These RCP scenarios are based on GHG emissions and atmospheric concentrations, other air pollutant emissions and land use (Moss *et al.* 2010). They were developed utilising integrated assessment models that consider an extensive range of climate model simulations, aiming to project consequences for the climate system (Meinshausen *et al.* 2011). The RCPs are named according to the degree of change in radiative forcing by 2100: +2.6, +4.5, +6.0 and +8.5 watts per square meter (Masui *et al.* 2011; Riahi *et al.* 2011; Thomson *et al.* 2011; van Vuuren *et al.* 2011). These concentration pathways can then be used in impact and adaptation experiments and assessments.

When considering the prediction models from previous climatological periods, RCP 4.5 and 8.5 projects the most likely future outcomes of the four RCPs (Collins *et al.* 2013; Gattuso *et al.* 2014). There are, however, uncertainties within these projections based on how the climate system responds to anthropogenic emissions and whether efforts are made to reduce these emissions (Collins *et al.* 2013). The further ahead these models are used to project, the higher the uncertainties become. The certainty, also referred to as the confidence level, that climate change impacts and associated events might occur can be graphically represented (see Fig. 1.4.1). These transient, scenario-based simulations make it possible to analyse projected changes based on a given global average temperature threshold (NRC 2011). Representative concentration pathway scenarios derived from global average temperatures offer the public and policymakers a way to understand the effects of any given temperature threshold. Numerous physical changes and related results have demonstrated scaling with global average sea-surface temperature, including shifts in average precipitation, extreme heat events, and higher risks of coral bleaching (NRC 2011; Frieler *et al.* 2013).

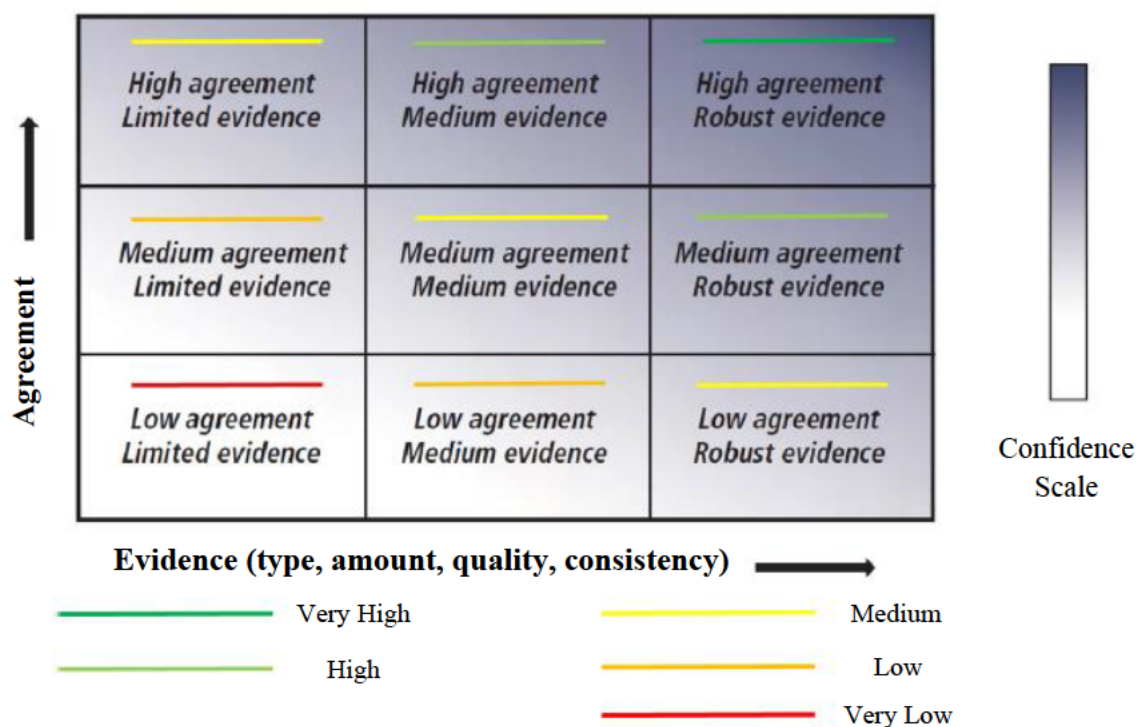


**Figure 1.4.1** Confidence levels of climate change affecting the marine environment based on evidence and consensus. The increased levels of evidence and degrees of agreement are associated with increasing confidence, as indicated by the increasing strength of shading in the confidence scale (adapted from IPCC 2013).

The ocean will continue to absorb anthropogenic carbon dioxide (CO<sub>2</sub>) under all RCP scenarios through and surpassing the year 2100, being especially elevated for the higher RCPs (*very high confidence*; Figs. 1.4.1, 1.4.2). RCP 2.6 envisages that GHG emissions peak between 2010 and 2020 but then decline considerably after that (Collins *et al.* 2013, Meinshausen *et al.* 2011). For RCP 4.5, a peak in GHG emissions is experienced by 2040, followed by a subsequent decline. In the case of the RCP 6.0, GHG emissions peak by 2080 and then decline, whereas GHG will be progressively emitted throughout the 21<sup>st</sup> century under the RCP 8.5 scenario (Meinshausen *et al.* 2011; Fig. 1.4.3).

Based on the Earth system and integrated assessment models, there is *high confidence* that climate change and associated changes in the carbon cycle are amplifying global warming (Figs. 1.4.1, 1.4.2; IPCC 2013, 2014). These models further project a global increase in ocean acidification (OA) for all RCP scenarios before the end of the 21<sup>st</sup> century, with slow recoveries past the mid-century under RCP 2.6 (see IPCC 2014). For RCP scenarios 4.5, 6.0 and 8.5, OA and global warming will influence the formation and maintenance of coral reefs (*high confidence*; Fig. 1.4.1; Gattuso *et al.* 2014) and the goods and services these ecosystems provide (Kroeker *et al.* 2013).

The effects of OA and global warming will primarily affect coastal regions and small islands that heavily depend on ecological goods and services from coral reefs (Turley & Gattuso 2012). The increases in global average sea surface temperatures (SST) for the different RCP scenarios are more certain for the higher latitudes (Hoegh-Guldberg *et al.* 2014). The one-year intervals of interannually varying SST isotherms (i.e. lines of equal temperature) are moving to higher latitudes at approximate rates of 40 km year<sup>-1</sup> (Burrows *et al.* 2014; García Molinos *et al.* 2015). The change in surface layer temperatures towards higher latitudes will cause intensifying marine heatwaves (MHW), resulting in more episodic bleaching events in affected areas. The global average duration of a MHW, has nearly doubled over the satellite record for especially high-latitude regions across all ocean basins (Oliver *et al.* 2018). Furthermore, changes in MHW characteristics have been strongly correlated to changing SSTs globally. The increases are expected to continue under projected future RCP scenarios (Oliver *et al.* 2019).

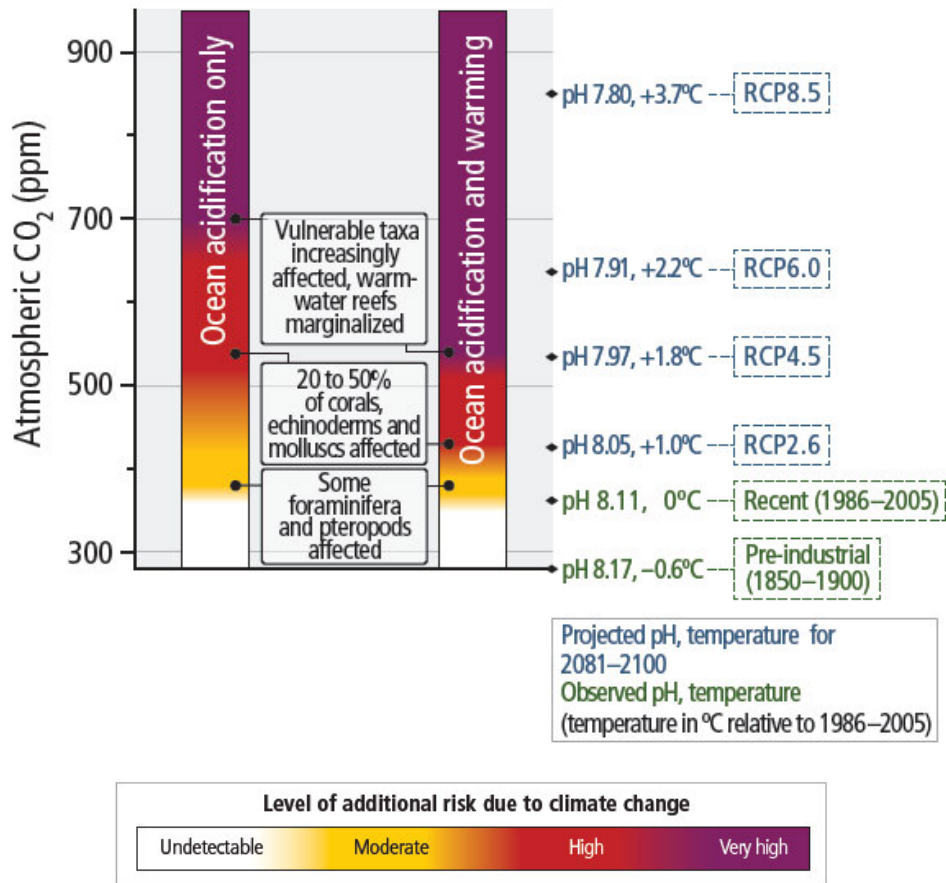


**Figure 1.4.2** A risk level criterion of the impacts of climate change concerning ocean warming and acidification on calcifying marine species (with a focus on corals and reefs). The risk level criterion is consistent with the confidence levels that are further based on evidence and the degree of scientific agreement (see Fig 1.4.1). Accordingly, the level of additional risk is indicated by the colour bar (adapted from IPCC 2014).

Similar results were found to occur in average ocean temperatures (*high confidence*), where an increase in climate extremes correlated with rising global average SSTs (Hoegh-Guldberg *et al.* 2014; García Molinos *et al.* 2015). Additionally, more intense climate variability has become evident, for example, the intensification of El Niño-Southern Oscillation (ENSO) events associated with climate change (Hoegh-Guldberg *et al.* 2014; Oliver *et al.* 2018). Consequently, the increased frequency and amplitude of ENSO events have induced warming of the WIO (Roxy *et al.* 2014). During 1998, when a major ENSO event occurred, above-average SSTs were recorded on a global scale, and accordingly, it was estimated that 16% of coral communities bleached globally and died (Hoegh-Guldberg 1999; Wilkinson 2008). Since then, more coral bleaching events have occurred, and the extent of these impacts have also increased over time (Hoegh-Guldberg *et al.* 2014; Hughes *et al.* 2018).

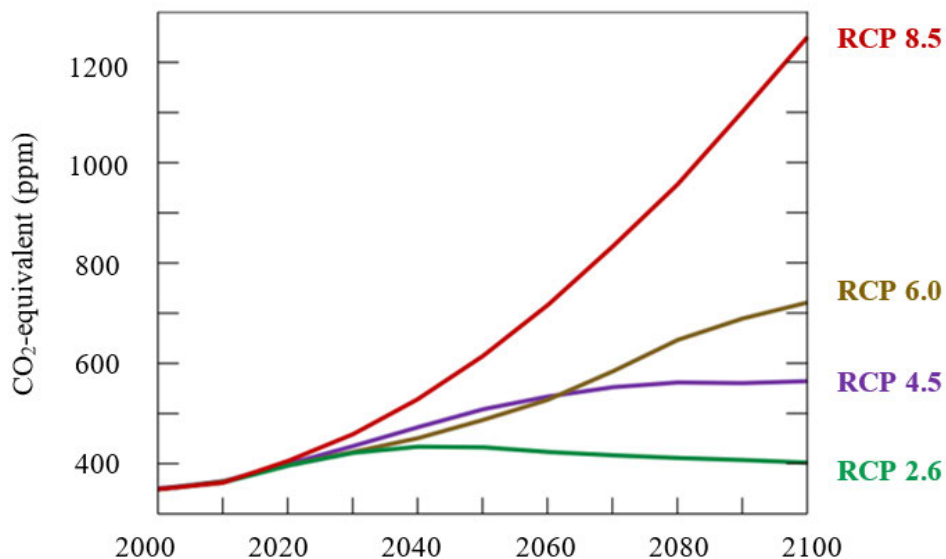


**Figure 1.4.3** Projected trajectories of the four Representative Concentration Pathways (RCPs) to the year 2100 based on accumulative atmospheric greenhouse gases (i.e. CO<sub>2</sub>-equivalent concentrations) outlined by the fifth IPCC Assessment Report (adapted from van Vuuren *et al.* 2011).

Along with El Niño and La Niña events, the Indian Ocean Dipole (IOD) has also intensified with global warming. The IOD is an interannual mode of aperiodic oscillation of the SSTs, which causes climate variability within the Indian Ocean (Saji *et al.* 1999). Some corals found in the WIO have shown records of past relationships between atmospheric-ocean processes (Webster *et al.* 1998; Zinke *et al.* 2009; Watanabe *et al.* 2019). Reconstruction models using corals have further suggested that ever-increasing global warming might increase variation associated with ENSO events, as well as intensify the frequency and strength of warmer IOD occurrences (Abram *et al.* 2003; Watanabe *et al.* 2019).

Throughout the 20<sup>th</sup> century, the increase in atmospheric CO<sub>2</sub> has resulted in the average global ocean temperature rising by 0.74°C, seawater carbonate concentrations decreasing by ~30 μmol kg<sup>-1</sup> and ocean acidity increasing by 0.1 pH units (IPCC 2007; Fig. 1.4.3). Other physical parameters that have changed in the ocean include evidence of intensifying coastal upwelling (Bakun 1990), rising sea levels (IPCC 2007), a decrease in aragonite saturation (Hoegh-Guldberg *et al.* 2007), and an increase in the intensity of tropical hurricanes and cyclones (Webster *et al.* 2005). Due to global warming (Hughes 2000), biological consequences have resulted in corals experiencing tremendous thermal stress and bleaching, which have significantly affected global coral reef communities (Baker *et al.* 2008).

The influence of a 1.5°C increase in seawater temperature due to global warming (Fig. 1.4.3) is predicted to shift distributions of several marine species to higher latitudes, along with cumulative damage to many ecosystems (IPCC 2018). In the case of coral reefs, mass mortalities and increases in disease outbreaks will intensify as they are exposed to increasing temperatures (*very high confidence*; Figs. 1.4.1, 1.4.2) (Hoegh-Guldberg 1999; Hughes *et al.* 2017). Subsequently, the degradation of coral reefs will result in the loss of coastal resources and a reduction in the productivity of fisheries. Climate change impacts of a 2.0°C warming will cause more considerable losses (Gattuso *et al.* 2015).

Further research on how the ocean will respond to long-term changes associated with climatic phenomena and related anthropogenic influences will greatly enhance the understanding of how physiological responses of individual corals may change when they are thermally stressed (Riegl & Pillar 2003; Sheppard 2003; Le Treut *et al.* 2007). Climate change may substantially influence the physiologies of the organisms comprising coral reefs and their adaptive potential over spatial and temporal scales (Gunderson *et al.* 2016).

## **1.5 South African high-latitude coral reefs and global warming**

The tropical western Indo-Pacific is the largest marine biogeographic province globally, containing several of Earth's most important coral reef ecosystems (Spalding *et al.* 2007). It encompasses large areas of the tropical waters of the Indian and Pacific Oceans. Within it, the Western Indian Ocean (WIO) contains 16% of the world's coral reefs and encompasses the second highest peak in coral reef biodiversity globally (Obura *et al.* 2017). The most significant large-scale determining abiotic factors of coral community composition in the WIO appear to be temperature and wave-generated turbulence, as well as turbidity (Porter *et al.* 2014, 2017). The Delagoa Bioregion, one of the bioregions within the western Indo-Pacific province (Spalding *et*

*al.* 2007; Porter *et al.* 2013) and the focal area of this study, contains Africa's southernmost coral communities (Riegl *et al.* 1995; Schleyer 2000). The bioregion extends northwards from Leven Point, in the Maputaland region of South Africa, into southern Mozambique (Porter *et al.* 2013). The high-latitude coral reefs in Maputaland have not been affected by global bleaching events to any great extent (Gudka *et al.* 2018; Schleyer *et al.* 2018). Being at the marginal limits of reef-building coral distribution, it has been suggested that these high-latitude reefs may manifest symptoms related to climatic changes in advance of those at low latitude (Schleyer & Celliers 2003a). This is mainly due to climate-affected factors such as aragonite saturation states and limiting temperatures at high latitudes (Kleypas *et al.* 1999).

In Maputaland, coral communities attain high biodiversity with soft coral cover (~32%, 39 species) exceeding the ~27% scleractinian cover (93 species) across a considerable area of the reef (Riegl *et al.* 1995; Schleyer 1995; Schleyer 1999, 2000; Schleyer & Porter 2018). Coral communities comprise a combination of both tropical and subtropical Indo-Pacific species (Celliers & Schleyer 2008). Soft corals dominate these reef-top communities (Riegl *et al.* 1995) and cover approximately the same surface area as hard corals at the reef-sediment interface (Schleyer & Celliers 2003b). The coral communities flourish at this high-latitude due to the warm, clear waters that result from the mixing of the tropical Mozambique and south-east Madagascar currents, generating the Agulhas Current, the characteristically narrow continental shelf, and the negligible riverine input (Porter *et al.* 2017a). These oceanic conditions result in average water temperatures of 24.4°C at Sodwana Bay (Porter & Schleyer 2017). Warmer coastal waters may result in coral communities shifting towards a more hard coral-dominated community. However, this change might be transitory since ocean temperatures occasionally reach the local coral bleaching threshold of 28.8°C (Schleyer & Celliers 2003a).

Sodwana Bay has typical high-latitude reef communities of Maputaland that may be valuable for environmental-stressor studies due to the reefs' marginal nature (Schleyer & Celliers 2003a). Although coral reefs in Sodwana Bay were discovered in the 1970s, long-term monitoring of these reefs only commenced in 1993. As monitoring on these reefs progressed, recent coral bleaching events have also been recorded (Schleyer 2000; Celliers & Schleyer 2008; Gudka *et al.* 2018). It was found that the bleaching event that occurred during 1998 was a result of oceanic warming that gradually progressed from the year 1995 (Schleyer 2000). As more heat build-up occurred in the ocean over the years, it caused another global coral bleaching event to occur in 2016 (Eakin *et al.* 2018; Eakin *et al.* 2019). According to Reynolds' sea-surface temperatures (SSTs), it is evident from regional data that ocean temperatures have been increasing since the 1950s and will continue to rise throughout the 21<sup>st</sup> century (Schleyer *et al.* 2008). An estimated 50 to 60% of

corals were affected by the 1998 El Niño-Southern Oscillation (ENSO) event in the WIO (Obura 2005). Thus far, the Delagoa Bioregion has experienced ENSO and minor bleaching events during the summers of 2000 to 2001 (Celliers & Schleyer 2002), in 2005 and again in 2016 (Schleyer *et al.* 2018). An increase in the intensity of the El Niño effect across South Africa (Richard *et al.* 2000), along with more dramatic coral bleaching events, can be expected due to increasing SSTs in the region (Celliers & Schleyer 2002). A recent study conducted by Porter and Schleyer (2017) found that SSTs have been decreasing by 0.03°C per annum at Sodwana Bay. Despite the nominal decrease, minor bleaching episodes due to ENSO events and changes in coral composition were still evident (Porter & Schleyer 2017).

Generally, high-latitude coral reefs persist in more stressful environments than their tropical counterparts. For example, the Arabian Gulf reefs survive the highest yearly temperature variabilities experienced by any reef ecosystem (14 to 37°C; Sheppard *et al.* 2000). As a result, some reefs situated at higher latitudes have already started experiencing thermal stress, which may become more evident among coral reefs found at broader distribution and temperature ranges. Similarly, Ateweberhan *et al.* (2011) determined that regional patterns in coral cover distribution in the Indian Ocean are driven primarily by intermittent and acute environmental stressors such as higher ocean temperatures, increased storm and cyclone occurrences due to global warming and increased solar radiation.

The wave energy characterising the Delagoa Bioregion is found to be fundamentally important, hindering more delicately branched acroporids and other structurally complex reef-building corals from flourishing, and thus, favour encrusting growth forms of soft corals, especially on shallow reaches of these types of reef (Schleyer *et al.* 2003; Porter *et al.* 2017a). Corals nevertheless get damaged by episodic storms which contribute to differences in community structures on these reefs (Riegl & Riegl 1996). Regular high-energy wave events may limit some hard coral species to such an extent that reef frameworks can neither be formed nor maintained (Riegl 2001). The result of high-energy wave events in the face of ever-increasing global warming needs to be taken into consideration for coral reef conservation management (Riegl 2001; Webster *et al.* 2005; Celliers & Schleyer 2008). Cyclones, specifically, are projected to increase in frequency and intensity, and to reach higher latitudes due to increasing climate change effects (Webster *et al.* 2005). Furthermore, Agulhas Current eddies also move southwards along the coastline and alter the current dynamics and cause temperatures to rapidly increase or decrease (Morris *et al.* 2013; Porter & Schleyer 2017). A recent study by Halo and Raj (2020) found that the intensification of eddies in the Agulhas Current along the Maputaland coastline is indeed occurring due to increasing global warming. These intensified eddies may cause oceanic lateral fluxes to become

stronger and ocean-atmosphere fluxes to occur more frequently. Consequently, environmental conditions (i.e. air-sea heat flux exchanges, broadening and weakening of the Agulhas Current, excessive SST warming, seasonality), both within the atmosphere and the ocean, are more strongly influenced based on the oceanic variability in the WIO (Halo & Raj 2020).

Considerable research has been conducted on the biodiversity (Schleyer & Celliers 2005; Celliers & Schleyer 2008; Porter *et al.* 2013), local oceanography (Morris 2009), coral systematics, distribution, reproduction and settlement (Glassom *et al.* 2006; Schleyer *et al.* 2008; Hart 2018) on Maputaland coral reefs. More recent studies were undertaken on the dynamics in reef cover, mortality in different corals and their recruitment success to determine the effects, if any, of climate change (Porter & Schleyer 2017; Hart 2018). Freeman (2015) suggested that coral habitats classified as marginal will perform best under the IPCC projected RCP scenarios relative to their more tropical counterparts. Hence, the marginal reefs at Sodwana Bay and in Maputaland may be more resilient to climate change, even when considering their physical and chemical environmental limitations (Kleypas *et al.* 1999). However, marginality or environmental limitations do not account for the effects that episodic bleaching and ENSO events may have on marginal reefs due to marine heatwaves. Nevertheless, high connectivity across latitudes is essential for high-latitude coral reef communities to function as refugia from global warming (Beger *et al.* 2014; Camp *et al.* 2018).

## **1.6 Mesocosm experiments and their importance in coral reef studies**

When studying coral reefs at the community level, mesocosms provide opportunities to investigate mechanisms of community assembly and, thus, more accurately determine how climate shifts are likely to affect biodiversity, community structure and ecosystem functioning (Logue *et al.* 2011). Mesocosms are closed or partially enclosed indoor or *in situ* experimental systems that closely simulate the natural environment (Odum 1984). These systems have numerous advantages such as replicability, consideration of species interactions, and tight (microcosm) or realistic (mesocosm) control of physico-chemical parameters; they are thus able to limit confounding factors (Leblud *et al.* 2014).

Mesocosm experiments can play an essential role in projecting the impact of climatic conditions at different physiological levels on coral reefs, ranging from individual species to representative communities and entire ecosystems (Bestion *et al.* 2015). Data on physiological tolerances obtained from mesocosm experiments can be coupled with spatial geographic information system (GIS) layers of the present- and future climatic conditions to project probable ranges of a species

or even a community (Kearney *et al.* 2009). Experimental designs utilising mesocosms are advantageous as they more closely mimic natural environmental variabilities and interspecific interactions in an ecosystem. Experiments that include both GIS layering with physico-chemical parameters can further our knowledge of fundamental principles of population ecology that include the importance of plasticity in life-history traits of coral reefs, along with predator-prey dynamics on the persistence of reef communities (Chevin *et al.* 2010). Furthermore, the data can be used in metapopulation and demographic models to test and improve theoretical projections. Accordingly, spatial models that combine physico-chemical parameters will improve forecasting of bleaching areas, extinction risks and distribution dynamics (Pearson *et al.* 2014).

Net losses of calcium carbonate ( $\text{CaCO}_3$ ) have been recorded (Andersson *et al.* 2009) in simulated climate scenarios in reef community-level mesocosm experiments. Numerous laboratory studies that include mesocosm experiments have effectively demonstrated the sensitivity of coral calcification rates to increasing water temperatures and decreasing pH (Kroeker *et al.* 2013). In other mesocosm-related studies, Leclercq *et al.* (2002) and Langdon *et al.* (2000) found a linear decrease in net calcification with an increase in the partial pressure of carbon dioxide ( $p\text{CO}_2$ ), as well as a 40% reduction in overall reef calcification. Moreover, a mesocosm-based study projected that a 21% decrease in calcification and a doubling effect in  $p\text{CO}_2$  can be expected between the pre-industrial era and year 2065 (Leclercq *et al.* 2000).

Previous experimental results have not yet reached a clear consensus on whether global warming affects responses and changes in calcification rates in the case of individual coral species, live rock specimens and reef communities (Langdon & Atkinson 2005; Jokiel *et al.* 2008). The uncertainty could be due to a lack of mesocosm experiments that investigate such aims and objectives (Pandolfi *et al.* 2011). The effect of one species dominating another due to processes such as accretion, together with interactions by co-inhabitants and dissolution of the reef framework can also influence reef responses (Ries *et al.* 2009; Pandolfi *et al.* 2011). The forecasting of physiological responses to global warming will be comprehensive if mesocosm experiments cover a wide range of future climate change scenarios (Stewart *et al.* 2013).

## **1.7 Physiological responses to global warming**

### **1.7.1 Coral growth according to size and buoyant weight**

A variety of methods have been employed to quantify coral growth. A common metric used to measure coral growth is linear extension (Holcomb *et al.* 2013; Pratchett *et al.* 2015). Linear extension in corals can be defined as the outward development of coral skeletons toward the edge

of a colony (Cronin 1999). Growth can be measured as a unidirectional change in branch length, plate diameter or colony circumference. Linear extensions of coral branches maintain an approximately similar growth direction and function as a determinant of coral fitness and ecological success (Kleypas & Langdon 2006).

The rate at which corals grow is largely influenced by various environmental factors (Lough & Barnes 2000; Cooper *et al.* 2011). Previous research conducted in Hawaii and the Great Barrier Reef (GBR) showed a correlation between coral densities and latitude, i.e. the higher the latitudinal position of the coral species, the denser the coral skeleton and, conversely, the slower the linear extension rate (Hoeke *et al.* 2011; Woolsey *et al.* 2015; Anderson *et al.* 2017). Other environmental factors that influence growth rate include temperature (Storz & Gischler 2011), wave and tidal current (Reid *et al.* 2019), sedimentation (McClanahan & Obura 1997; Crabbe & Smith 2005), topography of colonies (Cohen & Hart 1997) and sunlight availability (Bessell-Browne *et al.* 2017). Perturbations to coral reef ecosystems, again, may negatively affect the growth rate of corals. For example, it is projected that the effects of anthropogenically-driven climate change will have a critical, negative influence on coral growth (Kleypas & Langdon 2006). In the case of live rock, seasonal switching has been observed in coralline algae where the linear extension of articulated coralline algae decreases, changing from an upright (frondose) phase to a crustose phase because of increasing temperatures (Guy-Haim *et al.* 2016).

Despite such projections, Lough and Barnes (2000) observed an increase in calcification and growth rates of 3.5% for every 1°C increase in temperature for the coral *Porites lutea* on the GBR. However, the positive relationship between calcification and coral growth will only persist if temperatures do not increase further (McNeil *et al.* 2004). Recent work by Anderson *et al.* (2017) on branching corals from the GBR demonstrated a decline in linear extension that was possibly attributable to temperatures above the limits for optimal coral growth. Annual growth patterns of corals are often not readily preserved in the skeleton (Roche *et al.* 2010). Therefore, temporal changes in growth rates may only be detectable by direct measurements of the corals at specific time intervals (Bak *et al.* 2009). Unsurprisingly, limited data and studies are available on changes in linear extension of both hard and soft coral species due to most studies focusing on buoyant weights and calcification rates as metrics (Anderson *et al.* 2014, 2017).

The most comparable measure of coral growth, which results in unbiased growth estimations across various growth forms, is the change in skeletal weight or average calcification (Pratchett *et al.* 2015). Skeletal weight, specifically, can be determined through buoyant weighing. The buoyant weighing technique was initially developed in the 1960s by Bak (1973) and is based on

Archimedes' principle (Bak 1973; Jokiel *et al.* 1978). The method entails weighing living coral fragments while suspending the fragment in a known density of seawater (determined from salinity and temperature measurements).

Optimal calcification of corals and live rock, which facilitates healthy growth rates, is essential for enabling corals to colonise reefs (Darling *et al.* 2012). Calcification processes further enable the outgrowing abilities of corals when having to compete for light, space and food (Allemand *et al.* 2011). Additionally, dense coral skeletons allow numerous corals to persist in areas where considerable wave-action occurs (Hughes 1987). Both the linear-extension and the buoyant-weight measuring techniques provide time-integrated measurements of coral growth.

### **1.7.2 Photosynthetic efficiency**

Corals form symbioses with photosynthetic dinoflagellate protists called zooxanthellae. The host coral is supplied with dissolved organic matter, microbial interactions and copious amounts of sugars, glycerol, lipids, amino acids and other organic compounds via the photosynthesising zooxanthellae within coral tissues (Stat *et al.* 2006; Blackall *et al.* 2015). Over the past three decades, numerous studies conducted globally have reported cases of disruption of this symbiosis resulting in mass bleaching events. These events render the corals on reefs white through the loss of symbionts or pigments within them, leading to a phenomenon known as coral bleaching. The loss of these symbiotic zooxanthellae, due to environmental stresses such as global warming, affect coral energy and carbon budgets and may even cause death if severe stress persists (Lesser 2011), unless the symbiosis is re-established from surviving zooxanthellae (Koren *et al.* 2008). The main reason for these bleaching events is elevated ocean temperatures which often act synergistically with high irradiance (Brown 1997; Jones & Hoegh-Guldberg 2001) and ultraviolet radiation (Iluz *et al.* 2008). The stress caused by above-average ocean temperatures results in a decrease in the maximum photochemical quantum yield (Kitajima & Butler 1975), which indicates a decline in the photosynthetic efficiency of the zooxanthellae (Jones *et al.* 1999). Photosynthetic efficiency is considered a key proxy for coral health (Lichtenberg *et al.* 2016).

Progress in photosynthetic research has been facilitated by the Pulse-Amplitude-Modulated (PAM) fluorometer, invented in the mid-1980s. Since then, photosynthetic efficiency has been determined in several marine angiosperms (Beer *et al.* 1998; Beer & Bjork 2000), marine macroalgal genera *Ulva* (Beer *et al.* 2000; Franklin & Badger 2001; Longstaff *et al.* 2002), *Porphyra* and *Zonaria* (Franklin & Badger 2001), as well as many hard corals including *Stylophora pistillata* and *Acropora aspera* (Jones *et al.* 1999; Winters *et al.* 2003), *A. millepora*, *A. nobilis*, *Cyphastrea serailia*, *Montipora tuberculosa*, *Pocillopora damicornis*, *Porites*

*cylindrica* (Ralph *et al.* 2002) and *Balanophyllia europaea* (Caroselli *et al.* 2015). Photosynthetic efficiency studies have also been done on soft corals such as *Sarcophyton* species (Hegazy *et al.* 2012; Al-Footy *et al.* 2015; Farag *et al.* 2017), *Sinularia flexibilis* (Rocha *et al.* 2013) and *Xenia elongata* (Studivan *et al.* 2015).

By using PAM fluorometry, the potential maximum quantum yield of photosystem II (PS II) is obtained by measuring a species' *in vivo* chlorophyll fluorescence induction, after it has been dark-adapted. PAM fluorometry has also made it possible to measure the effective quantum yield (Genty *et al.* 1989) of PS II ( $Y$ , or  $\Phi_{PS II}$ ) under ambient light (Schreiber *et al.* 1986; reviewed by Schreiber & Bilger 1993). Related studies have proposed that the negative effects of climate change may result in a reduction in a coral's photosynthetic ability (see Goffredo *et al.* 2008, 2009), which ultimately results in a decrease of energetic resources for all metabolic processes of the host (Caroselli *et al.* 2011).

Furthermore, recurring bleaching within a short period significantly reduces the abilities of corals to recover from successive bleaching episodes (Grottoli *et al.* 2014). During such heat-stress episodes, the rate at which the coral photosynthesises declines, with the decrease in available energy generated from the disrupted *Symbiodinium* cells (Hoegh-Guldberg 1999). Though photosynthetic rates of crustose coralline algae (CCA) on live rock increase as temperatures are elevated, prolonged ocean warming and persistent bleaching episodes could potentially reverse any such short-term benefits (Anthony *et al.* 2008). Sustained warming and bleaching exacerbate the negative effects on CCA, causing them to become necrotic and eventually die (Martone *et al.* 2010). Hence, photosynthetic pigments are lost when coralline algae turn white from bleaching, which results in a dramatic drop in photosynthetic rates (Diaz-Pulido *et al.* 2011; Cornwall *et al.* 2017).

When corals remain thermally stressed, they cannot photosynthesise efficiently, resulting in a significant reduction of coral metabolic activity rates (Hughes *et al.* 2010). As coral photosynthesis is compromised, a decrease in the available energy is experienced, causing a decline in growth and maintenance and the eventual death of the coral host (McClanahan 2004; Anthony *et al.* 2009). Consequently, future ocean temperatures can lead to a decline in photosynthetic efficiency, which would cause a decrease in coral health.

### 1.7.3 Net community calcification

There is a pressing need to investigate coral calcification in the context of global climate change (Kleypas *et al.* 1999; Hoegh-Guldberg *et al.* 2007; Cantin *et al.* 2010; Chan & Connolly 2013). Hoegh-Guldberg (1999) presented a model of future coral reef degradation based predominantly on modelled climate-change-related temperature projections and coral mortalities because of above-average temperature regimes, with further declines resulting from projected shifts in seawater  $\Omega_{\text{aragonite}}$  saturation state ( $\Omega$  being the degree of saturation). Calcification is the primary process for skeleton formation via precipitation of calcium carbonate ( $\text{CaCO}_3$ ) in the form of aragonite (Gattuso *et al.* 1999). The effects of global warming caused by increasing carbon dioxide ( $\text{CO}_2$ ) reduce  $\text{CO}_3^{2-}$  concentrations in the ocean, which further lowers the saturation state of carbonate (Sarmiento & Gruber 2006). Adequate carbonate concentration is imperative in the biogeochemical process that forms  $\text{CaCO}_3$ , which contributes to the calcifying of many marine organisms such as scleractinian corals. As the aragonite saturation state becomes less favourable to calcifying organisms, the recycling of  $\text{CaCO}_3$  and the survival of such organisms in the ocean declines (Shi *et al.* 2019).

Cold- and warm-water scleractinian corals accrete  $\text{CaCO}_3$  skeletons to create a three-dimensional reef framework that offers liveable habitats for fish populations and other species over time. High rates of calcification are required to overcome significant bioerosion rates and wave-driven physical erosion (Fisher *et al.* 2015). Biogenic accretion and dissolution processes entail maintaining an intricate balance to form such rigid coral reef frameworks (Cohen & Holcomb 2009). These two processes, which together are known as net calcification, regulate the growth of coral reef organisms and the entire reef ecosystem, which is further referred to as net community calcification (NCC). Accurate calcification measurements of coral reef components and communities are necessary to understand the role of the carbon cycle on reefs and to project and monitor the effects of global warming on these biogenic ecosystems.

Reef-community accretion processes become more energy-intensive as pH drops due to the chemical kinetics involved in calcification (Brown 1997; Pandolfi *et al.* 2011). Resultantly, NCC will decline as corals fail to calcify and build skeletons to form adequate reef structures (Langdon *et al.* 2000; Doney *et al.* 2009; Hoegh-Guldberg 2011). High-latitude reefs are more of a concern as a reduction in calcification processes is more likely in cooler waters (Guinotte *et al.* 2003). The decline occurs because accretion processes are proportional to seawater temperatures and increase from the poles towards the equator (Orr *et al.* 2005). However, anomalously warm temperatures have the potential to reduce net calcification rates in reef communities, especially during

bleaching events (Colombo-Pallota *et al.* 2010). Accordingly, reef processes and resilience are affected as a whole, which negatively influences coral communities.

To efficiently detect changes in calcification rates and ascribe them to global warming entails a proper understanding of the natural ranges and irregularities in calcification rates that are evident at present (Maier *et al.* 2013). Several methods are available to quantify rates of calcification such as the buoyant weight technique (Jokiel *et al.* 1978), incorporating radiolabelled carbon or calcium of the skeleton (Goreau 1959) and by quantifying changes in seawater constituents through total alkalinity measurements (Smith & Key 1975). The alkalinity depletion method (Kinsey 1978; Smith & Kinsey 1978), also known as the alkalinity anomaly technique (Chrisholm & Gattuso 1991), has been the primary means of measuring net calcification rates of corals and reef ecosystems using seawater samples (Holcomb *et al.* 2010; Maier *et al.* 2013). Not only has the technique been utilised widely in experiments, but the way total alkalinity is directly influenced by bicarbonate ( $HCO_3^-$ ) and carbonate ( $CO_3^{2-}$ ) ion concentrations allow for more accurate net calcification determinations (Wolf-Gladrow *et al.* 2007; Schoepf *et al.* 2017).

Experiments conducted under controlled conditions using global warming rates and exposing coral communities to constant temperatures as high as those expected by 2100 (IPCC 2014), suggest compromised calcification efficiency and a change in coral morphology (Goffredo *et al.* 2014; Fantazzini *et al.* 2015). The studies conducted by Cornwall *et al.* (2019) and Kornder *et al.* (2018) found that coralline algae on live rock were relatively robust to warmer seawater compared to coral species with an increase in calcification in response to increasing temperatures. Consequently, projected increases in ocean temperature and acidity (IPCC 2014) are likely to reduce calcification (Langdon & Atkinson 2005; Jokiel *et al.* 2008) and increase dissolution (Anthony *et al.* 2008; Andersson *et al.* 2009; Diaz-Pulido *et al.* 2011) of corals and crustose coralline algae; but more so under conditions of a worst-case scenario such as under RCP 8.5 (Gattuso *et al.* 2015).

## 1.8 Aims, objectives and hypotheses

As contextualised throughout this introductory chapter, the physiological responses of coral and live rock were investigated within the context of the marginal nature of the reefs found in the south-west Indian Ocean, to establish whether global warming will significantly affect their survival by the year 2100. The study evaluated how different temperatures that are directly relatable to local current conditions as well as those projected to occur in the future, according to the Representative Concentration Pathway (RCP) scenarios, may affect the physiological responses of corals and CCA associated with live rock using mesocosm experiments.

This study aimed to undertake a global-warming, climate-change experiment that would test the effects of thermal stress on a representative high-latitude coral community in terms of its hard and soft coral components, as well as the live rock.

Given this context, the objectives of this study were to:

- 1) Quantify any changes in the physiology (linear extension, buoyant weight and photosynthetic efficiency) of two hard and soft coral species (*Acropora appressa* and *Sinularia brassica*), and fragments of matured live rock from Sodwana Bay, subjected to three temperature scenarios: long-term historical-average (24.4°C), year-2100 average RCP 4.5 (26.9°C) and bleaching-threshold (28.8°C) temperatures.
- 2) Quantify net community calcification of a representative Sodwana Bay coral community (hard coral species, soft coral species and live rock) subjected to the three temperature scenarios given in Objective 1.

Physiological responses were quantified to determine how each organism may be affected by each temperature scenario as an individual component (Objective 1) and collectively as a representative reef community (Objective 2).

The following null hypothesis and alternative hypotheses were tested:

H<sub>0</sub>: The coral species (*A. appressa* and *S. brassica*, respectively) and live rock will physiologically respond positively to elevated temperature conditions exceeding the local historical-average sea temperature recorded at Sodwana Bay.

H<sub>1</sub>: Coral growth (dimension and buoyant weight) of both species will increase in historical-average sea temperatures recorded at Sodwana Bay, whereas growth will be negatively influenced in heat-stressed conditions.

H<sub>2</sub>: Both the coral species and live rock will remain photosynthetically efficient in the historical-average sea temperature recorded at Sodwana Bay, whereas photosynthetic efficiency will be adversely affected in heat-stressed conditions.

H<sub>3</sub>: Exposure of coral communities (*A. appressa*, *S. brassica* and live rock) to temperatures higher than the historical-average sea temperature recorded at Sodwana Bay will cause a decrease in net community calcification.

## CHAPTER 2 | METHODS

### 2.1 Collection site

Sodwana Bay is a popular recreational diving site located in the Maputaland region of the KwaZulu-Natal (KZN) political province of South Africa (Fig. 2.1). These reefs lie within the Delagoa Bioregion and are the southernmost coral reefs on the east African coast (Ramsay 1994; Porter *et al.* 2013) occurring in subtropical waters (Schleyer *et al.* 2018). Due to their high-latitude location, the reefs are non-accretive and exist as fossilised sandstone substrata (Ramsay 1994). Sodwana Bay is situated in the Maputaland Marine Reserve of the iSimangaliso Wetland Park World Heritage Site that was inscribed in 1999 (UNESCO 2000; McIntosh 2010), where conservation efforts are made to protect Sodwana Bay from negative anthropogenic influences that could result in its degradation. Biological material was collected from Two-mile Reef, Sodwana Bay located within the Central Reef Complex – one of three reef complexes within the Maputaland region (Fig. 2.1; Riegl *et al.* 1995; Schleyer & Porter 2018). Two-mile Reef experiences relatively high turbulence and is much steeper than many other reefs in the region (Schleyer & Celliers 2003a, b; Schleyer & Porter 2018; Schleyer *et al.* 2018), lying parallel to the shoreline at approximately 1 km offshore (Ramsay 1996). Two-mile Reef is a patch reef that ranges in depth from 6 to 27 m and comprises shallow pinnacles, extensive deep subtidal reef flats and a small fore reef edge (Riegl *et al.* 1995; Schleyer 2000; Celliers & Schleyer 2002).

Sodwana Bay reefs are located on a straight, exposed coastline that experiences prevailing north-easterly and south-to-south-westerly winds, resulting in substantial swells (Schumann 1988; Celliers & Schleyer 2008). The straight exposed coastline contributes to some oceanographic processes occurring in this area (Ramsay 1994). These processes include warm water pulses that travel southward, shelf-edge upwelling (on Sodwana Bay's extremely narrow shelf), inshore current reversal, as well as offshore migration of the Agulhas Current (Ramsay 1994; Celliers & Schleyer 2002; Morris 2009). Resultantly, high variability on an intra- and inter-annual timescale occurs in the region (Celliers & Schleyer 2002). Hence, a subtropical climate characterises the KZN coastline with significant influence from the strong, warm Agulhas Current (Lutjeharms 2004, 2006).

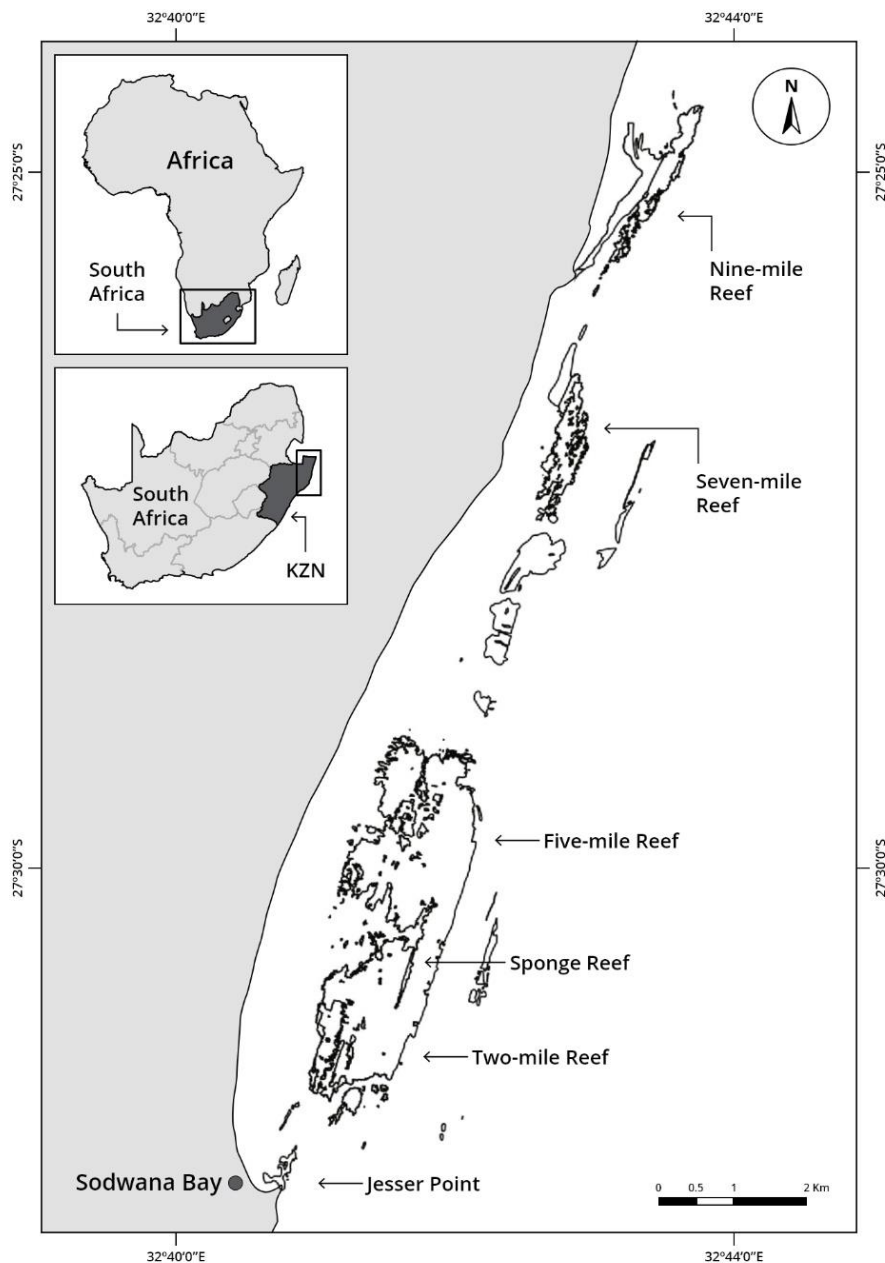


**Figure 2.1** Collection site on Two-mile Reef situated in Sodwana Bay, KwaZulu-Natal, South Africa where biological material was collected for mesocosm experiments.

The sea temperatures are critical for evaluating climate change and global warming impacts on ecosystems and biodiversity. Incidentally, the warm Agulhas Current causes seasonal variation in sea surface temperatures ranging between 22 and 28°C (Lutjeharms 2004). As the Agulhas Current plays a substantial role within the global thermohaline circulation, it is likely to cause significant global climate change and variability (Beal *et al.* 2011). Accordingly, the Agulhas Current has a considerable effect in shaping marine ecosystems due to how highly variable the system operates, including its ongoing formation of abundant mesoscale eddies and dipoles (de

Ruijter *et al.* 2013). The eddies function as distributors of plankton and pelagic fish and connect remote ecosystems (Roberts *et al.* 2010; Clayton *et al.* 2013). As the Agulhas Current is a typical western boundary current, it creates hot spots in the ocean that release heat into the atmosphere and, in return, take up carbon dioxide (Lutjeharms 2006).

In addition to the Agulhas Current system's influence, reefs on the Maputaland coastline are exposed to intermittent storms and occasional cyclonic activity (Kovacs *et al.* 1985; Reason & Keibel 2004) and cut-off lows (Rouault *et al.* 2002). Large swells frequently move the sand on the shallower and inshore western parts of the reefs, which function as key disturbances in regulating these communities (Porter *et al.* 2017a, b; Schleyer *et al.* 2018). Other key factors such as relatively lower temperature, light and aragonite saturation state further limit high-latitude coral growth and reef accretion (Kleypas *et al.* 1999). The reef communities support at least 399 fish species (Floros 2010), 93 scleractinian species and 39 alcyonacean species (Schleyer 2000; Celliers & Schleyer 2008). Soft coral cover of ~27% exceeds hard coral cover by approximately 5% (Celliers & Schleyer 2008). These reef communities comprise a mix of both tropical and subtropical species, establishing rich biodiversity at this high latitude on the East African coast (Schleyer & Celliers 2003a; Celliers & Schleyer 2008; Spalding *et al.* 2007).

Live material was collected on Two-mile Reef (27°31'3.6" S, 32°41'12.54" E) from reef communities in Sodwana Bay for experimentation (Fig. 2.1). As Two-mile Reef consists of sandstone dunes, it is ideal for hard and soft coral species. Hard corals tend to characterise the gully sub-communities, whereas soft corals proliferate on the reef-top sub-communities (Schleyer 1999). These coral communities colonise the beach rocks and aeolianite substrata due to glacial maximum sea-level rise (Ramsay 1994) and occur at depths of 8 - 35 m.

The collection site has largely been unaffected by major coral bleaching (Porter & Schleyer 2017) and disease (Schleyer *et al.* 2018). Additionally, Sodwana Bay does not experience any large river-flow inputs from the coast (Schleyer 2000), and the clarity of the horizontal water is seldom less than 15 m (Ramsay 1991). Resultantly, Two-mile Reef is considered mostly healthy (Schleyer & Porter 2018). Sodwana Bay is remote from any large cities or heavy industry. Still, over 6.7 million people live near or on the Maputaland coastline, mostly in rural communities which practice subsistence agriculture and rely on tourism for formal employment (Mograbi & Rogerson 2007). As many livelihoods depend on the region's biodiversity resources, it accentuates the importance of conservation and ecological research in this area.

## 2.2 Study species, their collection and preparation

The collected biological material from Two-mile Reef included three colonies each of the scleractinian *Acropora appressa* (Ehrenberg 1834) and alcyonacean *Simularia brassica* (May 1898). Additionally, similarly sized pieces of matured ‘live rock,’ i.e. coral rubble encrusted with crustose coralline algae (CCA), were also collected (Fig. 2.2). The collection of material for experimentation purposes was performed during the austral spring period in November 2018. The hard coral *A. appressa*, commonly known as staghorn coral, is found across the Indo-West Pacific Ocean’s tropical waters on upper reef slopes and flats (Veron 2000). The soft coral *S. brassica*, commonly known as cabbage leather-coral, also has a distribution across the Indo-West Pacific Ocean and can be found inhabiting relatively shallow areas with strong currents (Fabricius & McCorry 2006). *Simularia brassica* was the most commonly found species within this Central Reef Complex (Schleyer & Celliers 2003a, b). However, soft coral cover has shown a decrease at 0.95% per annum on Nine-mile Reef, which further accentuated the importance of studying a soft coral species (Porter & Schleyer 2017). *Simularia brassica*, *A. appressa* and live rock were selected to represent the three main components comprising coral reefs in the region – namely soft coral, hard coral and the reef substratum, respectively (Fig. 2.2; Schleyer & Porter 2018; Porter & Schleyer 2019).

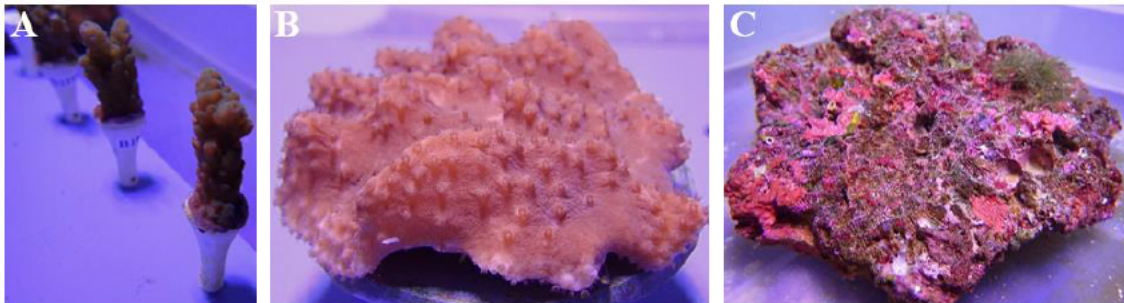


**Figure 2.2** The study species *Acropora appressa* (A), *Simularia brassica* (B) and live rock (C), collected from Two-mile Reef, Sodwana Bay, South Africa and used in mesocosm experiments.

The organisms were collected with SCUBA by scientific commercial divers operating under the South Africa Department of Labour Codes of Practice Inshore Diving with a research permit, granted to the Oceanographic Research Institute by the Department of Forestry, Fisheries and the Environment. As the work was conducted within the iSimangaliso Wetland Park World Heritage Site, prior approval was obtained from the Park Authority and Ezemvelo KZN Wildlife.

Haphazardly selected colonies of *A. appressa* were carefully removed with a hammer and chisel, while colonies of *S. brassica* were removed with a paint scraper. Additional precautions were taken to remove colonies of *S. brassica*, which included removing each colony with adherent reef matrixes to prevent damage to the basal coenenchyme. After collection, each colony was packed separately in a transparent plastic bag filled with seawater and oxygen and sealed with an elastic band. Live rock was harvested by hand at a similar location on Two-mile reef. After collection, the live rock specimens were kept in a cooler box filled with seawater and oxygen for transport.

All biological material was transported back to the laboratory at the Oceanographic Research Institute, Durban in several cooler boxes within 5 hours of collection. Upon arrival, the bags were floated in the holding tanks to prevent thermal shock until the water temperature reached a suitable maintenance temperature of 24.4°C. A temperature of 24.4°C was chosen as it corresponded to the long-term historical-average seawater temperature measured at Sodwana Bay (Porter & Schleyer 2017). As the live rock specimens were not in bags, the 24.4°C seawater from the holding tank was slowly introduced into the cooler box until both the holding tank and the cooler box's temperatures were the same. The live rock specimens were then spread out in the holding tank for several weeks prior to experimentation. The corals were acclimatised to ambient light and water conditions for four weeks to ensure that all colonies appeared visibly healthy before experimentation.

Subsequently, the *A. appressa* colonies were carefully broken up into smaller, manageable pieces with a hammer and chisel, keeping part of the colony's base intact. Individual fragments were then snapped off from the base and were cut to ~30 mm lengths using side-cutters. Studies have shown that *Acropora* species fragments cut to lengths of 30 to 50 mm are optimal for recovery and growth (Lirman *et al.* 2010; Shafir & Rinkevich 2013). Each fragment was then buoyantly weighed before being mounted on a plastic mount with two-part epoxy putty (Pratley Putty® Original – Standard Setting) (see section 2.6.1 for details on the buoyant weighing technique). Hard coral mounts were made from polypropylene golf tees that were cut to a length of 23 mm and made to fit securely into drilled incisions in a sheet of polyvinyl chloride (PVC). Additionally, the golf tees were negatively buoyant, inert and had a smooth surface that restricted excessive algal growth. Previous studies have proved similar mounting techniques to be successful for various hard coral species (see Borneman & Lowrie 2001; Osinga *et al.* 2012; Shafir & Rinkevich 2013). Mounted coral fragments were then left to set and recover for two weeks at 24.4°C.

The *S. brassica* colonies were sectioned using a sharpened, circular cookie cutter with a 50-mm diameter. The sectioned sizes were chosen with due consideration for the size of the original individual colonies collected. They corresponded with a study done by Shafir and Rinkevich

(2013) that sectioned soft coral to similar dimensions of 40 to 60 mm. A circular shape was chosen as it provided the minimal perimeter to surface area ratio relative to other shapes, which allowed for a smaller recovery area. Each of the soft coral sections were then mounted on a customised disc and pinned to it with a hypodermic needle after each component was buoyantly weighed. The 55 mm diameter discs were cut from PVC sheets with a thickness of 4 mm. The discs' edges were smoothed with a wood lathe and abraded on the surface with 50-grit sanding paper to facilitate the natural attachment of soft coral sections to the mounts. A 10 mm diameter countersunk hole was drilled, with a speed-drill press, into the middle of the PVC disc. Each disc was then glued at the bottom center to a golf tee's top-edge with non-toxic cyanoacrylate glue. The countersunk hole was filled with Bostik® marine silicone sealant, which allowed each section of soft coral to be pinned to the mount with a sterile hypodermic needle (21 gauge) before the soft coral could naturally grow and adhere to the mount. The mounting technique minimised stress to the coral and allowed for complete recovery without tissue necrosis. After each soft coral section had been pinned, they were left to recover and attach to the mount in a holding tank for four weeks. Once each section had naturally attached to the mount, the needle was removed.

### **2.3 Experimental design**

Experiments were conducted at the research aquarium of the Oceanographic Research Institute, Durban, South Africa (Fig. 2.3.1). A continuous 24-h flow-through seawater experimental system was constructed. The system consisted of one 5 000 L reservoir JoJo (Pty) Ltd. tank connected to three 300 L header JoJo tanks, each of which was connected to three 68 L (each) transparent polypropylene tanks that represented triplicate mesocosms functioning as a pseudo-replicated system (Fig. 2.3.1). The raw seawater inflow was obtained directly from the ocean at the Durban beach wellpoints. The water was pumped into the 5000 L reservoir tank, which fed each of the three 300 L header tanks. The seawater was filtered through three differently-graded sediment-filter cartridges (in the order 10, 5 and 0.2 microns), positioned in canisters, and a heat exchanger set to ~24°C before each of the three header tanks received it. Each header tank also had a canister containing a 0.2-micron sediment filter cartridge, which removed any other abiotic and biotic material that might have built up in the pipes or on the header tanks' walls. The water from each of the three header tanks flowed via gravity into triplicate mesocosms via Astore Keymak® rotameter variable area flow meters set at 12 L min<sup>-1</sup>. Triplicate mesocosms were immersed in their respective white polypropylene 2000 L water baths to minimise temperature variations (Figs. 2.3.1, 2.3.2).

A GHL<sup>®</sup> ProfiLux III Aquarium Controller was installed above the three header tanks and connected to six pre-calibrated probes: a temperature probe (GHL<sup>®</sup> temperature sensor) and a dual pH-conductivity probe (GHL<sup>®</sup> pH electrode) in each of the three header tanks. Furthermore, a temperature- and dual pH-conductivity probe was also placed in each of the 2000 L water baths accommodating the mesocosms, connected via a GHL<sup>®</sup> ProfiLux Aquatic Bus (PAB). The PAB was supported by the primary GHL<sup>®</sup> ProfiLux III Aquarium Controller, which was installed in series. Additionally, a short message service (SMS) module III with a sim card was connected to the PAB to provide potential alert notifications if temperatures deviated outside ( $\pm 0.5^{\circ}\text{C}$ ) of their set ranges. The SMS module also functioned as a reporter for the system, which sent a daily summary of the average temperature and pH/conductivity for each header tank and water bath. The ProfiLux<sup>®</sup> system (i.e. controller, PAB, SMS-module) was assigned an internet protocol (IP) address and connected to a computer that provided access to real-time data. For data to be downloaded and probes to be programmed, GHL<sup>®</sup> Control Center software for a Windows 10 operating system was installed and connected via a local area network to the controller.

In addition to the temperature and dual pH-conductivity probes, each header tank included the following: a ball valve connected to the inlet pipe that was set to stop and start the seawater flow according to the set water level; an overflow in case the ball valve failed or excess seawater was pumped into the tank; a 1 kW submersible titanium electric heater with a linked PT100 temperature probe (Omega<sup>®</sup> immersion titanium heater, Chuan Kuan Enterprise Co., Ltd., Taiwan); an aerator pump; and a bottom circulation pump that mixed the water evenly and kept the water from becoming stagnant (Fig. 2.3.1). The PT100 probes were connected to intelligent proportional integral derivative (PID) temperature controllers that consisted of a double digital display with multisensory functions. These controllers were kept in a self-designed Ingress Protection Code 67-rated panel above the header tanks (Fig. 2.3.2), manually controlled and adjusted for each temperature treatment (see section 2.4). The titanium electric heaters were utilised to warm and maintain the different treatments at their set temperatures. The PIDs controlled the titanium heaters' operation to heat and maintain the seawater temperature up to an accuracy of  $0.1^{\circ}\text{C}$  with a 0.5-second sampling cycle. The hysteresis was set at  $0.2^{\circ}\text{C}$  of the setpoint temperature.

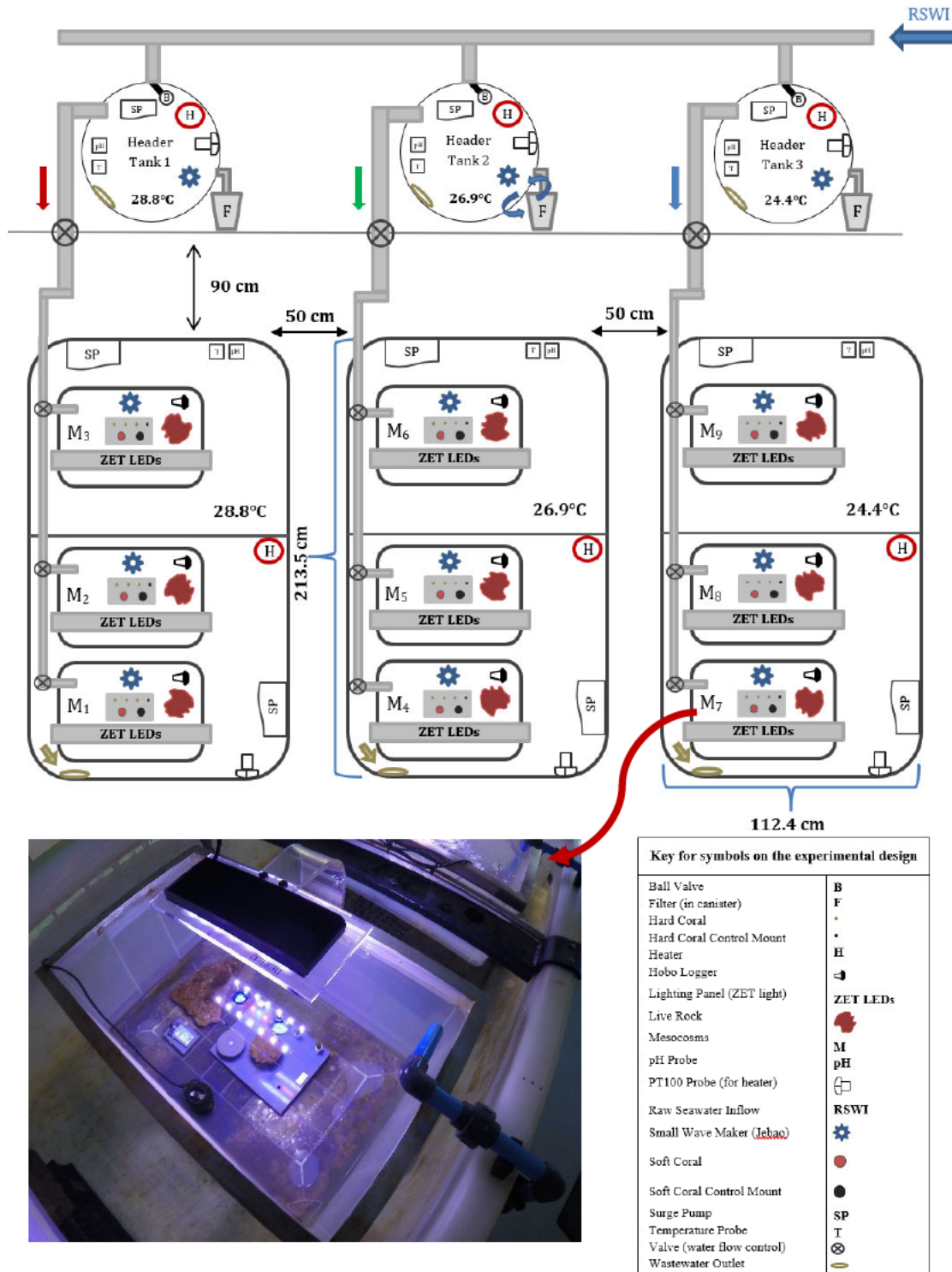


**Figure 2.3.1** A schematic representation of the experimental setup. The top part of the figure shows the incoming seawater and the three header tanks for each treatment. Water flows from each header tank that is pseudo-replicated into triplicate mesocosms (M<sub>1</sub> to M<sub>9</sub>) located in their respective water baths. A photograph of a typical mesocosm is provided at the bottom-left corner of the figure.

Furthermore, the water baths each contained a 3 kW submersible titanium electric heater (Omega<sup>®</sup> immersion titanium heater, Chuan Kuan Enterprise Co., Ltd., Taiwan) linked to a PT100 probe and PID temperature controller that assisted in maintaining the set temperatures in the water baths and mesocosm; two circulation pumps on opposite sides of the bath to assist in optimal water flow and the distribution of warmer and colder water and an overflow outlet with a plastic mesh basket that prevented any potential foreign objects from blocking the outflow and causing the water baths to overflow (Fig. 2.3.2). As the experiment was conducted during summer, a portable chiller (Hailea aquarium chiller HC-1000A, pumping at a flow rate of 4 000 L/h) was installed to chill and maintain the water temperature within water baths when necessary. The temperature control in each header tank and water bath effectively maintained the water temperature within pseudo-replicated triplicate mesocosms. The water in the baths was never in contact with the water in the mesocosms as the water overflowed from triplicate mesocosms into their respective bath.



**Figure 2.3.2** The research aquarium at the Oceanographic Research Institute showing the experimental system built to test the effects of global warming on coral communities, including header tanks, water baths, mesocosms and various electronic peripheral equipment.

Each mesocosm was illuminated with a Zetlight<sup>®</sup> Aqua Series LED light (Series: ZA 1201-L) set on a 12:12-h light:dark cycle, simulating different phases of the day (ramped up over 6 hours). The lights were programmed to turn on and start the 12-h light cycle at 05:00 with a dawn setting for two hours, then ramped up in intensity to simulate sunrise for two hours followed by daytime for four hours. The lights then reduced in intensity to simulate sunset for two hours before they

were further decreased in intensity for another two hours to simulate dusk. The lights, therefore, switched off at 17:00 and started a 12-h dark cycle. Hence, a whole day was simulated as closely as possible to the typical diurnal and nocturnal light regimes experienced by coral reef environments. The LED lights ranged in wavelengths between 400 and 700 nm (actinic) and emitted a maximum colour temperature of 12 000 K for the white-light spectrum (daylight only).

A Jebao® OW-10 Series wavemaker (submersible pump) was placed within each mesocosm and set as closely as possible to replicate water movement experienced on a typical coral reef at Sodwana Bay. The settings included mode “W1 – wave mode”, which allowed for regular pulsing at a 90% wave pattern and full intensity pulse speed. These settings provided pulses of water that simulated natural surge as closely as possible. There was one master controller that controlled the other eight wavemakers via a slave system to achieve identical surge conditions in each mesocosm. During measurements and feeding of the specimens, “feed mode” was activated, which paused the pumps for 10 minutes. The last electronic component within each mesocosm included a submersible HOBO Pendant® temperature/light 8K data logger that logged the water temperature and light intensity at 30-minute intervals. A HOBO® Optic USB Base Station with a Pendant Coupler™ was used to set up the HOBO Pendant® loggers and to download the logged data in the HOBOWare® version 3.7.17 created by Onset Computer Corporation. The temperature loggers had an accuracy of 0.53°C, a precision of 0.14°C and drift of <0.1°C year<sup>-1</sup>. The loggers’ hysteresis was set at 0.05°C, which allowed for accurate seawater temperature recordings between 0.05 and 0.1°C.

The non-electronic components and live material within each mesocosm comprised the following: a 190 x 150 mm custom coral stand consisting of PVC material with a 15 mm thickness to hold three hard coral fragments on their respective mounts; a hard coral control mount; one soft coral section on its respective mount; a soft coral control mount; and a piece of live rock. The PVC coral stand was chosen and designed to provide a solid foundation for the coral mounts due to its weight and restrict excessive algae growth and facilitate ease of maintenance and coral material measurement.

As there were three hard coral colonies of *A. appressa* purposely collected in total, mounted fragments from each colony were randomly assigned per treatment so that each treatment comprised the same three colonies. Therefore, each mesocosm within a treatment had material from one of the three different colonies (i.e. pseudo-replicated), but the same three colonies were split among the three treatments (Figs. 2.3.1, 2.3.3). Such a distribution meant that the colonies effectively functioned as clones across the three treatments and is analogous to using genetically

identical triplets as is employed in human medical studies. As there were three genetically distinct colonies per treatment, potential population-level effects can also be investigated. Clones allow for improved testing of a treatment effect by minimising genetic variation (Rosenberg & VanLiere 2009), the possible detection of cloned-fragment effects (Cunning *et al.* 2018), and future replicate genetic-association studies of the same genotypes (Davies & Gray 2015; Cunning *et al.* 2018). To ensure that there was enough biological material for calcification experiments and that the relative amount of hard coral to soft coral approximated that on local Maputaland Reefs, three fragments were included from a single colony of *A. appressa* in each mesocosm, effectively acting as technical replicates. Therefore, nine fragments from each of the three *A. appressa* colonies were split across the three temperature treatments.

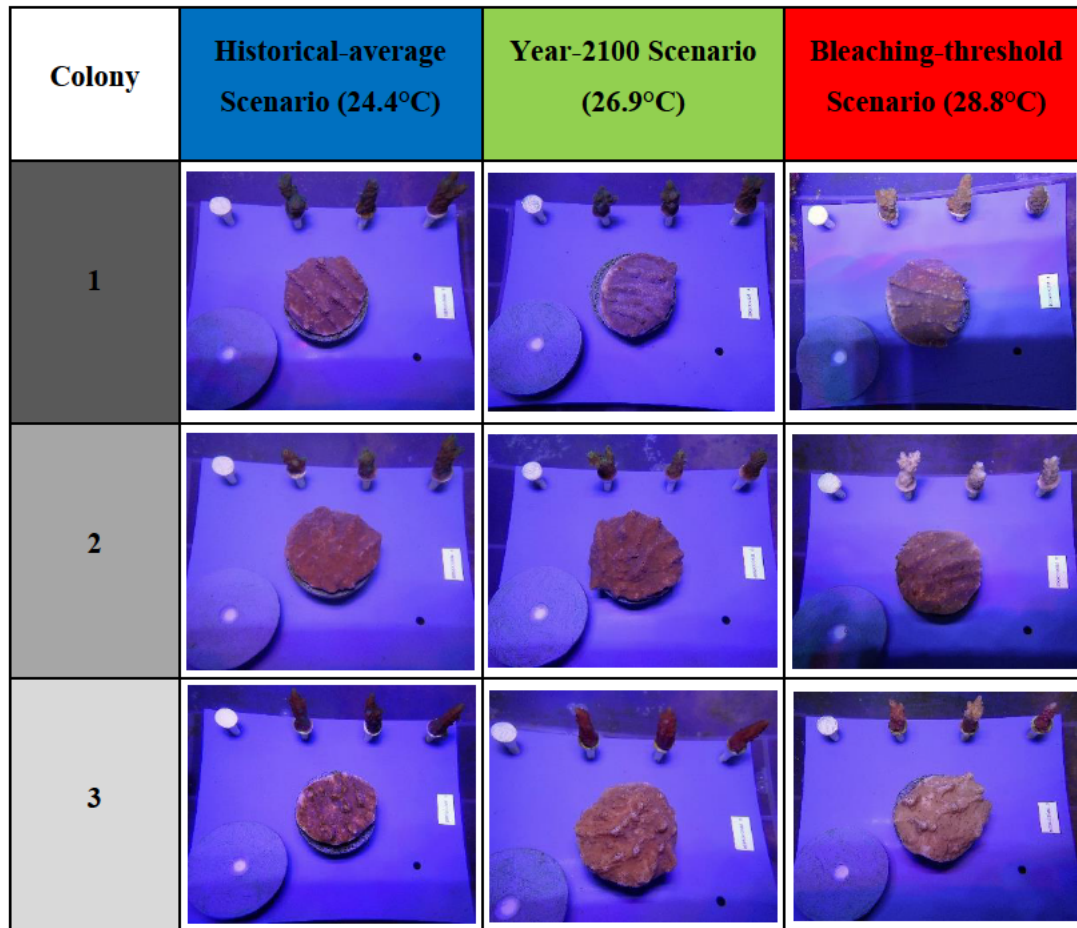


**Figure 2.3.3** Photographs of the representative coral communities in the different temperature treatments. Each of the three colonies of both *Acropora appressa* and *Sinularia brassica* were split and randomly assigned per treatment (historical-average (24.4°C), RCP 4.5 year-2100 (26.9°C) and bleaching-threshold (28.8°C) scenarios). Each photograph, taken during week 8 of the experiment, represented a mesocosm that was pseudo-replicated per treatment with the respective hard coral control mount (top-left corner) and soft coral control mount (bottom-left corner).

The same method used above was also used for allocating mounted sections of *S. brassica* from the three colonies collected, except that the sections of *S. brassica* were large enough for each mesocosm and the following experiments to avoid the need for technical replicates (Fig. 2.3.1). There were three mounted sections per *S. brassica* colony, with one section assigned to each mesocosm. Every treatment consisted of three colonies that were split among the triplicate mesocosms to effectively function as a pseudo-replicated system. Altogether, each treatment therefore comprised three distinct colonies of *A. appressa* and three distinct colonies of *S. brassica*, with three fragments of one colony of *A. appressa* and a section of one colony of *S. brassica* in each mesocosm (Fig. 2.3.3), as well as one piece of live rock. All nine live rock pieces were of similar size and volume ( $363.33 \pm 67.92$  ml) as determined through the water displacement method and were randomly assigned to each mesocosm. All living components effectively constituted a basic coral community and were moved to their selected mesocosms to acclimatise for a further four weeks (at the control temperature of  $24.4^{\circ}\text{C}$ ) prior to ramping of temperatures. These coral communities collected from Two-mile Reef were then cultured at three different seawater temperatures (see section 2.4) for 10 weeks from the end of January 2019 until mid-April 2019. Besides the biological material, each replicate mesocosm contained a hard coral control mount and a soft coral control mount. The control mounts functioned as standards within the replicate mesocosms. Accordingly, control mounts were weighed and used to account for any potential biofouling on all mounts.

In terms of testing the effects of temperature on coral communities, temperatures were kept constant in the control treatment and slowly raised in the RCP 4.5 and bleaching-threshold treatments over a period of four weeks until their setpoint temperatures were reached during the initial phase of the experiment (see section 2.4 on water temperature selection). Once temperatures in each treatment had reached their setpoints, they were held constant for another four weeks (hereon referred to as the middle phase). Lastly, the experiment terminated with a final increase of temperatures in the warmest treatment over two weeks (hereon referred to as the final phase), while temperatures in the other two treatments were held constant (Fig. 2.3.3). Thus, the experiment lasted for 10 weeks.

## **2.4 Water temperature selection**

Temperature selections were based on long-term temperature records from Sodwana Bay (Celliers & Schleyer 2002; Porter & Schleyer 2007) and projected scenarios based on the Representative Concentration Pathways (RCPs) adopted by the Intergovernmental Panel on Climate Change (IPCC; Moss *et al.* 2010). The most recent historical-average temperature in Sodwana Bay has

been determined by Porter and Schleyer (2017) over 25 years. This temperature was employed as the control scenario for the experiment and set at 24.4°C. A future scenario for the year-2100 was determined from the Coupled Model Intercomparison Project Phase 5 Representative Concentration Pathway projections of sea surface temperature for the region covering Sodwana Bay (Taylor *et al.* 2012). The monthly data were downloaded from the National Center for Atmospheric Research Climate Data Gateway and extracted from network Common Data Form (NetCDF) files containing a multi-model ensemble (MME) of projected future sea surface temperatures. The MME monthly temperature for 2006 to 2100 for emissions scenarios RCP 2.6, 4.5, 6.0 and 8.5 (Amman *et al.* 2018; IPCC 2018) were extracted from the NetCDF files by importing the files into QGIS version 2.18.23 as raster layers. Subsequently, the average annual SSTs for each RCP scenario encompassing the Sodwana Bay area were computed for the year 2100.

After inspection of the data, we found that the average annual temperature (26.9°C) for the RCP 4.5 scenario projected for the year 2100 most closely corresponded to the mid-point temperature (26.6°C) between Sodwana Bay's long-term historical-average (24.4°C) and the local bleaching-threshold (28.8°C) temperature (Celliers & Schleyer 2002). Furthermore, as per the literature, RCP 4.5 is the most likely future scenario based on climate projection models (Collins *et al.* 2013; Gattuso *et al.* 2014). Hence, the year-2100 global warming scenario (hereafter referred to as RCP 4.5) for Sodwana Bay employed in the experiment was set at a temperature of 26.9°C. The third temperature treatment used in this study, referred to as the bleaching-threshold scenario, was selected to represent a bleaching scenario on the local high-latitude reefs of Sodwana Bay. The bleaching-threshold temperature for Sodwana Bay has been previously determined at 28.8°C (Celliers & Schleyer 2002), which also closely approximates the monthly-maximum temperatures projected by the RCP 4.5, 6.0 and 8.5 scenarios by the year 2100.

Additionally, the bleaching-threshold temperature also approximates the average annual RCP 8.5 SST for the year 2100 at 28.6°C in Sodwana Bay. A further increase of 1°C in the bleaching-threshold scenario during the last two weeks of the experiment was done to simulate an extreme warming scenario for Sodwana Bay reefs, which corresponded with the warmest months projected by the RCP 8.5 scenario in 2100. Consequently, the average daily rates of temperature increase during the initial phase of the experiment (when temperatures were ramped to reach their respective treatment setpoints) were 0.00°C d<sup>-1</sup> in the control, 0.09°C d<sup>-1</sup> in the RCP 4.5 treatment, and 0.16°C d<sup>-1</sup> in the bleaching-threshold treatment (see Fig. 3.1; Table 3.1).

## **2.5 Coral feeding and general maintenance**

During experiments, corals were fed with pre-weighed (~0.04 g) cooked egg yolk, stored at -20°C. The egg was defrosted at room temperature one hour before feeding the corals. Feeding was conducted twice weekly in the morning. During feeding, the water supply from the header tanks to the mesocosms was switched off for 90 minutes to ensure that the egg was not removed with the overflowing water and to allow for enough feeding time. The egg was homogenised with 15 ml of mesocosm water before it was poured into each mesocosm.

As with any such system, a regular-maintenance schedule was required. In order to prevent the build-up of sludge in the main 5000 L reservoir tank, a 1-minute bottom flush was performed weekly. The three-graded filter system was also washed and replaced with clean sediment filters weekly. The same maintenance approach was undertaken with the filters inside the header tanks. The Astore Keymak<sup>®</sup> rotameter variable area flow meters, controlling the water supply to each mesocosm received from the header tanks, were also dismantled weekly and cleaned thoroughly. The variable area flow meters were then put on their maximum flow rate while the rest of the equipment was cleaned inside each of the mesocosms.

All the coral mounts were also cleaned weekly with a toothbrush prior to experimental measurements being undertaken to ensure their accuracy. The flow rate into the mesocosms was set back to 12 L/h after flushing the cleaned mesocosms for another 20 minutes. Additionally, the LEDs were wiped twice weekly to remove any salt build-up that may have affected the corals' physiological responses and confounded results. Further maintenance was completed in the water baths by checking and cleaning the circulation pumps, cleaning the inside walls, wiping all the probes and checking the waste outlets. General maintenance checks were performed during the day, which included making sure the system was operating efficiently.

## **2.6 Data collection**

The collecting of data was done weekly throughout the three experimental phases (initial, middle and final). Throughout these phases, the physiological parameters of growth (size and buoyant weight) and photosynthetic efficiency were measured at weekly intervals, and net community calcification (NCC) was measured at 6-hour intervals within a 24-hour diel period in the last week of the initial phase (week 4, diel period 1), in week 6 (diel period 2) during the middle phase and again at the end of the middle phase (week 8, diel period 3).

### 2.6.1 Growth

Coral growth was assessed using the linear extension and buoyant weight measurements. For linear extension measurements, repeated measures are required from a fixed reference point on branching hard corals to their branch tips and cross-section measurements for plated soft corals (Hughes & Jackson 1985; Roche *et al.* 2010). Throughout this study, the *A. appressa* fragments were measured with a plastic Vernier calliper from the fragment's base to the tip of the fragment. For *S. brassica* sections, their diameter cross-section measurements were measured with Vernier callipers as they were disc-shaped. With the help of two permanent marks on the mount, the same long mid-section and short mid-section were measured weekly for consistency.

For the buoyant weight determinations, both *A. appressa* and *S. brassica*, as well as their respective control mounts, were weighed at weekly intervals until the experiment was terminated. This technique is based on Archimedes' principle (Bak 1973; Jokiel *et al.* 1978). The buoyant weight technique was ideal as it reduced the amount of handling and stress of the corals compared to a standard weighing technique. It further reduced the amount of air exposure the corals experienced and allowed for the displacement of the water around corals, providing only the weight of the skeletal density (hard corals) or mainly the calcite sclerites (soft corals) (Davies 1989; Kleypas & Langdon 2006; Jokiel *et al.* 2008). Archimedes' principle can be expressed as:

$$W_a = W_w + (V_a \cdot D_w) \quad (2.6.1),$$

where “ $W_a$ ” is the total dry weight of skeletal material, i.e. mainly aragonite in hard corals and calcite sclerites in soft corals; “ $W_w$ ” is the measured buoyant weight of the specimen; “ $V_a$ ” is the volume of skeletal material in the specimen; and “ $D_w$ ” is the density of the buoyant fluid (seawater in this instance) used in the weighing process. Assumptions, according to Jokiel *et al.* (1978), that have to be met for this technique are: (1) the coral skeleton should be comprised entirely of aragonite (hard coral) or tissue containing calcite sclerites (soft coral); (2) live coral tissue have similar densities to the seawater; (3) any cryptic coral-associated fauna should primarily contain neutrally buoyant tissue and therefore not affect the buoyant weight; and (4) holes and spaces within the porous skeleton should be filled with a medium of equal density compared to that of the buoyant weight medium (Jokiel *et al.* 1978). The measurement of corals in the air to determine their weights has obvious and significant limitations, such as corals being subjected to prolonged aerial exposure and the fact that an unknown amount of water covering the coral is also measured. Hence, after further refinement of the buoyant weighing technique, regular use has been made of this measuring technique for experiments based on the growth of both small coral fragments and large colonies *in situ* (Herler & Dirnwöber 2011) and *ex situ* (Kuffner *et al.* 2017).

An electronic Sartorius® 1712 analytical/semi-micro balance, accurate to 0.00001 g, was used to quantify the individual corals' buoyant weights and their controls at weekly intervals. The mounts were thoroughly and carefully scrubbed with a toothbrush to remove any biofouling prior to weighing. The weighing station comprised an enclosed marine plywood box with a centered hole at the top, through which a 150 mm piece of 2 kg breaking strain monofilament and hook was suspended. The balance was positioned on the top of the box, calibrated by ensuring that the levelling eye was centred after attaching a section of fishing line and hook to the balance's bottom-weighing hook. The enclosed space in which the fishing line and hook were suspended served to eliminate air influences while weighing. A known volume and density of seawater, calculated from the seawater conductivity and temperature using a Eutech Instruments® Pte. Ltd. Cyberscan Series 600 probe, was collected in a 2 L borosilicate beaker and placed inside the box.

A pilot study using marbles with pre-determined weights were used as standards and marbles were weighed in the water of each temperature treatment before weighing any of the mounts, i.e. three differently sized marbles weighed individually per treatment throughout the experiment. The marble standards thus functioned in indicating the effects of different temperature treatments on the measured buoyant weights. The coral and the control mounts were then individually weighed in each treatment by suspending the mount beneath the scale and lowering it into the beaker of water until the sample was completely immersed. The seawater in the borosilicate beaker was collected from each treatment where the sample was from. Resultantly, the corals were not thermally stressed during measuring. The results of the marble buoyant weights measured across the different temperature treatments were used to support the fact that a correction factor for different densities of seawater due to temperature was not needed prior to analysing the buoyant weight data derived across the different temperature treatments.

### **2.6.2 Photosynthetic efficiency**

The photosynthetic efficiency was determined for *A. appressa*, *S. brassica* and live rock, which related directly to their mode of energy acquisition and energetics. A Junior Pulse-Amplitude-Modulated chlorophyll fluorometer (JR-PAM; Heinz Walz GmbH®, Effeltrich, Germany) was utilised to measure the photosynthetic efficiency of the corals and live rock. The JR-PAM was equipped with a 1.5 mm diameter fibre-optic cable, 100 cm in length, to allow for underwater measurements, powered by a laptop running a Windows 10 operating system with the installed PAM WinControl-3 Software®. As a measure of how photosynthetically efficient the coral communities were within their respective treatments was required, both daytime and dark-acclimated (i.e. night-time) measurements were necessary. Calibration of the JR-PAM was done

prior to recordings by testing the fibre-optic cable's signal in both air and water. A similar test was also performed on a piece of hard coral to determine the appropriate measuring distance. Consequently, all measurements were taken by direct contact of the fibre-optic tip to the coenosarc (i.e. living coral tissue) of the coral. Before measurements were taken, each coral was disturbed with the fibre-optic tip to allow any polyps to retract and thus, minimise variations in photosynthetic activities between the two different parts (polyps and coenosarc) of the corals' external anatomy (Ralph *et al.* 2002).

For the daytime measurements, rapid light curves (RLCs) were produced to determine maximum and relative electron transport rates (rETRs). Whereas dark-adapted induction curves during the dark-acclimated measurements were generated to obtain the maximum quantum yield ( $F_v/F_m$ ). Accordingly, the maximum potential- and effective quantum yield ( $Y(II)$ ) of photosystem two (PS II) was calculated as:

$$Y(II) = \frac{F'_M - F'}{F'_M} \quad (2.6.2),$$

where “ $F'_M$ ” is the maximum fluorescence levels during the application of saturating light pulses (SLPs), which temporarily closes all PS II reaction centres; and “ $F'$ ” is the level of the fluorescence curve during application of SLPs and shortly before a SLP is applied (Klughhammer & Schreiber 2008). The PS II can then be multiplied by the photosynthetically active radiation (PAR, in  $\mu\text{mol quanta m}^{-2} \text{s}^{-1}$ ) absorbed by the pigments associated with  $Y(II)$ , where  $\Phi_{PS II}$  is the effective quantum yield of PS II photochemistry, to obtain relative electron transport rates (rETRs, in  $\mu\text{mol electrons m}^{-2} \text{s}^{-1}$ ; Genty *et al.* 1989). An estimate of the relative PS II-derived photosynthetic ETR was calculated as (Ralph & Gademann 2005):

$$rETR = \Phi_{PS II} \times PAR \quad (2.6.3).$$

The following settings were applied to obtain the RLCs and rETRs: the blue (450 nm) LED measuring light (i.e. fluorometer's excitation radiation) was set on intensity level 8; the SLP on level 8 for 0.8 s; the gain on one at 680 nm excited light intensity; and the ETR at 20 s intervals. The blue LED functioned as the measuring light (evenly pulsed measuring beam), the actinic light (continuous radiation), and produced the SLP (photochemical quenching). For the RLCs, the actinic light remained switched on for all the daylight measurements, except during the  $F_0'$ -mode when the far-red (745 nm) LED switched on to measure  $F_0'$  (minimum fluorescence yield). Thus, light curves were obtained by repeating the SLPs on six random spots on each coral and live rock replicate. The daylight measurements were conducted weekly, from 09:00 until 12:00, and provided data for the rETR.

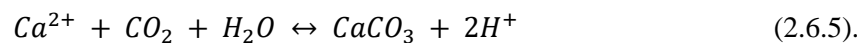
For the dark-acclimated measurements, the coral communities were dark-adapted for at least an hour prior to measurements. Induction curves were obtained by keeping the actinic light switched off and measuring  $F_0$  (basic fluorescence yield). The measuring light switched on only during the SLPs when three  $F_M$ -values (maximum chlorophyll fluorescence yield) were attained on three random spots on each of the coral and live rock replicates. The dark-acclimated measurements were also conducted weekly from 19:00 until 22:00, allowing the coral communities enough time to acclimatise to the dark. These dark-acclimated measurements provided data for  $F_v/F_M$  of PS II. Similar studies have applied comparable methods to determine coral photosynthetic efficiency in different *ex-situ* experiments (Rodolfo-Metalpa *et al.* 2010; Roth *et al.* 2012; Zartler 2012; Schoepf *et al.* 2015).

### 2.6.3 Net community calcification

The alkalinity anomaly technique (AAT; Smith & Key 1975; Chisholm & Gattuso 1991) was used to determine net coral community calcification (NCC) for each of the three different temperature treatments. Numerous mesocosm studies have applied the AAT successfully (see Rodolfo-Metalpa *et al.* 2010; Dove *et al.* 2013; Comeau *et al.* 2015; Courtney *et al.* 2017). The AAT was used to quantify how the coral community responded as a whole (i.e. net community calcification) to the different temperature treatments, as opposed to individual component responses as assessed by the growth and photosynthetic efficiency measurements. As per Dickson (1981), total alkalinity (TA) can be defined as the “total buffering capacity of seawater or the excess of proton acceptors over proton donors” as follows:

$$\begin{aligned} \text{TA} = & [\text{HCO}_3^-] + 2[\text{CO}_3^{2-}] + [\text{B}(\text{OH})_4^-] + [\text{OH}^-] + [\text{HPO}_4^{2-}] + \\ & 2[\text{PO}_4^{3-}] + [\text{SiO}(\text{OH})_3^-] + [\text{NH}_3] + [\text{HS}^-] - [\text{HSO}_4^-] - [\text{H}^+]_{\text{F}} \\ & - [\text{HF}] - [\text{H}_3\text{PO}_4] + [\text{minor acids} - \text{minor bases}] \end{aligned} \quad (2.6.4).$$

Total alkalinity is influenced mainly by bicarbonate and carbonate ion concentrations together with many other minor compounds (Eq. 2.6.4). When coral reefs release protons due to calcification, the TA is lowered (Smith & Key 1975). This reaction is described as follows:



Equation 2.6.5 indicates that two protons are produced for every single mole of  $\text{CaCO}_3$  precipitated from the water with the subsequent reduction of TA by two moles for each mole of  $\text{CaCO}_3$  produced. The reverse reaction occurs during dissolution. The net effect of these two

processes is measured by the AAT, which has been extensively utilised to determine calcification rates of corals and reef communities.

The water volume to biomass ratio required to adequately detect changes in TA levels approximates 2 L of seawater for one piece of coral (with a linear size between 30 and 120 mm; see Rodolfo-Metalpa *et al.* 2010; Roth *et al.* 2012; Dove *et al.* 2013) or ~12 L of seawater for a community of coral (with an approximate size of 200 x 150 mm; see Fujise *et al.* 2014; Comeau *et al.* 2015; Schoepf *et al.* 2015). Therefore, a pilot study was conducted over a 24-h period prior to experimentations to determine the appropriate volume of water to use that would ensure that changes in TA could be detected while oxygen saturation and concentrations of ammonia remained within safe limits.

This pilot study entailed incubating a representative coral community in a closed 12-L holding tub for the collection of TA and water chemistry measurements (oxygen, pH, conductivity and temperature) over a 24-h diel period. The collection of water samples and the water chemistry measurements were taken at intervals of four hours. Water samples were processed as per the AAT (see below), which confirmed that 12 L of seawater harbouring a coral community with a footprint of approximately 240 x 110 mm, was adequate volume for the detection of TA changes with due consideration for the build-up of toxins and the potential decline of oxygen concentrations.

Consequently, this component of the study required adding 10 L of seawater from each of the nine 68-L mesocosms to replicate 12-L incubation tubs before coral communities were transferred for the duration of the TA measurements. All mesocosm components (equipment, live specimens, coral mounts) were thoroughly cleaned before being transferred into the incubation tubs. The water supply to each incubation tub was turned off for 24 hours and the water surfaces of each tub were covered with a transparent acetate sheet (200-micron thickness), suspended by a frame of polystyrene. The acetate sheet created a closed system and minimised gaseous exchange that could negatively influence TA's determinations (Schoepf *et al.* 2016; Cohen *et al.* 2017). The wavemaker pumps were adjusted to accommodate the smaller water volumes and acetate sheet.

Replicate water samples were then collected from each incubation tub immediately after coral communities were transferred to the respective tubs at 18:00. Thereafter, the rest of the water samples were collected at 6-h intervals until a 24-h diel cycle of sampling was completed. As such, five sampling sessions (intervals) with nine water bottles each were collected during a 24-h diel period (45 bottles per alkalinity diel period). There were three diel periods allocated during the experiment: Diel period 1, which was at the end of week 4; Diel period 2 at the end of week 6; and Diel period 3 at the end of week 8. Samples were collected at the end of week 4 at the end

of the initial phase of the experiment as it was important to determine community-level responses after all treatments had reached their setpoint temperatures to assess the effect of rate of change of temperature on NCC. Further sampling was conducted during Week 6 (Diel period 2) as this was the halfway mark of the middle phase of the experiment and was chosen to investigate possible signs of early stress in community-level responses in the RCP 4.5 and bleaching-threshold scenarios two weeks after temperatures had reached their setpoints. Week 8 was at the end of the middle phase, when Diel period 3 samples were collected to determine NCC after coral communities had been kept at their setpoint temperatures for four weeks.

The collection of water samples for total alkalinity measurements was conducted according to Chisholm and Gattuso (1991). Amber borosilicate glass bottles of 250 ml volume were used to collect water samples from each replicate incubation tub. The bottles were washed in an acid bath (HTH<sup>®</sup> Easy Acid diluted to a ratio of 1:20 acid to water) and rinsed with distilled water prior to sampling. The water samples were then collected after the bottle was pre-rinsed twice with the incubation tub's water, ensuring uncontaminated sample collection. The seawater was siphoned from the incubation tub into the bottle, using a 1-m long (4 mm inner-diameter) clear silicone airline tubing, allowing it to overfill for three seconds to displace any air in the bottle. Subsequently, between 8 and 11 ml of the sample was extracted from the top with an electronically operated serological pipette to ensure that mercuric chloride (HgCl<sub>2</sub>) could be added and prevent the grease stopper from coming into contact with the water sample.

A saturated solution of HgCl<sub>2</sub> (50 µl<sup>-1</sup> per 250 ml) was added to each sample bottle to kill any potential microorganisms that may have influenced alkalinity levels after sampling was conducted. The glass stopper of the amber bottle was then greased with ultra-high vacuum grease (Apiezon<sup>®</sup> L), inserted into the neck of the bottle, closed with a twist to spread the lubricant evenly and thus, form an airtight seal. A further seal was guaranteed by wrapping a thick rubber band over the top of the lid and the bottom of the bottle. After labelling the bottle accordingly, it was wrapped with heavy-duty aluminium foil to prevent the water chemistry from potentially changing due to light exposure. Labelling was performed again on the outside of the foil-wrapped bottle. The bottles were refrigerated at 4°C until titration analyses were performed. The seawater temperature, pH and conductivity of each incubation tub was recorded when each water sample was collected using a waterproof temperature/conductivity portable meter (Eutech Instruments<sup>®</sup> Pte. Ltd. Cyberscan Series 600). Additionally, the time at which the water sample was collected was recorded.

The seawater samples' TA concentrations were determined potentiometrically using an automated titrator (<sup>®</sup>Metrohm AG 888 Titrand and magnetic 801 Stirrer) with a 20 ml exchange

unit and “Ecotrode plus” pH glass electrode. Before titrations, the laboratory’s temperature in which the analyses were conducted was set to the titration temperature of 20°C. The samples were removed from the fridge and left to reach the room temperature first, then were added to a water bath for 40 minutes before starting the titrations. The same temperature of 20°C was set for the water bath in which the water samples were held prior to analysis to equilibrate their temperatures with the titration temperature. The water bath was filled with distilled water up to the shoulder of the bottles.

The ©Metrohm AG 888 Titrande was then switched on, the hydrochloric acid supply to the titrator was opened and the Tiamo™ version 2.3 software was run. Before every set of titrations (approximately 12 to 15 titrations per day), the automated titrator went through a dosing cycle after running the Tiamo™ version 2.3 software, which cleaned the dosing device (burette), refilled the dosing medium that was connected to a standard 0.1 N hydrochloric acid (HCl) supply, and reconnected all the sensors and devices. The dosing cycle ensured accurate titrations were done and that the ©Metrohm AG 888 Titrande titrator operated correctly. The pH glass electrode was calibrated weekly with three different pH buffers of pH 4, 7 and 9. These buffers were also kept in the 20°C water baths prior to utilisation for calibration purposes.

The automated titrator was set up for the titrations by positioning the pH glass electrode and preparing the titrating stir plate, which suffices as a small water bath for the measured sample. The titrating stir plate also contains magnetic properties that help keep the stir bar in place during the titration procedure. Hereafter, a 100 ml beaker, 50 ml volumetric flask and the stir bar were rinsed with distilled water. The first water sample was removed from the water bath and carefully opened before approximately 20 ml of sample was pipetted and utilised for further rinsing of the beaker, flask and stir bar. Particular caution was taken to reduce gaseous exchange from the water sample to the flask and again from the flask to the beaker by meticulous pipetting techniques and slow water transfer. A further 50 ml of the sample was pipetted into the volumetric flask, the stopper was inserted, and the flask was weighed with an analytical balance. The weighed amount was tared on the scale, the flask removed, the contents emptied into the rinsed 100 ml beaker and the stir bar slid into the beaker using a Kim wipe. The flask was put back onto the balance without taring it, providing the weight of the contents in the beaker. The beaker containing the 50 ml water sample was then placed into the smaller water bath situated on the titrating stir plate. The pH glass electrode and the dosing burette, positioned on a stand at similar heights to one another without touching, were rinsed with distilled water and wiped down with Kim wipes. They were then simultaneously submerged into the beaker above the stir bar.

Within the Tiamo™ software interface, all required information was inserted, such as the sample name, weight, collection date and time of the sample, and the titration number. An electromotive force titration was initiated as the titration method, setting the stirring speed to six. The automated titration procedure was completed after a stable mV reading was reached, according to the dosed HCl for the given TA water sample's weight, and a Gran plot with an inflection point was generated (Gran 1952). The titrated sample was then safely disposed of into the labelled carcinogenic waste bin and all the apparatuses were rinsed with distilled water. The entire sample preparation and titration process was repeated for each new titration. Repetitive titrations on the same TA water sample were only performed on the first titration of the day. The rest of the titrations included only one titration per sample bottle unless the mV readings and Gran plot were out of range, then two further titrations were done for that bottle. Further titrations were only necessary for 6.5% of the samples from a total of 170 titrations.

## 2.7 Data analysis

As the *Acropora appressa* had three cloned fragments from a single colony that acted as technical replicates within each mesocosm, the values derived from the clones within each mesocosm were averaged to provide a single value prior to data analysis. Consequently, the experimental setup consisted of three temperature treatments (factor: treatment) with three replicate mesocosms (factor: mesocosms nested in treatment) per treatment. Each mesocosm contained three hard coral *A. appressa* fragments, a hard coral control mount, the soft coral *Sinularia brassica* segment, a soft coral control mount and a piece of live rock (collective factor: species with contrasts: hard coral versus soft coral; hard coral versus hard coral control mount; soft coral versus soft coral control mount). The collected *A. appressa* and *S. brassica* species made up three independent colonies each (factor: colony nested in species). As weekly measurements were done during each of the three phases of the experiment for growth and photosynthetic efficiency, week was nested in phase. Treatment, species and phase were therefore considered orthogonal. The NCC measuring periods were done at specific interval times (factor: Diel Period) and specific weeks (factor: Intervals nested in Diel Period).

Temperatures recorded within the replicate mesocosms were analysed with Microsoft Excel 2010. All other datasets that included the physiological parameters of the coral communities such as growth (linear extension and buoyant weight), photosynthetic efficiency and net community calcification were analysed with univariate permutational analyses of variance (perMANOVA) (Anderson *et al.* 2008). Several other univariate statistical approaches were applied before continuing with a perMANOVA approach, but the limitations of these models indicated that they

were inappropriate. These methods included statistical tests of normality, i.e. K-S normality test, adjusting of the values using the Holm method and log-transforming the data. Furthermore, due to the complexity of the experimental design (i.e. multiple factors and levels with a nested design), and the non-parametric repeated measures nature of the data, standard ANOVA models were unsuitable.

For each response variable of coral physiology quantified, permANOVA analyses were performed on the resemblance matrix of Euclidean distances among replicates, using 9999 permutations of the residuals under a reduced model (Anderson *et al.* 2008). Monte-Carlo permutation tests were employed to obtain the desired number of permutations to derive accurate *P*-values. The permANOVA analyses were conducted with PRIMER-E<sup>®</sup> version 7 software and the PERMANOVA<sup>®</sup>+ add-on package (Anderson *et al.* 2008). The *a priori* analyses were undertaken using type I sequential sum of squares and *post hoc* tests conducted on the fixed effects found to be significant ( $\alpha \leq 0.05$ ) in the *a priori* analysis. Wherever the terms resulted in significant differences after *a priori* permANOVA analyses, supplementary permutational analysis of dispersions (permDISP) were performed to test for homogeneity of multivariate dispersions among groups. Accordingly, the distance-based permDISP analysis was performed on the resemblance matrix for the different interactive factors of each dataset based on deviations from the group centroids with *P*-values derived from 9999 permutations. The subsections below provide further details on the specifics of each analysis performed for the respective variables quantified during the experiment.

### **2.7.1 Temperature**

All temperature values recorded during the ten weeks of experimentation were plotted as a time series and statistically summarised (minimum, maximum, average and  $\pm$  SD). The plotted values and summary statistics indicated 1) how close the temperatures within the three treatments were to the setpoint values (see Fig. 3.1 and Table 3.1), 2) what the within-treatment variability was, and 3) how temperatures changed over the three different phases (initial, middle, final) of the experiment. The plots and summary statistics were created using Microsoft Excel 2010.

### **2.7.2 Growth**

The averaged (weekly and per treatment) linear extension and buoyant weight of *A. appressa* and *S. brassica* were plotted independently, along with the buoyant weight of their corresponding control mounts. The average  $\pm$  standard deviations (SDs) were plotted at weekly intervals for each temperature treatment, plotting the change in growth with time relative to the initial weight. The

marbles' measured buoyant weights were averaged weekly and per treatment for each marble and plotted per temperature with their respective SDs. The maximum range  $\pm$  SD in buoyant weight of any of the three marbles, attributable to the differences in water density associated with the different temperature treatments, were calculated accordingly. The average  $\pm$  SD change in the buoyant weight of the control mounts for each treatment was also plotted at weekly intervals for the experiment's duration.

The coral growth data (linear extension and buoyant weight, respectively) were analysed using a non-parametric permANOVA with the following factors (in order): treatment, species, phase, mesocosm (nested in treatment), colony (nested in species) and week (nested in phase). The permANOVA design included a six-factorial design with both fixed (treatment, species, phase, week) and random (mesocosm, colony) effects assigned. If the fixed factors and their respective interactions were significant ( $\alpha \leq 0.05$ ) in the *a priori* analysis, further post hoc pair-wise tests were conducted to test which levels within a particular factor differed. The *a priori* pairwise contrasts for the species factor were hard coral versus soft coral.

### 2.7.3 Photosynthetic efficiency

As described in subsection 2.6.2, multiple locations were measured on each fragment of *A. appressa*, section of *S. brassica* and piece of live rock. Therefore, the numerous  $F_V/F_M$  and rETR technical replicates were averaged for the dark-acclimated and daytime measurements, respectively. As the  $F_V/F_M$  values are obtained from dark-acclimated measurements and are generally used as a proxy for heat sensitivity in corals (Warner *et al.* 2010), the average  $\pm$  SD values were plotted throughout the experiment at weekly intervals. The respective plots, i.e. *A. appressa*, *S. brassica* and live rock, illustrated how the photosynthetic efficiency of the two coral species and live rock changed according to the different temperature treatments over the course of the experiment.

The permANOVA analysis was performed on the overall  $F_V/F_M$  for PS II values derived by averaged rETR (day) values and  $F_V/F_M$  (night) values. The same six-factorial permANOVA model used for coral growth was employed to analyse photosynthetic efficiency (refer to subsection 2.7.2). However, the *a priori* pairwise contrasts were hard coral versus soft coral, hard coral versus live rock and soft coral versus live rock for the species factor.

#### 2.7.4 Net community calcification

The net community calcification (NCC) values were determined by using the changes in total alkalinity (TA) values as a proxy. Accordingly, the TA values were determined before and after the incubation period at the points when dissolution (prevalent at night) and accretion (stronger during daylight) occurred (Gattuso *et al.* 1999). The NCC per treatment was then calculated by subtracting the dissolution and accretion points (Pandolfi *et al.* 2011; van Hooidek *et al.* 2014) per the 6-h sampling interval of each mesocosm. The calculated value was further divided by two as each one mole of  $\text{CaCO}_3$  precipitated alkalinity gets reduced by two molar equivalents (Chisholm & Gattuso 1991).

Components of the carbonate system that were measured during the alkalinity anomaly technique (AAT) were calculated from the titrated TA values, sample weights, pH, temperature and conductivity (converted to salinity) measurements, using the apparent dissociation constants of Mehrbach *et al.* (1973) that have been refitted by Dickson and Millero (1987). The average  $\pm$  standard error (SE) concentration of calcium carbonate ( $\text{CaCO}_3$ ) indicating NCC for each 6-h sampling interval across the three diel periods was calculated and plotted using Microsoft Excel 2010 per treatment to provide a visual indication of coral community responses to the different temperature treatments. Additionally, the average  $\pm$  SD  $\text{CaCO}_3$  concentrations were plotted for each 6-h interval during each diel period per temperature treatment.

The NCC data of  $\text{CaCO}_3$  concentrations were analysed using a four-factorial permANOVA design that included the following factors: treatment, diel period, mesocosm (nested in treatment), and interval (nested in diel period). The fixed factors included treatment and diel period, whereas the random factors were mesocosm (nested in treatment) and interval (nested in diel period).

# CHAPTER 3 | RESULTS

## 3.1 Water temperature

The hourly temperature measurements recorded within mesocosms across each of the three phases of the experiment are indicated in Figure 3.1 and summarised in Table 3.1. During the initial phase of increasing temperature, the control treatment had an average  $\pm$  standard deviation (SD) temperature of  $24.94 \pm 0.23^\circ\text{C}$  and a maximum range of  $1.46^\circ\text{C}$ . During the same phase, the Representative Concentration Pathway 4.5 (RCP 4.5) treatment and bleaching-threshold treatment had average  $\pm$  SD temperatures of  $25.64 \pm 0.72^\circ\text{C}$  and  $26.26 \pm 1.16^\circ\text{C}$  respectively, with corresponding ranges of  $2.43$  and  $3.91^\circ\text{C}$ . Average  $\pm$  SD temperatures obtained during the stable temperature middle phase were  $24.73 \pm 0.15^\circ\text{C}$  for the control treatment (target =  $24.4^\circ\text{C}$ ),  $27.10 \pm 0.16^\circ\text{C}$  for the RCP 4.5 treatment ( $26.9^\circ\text{C}$ ) and  $28.88 \pm 0.23^\circ\text{C}$  for the bleaching-threshold treatment ( $28.8^\circ\text{C}$ ). During the extended final phase, when temperatures in the warmest treatment ( $28.8^\circ\text{C}$ ) were increased by  $1^\circ\text{C}$  to a setpoint of  $29.8^\circ\text{C}$ , an average  $\pm$  SD value of  $29.40 \pm 0.35^\circ\text{C}$  was achieved, whilst temperatures in the other two treatments remained similar to their corresponding measurements during the middle phase (Fig. 3.1).

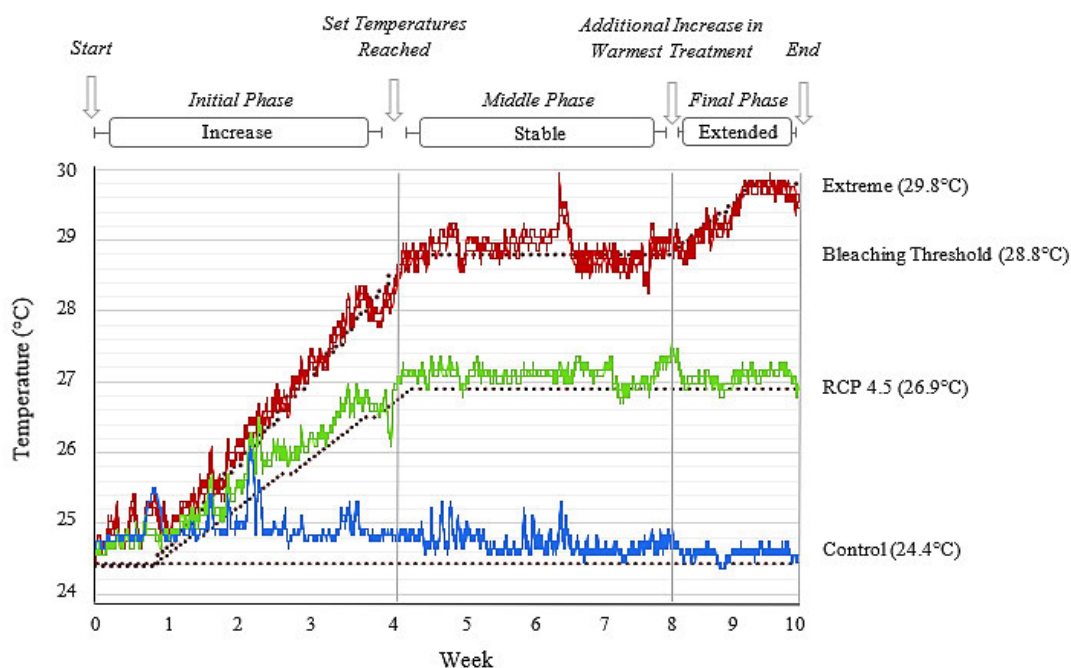


**Figure 3.1** Hourly temperature time series over the 10-week experiment for each replicate mesocosm according to each temperature treatment and their associated climate scenarios. Solid grey vertical lines denote the three different phases of temperature change during the experiment and dotted lines indicate the setpoint temperatures (also in brackets) for each treatment including the extended final phase when temperatures were increased by  $1^\circ\text{C}$  to  $29.8^\circ\text{C}$  in the warmest treatment ( $28.8^\circ\text{C}$ ).

**Table 3.1** Temperature (°C) summary statistics based on hourly measurements obtained for all three temperature treatments during each of the three phases of the experiment. The target rate of increase (°C.d<sup>-1</sup>) for the initial phase as well as setpoint temperatures for the other phases are also provided. RCP = Representative concentration pathway. SD = standard deviation. Min. = minimum. Max. = maximum.

<i>Treatment</i>	Initial Phase (Increase)				Middle Phase (Stable)				Final Phase (Extended Increase)			
	<i>Rate of Increase</i>	<i>Average ± SD</i>	<i>Min.</i>	<i>Max.</i>	<i>Setpoint Temperature</i>	<i>Average ± SD</i>	<i>Min.</i>	<i>Max.</i>	<i>Setpoint Temperature</i>	<i>Average ± SD</i>	<i>Min.</i>	<i>Max.</i>
24.4°C (Control)	0.00	24.94 ± 0.23	24.64	26.10	24.4 ± 0.5	24.73 ± 0.15	24.45	25.32	24.4 ± 0.5	24.57 ± 0.08	24.35	24.74
26.9°C (RCP 4.5)	0.09	25.64 ± 0.72	24.55	26.98	26.9 ± 0.5	27.10 ± 0.16	26.10	27.57	26.9 ± 0.5	27.08 ± 0.12	26.78	27.47
28.8°C (Bleaching Threshold)	0.16	26.26 ± 1.16	24.45	28.36	28.8 ± 0.5	28.88 ± 0.23	27.96	29.95	29.8 ± 0.5	29.40 ± 0.35	28.66	29.95

### 3.2 Buoyant weights of marbles at different temperatures

The different water temperatures and their corresponding densities of water did not materially influence the buoyant weight measurements, as the three marbles measured in the different water temperatures employed in the experiment revealed negligible variability (Fig. 3.2). The maximum range in buoyant weight of any of the three marbles attributable to the differences in water density associated with the different temperature treatments was 0.00165 g, with a standard deviation of 0.0009 g. This value of 0.00165 g was approximately one order of magnitude lower (14.9 times) than the minimum growth (0.02459 g) measured for any particular coral throughout the experiment (see subsection 3.3.1.2).

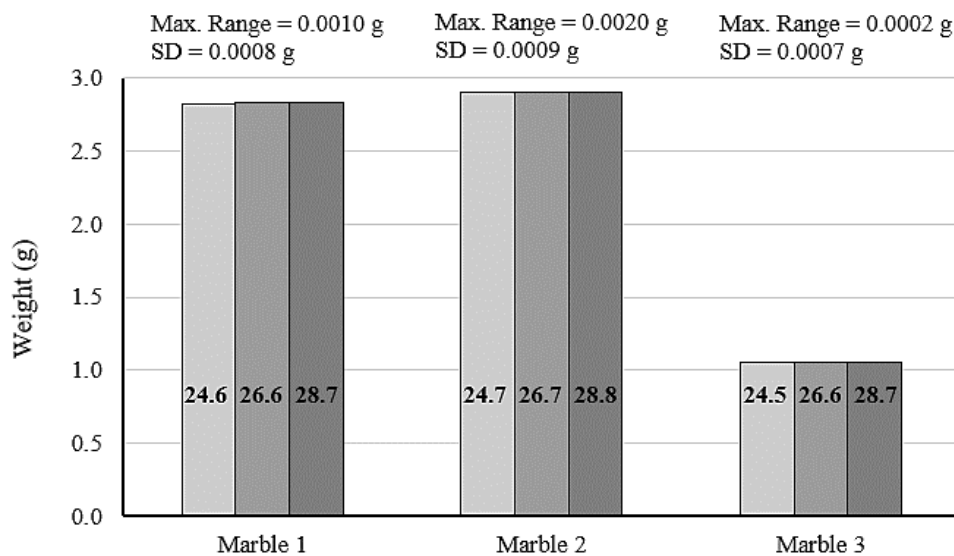


**Figure 3.2** Raw marble buoyant weight (g) comparisons measured at each of the three setpoint temperature treatments (24.4°C, 26.9°C and 28.8°C) with maximum (max.) ranges and standard deviations (SD) according to each marble across the three different temperatures. Values inside the bars indicate the instantaneous temperatures (°C) a particular marble was measured at.

### 3.3 Physiological responses

#### 3.3.1 Growth

##### 3.3.1.1 Growth according to size (linear extension and diameter increase)

The average  $\pm$  standard deviation (SD) linear extension in *Acropora appressa* fragments for the experiment was  $1.45 \pm 1.18$  mm in the 24.4°C control treatment,  $0.65 \pm 1.19$  mm in the 26.9°C treatment and  $1.17 \pm 0.61$  mm in the 28.8°C treatment (Fig. 3.3.1). *Acropora appressa* fragments at 24.4°C underwent a weekly average  $\pm$  SD extension of  $0.21 \pm 0.16$  mm, whereas fragments in

the 26.9°C treatment underwent a slower weekly extension rate of  $0.09 \pm 0.05$  mm from the fourth week until termination of the experiment. The 28.8°C treatment manifested a slower extension rate in the fragments at  $0.17 \pm 0.10$  mm from week 4 until week 6 compared to the first three weeks at  $0.42 \pm 0.31$  mm. *Acropora appressa* fragments at 28.8°C then declined in extension from the end of week 6 until the end of the experiment (Fig. 3.3.1).

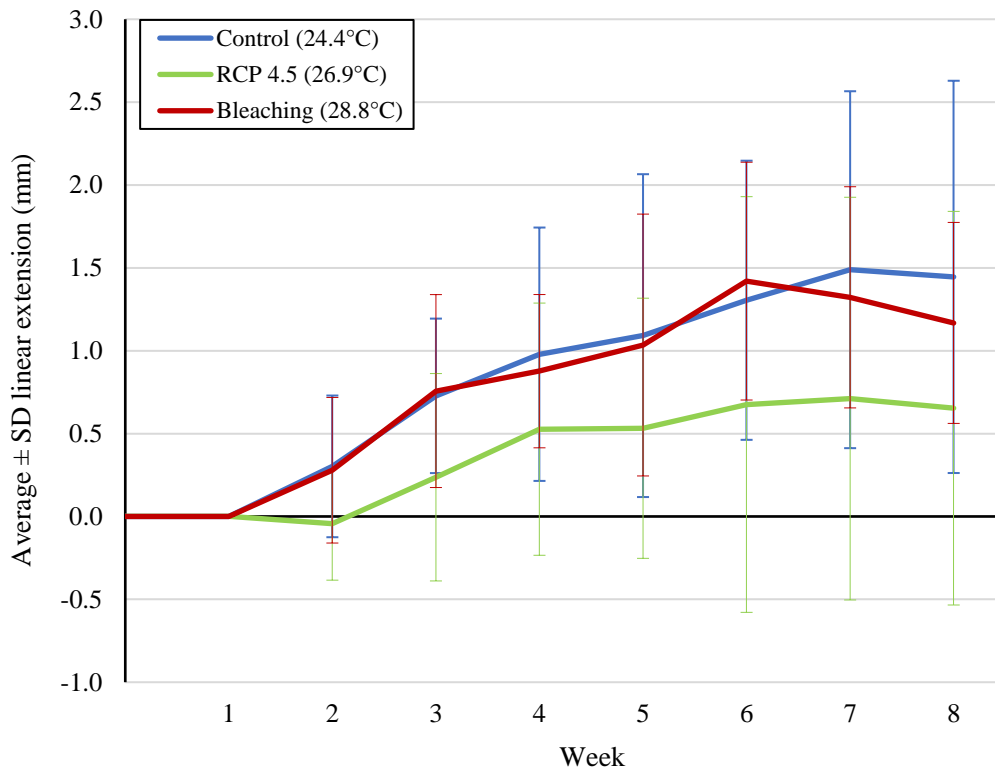


**Figure 3.3.1** Average  $\pm$  standard deviation (SD) linear extension (mm) of *Acropora appressa* fragments measured at weekly intervals plotted according to three temperature treatments associated with different climate change scenarios.

In the soft coral *Sinularia brassica*, the average  $\pm$  SD growth in diameter in the 24.4°C control treatment was  $8.57 \pm 0.47$  mm over nine weeks (Fig. 3.3.2). During the same period, the average  $\pm$  SD growth in diameter was  $12.73 \pm 0.09$  mm for soft corals at 26.9°C and  $8.7 \pm 0.15$  mm for soft corals at 28.8°C. However, average  $\pm$  SD losses of  $10.69 \pm 0.17$  and  $4.79 \pm 0.46$  mm in diameter were evident over the last five weeks at 26.9°C and 28.8°C, respectively, once temperatures had reached their setpoints. Contrastingly, an average  $\pm$  SD growth of  $2.51 \pm 0.43$  mm in diameter was evident over the last five weeks at 24.4°C (Fig. 3.3.2). During the last week of the bleaching-threshold treatment, there was an obvious reduction in diameter by 2.46 millimetres when temperatures were increased to 29.8°C, which was not detected in the other two treatments.

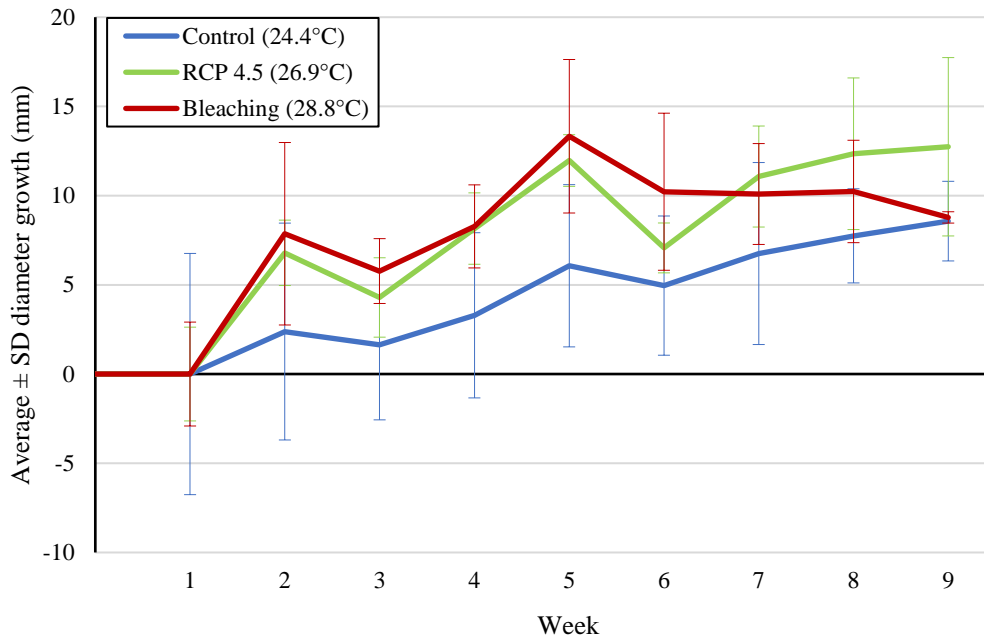


**Figure 3.3.2** Average  $\pm$  standard deviation (SD) change in diameter (mm) of *Sinularia brassica* discs measured at weekly intervals plotted according to three temperature treatments associated with different climate change scenarios.

The *a priori* permutational analysis of variance (permANOVA) investigating variation in linear extension of *A. appressa* and change in the diameter of *S. brassica*, respectively, revealed significant differences in size between phases ( $F_{(\text{Pseudo})} = 5.16$ ;  $P_{(\text{MC})} = 0.0480$ ), week nested in phase ( $F_{(\text{Pseudo})} = 4.63$ ;  $P_{(\text{MC})} = 0.0003$ ), and in the interaction between species and week nested in phase ( $F_{(\text{Pseudo})} = 6.85$ ;  $P_{(\text{MC})} = 0.0001$ ) (Table 3.3.1). All terms involving the random effect of colony nested in species and their interactions with fixed effects terms, were also significant ( $P_{(\text{MC})} < 0.0005$ ). No significant differences were detected according to the fixed effects in treatment ( $P_{(\text{MC})} = 0.3501$ ), species ( $P_{(\text{MC})} = 0.3938$ ) and their interactions, including the three-way interaction of treatment-species-phase ( $P_{(\text{MC})} = 0.9848$ ). The *a priori* permutational analyses of dispersion (permDISP) detected significant dispersions for all terms in the model ( $P_{(\text{perm})} < 0.05$ ), except for the overall treatment term ( $F = 0.4321$ ;  $P_{(\text{perm})} = 0.8046$ ).

**Table 3.3.1** Permutational ANOVA (permANOVA) and permutational analyses of dispersion (permDISP) investigating variation in the change in size of hard and soft corals exposed to three different temperature treatments, based on weekly measurements of their linear extension and diameter, respectively. Significant differences are indicated in bold ( $\alpha \leq 0.05$ ).

Source of variation	permANOVA				permDISP	
	df	MS	$F_{(Pseudo)}$	$P_{(MC)}$	$F$	$P_{(perm)}$
Treatment	2	3.2163	1.3165	0.3501	0.4321	0.8046
Species	1	96.730	1.1312	0.3938	81.750	<b>0.0001</b>
Phase	2	86.643	5.1599	<b>0.0480</b>	19.752	<b>0.0001</b>
Mesocosm (Treatment)	6	23.548	0.5822	0.7356	4.3445	<b>0.0089</b>
Colony (Species)	2	85.498	41.437	<b>0.0001</b>	21.616	<b>0.0001</b>
Week (Phase)	7	9.9845	4.6267	<b>0.0003</b>	9.2438	<b>0.0001</b>
Treatment x Species	2	6.3798	0.4978	0.6445	16.337	<b>0.0001</b>
Treatment x Phase	4	10.794	1.3258	0.3203	5.5066	<b>0.0004</b>
Species x Phase	1	56.040	2.3088	0.1781	39.356	<b>0.0001</b>
Treatment x Colony (Species)	4	12.813	6.2099	<b>0.0002</b>	8.2048	<b>0.0001</b>
Treatment x Week (Phase)	12	2.5966	1.2475	0.2652	3.8308	<b>0.0005</b>
Species x Week (Phase)	6	14.202	6.8539	<b>0.0001</b>	13.116	<b>0.0001</b>
Colony (Species) x Phase	6	19.058	9.2368	<b>0.0001</b>	6.6658	<b>0.0001</b>
Treatment x Species x Phase	2	0.9062	0.1279	0.9848	14.608	<b>0.0001</b>
Treatment x Species x Week (Phase)	12	2.3724	1.1442	0.3301	4.7871	<b>0.0114</b>
Treatment x Colony (Species) x Phase	12	9.1069	4.4138	<b>0.0001</b>	3.1694	<b>0.0331</b>
Res	71	2.0633				
Total	152					

*Post hoc* pairwise analyses, however, yielded no significant differences in growth between phases of the experiment, although the initial versus the middle phase was marginally non-significant ( $t = 2.51$ ;  $P_{(MC)} = 0.0627$ ) (Table 3.3.2). *Post hoc* analyses of dispersion, however, were all significantly different between phases ( $P_{(perm)} < 0.05$ ) (Table 3.3.2).

**Table 3.3.2** *Post hoc* pairwise permutational ANOVA (permANOVA) and permutational analyses of dispersion (permDISP) comparisons of growth between all phases (initial, middle and final) of the experiment for hard and soft corals combined. Significant differences are indicated in bold ( $\alpha \leq 0.05$ ).

Source of variation	permANOVA		permDISP	
	pairwise comparisons		pairwise comparisons	
	$t$	$P_{(MC)}$	$t$	$P_{(perm)}$
Initial Phase vs Middle Phase	2.5144	0.0627	4.8224	<b>0.0002</b>
Initial Phase vs Final Phase	1.8086	0.2142	6.2310	<b>0.0001</b>
Middle Phase vs Final Phase	1.1473	0.3735	2.5633	<b>0.0467</b>

*Post hoc* pairwise permANOVA revealed that growth was significantly lower in the initial phase of the experiment during the following weeks: weeks 1 and 2 ( $t = 5.46$ ;  $P_{(MC)} = 0.0002$ ), 1 and 4 ( $t = 2.44$ ;  $P_{(MC)} = 0.0341$ ), 2 and 3 ( $t = 4.57$ ;  $P_{(MC)} = 0.0008$ ), 3 and 4 ( $t = 9.67$ ;  $P_{(MC)} = 0.0001$ ). During the middle phase, growth in week 5 was significantly less than growth in week 6 ( $t = 2.66$ ;  $P_{(MC)} = 0.0211$ ; Table 3.3.3). *Post hoc* pairwise permDISP analyses of dispersion revealed that weeks 1 and 2 ( $t = 5.80$ ;  $P_{(perm)} = 0.0001$ ), 1 and 3 ( $t = 6.61$ ;  $P_{(perm)} = 0.0001$ ), and 1 and 4 ( $t = 5.01$ ;  $P_{(perm)} = 0.0001$ ) of the initial phase differed in their levels of dispersion. During the middle phase, weeks 5 and 6 ( $t = 3.97$ ;  $P_{(perm)} = 0.0005$ ), 5 and 8 ( $t = 2.64$ ;  $P_{(perm)} = 0.0186$ ), and 6 and 7 ( $t = 4.09$ ;  $P_{(perm)} = 0.0003$ ) differed in dispersion. The permANOVA could not test between week 9 and 10, as no measurements were taken in week 10. Therefore, the difference between week 9 and week 10 (i.e. null) resulted in a “no test” output (Table 3.3.3).

**Table 3.3.3** *Post hoc* pairwise permutational ANOVA (permANOVA) and permutational analysis of dispersion (permDISP) comparisons of the variation in growth between weeks for each phase of the experiment for hard and soft corals combined. Significant differences are indicated in bold ( $\alpha \leq 0.05$ ).

Source of variation	permANOVA pairwise comparisons		permDISP pairwise comparisons	
	$t$	$P_{(MC)}$	$t$	$P_{(perm)}$
<i>Initial Phase</i>				
Week 1 vs Week 2	5.4611	<b>0.0002</b>	5.7965	<b>0.0001</b>
Week 1 vs Week 3	1.8202	0.0949	6.6083	<b>0.0001</b>
Week 1 vs Week 4	2.4387	<b>0.0341</b>	5.0083	<b>0.0001</b>
Week 2 vs Week 3	4.5665	<b>0.0008</b>	0.2493	0.8059
Week 2 vs Week 4	1.4966	0.1685	2.0878	0.0663
Week 3 vs Week 4	9.6672	<b>0.0001</b>	2.0568	0.1145
<i>Middle Phase</i>				
Week 5 vs Week 6	2.6636	<b>0.0211</b>	3.9666	<b>0.0005</b>
Week 5 vs Week 7	1.1344	0.2853	1.1784	0.2738
Week 5 vs Week 8	0.1223	0.9062	2.6448	<b>0.0186</b>
Week 6 vs Week 7	1.5116	0.1547	4.0853	<b>0.0003</b>
Week 6 vs Week 8	1.6473	0.1237	2.2586	0.0888
Week 7 vs Week 8	0.8430	0.4091	0.6353	0.6430
<i>Final Phase</i>				
Week 9 vs null	No test			

*Post hoc* pairwise permANOVA detected a significant difference in growth between the hard coral *A. appressa* and soft coral *S. brassica* only during week 2 ( $t = 8.90$ ;  $P_{(MC)} = 0.0129$ ) (Table 3.3.4). All *post hoc* pairwise permDISP analyses were found to indicate significant dispersion,

except in week 1 that yielded no differences, as there was no change detected in the diameter of the soft corals during the first week of the experiment.

**Table 3.3.4** *Post hoc* pairwise permutational ANOVA (permANOVA) and permutational analysis of dispersion (permDISP) comparisons investigating the variation in growth between hard and soft coral for the different weeks within each phase of the experiment. Significant differences are indicated in bold ( $\alpha \leq 0.05$ ).

Source of variation	permANOVA pairwise comparisons		permDISP pairwise comparisons	
	<i>t</i>	$P_{(MC)}$	<i>t</i>	$P_{(perm)}$
<i>Hard Coral vs Soft Coral</i>				
<i>Initial Phase</i>				
Week 1	0	1	0	1
Week 2	8.8954	<b>0.0129</b>	5.9864	<b>0.0002</b>
Week 3	2.1746	0.1652	3.6560	<b>0.0007</b>
Week 4	0.0681	0.9957	3.1118	<b>0.0089</b>
<i>Hard Coral vs Soft Coral</i>				
<i>Middle Phase</i>				
Week 5	1.9367	0.1882	3.6389	<b>0.0003</b>
Week 6	0.3988	0.7365	2.7172	<b>0.0162</b>
Week 7	0.9947	0.4215	4.0469	<b>0.0003</b>
Week 8	1.0762	0.3835	5.7633	<b>0.0002</b>

*Post hoc* pairwise permANOVA analyses revealed that there were significant differences in linear extension in the hard coral *A. appressa* between all weeks of the initial phase, with successive weeks indicating significant growth relative to preceding weeks (Table 3.3.5). Comparisons between weekly changes in extension in the middle phase were not significant, although weeks 5 and 6 ( $t = 2.16$ ;  $P_{(MC)} = 0.0722$ ), and 5 and 7 ( $t = 2.07$ ;  $P_{(MC)} = 0.0831$ ), were only marginally non-significant. The *post hoc* pairwise permDISP revealed significant differences in dispersion between most weeks in the initial phase of the experiment but not in the middle phase.

For the soft coral *S. brassica*, *post hoc* pairwise permANOVA analyses detected differences in diameter increase between most weeks in the initial phase of the experiment, with successive weeks generally exhibiting larger values in diameter (Table 3.3.5). However, in the middle phase, growth only differed between week 5 and 6, with week 6 having significantly less growth ( $t = 2.92$ ;  $P_{(MC)} = 0.0271$ ). *Post hoc* pairwise permDISP analyses were generally not significant but, when they were, it was associated with week 1, when there was no change in diameter recorded in the soft corals. No tests were conducted between week 9 and 10 as previously explained.

**Table 3.3.5** *Post hoc* pairwise permutational ANOVA (permANOVA) and permutational analyses of dispersion (permDISP) comparisons investigating the variation in growth between the different weeks of each experimental phase for hard and soft coral. Significant differences are indicated in bold ( $\alpha \leq 0.05$ ).

Source of variation	permANOVA pairwise comparisons		permDISP pairwise comparisons	
	<i>t</i>	<i>P</i> <sub>(MC)</sub>	<i>t</i>	<i>P</i> <sub>(perm)</sub>
<b>Hard Coral</b>				
<i>Initial Phase</i>				
Week 1 vs Week 2	2.6273	<b>0.0389</b>	3.2718	<b>0.0001</b>
Week 1 vs Week 3	3.8671	<b>0.0083</b>	3.7697	<b>0.0002</b>
Week 1 vs Week 4	4.1216	<b>0.0069</b>	4.4159	<b>0.0001</b>
Week 2 vs Week 3	4.1776	<b>0.0053</b>	1.6337	0.1146
Week 2 vs Week 4	4.1736	<b>0.0070</b>	2.3072	<b>0.0299</b>
Week 3 vs Week 4	2.7546	<b>0.0341</b>	0.6103	0.5641
<i>Middle Phase</i>				
Week 5 vs Week 6	2.1648	0.0722	0.10004	0.9311
Week 5 vs Week 7	2.0669	0.0831	0.67522	0.5300
Week 5 vs Week 8	1.1416	0.3022	0.55121	0.5819
Week 6 vs Week 7	0.4550	0.6689	0.47638	0.6792
Week 6 vs Week 8	0.3649	0.7295	0.39070	0.8008
Week 7 vs Week 8	1.4532	0.1981	0.05690	0.9217
<b>Soft Coral</b>				
<i>Initial Phase</i>				
Week 1 vs Week 2	5.1785	<b>0.0017</b>	6.7785	<b>0.0001</b>
Week 1 vs Week 3	2.7582	<b>0.0344</b>	4.9517	<b>0.0001</b>
Week 1 vs Week 4	1.1057	0.3204	4.8766	<b>0.0002</b>
Week 2 vs Week 3	5.0164	<b>0.0026</b>	0.6073	0.5436
Week 2 vs Week 4	2.2147	0.0773	1.1440	0.2543
Week 3 vs Week 4	9.2820	<b>0.0003</b>	0.4558	0.6686
<i>Middle Phase</i>				
Week 5 vs Week 6	2.9170	<b>0.0271</b>	0.7279	0.4805
Week 5 vs Week 7	1.5400	0.1766	0.4618	0.6515
Week 5 vs Week 8	0.2999	0.7715	1.6989	0.1203
Week 6 vs Week 7	1.4834	0.1910	1.2081	0.2787
Week 6 vs Week 8	1.6798	0.1451	2.4866	<b>0.0241</b>
Week 7 vs Week 8	0.9452	0.3827	1.2422	0.2004
<i>Final Phase</i>				
Week 9 vs null	No test			

### 3.3.1.2 Growth according to buoyant weight

The hard coral control mounts manifested minimal changes in weight across all temperature treatments, which ranged between zero and 0.025 g. Overall, the average  $\pm$  SD changes in weight of the control mounts for the 24.4°C, 26.9°C and 28.8°C treatments were  $0.019 \pm 0.007$  g,  $0.016 \pm 0.006$  g and  $0.013 \pm 0.005$  g, respectively. *Acropora appressa* yielded a consistently positive change in buoyant weight, with an average  $\pm$  standard deviation (SD) in weekly growth of  $0.025 \pm 0.008$  g for the duration of the experiment in the 24.4°C control treatment (Fig. 3.3.3). At 26.9°C, *A. appressa* displayed a positive change in weight until week 6, then slower growth became evident with a decrease in the last two weeks of the experiment (Figs. 2.3.3, 3.3.3). The weekly average  $\pm$  SD growth of *A. appressa* decreased within the 28.8°C treatment ( $0.009 \pm 0.008$  g) over the last three weeks of the experiment, yielding a lower weekly growth from week 6 onward (Fig. 3.3.3).

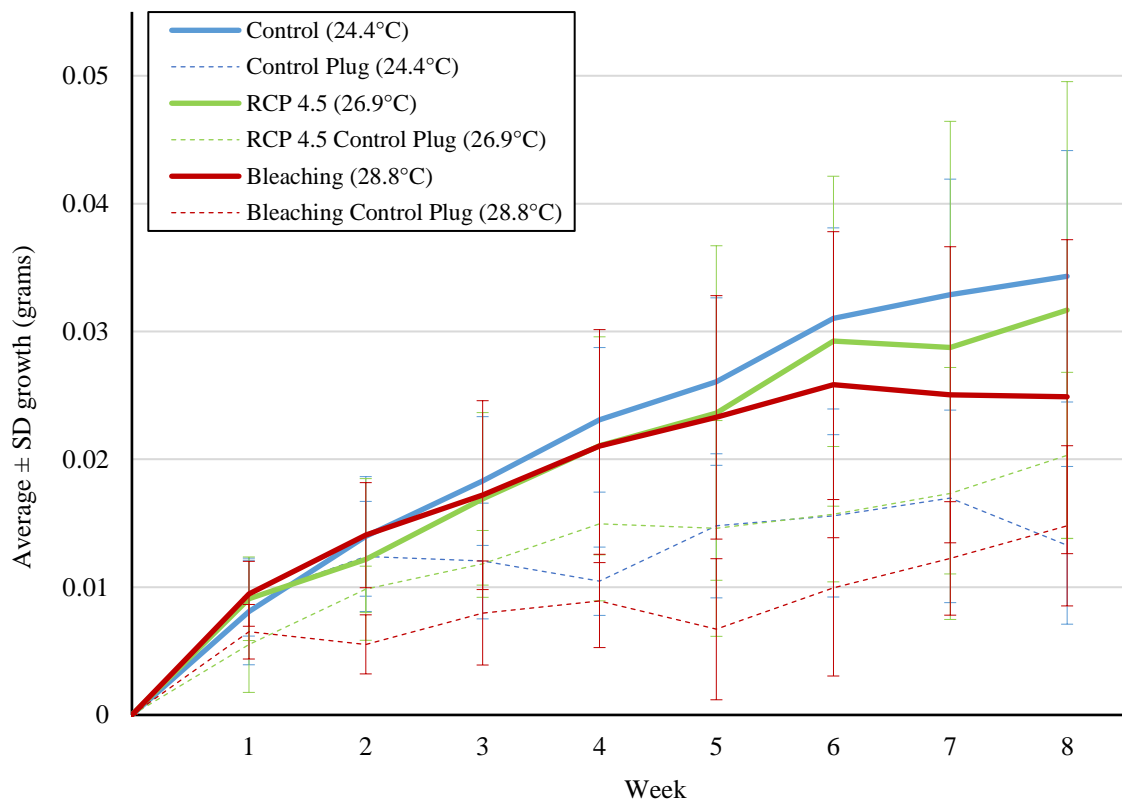


**Figure 3.3.3** Average  $\pm$  standard deviation (SD) growth (g) of *Acropora appressa* throughout the experiment based on weekly buoyant weight measurements plotted according to each temperature treatment. Solid lines indicate a change in coral growth and dotted lines indicate a change in the control mounts.

Relatively minor weight changes were measured among the soft coral control mounts, ranging between 0 and 0.015 g. Overall the average  $\pm$  SD changes in weight of the controls at 24.4°C, 26.9°C and 28.8°C were  $0.007 \pm 0.0009$  g,  $0.006 \pm 0.0004$  g and  $0.001 \pm 0.0001$  g, respectively. *Simularia brassica*, experienced a loss in weight across all treatments for the first four weeks when temperatures were being manipulated at different rates. However, a positive and consistent change in weight was evident at 24.4°C from the fifth week until the end of the experiment (Fig. 3.3.4). A similar pattern was evident for *S. brassica* in the 26.9°C treatment, but with a slower weekly growth. However, *S. brassica* underwent a rapid loss in weight during the last week at 26.9°C (Fig. 3.3.4). In the 28.8°C treatment, a consistent decline in weekly weight was measured during all three phases of the experiment, especially when the water temperature in this treatment was increased to 29.8°C during the last two weeks (final phase) of the experiment (Figs. 2.3.3, 3.3.4).

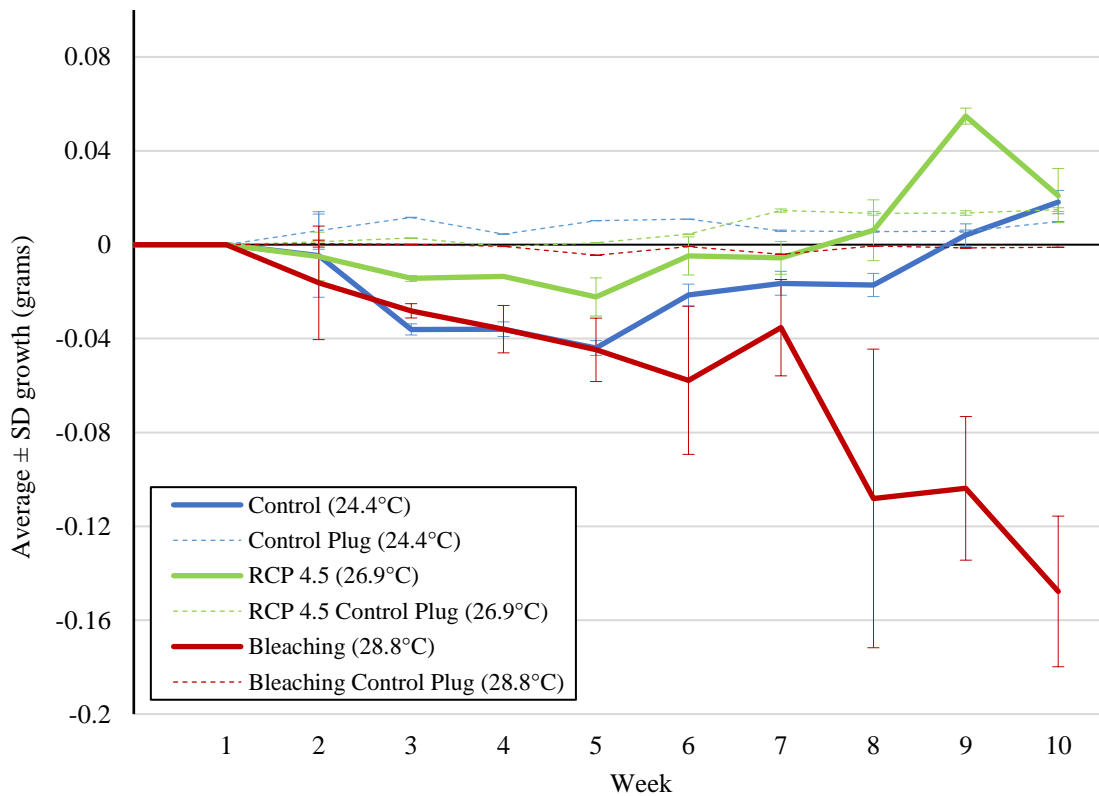


**Figure 3.3.4** Average  $\pm$  standard deviation (SD) growth (g) of *Simularia brassica* throughout the experiment based on weekly buoyant weight measurements plotted according to each temperature treatment. Solid lines indicate a change in coral growth and dotted lines indicate a change in the control mounts.

The *a priori* perMANOVA investigating variation in the growth of hard and soft corals (including the *a priori* pairwise contrasts and controls) based on their buoyant weights revealed significant

differences in the interaction between treatment and phase ( $F_{(Pseudo)} = 3.73$ ;  $P_{(MC)} = 0.0158$ ), species, and week nested in phase, for hard coral and its control plug ( $F_{(Pseudo)} = 4.42$ ;  $P_{(MC)} = 0.0010$ ), and between the three-way interaction of treatment-species-week nested in phase for hard coral and their control mounts ( $F_{(Pseudo)} = 1.94$ ;  $P_{(MC)} = 0.0426$ ; Table 3.3.6). The random effect of colony nested in species and its interaction with most fixed effects was usually significant. Treatment, treatment crossed with species and the treatment-species-phase interaction terms were not significant. *A priori* permDISP analyses of dispersion detected significant differences for nearly all tests, including all those found to differ significantly in the permANOVA (Table 3.3.6). Marginally non-significant differences in dispersion were found for the interaction of treatment and species for hard coral and its control ( $F = 2.24$ ;  $P_{(perm)} = 0.0868$ ), and for treatment-species-week nested in phase, especially for hard and soft corals and their associated controls ( $F = 5.07$ ;  $P_{(perm)} = 0.0720$  and  $F = 5.30$ ;  $P_{(perm)} = 0.0686$ , respectively).

**Table 3.3.6** Permutational ANOVA (permANOVA) and permutational analysis of dispersion (permDISP) investigating variation in the growth (change in weekly buoyant weight) of hard and soft corals exposed to three different temperature treatments. The relevant *a priori* pairwise contrasts for species (i.e. hard or soft corals and their controls) have been included and are indicated in italics. Significant differences are indicated in bold ( $\alpha \leq 0.05$ ).

Source of variation	permANOVA				permDISP	
	df	MS	$F_{(Pseudo)}$	$P_{(MC)}$	$F$	$P_{(perm)}$
Treatment	2	0.011848	1.09740	0.4467	5.7085	<b>0.0350</b>
Species	3	0.045418	1.73020	0.2138	63.100	<b>0.0001</b>
<i>Hard Coral vs Soft Coral</i>	1	0.118610	2.64200	0.1613	57.671	<b>0.0001</b>
<i>Hard Coral vs Hard Coral Control</i>	1	0.004825	7.80080	0.1072	7.6694	<b>0.0112</b>
<i>Soft Coral vs Soft Coral Control</i>	1	0.035110	0.80565	0.3975	72.162	<b>0.0001</b>
Phase	2	5.95x10 <sup>-5</sup>	0.02054	0.9788	16.753	<b>0.0011</b>
Mesocosm (Treatment)	6	0.018673	0.88776	0.5213	16.670	<b>0.0001</b>
Colony (Species)	12	0.016054	62.7860	<b>0.0001</b>	31.178	<b>0.0001</b>
<i>Hard Coral vs Soft Coral</i>	5	0.023843	49.1040	<b>0.0001</b>	21.897	<b>0.0001</b>
<i>Hard Coral vs Hard Coral Control</i>	2	0.000618	83.8510	<b>0.0001</b>	6.7485	<b>0.0036</b>
<i>Soft Coral vs Soft Coral Control</i>	8	0.018240	36.1890	<b>0.0001</b>	10.450	<b>0.0021</b>
Week (Phase)	7	0.000464	1.62240	0.1269	4.3228	<b>0.0302</b>
Treatment x Species	6	0.005730	0.46945	0.8409	32.608	<b>0.0001</b>
<i>Hard Coral vs Soft Coral</i>	2	0.011918	0.53229	0.6206	25.308	<b>0.0001</b>
<i>Hard Coral vs Hard Coral Control</i>	2	6.51x10 <sup>-5</sup>	0.19076	0.8336	2.2448	0.0868
<i>Soft Coral vs Soft Coral Control</i>	2	0.010370	0.50512	0.6296	30.908	<b>0.0001</b>
Treatment x Phase	4	0.007582	3.73030	<b>0.0158</b>	9.2091	<b>0.0011</b>
Species x Phase	4	0.000897	0.30963	0.8630	39.958	<b>0.0001</b>
<i>Hard Coral vs Soft Coral</i>	1	0.003202	0.55026	0.4870	33.658	<b>0.0001</b>
<i>Hard Coral vs Hard Coral Control</i>	1	0.000564	3.96430	0.1177	3.8207	<b>0.0171</b>
<i>Soft Coral vs Soft Coral Control</i>	2	0.000540	0.12756	0.8812	31.034	<b>0.0001</b>
Treatment x Colony (Species)	24	0.007651	29.9230	<b>0.0001</b>	28.423	<b>0.0001</b>
<i>Hard Coral vs Soft Coral</i>	10	0.012279	25.2870	<b>0.0001</b>	10.009	<b>0.0001</b>
<i>Hard Coral vs Hard Coral Control</i>	4	0.000341	46.2560	<b>0.0001</b>	5.5379	<b>0.0002</b>

<i>Soft Coral vs Soft Coral Control</i>	16	0.009007	17.8700	<b>0.0001</b>	12.257	<b>0.0001</b>
Treatment x Week (Phase)	14	0.000312	1.12600	0.3370	2.8642	0.1495
Species x Week (Phase)	17	0.000316	1.23420	0.2475	11.063	<b>0.0001</b>
<i>Hard Coral vs Soft Coral</i>	5	0.000619	1.27420	0.2827	8.8384	<b>0.0001</b>
<i>Hard Coral vs Hard Coral Control</i>	6	3.22x10 <sup>-5</sup>	4.41930	<b>0.0010</b>	1.4561	0.2182
<i>Soft Coral vs Soft Coral Control</i>	6	0.000568	1.12770	0.3566	9.0264	<b>0.0001</b>
Colony (Species) x Phase	12	0.002871	11.2270	<b>0.0001</b>	17.998	<b>0.0001</b>
<i>Hard Coral vs Soft Coral</i>	6	0.005576	11.4820	<b>0.0001</b>	14.646	<b>0.0001</b>
<i>Hard Coral vs Hard Coral Control</i>	4	0.000142	19.3010	<b>0.0001</b>	7.3447	<b>0.0001</b>
<i>Soft Coral vs Soft Coral Control</i>	8	0.004235	8.40230	<b>0.0001</b>	8.7769	<b>0.0002</b>
Treatment x Species x Phase	8	0.002997	1.42300	0.2436	20.564	<b>0.0001</b>
<i>Hard Coral vs Soft Coral</i>	2	0.000918	0.22092	0.8237	16.650	<b>0.0001</b>
<i>Hard Coral vs Hard Coral Control</i>	2	2.39x10 <sup>-5</sup>	2.35880	0.1582	2.4643	<b>0.0208</b>
<i>Soft Coral vs Soft Coral Control</i>	4	0.005654	1.81360	0.1839	15.879	<b>0.0001</b>
Treatment x Species x Week (Phase)	34	0.000285	1.11600	0.3251	6.2367	0.7955
<i>Hard Coral vs Soft Coral</i>	10	0.000468	0.96453	0.4815	5.0652	0.0720
<i>Hard Coral vs Hard Coral Control</i>	12	1.43x10 <sup>-5</sup>	1.93930	<b>0.0426</b>	1.1622	0.9816
<i>Soft Coral vs Soft Coral Control</i>	12	0.000589	1.16890	0.3115	5.2991	0.0686
Treatment x Colony (Species) x Phase	24	0.002082	8.14150	<b>0.0001</b>	28.947	<b>0.0001</b>
<i>Hard Coral vs Soft Coral</i>	12	0.004059	8.36010	<b>0.0001</b>	4.3926	0.1665
<i>Hard Coral vs Hard Coral Control</i>	8	1.01x10 <sup>-5</sup>	1.37130	0.2230	9.2807	<b>0.0001</b>
<i>Soft Coral vs Soft Coral Control</i>	16	0.003118	6.18550	<b>0.0001</b>	16.853	<b>0.0001</b>
Res	144	0.000256				
Total	323					

*Post hoc* perMANOVA analyses of the interaction between treatment and phase revealed no significant differences in buoyant weight in any of the pairwise comparisons between temperature treatments (Table 3.3.7). It did, however, detect significant differences between the middle and final phase at 24.4°C ( $t = 6.35$ ;  $P_{(MC)} = 0.0033$ ) and 26.9°C ( $t = 4.52$ ;  $P_{(MC)} = 0.0124$ ) (Table 3.3.8). A marginally non-significant difference was evident between the middle and final phase in the warmest treatment ( $t = 2.16$ ;  $P_{(MC)} = 0.0980$ ). The majority of *post hoc* pairwise permDISP analyses were not significant but, when they were, they were not when significant perMANOVA differences were evident (Tables 3.3.7, 3.3.8).

**Table 3.3.7** *Post hoc* pairwise permutational ANOVA (permANOVA) and permutational analysis of dispersion (permDISP) comparisons investigating variation in the growth of hard and soft corals between the different temperature treatments for each phase of the experiment. Significant differences are indicated in bold ( $\alpha \leq 0.05$ ). \*Temperatures were increased to 29.8°C during the final phase of the bleaching-threshold treatment.

Source of variation	permANOVA pairwise comparisons		permDISP pairwise comparisons	
	<i>t</i>	<i>P</i> <sub>(MC)</sub>	<i>t</i>	<i>P</i> <sub>(perm)</sub>
<i>Initial Phase</i>				
24.4°C vs 26.9°C	0.66769	0.8788	1.0145	0.3770
24.4°C vs 28.8°C	0.86316	0.6910	0.2076	0.8626
26.9°C vs 28.8°C	0.76159	0.7454	1.0699	0.3570
<i>Middle Phase</i>				
24.4°C vs 26.9°C	0.92931	0.5965	0.6189	0.6567
24.4°C vs 28.8°C	1.05020	0.4822	1.7917	0.2371
26.9°C vs 28.8°C	0.98377	0.4988	1.3965	0.3562
<i>Final Phase</i>				
24.4°C vs 26.9°C	1.33090	0.2825	1.2807	0.2582
24.4°C vs 29.8°C*	1.68380	0.1779	3.2579	<b>0.0078</b>
26.9°C vs 29.8°C*	1.88500	0.1326	2.5138	0.0604

**Table 3.3.8** *Post hoc* pairwise permutational ANOVA and permutational analysis of dispersion (permDISP) comparisons investigating variation in the growth of hard and soft corals between different phases of the experiment for each temperature treatment. Significant differences are indicated in bold ( $\alpha \leq 0.05$ ). \*Temperatures were spiked to 29.8°C during the final phase of the bleaching-threshold treatment.

Source of variation	permANOVA pairwise comparisons		permDISP pairwise comparisons	
	<i>t</i>	<i>P</i> <sub>(MC)</sub>	<i>t</i>	<i>P</i> <sub>(perm)</sub>
<i>24.4°C (Control)</i>				
Initial Phase vs Middle Phase	1.0069	0.3356	1.6418	0.2147
Initial Phase vs Final Phase	1.7915	0.1288	2.2779	0.0502
Middle Phase vs Final Phase	6.3499	<b>0.0033</b>	0.8309	0.5459
<i>26.9°C (RCP 4.5)</i>				
Initial Phase vs Middle Phase	0.6969	0.5015	3.0376	<b>0.0035</b>
Initial Phase vs Final Phase	1.6075	0.1835	6.6721	<b>0.0001</b>
Middle Phase vs Final Phase	4.5223	<b>0.0124</b>	1.7770	0.1252
<i>28.8°C (Bleaching-threshold)</i>				
Initial Phase vs Middle Phase	0.5014	0.6326	2.4882	0.0697
Initial Phase vs Final Phase*	1.6538	0.1682	6.9778	<b>0.0002</b>
Middle Phase vs Final Phase*	2.1644	0.0980	2.5110	0.0643

*Post hoc* pairwise permANOVA and permDISP comparisons between hard corals and their control mounts revealed no significant differences in buoyant weight during any of the weeks,

neither in the initial or the middle phase, despite consistently larger changes in hard corals being evident relative to the control mounts. There were, however, marginally non-significant differences between hard corals and their control mounts at week 4 ( $t = 2.92$ ;  $P_{(MC)} = 0.0983$ ) of the initial phase, and at weeks 6 ( $t = 3.29$ ;  $P_{(MC)} = 0.0814$ ), 7 ( $t = 3.16$ ;  $P_{(MC)} = 0.0886$ ) and 8 ( $t = 3.14$ ;  $P_{(MC)} = 0.0871$ ) of the middle phase (Table 3.3.9).

**Table 3.3.9** *Post hoc* pairwise permutational ANOVA and permutational analysis of dispersion (permDISP) comparisons investigating variation in growth between hard coral and its control for each experimental phase during the different corresponding weeks. Significant differences are indicated in bold ( $\alpha \leq 0.05$ ).

Source of variation	permANOVA		permDISP	
	pairwise comparisons		pairwise comparisons	
	<i>t</i>	$P_{(MC)}$	<i>t</i>	$P_{(perm)}$
<b>Hard Coral vs Hard Coral Control</b>				
<i>Initial Phase</i>				
Week 1	1.1538	0.3672	0.38899	0.7394
Week 2	2.2196	0.1519	0.10117	0.9223
Week 3	2.4543	0.1308	0.59777	0.5359
Week 4	2.9218	0.0983	0.68231	0.5076
<i>Middle Phase</i>				
Week 5	2.7954	0.1125	0.10092	0.9332
Week 6	3.2878	0.0814	0.64286	0.5106
Week 7	3.1562	0.0886	0.35511	0.7389
Week 8	3.1363	0.0871	1.57850	0.1761

Nevertheless, when *post hoc* permANOVA analyses were conducted between hard corals and their control mounts for each specific temperature treatment, changes in weight in hard corals were found to be significantly higher compared to control mounts (Table 3.3.10). At 24.4°C during the middle phase, there was a significant difference at week 8 ( $t = 6.70$ ;  $P_{(MC)} = 0.0226$ ), with a marginally non-significant difference the week before ( $t = 3.72$ ;  $P_{(MC)} = 0.0652$ ). At 28.8°C, growth in hard corals was significantly higher relative to their control mounts during all the weeks in the initial phase ( $P_{(MC)} < 0.05$ ), as well as in weeks 5 ( $t = 5.85$ ;  $P_{(MC)} = 0.0274$ ) and 6 ( $t = 7.67$ ;  $P_{(MC)} = 0.0173$ ) during the middle phase. Results for week 7 ( $t = 4.01$ ;  $P_{(MC)} = 0.0570$ ) and week 8 ( $t = 3.74$ ;  $P_{(MC)} = 0.0632$ ) were marginally non-significant (Table 3.3.10). No differences in weight change were detected between the hard corals and their control mounts at 26.9°C. All the *post hoc* pairwise permDISP analyses detected no significant differences in dispersion (Table 3.3.10).

**Table 3.3.10** *Post hoc* pairwise permutational ANOVA and permutational analysis of dispersion (permDISP) comparisons investigating variation in growth between hard coral and its control for each temperature treatment during the different experimental phases and their corresponding weeks. Significant differences are indicated in bold ( $\alpha \leq 0.05$ ).

Source of variation	permANOVA		permDISP	
	pairwise comparisons		pairwise comparisons	
	<i>t</i>	<i>P</i> <sub>(MC)</sub>	<i>t</i>	<i>P</i> <sub>(perm)</sub>
<b>Hard Coral vs Hard Coral Control</b>				
<i>24.4°C (Control)</i>				
<i>Initial Phase</i>				
Week 1	0.41066	0.7200	0.30056	0.7924
Week 2	0.08458	0.9407	0.26259	0.8005
Week 3	0.82803	0.4986	0.23925	0.9012
Week 4	2.58880	0.1213	0.14307	0.8006
<i>Middle Phase</i>				
Week 5	1.7922	0.2168	0.73020	0.5954
Week 6	2.1922	0.1579	1.30620	0.6124
Week 7	3.7224	0.0652	0.83823	0.3934
Week 8	6.6900	<b>0.0226</b>	0.08555	0.8980
<i>26.9°C (RCP 4.5)</i>				
<i>Initial Phase</i>				
Week 1	0.99841	0.4210	0.64082	0.6982
Week 2	0.97819	0.4318	0.70042	0.5996
Week 3	1.27240	0.3279	0.71166	0.4011
Week 4	1.16130	0.3657	0.09319	0.8964
<i>Middle Phase</i>				
Week 5	1.0481	0.4030	0.12883	0.7999
Week 6	2.1483	0.1637	1.62110	0.2985
Week 7	1.3217	0.3194	0.68566	0.6090
Week 8	1.3042	0.3223	2.00450	0.1992
<i>28.8°C (Bleaching-threshold)</i>				
<i>Initial Phase</i>				
Week 1	13.420	<b>0.0065</b>	0.30569	0.4948
Week 2	7.7963	<b>0.0168</b>	0.09987	0.9008
Week 3	6.9731	<b>0.0208</b>	0.70014	0.3976
Week 4	6.2261	<b>0.0271</b>	1.17890	0.6011
<i>Middle Phase</i>				
Week 5	5.8528	<b>0.0274</b>	0.87392	0.6925
Week 6	7.6689	<b>0.0173</b>	0.96145	0.6052
Week 7	4.0085	0.0570	1.58980	0.2994
Week 8	3.7399	0.0632	1.39860	0.4993

The *a priori* analysis of change in weight of soft corals relative to their control mounts measured at weekly intervals in different treatments did not yield significant differences and thus no *post hoc* tests were carried out for this interaction term (Table 3.3.1).

### 3.3.2 Photosynthetic efficiency

All corals and live rock were visibly healthy up to week 5 of the experiment in all temperature treatments (Fig. 2.3.3). Furthermore, all specimens held at the control temperature of 24.4°C appeared to remain healthy for the full duration of the experiment. It is also noteworthy that, in the control treatment held at a constant temperature, none of the corals or live rock developed tissue necrosis, nor was any bleaching or mortality detected. The average  $\pm$  standard deviation (SD) photosynthetic efficiency ( $F_V/F_M$ ) stayed fairly consistent over time for both *Acropora appressa* ( $0.643 \pm 0.029 \mu\text{mol m}^{-2} \text{s}^{-1}$ ) and *Sinularia brassica* ( $0.627 \pm 0.021 \mu\text{mol m}^{-2} \text{s}^{-1}$ ) in the 24.4°C treatment (Figs. 3.3.5, 3.3.6).

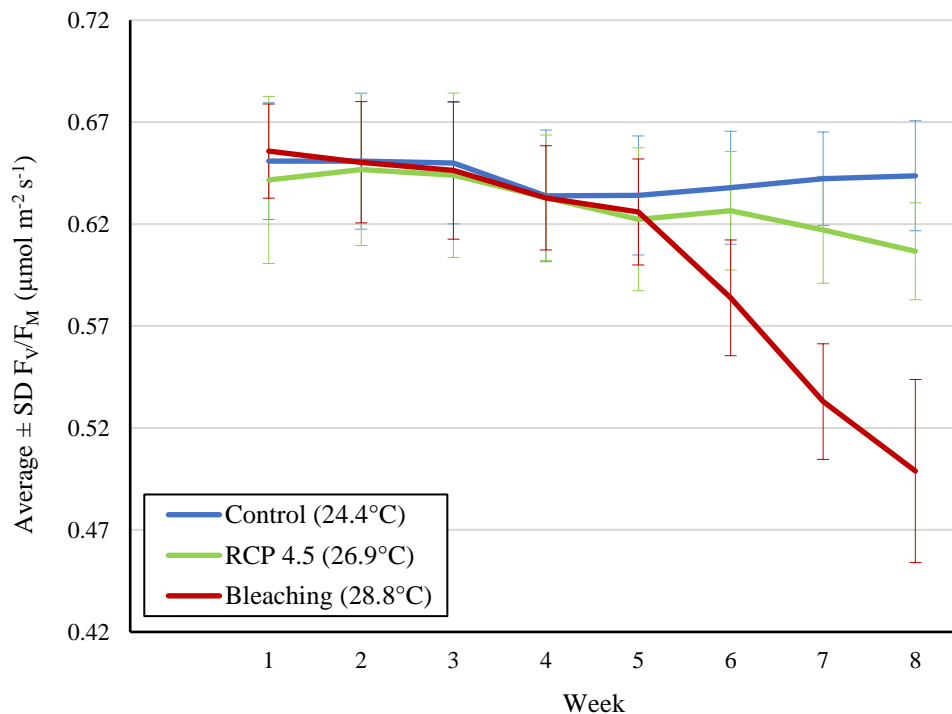


**Figure 3.3.5** Average  $\pm$  standard deviation (SD) photosynthetic efficiency ( $F_V/F_M$ ) of the hard coral *Acropora appressa* throughout the experiment.

Contrastingly, the  $F_V/F_M$  for both *A. appressa* and *S. brassica* decreased with time at 26.9 °C and especially at 28.8°C (Figs. 3.3.5, 3.3.6). These decreases in  $F_V/F_M$  became more evident during weeks 5 and 6 of the experiment. Furthermore, the  $F_V/F_M$  for corals exposed to the 28.8°C treatment declined sooner and faster than those corals exposed to the 26.9°C treatment (Figs. 3.3.5, 3.3.6). Despite a similar trend in the  $F_V/F_M$  at 28.8°C for both corals, *A. appressa* indicated much greater stress than *S. brassica*, with an average weekly reduction  $\pm$  SD  $F_V/F_M$  of  $22.49 \pm$

1.66% relative to a reduction of  $11.69 \pm 1.65\%$  for *S. brassica*. Overall, *A. appressa* was  $12.49 \pm 1.54\%$  less photosynthetically efficient than *S. brassica* at  $28.8^\circ\text{C}$ .

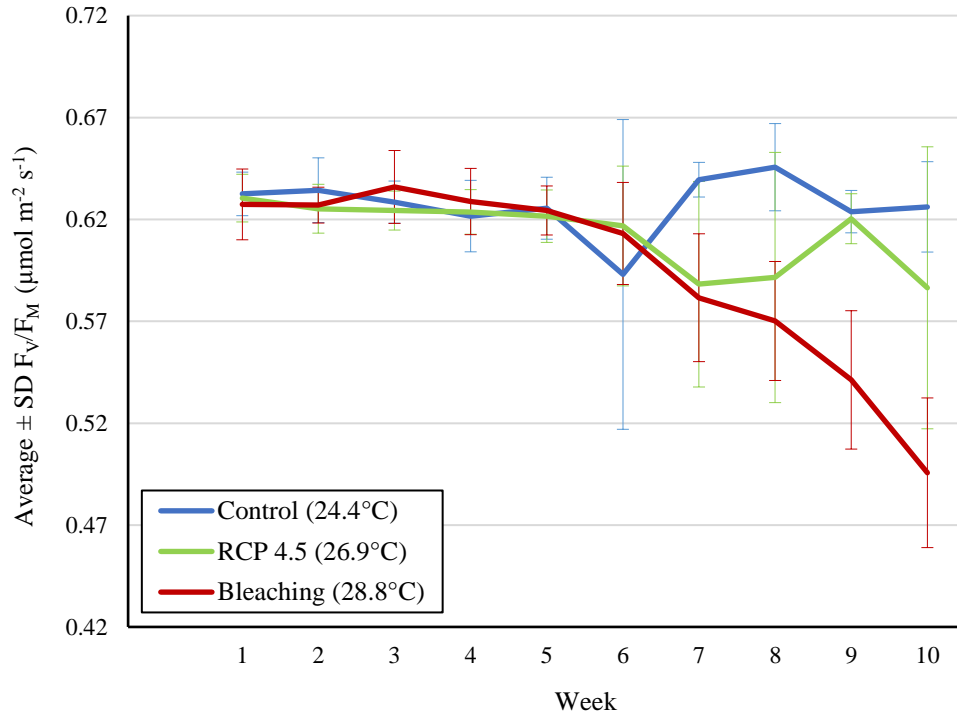


**Figure 3.3.6** Average  $\pm$  standard deviation (SD) photosynthetic efficiency ( $F_v/F_M$ ) of the soft coral *Sinularia brassica* throughout the experiment.

Live rock yielded relatively consistent average  $\pm$  SD levels of photosynthetic efficiency throughout the 10 weeks of experimentation at all the temperature treatments ( $0.505 \pm 0.033 \mu\text{mol m}^{-2} \text{s}^{-1}$  at  $24.4^\circ\text{C}$ ,  $0.510 \pm 0.014 \mu\text{mol m}^{-2} \text{s}^{-1}$  at  $26.9^\circ\text{C}$  and  $0.508 \pm 0.022 \mu\text{mol m}^{-2} \text{s}^{-1}$  at  $28.8^\circ\text{C}$ ) (Fig. 3.3.7).

The *a priori* perMANOVA investigating variation in photosynthetic efficiency of hard and soft corals, as well as live rock, revealed that the following terms differed significantly: species ( $F_{(\text{Pseudo})} = 51.07$ ;  $P_{(\text{MC})} = 0.0003$ ), phase ( $F_{(\text{Pseudo})} = 16.70$ ;  $P_{(\text{MC})} = 0.0003$ ), week nested in phase ( $F_{(\text{Pseudo})} = 9.13$ ;  $P_{(\text{MC})} = 0.0001$ ), the interaction of treatment and phase ( $F_{(\text{Pseudo})} = 14.22$ ;  $P_{(\text{MC})} = 0.0001$ ), treatment and week nested in phase ( $F_{(\text{Pseudo})} = 2.78$ ;  $P_{(\text{MC})} = 0.0010$ ), species and week nested in phase ( $F_{(\text{Pseudo})} = 2.57$ ;  $P_{(\text{MC})} = 0.0053$ ) and the three-way interaction of treatment-species-phase ( $F_{(\text{Pseudo})} = 2.89$ ;  $P_{(\text{MC})} = 0.0450$ ) (Table 3.3.11). The interaction of treatment and species ( $F_{(\text{Pseudo})} = 3.27$ ;  $P_{(\text{MC})} = 0.0930$ ), and treatment-species-week nested in phase ( $F_{(\text{Pseudo})} = 1.54$ ;  $P_{(\text{MC})} = 0.0680$ ) were marginally non-significant.

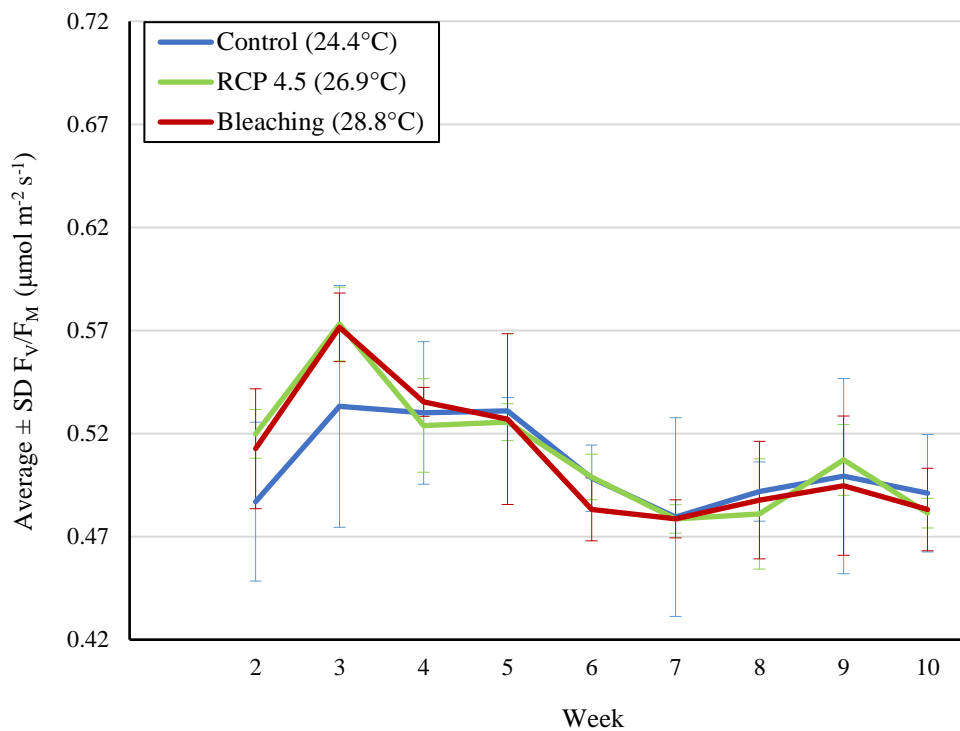


**Figure 3.3.7** Average  $\pm$  standard deviation (SD) photosynthetic efficiency ( $F_v/F_M$ ) of live rock throughout the experiment.

Several *a priori* pairwise contrasts between species were also significant and these usually involved both coral species with live rock, but not between coral species themselves. Exceptions were between hard and soft corals involving the random effect of colony nested within species and interactions of colony nested within species with the fixed effect of phase (Table 3.3.11).

*A priori* permDISP analyses revealed significant differences in dispersion according to phase ( $F = 8.20$ ;  $P_{(\text{perm})} = 0.0020$ ), week nested in phase ( $F = 5.35$ ;  $P_{(\text{perm})} = 0.0001$ ), the interactions between treatment and species ( $F = 4.90$ ;  $P_{(\text{perm})} = 0.0006$ ), treatment and phase ( $F = 3.58$ ;  $P_{(\text{perm})} = 0.0060$ ), species and phase ( $F = 9.28$ ;  $P_{(\text{perm})} = 0.0001$ ), treatment and week nested in phase ( $F = 2.55$ ;  $P_{(\text{perm})} = 0.0032$ ), species and week nested in phase ( $F = 5.27$ ;  $P_{(\text{perm})} = 0.0001$ ), and the three-way interaction of treatment, species and phase ( $F = 2.32$ ;  $P_{(\text{perm})} = 0.0092$ ) (Table 3.3.11).

**Table 3.3.11** Permutational ANOVA (permANOVA) and permutational analysis of dispersion (permDISP) investigating variation in photosynthetic efficiency among hard and soft coral, as well as live rock, exposed to different temperature treatments. *A priori* pairwise contrasts between species are given in italics. Significant differences are indicated in bold ( $\alpha \leq 0.05$ ).

Source of variation	permANOVA				permDISP	
	df	MS	$F_{(Pseudo)}$	$P_{(MC)}$	$F$	$P_{(perm)}$
Treatment	2	0.011090	2.6278	0.1407	0.7918	0.5898
Species	2	0.330790	51.073	<b>0.0003</b>	1.7990	0.2604
<i>Hard Coral vs Soft Coral</i>	1	0.008138	1.1925	0.3632	2.4566	0.2375
<i>Hard Coral vs Live Rock</i>	1	0.530100	53.810	<b>0.0064</b>	2.9520	0.0940
<i>Soft Coral vs Live Rock</i>	1	0.458130	134.01	<b>0.0016</b>	0.0034	0.9645
Phase	2	0.035305	16.700	<b>0.0003</b>	8.2006	<b>0.0020</b>
Mesocosm (Treatment)	6	0.004810	1.5341	0.2604	2.0741	0.2672
Colony (Species)	6	0.005053	11.058	<b>0.0001</b>	6.0002	<b>0.0174</b>
<i>Hard Coral vs Soft Coral</i>	3	0.005175	13.828	<b>0.0001</b>	1.3536	0.5665
<i>Hard Coral vs Live Rock</i>	3	0.007357	19.068	<b>0.0001</b>	10.944	<b>0.0001</b>
<i>Soft Coral vs Live Rock</i>	3	0.002875	4.7494	<b>0.0044</b>	4.6560	<b>0.0123</b>
Week (Phase)	7	0.004291	9.1307	<b>0.0001</b>	5.3513	<b>0.0001</b>
Treatment x Species	4	0.002738	3.2653	0.0930	4.8978	<b>0.0006</b>
<i>Hard Coral vs Soft Coral</i>	2	3.90x10 <sup>-6</sup>	0.0078	0.9930	6.7811	<b>0.0006</b>
<i>Hard Coral vs Live Rock</i>	2	0.003921	4.7566	0.1179	5.0097	<b>0.0009</b>
<i>Soft Coral vs Live Rock</i>	2	0.004271	3.6445	0.1572	3.3411	<b>0.0206</b>
Treatment x Phase	4	0.008438	14.221	<b>0.0001</b>	3.5814	<b>0.0060</b>
Species x Phase	3	0.001960	0.9188	0.4599	9.2847	<b>0.0001</b>
<i>Hard Coral vs Soft Coral</i>	1	0.003773	1.6840	0.2397	13.490	<b>0.0001</b>
<i>Hard Coral vs Live Rock</i>	1	3.08x10 <sup>-5</sup>	0.0715	1	3.9564	<b>0.0058</b>
<i>Soft Coral vs Live Rock</i>	2	0.002009	1.0496	0.3859	11.831	<b>0.0001</b>
Treatment x Colony (Species)	6	0.000839	1.8353	0.0964	2.8499	0.0923
<i>Hard Coral vs Soft Coral</i>	3	0.000500	1.3371	0.2705	8.2849	<b>0.0001</b>
<i>Hard Coral vs Live Rock</i>	3	0.000824	2.1362	0.1039	5.4004	<b>0.0001</b>
<i>Soft Coral vs Live Rock</i>	3	0.001179	1.9362	0.1314	3.1605	<b>0.0079</b>
Treatment x Week (Phase)	14	0.001273	2.7789	<b>0.0010</b>	2.5514	<b>0.0032</b>
Species x Week (Phase)	12	0.001173	2.5666	<b>0.0053</b>	5.2672	<b>0.0001</b>
<i>Hard Coral vs Soft Coral</i>	6	0.000416	1.1035	0.3660	6.2663	<b>0.0001</b>
<i>Hard Coral vs Live Rock</i>	5	0.001936	5.0161	<b>0.0008</b>	3.4681	<b>0.0011</b>
<i>Soft Coral vs Live Rock</i>	6	0.001466	2.4222	<b>0.0336</b>	5.6332	<b>0.0001</b>
Colony (Species) x Phase	14	0.001841	4.0284	<b>0.0001</b>	4.8001	<b>0.0002</b>
<i>Hard Coral vs Soft Coral</i>	8	0.001659	4.4341	<b>0.0004</b>	6.0108	<b>0.0003</b>
<i>Hard Coral vs Live Rock</i>	8	0.001522	3.9453	<b>0.0008</b>	7.3346	<b>0.0001</b>
<i>Soft Coral vs Live Rock</i>	12	0.001719	2.8395	<b>0.0028</b>	3.7738	<b>0.0009</b>
Treatment x Species x Phase	6	0.001397	2.8927	<b>0.0450</b>	2.3172	<b>0.0092</b>
<i>Hard Coral vs Soft Coral</i>	2	0.000672	1.6614	0.2438	3.2123	<b>0.0048</b>
<i>Hard Coral vs Live Rock</i>	2	0.001023	1.9510	0.1897	1.9796	<b>0.0444</b>
<i>Soft Coral vs Live Rock</i>	4	0.001548	2.8494	0.0695	1.7637	0.1392
Treatment x Species x Week (Phase)	24	0.000705	1.5429	0.0680	2.3197	0.2065
<i>Hard Coral vs Soft Coral</i>	12	0.000435	1.1635	0.3126	2.1756	0.4342
<i>Hard Coral vs Live Rock</i>	10	0.001143	2.9608	<b>0.0032</b>	1.6314	0.7114
<i>Soft Coral vs Live Rock</i>	12	0.000687	1.1358	0.3451	3.0642	0.0626

Treatment x Colony (Species) x Phase	16	0.000483	1.0573	0.3967	3.1657	<b>0.0009</b>
<i>Hard Coral vs Soft Coral</i>	10	0.000383	1.0236	0.4257	4.5000	<b>0.0014</b>
<i>Hard Coral vs Live Rock</i>	10	0.000515	1.3335	0.2294	5.3792	<b>0.0001</b>
<i>Soft Coral vs Live Rock</i>	12	0.000540	0.8928	0.5565	3.8344	<b>0.0001</b>
Res	114	0.000457				
Total	242					

*Post hoc* pairwise permANOVA analyses revealed that photosynthetic efficiency was significantly higher in the initial phase compared to the middle ( $t = 4.81$ ;  $P_{(MC)} = 0.0013$ ) and final phases ( $t = 3.97$ ;  $P_{(MC)} = 0.0083$ ), but not between the middle and final phases ( $t = 1.7074$ ;  $P_{(MC)} = 0.1417$ ) (Table 3.3.12). Significant dispersion was only evident between the initial and middle phases ( $t = 4.00$ ;  $P_{(perm)} = 0.0010$ ) (Table 3.3.12).

**Table 3.3.12** *Post hoc* pairwise permutational ANOVA (permANOVA) and permutational analysis of dispersion (permDISP) comparisons of photosynthetic efficiency of hard and soft coral, as well as live rock, between different phases of the experiment. Significant differences are indicated in bold ( $\alpha \leq 0.05$ ).

Source of variation	permANOVA		permDISP	
	pairwise comparisons		pairwise comparisons	
	$t$	$P_{(MC)}$	$t$	$P_{(perm)}$
Initial Phase vs Middle Phase	4.8085	<b>0.0013</b>	4.0025	<b>0.0010</b>
Initial Phase vs Final Phase	3.9661	<b>0.0083</b>	1.9799	0.0755
Middle Phase vs Final Phase	1.7074	0.1417	0.79841	0.4341

*Post hoc* pairwise permANOVA comparisons between weeks nested in phase revealed significant differences in photosynthetic efficiency between weeks 1 and 4 ( $t = 2.95$ ;  $P_{(MC)} = 0.0116$ ), 2 and 3 ( $t = 2.62$ ;  $P_{(MC)} = 0.0169$ ), and 3 and 4 ( $t = 3.44$ ;  $P_{(MC)} = 0.0030$ ) during the initial phase, with preceding weeks having higher photosynthetic efficiency. Weeks 1 and 3 were marginally non-significant ( $t = 1.92$ ;  $P_{(MC)} = 0.0801$ ). Weeks 5 and 6 ( $t = 3.57$ ;  $P_{(MC)} = 0.0026$ ), 5 and 7 ( $t = 5.85$ ;  $P_{(MC)} = 0.0001$ ), and 5 and 8 ( $t = 6.32$ ;  $P_{(MC)} = 0.0001$ ) during the middle phase also differed, with photosynthetic efficiency being higher in week 5 than in each of the subsequent weeks. Photosynthetic efficiency between weeks 6 and 7 ( $t = 1.88$ ;  $P_{(MC)} = 0.0751$ ), and 6 and 8 ( $t = 1.95$ ;  $P_{(MC)} = 0.0654$ ) during the middle phase, was marginally non-significant (Table 3.3.13). In the final phase, photosynthetic efficiency was significantly higher in week 9 compared to week 10 ( $t = 2.32$ ;  $P_{(MC)} = 0.0409$ ). *Post hoc* pairwise permDISP analyses indicated significant differences in dispersion involving week 1 and 5 with most other weeks nested in their respective phases ( $P_{(perm)} < 0.05$ ), and between week 2 and 3 ( $P_{(perm)} = 0.0322$ ) of the initial phase (Table 3.3.13).

**Table 3.3.13** *Post hoc* pairwise permutational ANOVA (permANOVA) and permutational analysis of dispersion (permDISP) comparisons of photosynthetic efficiency between weeks for each phase of the experiment. Significant differences are indicated in bold ( $\alpha \leq 0.05$ ).

Source of variation	permANOVA		permDISP	
	pairwise comparisons		pairwise comparisons	
	<i>t</i>	$P_{(MC)}$	<i>t</i>	$P_{(perm)}$
<i>Initial Phase</i>				
Week 1 vs Week 2	0.6280	0.5388	4.7146	<b>0.0001</b>
Week 1 vs Week 3	1.9209	0.0801	2.0738	<b>0.0427</b>
Week 1 vs Week 4	2.9495	<b>0.0116</b>	3.6469	<b>0.0020</b>
Week 2 vs Week 3	2.6188	<b>0.0169</b>	2.7397	<b>0.0322</b>
Week 2 vs Week 4	0.1809	0.8570	1.8602	0.1956
Week 3 vs Week 4	3.4396	<b>0.0030</b>	1.1259	0.3881
<i>Middle Phase</i>				
Week 5 vs Week 6	3.5733	<b>0.0026</b>	2.07090	0.0964
Week 5 vs Week 7	5.8455	<b>0.0001</b>	2.39660	<b>0.0259</b>
Week 5 vs Week 8	6.3232	<b>0.0001</b>	2.72130	<b>0.0095</b>
Week 6 vs Week 7	1.8817	0.0751	0.48783	0.6309
Week 6 vs Week 8	1.9468	0.0654	0.72255	0.4775
Week 7 vs Week 8	0.4103	0.6817	0.19875	0.8320
<i>Final Phase</i>				
Week 9 vs Week 10	2.3230	<b>0.0409</b>	0.29662	0.8266

*Post hoc* pairwise permANOVA analyses of the interaction of treatment and phase for each phase established that photosynthetic efficiency was significantly higher in the 24.4°C control treatment compared to 28.8°C during the middle phase ( $t = 3.18$ ;  $P_{(MC)} = 0.0218$ ) (Table 3.3.14). During the final phase, when temperatures were increased to 29.8°C in the warmest treatment, photosynthetic efficiency was significantly higher at both 24.4°C and 26.9°C relative to 29.8°C ( $t = 2.96$ ;  $P_{(MC)} = 0.0301$  and  $t = 2.44$ ;  $P_{(MC)} = 0.0491$ , respectively) (Table 3.3.14). No significant differences in photosynthetic efficiency were detected between treatments during the initial phase and between 24.4°C and 26.9°C in the final phase ( $t = 0.55$ ;  $P_{(MC)} = 0.6340$ ).

**Table 3.3.14** *Post hoc* pairwise permutational ANOVA (permANOVA) and permutational analysis of dispersion (permDISP) comparisons of photosynthetic efficiency between different temperature treatments for the initial, middle and final phases of the experiment. Significant differences are indicated in bold ( $\alpha \leq 0.05$ ). \*Temperatures were spiked to 29.8°C during the final phase of the bleaching-threshold treatment.

Source of variation	permANOVA		permDISP	
	pairwise comparisons		pairwise comparisons	
	<i>t</i>	<i>P</i> <sub>(MC)</sub>	<i>t</i>	<i>P</i> <sub>(perm)</sub>
<i>Initial Phase</i>				
24.4°C vs 26.9°C	0.53982	0.8893	1.00050	0.4689
24.4°C vs 28.8°C	0.50854	0.8537	1.08520	0.4607
26.9°C vs 28.8°C	0.50531	0.9422	0.11251	0.9336
<i>Middle Phase</i>				
24.4°C vs 26.9°C	1.67960	0.1510	1.12190	0.4159
24.4°C vs 28.8°C	3.17660	<b>0.0218</b>	1.79410	0.1074
26.9°C vs 28.8°C	1.66250	0.1633	0.71076	0.4962
<i>Final Phase</i>				
24.4°C vs 26.9°C	0.54602	0.6340	0.40113	0.6761
24.4°C vs 29.8°C*	2.96060	<b>0.0301</b>	3.86580	<b>0.0005</b>
26.9°C vs 29.8°C*	2.44300	<b>0.0491</b>	4.07980	<b>0.0016</b>

*Post hoc* permANOVA analyses of the treatment-phase interaction for each treatment indicated that photosynthetic efficiency was significantly higher during the initial phase compared to the middle phase in the 26.9°C treatment ( $t = 3.55$ ;  $P_{(MC)} = 0.0121$ ), and marginally non-significant between the initial and final phases of this treatment ( $t = 2.53$ ;  $P_{(MC)} = 0.0707$ ) (Table 3.3.15). During the 28.8°C treatment, when temperatures were increased to 29.8°C in the final phase, photosynthetic efficiency was significantly higher in the initial phase compared to both the middle ( $t = 10.55$ ;  $P_{(MC)} = 0.0001$ ) and final phases ( $t = 9.96$ ;  $P_{(MC)} = 0.0005$ ). Photosynthetic efficiency was also significantly higher during the middle phase compared to the final phase ( $t = 3.21$ ;  $P_{(MC)} = 0.0337$ ) (Table 3.3.15). Contrastingly, no significant differences were detected in photosynthetic efficiency between any of the phases in the control temperature of 24.4°C.

The *post hoc* pairwise permDISP indicated that there was significant dispersion between 24.4°C and 29.8°C ( $t = 3.87$ ;  $P_{(perm)} = 0.0005$ ), and 26.9°C and 29.8°C ( $t = 4.08$ ;  $P_{(perm)} = 0.0016$ ) during the final phase (Table 3.3.14). Significant dispersion was also detected between the initial and final phase for the 26.9°C treatment ( $t = 2.30$ ;  $P_{(perm)} = 0.0379$ ), as well as between the middle and final phases ( $t = 2.67$ ;  $P_{(perm)} = 0.0113$ ) of the 28.8°C treatment that was finally increased to 29.8°C (Table 3.3.15).

**Table 3.3.15** *Post hoc* pairwise permutational ANOVA (permANOVA) and permutational analysis of dispersion (permDISP) comparisons of photosynthetic efficiency between different phases of the experiment for each temperature treatment. Significant differences are indicated in bold ( $\alpha \leq 0.05$ ). \*Temperatures were increased to 29.8°C during the final phase of the bleaching-threshold treatment.

Source of variation	permANOVA		permDISP	
	pairwise comparisons		pairwise comparisons	
	<i>t</i>	<i>P</i> <sub>(MC)</sub>	<i>t</i>	<i>P</i> <sub>(perm)</sub>
<i>24.4°C (Control)</i>				
Initial Phase vs Middle Phase	1.24660	0.2631	1.8378	0.2198
Initial Phase vs Final Phase	0.84413	0.4409	1.3766	0.3015
Middle Phase vs Final Phase	0.29404	0.7812	0.1443	0.9077
<i>26.9°C (RCP 4.5)</i>				
Initial Phase vs Middle Phase	3.54560	<b>0.0121</b>	2.3475	0.0605
Initial Phase vs Final Phase	2.53070	0.0707	2.2995	<b>0.0379</b>
Middle Phase vs Final Phase	0.41524	0.6989	0.6102	0.5828
<i>28.8°C (Bleaching-threshold)</i>				
Initial Phase vs Middle Phase	10.5520	<b>0.0001</b>	1.7615	0.1071
Initial Phase vs Final Phase*	9.96090	<b>0.0005</b>	1.1185	0.3469
Middle Phase vs Final Phase*	3.20980	<b>0.0337</b>	2.6734	<b>0.0113</b>

*Post hoc* pairwise permANOVA analyses between temperature treatments for each week nested within a phase revealed photosynthetic efficiency to be significantly higher at 24.4°C during week 7 of the middle phase compared to the same week at 28.8°C ( $t = 7.96$ ;  $P_{(MC)} = 0.0011$ ) (Table 3.3.16). Photosynthetic efficiency was also significantly higher during week 8 at 24.4°C compared to the same week at 28.8°C ( $t = 3.99$ ;  $P_{(MC)} = 0.0176$ ). In addition, photosynthetic efficiency during week 10 of the final phase was significantly higher at 24.4°C compared to levels when temperatures were increased to 29.8°C ( $t = 4.49$ ;  $P_{(MC)} = 0.0089$ ) (Table 3.3.16). Marginally non-significant differences were detected between 26.9° and 28.8°C ( $t = 2.24$ ;  $P_{(MC)} = 0.0848$ ), and 24.4°C and 26.9°C ( $t = 2.42$ ;  $P_{(MC)} = 0.0668$ ) at week 8 during the middle phase, and between 26.9°C and 29.8°C at week 9 ( $t = 2.46$ ;  $P_{(MC)} = 0.0670$ ) and 10 ( $t = 2.42$ ;  $P_{(MC)} = 0.0712$ ) during the final phase.

*Post hoc* pairwise permDISP analyses yielded significant differences in dispersion of photosynthetic efficiency at week 9 during the final phase between 24.4°C and 29.8°C ( $t = 2.08$ ;  $P_{(perm)} = 0.0456$ ), and between 26.9°C and 29.8°C ( $t = 2.55$ ;  $P_{(perm)} = 0.0262$ ). During week 10 of the final phase, there was also a significant difference in dispersion between 24.4° and 29.8°C ( $t = 4.12$ ;  $P_{(perm)} = 0.0046$ ) (Table 3.3.16).

**Table 3.3.16** *Post hoc* pairwise permutational ANOVA (permANOVA) and permutational analysis of dispersion (permDISP) comparisons of photosynthetic efficiency between each temperature treatment, for each week, according to the three phases of the experiment. Significant differences are indicated in bold ( $\alpha \leq 0.05$ ). \*Temperatures were increased to 29.8°C during the final phase of the bleaching-threshold treatment.

Source of variation	permANOVA		permDISP	
	pairwise comparisons		pairwise comparisons	
	<i>t</i>	<i>P</i> <sub>(MC)</sub>	<i>t</i>	<i>P</i> <sub>(perm)</sub>
<b>Initial Phase</b>				
<i>Week 1</i>				
24.4°C vs 26.9°C	0.76797	0.6472	0.46492	0.6804
24.4°C vs 28.8°C	0.40586	0.9349	0.29604	0.8133
26.9°C vs 28.8°C	0.55929	0.8511	0.23456	0.7966
<i>Week 2</i>				
24.4°C vs 26.9°C	0.78344	0.6897	1.10730	0.4659
24.4°C vs 28.8°C	0.65468	0.8288	0.81060	0.6038
26.9°C vs 28.8°C	0.39261	0.9778	0.29863	0.8323
<i>Week 3</i>				
24.4°C vs 26.9°C	0.64553	0.7335	1.08010	0.4108
24.4°C vs 28.8°C	0.69935	0.6367	1.18740	0.4055
26.9°C vs 28.8°C	0.80160	0.7141	0.16295	0.8660
<i>Week 4</i>				
24.4°C vs 26.9°C	0.78013	0.6812	0.22606	0.8608
24.4°C vs 28.8°C	0.81520	0.6955	0.08245	0.9525
26.9°C vs 28.8°C	0.60146	0.8103	0.34915	0.8183
<b>Middle Phase</b>				
<i>Week 5</i>				
24.4°C vs 26.9°C	1.10170	0.4292	0.10988	0.9320
24.4°C vs 28.8°C	0.51361	0.9282	0.02035	0.9896
26.9°C vs 28.8°C	0.52469	0.9337	0.11895	0.9272
<i>Week 6</i>				
24.4°C vs 26.9°C	1.0118	0.4919	1.13030	0.3430
24.4°C vs 28.8°C	1.1427	0.3839	1.40950	0.2106
26.9°C vs 28.8°C	1.8488	0.1427	0.18854	0.8898
<i>Week 7</i>				
24.4°C vs 26.9°C	1.9166	0.1218	0.73935	0.5771
24.4°C vs 28.8°C	7.9599	<b>0.0011</b>	2.15060	0.1003
26.9°C vs 28.8°C	2.2389	0.0848	1.70220	0.1003
<i>Week 8</i>				
24.4°C vs 26.9°C	2.4230	0.0668	0.5285	0.6993
24.4°C vs 28.8°C	3.9879	<b>0.0176</b>	2.1079	0.0796
26.9°C vs 28.8°C	1.9742	0.1173	1.8550	0.0673
<b>Final Phase</b>				
<i>Week 9</i>				
24.4°C vs 26.9°C	0.5065	0.8051	0.4151	0.7119
24.4°C vs 29.8°C*	1.9774	0.1159	2.0830	<b>0.0456</b>
26.9°C vs 29.8°C*	2.4639	0.0670	2.5540	<b>0.0262</b>

<i>Week 10</i>				
24.4°C vs 26.9°C	1.1893	0.3326	0.45588	0.6874
24.4°C vs 29.8°C*	4.4893	<b>0.0089</b>	4.11680	<b>0.0046</b>
26.9°C vs 29.8°C*	2.4214	0.0712	3.03490	0.0568

*Post hoc* pairwise permANOVA yielded no significant differences in photosynthetic efficiency between different weeks nested in phase in the 24.4°C control treatment (Table 3.3.17). However, photosynthetic efficiency at 26.9°C was significantly higher in week 2 compared to week 3 ( $t = 6.94$ ;  $P_{(MC)} = 0.0005$ ), and in week 3 compared to week 4 ( $t = 4.11$ ;  $P_{(MC)} = 0.0075$ ) during the initial phase when temperatures were raised. During the middle phase, when temperatures were held constant at 26.9°C, photosynthetic efficiency in weeks 5 and 6 was significantly higher than in week 7 ( $t = 3.35$ ;  $P_{(MC)} = 0.0152$  and  $t = 3.42$ ;  $P_{(MC)} = 0.0125$ , respectively). There were marginally non-significant differences during the middle phase at 26.9°C between weeks 5 and 8 ( $t = 2.37$ ;  $P_{(MC)} = 0.0558$ ), and 6 and 8 ( $t = 2.20$ ;  $P_{(MC)} = 0.0678$ ).

When temperatures were raised during the initial phase in the 28.8°C treatment, the photosynthetic efficiency was significantly higher in most preceding weeks relative to subsequent weeks, specifically between weeks 1 and 4 ( $t = 5.24$ ;  $P_{(MC)} = 0.0063$ ), 2 and 3 ( $t = 3.05$ ;  $P_{(MC)} = 0.0196$ ), and 3 and 4 ( $t = 3.52$ ;  $P_{(MC)} = 0.0131$ ). When the temperature was held constant at 28.8°C during the middle phase of this treatment, a similar pattern of significantly higher levels of photosynthetic efficiency relative to subsequent weeks was observed for weeks 5 and 6 ( $t = 5.04$ ;  $P_{(MC)} = 0.0025$ ), 5 and 7 ( $t = 5.09$ ;  $P_{(MC)} = 0.0025$ ), 5 and 8 ( $t = 7.17$ ;  $P_{(MC)} = 0.0005$ ), 6 and 7 ( $t = 2.53$ ;  $P_{(MC)} = 0.0452$ ), and 6 and 8 ( $t = 4.36$ ;  $P_{(MC)} = 0.0047$ ) (Table 3.3.17). Pairwise analyses of dispersion only indicated a significant difference between week 1 and 2 ( $t = 2.57$ ;  $P_{(perm)} = 0.0371$ ), during the initial phase of the 28.8°C treatment (Table 3.3.17).

**Table 3.3.17** *Post hoc* pairwise permutational ANOVA (permANOVA) and permutational analysis of dispersion (permDISP) comparisons of photosynthetic efficiency between different weeks during each experimental phase of the experiment for different temperature treatments. Significant differences are indicated in bold ( $\alpha \leq 0.05$ ). \*Temperatures were increased to 29.8°C during the final phase of the bleaching-threshold treatment.

Source of variation	permANOVA		permDISP	
	pairwise comparisons		pairwise comparisons	
	<i>t</i>	$P_{(MC)}$	<i>t</i>	$P_{(perm)}$
<i>24.4°C (Control)</i>				
<i>Initial Phase</i>				
Week 1 vs Week 2	0.36082	0.7302	3.2010	<b>0.0142</b>
Week 1 vs Week 3	1.64130	0.1768	1.7130	0.1259
Week 1 vs Week 4	1.60890	0.1823	1.8985	0.1037

Week 2 vs Week 3	0.75844	0.4869	1.2420	0.4154
Week 2 vs Week 4	0.29668	0.7831	1.6395	0.2807
Week 3 vs Week 4	0.76588	0.4695	0.2263	0.8772

*Middle Phase*

Week 5 vs Week 6	1.32860	0.2355	2.32580	<b>0.0316</b>
Week 5 vs Week 7	1.14370	0.2886	1.82320	0.2654
Week 5 vs Week 8	0.73351	0.4789	1.77380	0.2206
Week 6 vs Week 7	0.69134	0.5117	0.27883	0.8414
Week 6 vs Week 8	0.92777	0.3840	0.01173	0.9942
Week 7 vs Week 8	0.76954	0.4704	0.22815	0.8996

*Final Phase*

Week 9 vs Week 10	0.40244	0.7099	0.34019	0.7329
-------------------	---------	--------	---------	--------

*26.9°C (RCP 4.5)*

*Initial Phase*

Week 1 vs Week 2	0.0115	0.9907	2.1570	0.0840
Week 1 vs Week 3	0.6468	0.5664	0.8481	0.4036
Week 1 vs Week 4	1.3246	0.2575	2.0281	0.1421
Week 2 vs Week 3	6.9381	<b>0.0005</b>	1.6464	0.1452
Week 2 vs Week 4	1.0825	0.3134	0.3916	0.7788
Week 3 vs Week 4	4.1137	<b>0.0075</b>	1.3568	0.2380

*Middle Phase*

Week 5 vs Week 6	1.9413	0.1031	0.76615	0.5480
Week 5 vs Week 7	3.3501	<b>0.0152</b>	1.26810	0.2452
Week 5 vs Week 8	2.3669	0.0558	1.44370	0.2040
Week 6 vs Week 7	3.4210	<b>0.0125</b>	0.40165	0.7289
Week 6 vs Week 8	2.1964	0.0678	0.48632	0.6912
Week 7 vs Week 8	0.2208	0.8295	0.06361	0.9529

*Final Phase*

Week 9 vs Week 10	1.5730	0.1970	0.32240	0.8184
-------------------	--------	--------	---------	--------

*28.8°C (Bleaching-threshold)*

*Initial Phase*

Week 1 vs Week 2	0.9159	0.4167	2.5699	<b>0.0371</b>
Week 1 vs Week 3	1.1058	0.3226	0.8949	0.3808
Week 1 vs Week 4	5.2383	<b>0.0063</b>	2.1855	0.0771
Week 2 vs Week 3	3.0541	<b>0.0196</b>	2.0437	0.1094
Week 2 vs Week 4	0.3569	0.7285	1.0415	0.4771
Week 3 vs Week 4	3.5218	<b>0.0131</b>	1.2333	0.3016

*Middle Phase*

Week 5 vs Week 6	5.03600	<b>0.0025</b>	0.60617	0.6495
Week 5 vs Week 7	5.09200	<b>0.0025</b>	0.37592	0.7488
Week 5 vs Week 8	7.17330	<b>0.0005</b>	0.26083	0.8236
Week 6 vs Week 7	2.53310	<b>0.0452</b>	1.04990	0.3285
Week 6 vs Week 8	4.35750	<b>0.0047</b>	0.96572	0.3508
Week 7 vs Week 8	0.92998	0.3843	0.14781	0.8740

*Final Phase\**

Week 9 vs Week 10	1.69620	0.1672	1.0350	0.2973
-------------------	---------	--------	--------	--------

Additionally, *post hoc* permANOVA analyses were performed on the photosynthetic efficiency data across treatments to test for differences between weeks nested in their corresponding phases, for each species (Table 3.3.18). In the hard coral *Acropora appressa*, photosynthetic efficiency was significantly higher in preceding weeks relative to subsequent weeks, for weeks 1 and 4 ( $t = 2.85$ ;  $P_{(MC)} = 0.0296$ ), 2 and 4 ( $t = 3.17$ ;  $P_{(MC)} = 0.0204$ ), and 3 and 4 ( $t = 2.84$ ;  $P_{(MC)} = 0.0308$ ) of the initial phase across treatments. The same pattern was observed between all weeks, except for week 7 and 8, during the middle phase. In the soft coral *Sinularia brassica*, a marginally non-significant difference was only found between weeks 5 and 7 ( $t = 1.96$ ;  $P_{(MC)} = 0.0964$ ) during the middle phase.

Photosynthetic efficiency in live rock during the initial phase of the experiment was significantly lower in week 2 compared to week 3 ( $t = 2.89$ ;  $P_{(MC)} = 0.0260$ ), and significantly higher in week 3 compared to week 4 ( $t = 2.48$ ;  $P_{(MC)} = 0.0498$ ). During the middle phase, photosynthetic efficiency was significantly higher in week 5 relative to weeks 6 ( $t = 6.20$ ;  $P_{(MC)} = 0.0006$ ), 7 ( $t = 3.84$ ;  $P_{(MC)} = 0.0097$ ) and 8 ( $t = 5.56$ ;  $P_{(MC)} = 0.0016$ ). Significant differences in dispersion were only detected in soft coral between weeks 5 and 6 ( $t = 2.18$ ;  $P_{(perm)} = 0.0058$ ), 5 and 7 ( $t = 3.01$ ;  $P_{(perm)} = 0.0054$ ), and 5 and 8 ( $t = 3.31$ ;  $P_{(perm)} = 0.0018$ ) during the middle phase. No differences in dispersion were found between weeks for either hard coral or live rock during any of the experimental phases (Table 3.3.18).

**Table 3.3.18** *Post hoc* pairwise permutational ANOVA (permANOVA) and permutational analysis of dispersion (permDISP) comparisons of photosynthetic efficiency between different weeks during each of the experimental phases for hard and soft coral, as well as live rock. Significant differences are indicated in bold ( $\alpha \leq 0.05$ ).

Source of variation	permANOVA pairwise comparisons		permDISP pairwise comparisons	
	<i>t</i>	$P_{(MC)}$	<i>t</i>	$P_{(perm)}$
<b>Hard Coral</b>				
<i>Initial Phase</i>				
Week 1 vs Week 2	0.7313	0.4980	0.08790	0.9582
Week 1 vs Week 3	1.4242	0.2093	0.12788	0.9237
Week 1 vs Week 4	2.8510	<b>0.0296</b>	0.79448	0.6002
Week 2 vs Week 3	0.9878	0.3667	0.04674	0.9739
Week 2 vs Week 4	3.1684	<b>0.0204</b>	0.78389	0.5940
Week 3 vs Week 4	2.8406	<b>0.0308</b>	0.70329	0.5884

<i>Middle Phase</i>				
Week 5 vs Week 6	3.6401	<b>0.0113</b>	0.67035	0.5338
Week 5 vs Week 7	7.4083	<b>0.0002</b>	2.26020	0.0640
Week 5 vs Week 8	4.4537	<b>0.0054</b>	2.38560	0.0639
Week 6 vs Week 7	7.2657	<b>0.0003</b>	1.72010	0.1115
Week 6 vs Week 8	4.0656	<b>0.0082</b>	2.02040	0.0876
Week 7 vs Week 8	1.8671	0.1096	0.74548	0.5476
Soft Coral				
<i>Initial Phase</i>				
Week 1 vs Week 2	0.32922	0.7548	0.07574	0.9336
Week 1 vs Week 3	1.29910	0.2353	0.44037	0.6507
Week 1 vs Week 4	1.13690	0.2974	0.14771	0.8786
Week 2 vs Week 3	0.66324	0.5279	0.38398	0.7073
Week 2 vs Week 4	1.05640	0.3298	0.21110	0.8384
Week 3 vs Week 4	0.75673	0.4791	0.50491	0.6292
<i>Middle Phase</i>				
Week 5 vs Week 6	1.00440	0.3495	2.17700	<b>0.0058</b>
Week 5 vs Week 7	1.96130	0.0964	3.01100	<b>0.0054</b>
Week 5 vs Week 8	1.86630	0.1181	3.31090	<b>0.0018</b>
Week 6 vs Week 7	0.25462	0.8024	0.08173	0.9567
Week 6 vs Week 8	0.25796	0.8031	0.60636	0.6373
Week 7 vs Week 8	0.06292	0.9518	0.60826	0.5871
<i>Final Phase</i>				
Week 9 vs Week 10	1.85260	0.1077	2.35290	0.0705
Live Rock				
<i>Initial Phase</i>				
Week 2 vs Week 3	2.8942	<b>0.0260</b>	0.38434	0.7316
Week 2 vs Week 4	1.5070	0.1820	0.43599	0.7729
Week 3 vs Week 4	2.4811	<b>0.0498</b>	0.77390	0.6779
<i>Middle Phase</i>				
Week 5 vs Week 6	6.2024	<b>0.0006</b>	0.21518	0.8052
Week 5 vs Week 7	3.8389	<b>0.0097</b>	0.35510	0.7569
Week 5 vs Week 8	5.5589	<b>0.0016</b>	0.48242	0.6571
Week 6 vs Week 7	1.6538	0.1530	0.64749	0.6196
Week 6 vs Week 8	0.8790	0.4166	0.98130	0.3303
Week 7 vs Week 8	0.7055	0.5077	0.05482	0.9712
<i>Final Phase</i>				
Week 9 vs Week 10	1.4021	0.2100	1.32570	0.2375

When *post hoc* permANOVA tests were undertaken between different temperature treatments during each phase of the experiment for each species, photosynthetic efficiency in the hard coral *A. appressa* was significantly higher during the middle phase at the control temperature of 24.4°C compared to 28.8°C ( $t = 3.81$ ;  $P_{(MC)} = 0.0201$ ), and higher at 26.9°C compared to 28.8°C ( $t = 2.83$ ;  $P_{(MC)} = 0.0479$ ) (Table 3.3.19). No difference was detected in photosynthetic efficiency in *A. appressa* between treatments at 24.4°C and 26.9°C ( $P_{(MC)} \geq 0.4120$ ). Photosynthetic efficiency in

the soft coral *S. brassica*, manifested a marginally non-significant difference between the 24.4°C and 28.8°C treatments ( $t = 2.32$ ;  $P_{(MC)} = 0.0820$ ) during the middle phase, but was significantly higher at 24.4°C and at 26.9°C compared to 29.8°C ( $t = 5.20$ ;  $P_{(MC)} = 0.0066$  and  $t = 2.96$ ;  $P_{(MC)} = 0.0415$ , respectively) during the final phase. No significant differences in the photosynthetic efficiency of live rock were detected between different treatments during any of the experimental phases ( $P_{(MC)} \geq 0.1040$ ). *Post hoc* analyses of dispersion revealed differences for *A. appressa* during the middle phase between the 24.4°C control treatment and 28.8°C ( $t = 2.57$ ;  $P_{(perm)} = 0.0160$ ), and between 26.9°C and 28.8°C treatments ( $t = 2.38$ ;  $P_{(perm)} = 0.0253$ ), as well as between 24.4°C and 29.8°C ( $t = 2.41$ ;  $P_{(perm)} = 0.0221$ ) for *S. brassica* during the final phase (Table 3.3.19).

**Table 3.3.19** *Post hoc* pairwise permutational ANOVA (permANOVA) and permutational analysis of dispersion (permDISP) comparisons investigating variation in photosynthetic efficiency between temperature treatments for hard and soft coral, as well as live rock, during each of the experimental phases. Significant differences are indicated in bold ( $\alpha \leq 0.05$ ). \*Temperatures were increased to 29.8°C during the final phase of the bleaching-threshold treatment.

Source of variation	permANOVA		permDISP	
	pairwise comparisons		pairwise comparisons	
	<i>t</i>	$P_{(MC)}$	<i>t</i>	$P_{(perm)}$
<b>Hard Coral</b>				
<i>Initial Phase</i>				
24.4°C vs 26.9°C	0.22116	0.8357	1.16560	0.3457
24.4°C vs 28.8°C	0.04590	0.9678	0.29245	0.7853
26.9°C vs 28.8°C	0.18438	0.8680	1.42320	0.2351
<i>Middle Phase</i>				
24.4°C vs 26.9°C	0.93083	0.4120	0.47481	0.7000
24.4°C vs 28.8°C	3.81250	<b>0.0201</b>	2.56620	<b>0.0160</b>
26.9°C vs 28.8°C	2.82650	<b>0.0479</b>	2.38240	<b>0.0253</b>
<b>Soft Coral</b>				
<i>Initial Phase</i>				
24.4°C vs 26.9°C	0.39702	0.7098	1.54260	0.1349
24.4°C vs 28.8°C	0.11157	0.9201	0.16400	0.8622
26.9°C vs 28.8°C	0.20974	0.8429	1.22370	0.2789
<i>Middle Phase</i>				
24.4°C vs 26.9°C	0.90302	0.4186	0.70094	0.7078
24.4°C vs 28.8°C	2.31500	0.0820	0.06451	0.9660
26.9°C vs 28.8°C	0.31402	0.7644	0.83693	0.5250
<i>Final Phase</i>				
24.4°C vs 26.9°C	0.90607	0.4187	1.32990	0.5698
24.4°C vs 29.8°C*	5.20230	<b>0.0066</b>	2.41460	<b>0.0221</b>
26.9°C vs 29.8°C*	2.95640	<b>0.0415</b>	0.07189	0.9677
<b>Live Rock</b>				
<i>Initial Phase</i>				

24.4°C vs 26.9°C	1.72680	0.1532	0.94707	0.3672
24.4°C vs 28.8°C	2.08180	0.1040	1.17490	0.2547
26.9°C vs 28.8°C	0.08025	0.9427	0.45264	0.6578
<i>Middle Phase</i>				
24.4°C vs 26.9°C	0.34071	0.7520	0.93143	0.3467
24.4°C vs 28.8°C	0.37704	0.7286	0.36710	0.7757
26.9°C vs 28.8°C	0.16309	0.8826	0.39609	0.8006
<i>Final Phase</i>				
24.4°C vs 26.9°C	0.04020	0.9699	1.96670	0.0833
24.4°C vs 29.8°C*	0.27322	0.7973	1.10580	0.3335
26.9°C vs 29.8°C*	0.57982	0.5927	0.75490	0.5635

When testing for differences in photosynthetic efficiency between phases for each species exposed to a particular treatment, marginally non-significant differences were found between the initial and middle phases for hard coral in the 24.4°C treatment ( $t = 4.13$ ;  $P_{(MC)} = 0.0569$ ), but not for soft coral or live rock ( $P_{(MC)} \geq 0.5082$ ) (Table 3.3.20). In the 26.9°C treatment, photosynthetic efficiency was marginally non-significant in hard coral between the initial and middle phases ( $t = 3.61$ ;  $P_{(MC)} = 0.0664$ ) and did not vary significantly between phases in soft coral ( $P_{(MC)} \geq 0.3483$ ). However, photosynthetic efficiency in live rock was significantly higher during the initial phase compared to the middle phase ( $t = 7.13$ ;  $P_{(MC)} = 0.0195$ ), and marginally non-significant between the initial and final phase ( $t = 3.60$ ;  $P_{(MC)} = 0.0710$ ). In the 28.8°C treatment, photosynthetic efficiency was significantly higher in hard coral during the initial phase compared to the middle phase ( $t = 8.12$ ;  $P_{(MC)} = 0.0168$ ) (Table 3.3.20).

Photosynthetic efficiency of soft coral in this treatment was marginally non-significant between the initial and middle phases ( $t = 3.26$ ;  $P_{(MC)} = 0.0818$ ) and between the middle and final phases ( $t = 4.13$ ;  $P_{(MC)} = 0.0592$ ), but significantly higher during the initial phase compared to the final phase ( $t = 10.73$ ;  $P_{(MC)} = 0.0094$ ). In live rock, photosynthetic efficiency was significantly higher in the initial phase compared to the middle phase ( $t = 8.13$ ;  $P_{(MC)} = 0.0154$ ), and only marginally non-significant between the initial and final phases ( $t = 3.93$ ;  $P_{(MC)} = 0.0594$ ).

*Post hoc* pairwise analyses of dispersion revealed no significant differences between phases at the 24.4°C treatment for any of the species (Table 3.3.20). However, photosynthetic efficiency in soft coral in the 26.9°C treatment was significantly higher during the initial phase compared to the middle phase ( $t = 3.40$ ;  $P_{(perm)} = 0.0006$ ) and final phase ( $t = 2.43$ ;  $P_{(perm)} = 0.0224$ ). Significant differences in dispersion were detected in the 28.8°C treatment between the initial and middle phases for both hard ( $t = 2.53$ ;  $P_{(perm)} = 0.0148$ ) and soft coral ( $t = 2.09$ ;  $P_{(perm)} = 0.0423$ ), as well as between the initial and final phases ( $t = 3.64$ ;  $P_{(perm)} = 0.0016$ ) for soft coral (Table 3.3.20).

**Table 3.3.20** *Post hoc* pairwise permutational ANOVA (permANOVA) and permutational analysis of dispersion (permDISP) comparisons investigating variation in photosynthetic efficiency of hard and soft coral, as well as live rock, between different experimental phases for each temperature treatment. Significant differences are indicated in bold ( $\alpha \leq 0.05$ ). \*Temperatures were increased to 29.8°C during the final phase of the bleaching-threshold treatment.

Source of variation	permANOVA pairwise comparisons		permDISP pairwise comparisons	
	<i>t</i>	<i>P</i> <sub>(MC)</sub>	<i>t</i>	<i>P</i> <sub>(perm)</sub>
<b>24.4°C (Control)</b>				
<i>Hard Coral</i>				
Initial Phase vs Middle Phase	4.12570	0.0569	0.37670	0.7594
<i>Soft Coral</i>				
Initial Phase vs Middle Phase	0.40614	0.7249	1.21640	0.6246
Initial Phase vs Final Phase	0.49406	0.6656	0.46266	0.6802
Middle Phase vs Final Phase	0.59651	0.6126	0.74849	0.8188
<i>Live Rock</i>				
Initial Phase vs Middle Phase	0.80289	0.5082	1.06640	0.2901
Initial Phase vs Final Phase	0.74588	0.5303	0.47860	0.6388
Middle Phase vs Final Phase	0.24903	0.8273	0.51176	0.6398
<b>26.9°C (RCP 4.5)</b>				
<i>Hard Coral</i>				
Initial Phase vs Middle Phase	3.61020	0.0664	1.1596	0.3432
<i>Soft Coral</i>				
Initial Phase vs Middle Phase	0.97942	0.4362	3.3990	<b>0.0006</b>
Initial Phase vs Final Phase	1.00140	0.4247	2.4272	<b>0.0224</b>
Middle Phase vs Final Phase	1.19620	0.3483	0.0290	0.9771
<i>Live Rock</i>				
Initial Phase vs Middle Phase	7.12840	<b>0.0195</b>	1.0002	0.3299
Initial Phase vs Final Phase	3.59870	0.0710	1.7677	0.1573
Middle Phase vs Final Phase	0.25296	0.8240	1.0794	0.2940
<b>28.8°C (Bleaching-threshold)</b>				
<i>Hard Coral</i>				
Initial Phase vs Middle Phase	8.11990	<b>0.0168</b>	2.52710	<b>0.0148</b>
<i>Soft Coral</i>				
Initial Phase vs Middle Phase	3.26210	0.0818	2.09010	<b>0.0423</b>
Initial Phase vs Final Phase*	10.7340	<b>0.0094</b>	3.63900	<b>0.0016</b>
Middle Phase vs Final Phase*	4.13210	0.0592	0.90261	0.4065
<i>Live Rock</i>				
Initial Phase vs Middle Phase	8.13130	<b>0.0154</b>	0.08436	0.9447
Initial Phase vs Final Phase*	3.92670	0.0594	0.24756	0.7870
Middle Phase vs Final Phase*	0.29070	0.8006	0.35088	0.8505

Significant differences in photosynthetic efficiency were evident between hard coral and live rock in the significant *a priori* pairwise contrast ( $F_{(\text{Pseudo})} = 2.95$ ;  $P_{(\text{MC})} < 0.0032$ ) for the treatment-species-week nested in the phase interaction term (Table 3.3.11). The *post hoc* pairwise permANOVA revealed that photosynthetic efficiency was significantly higher in hard coral compared to live rock during all weeks at 24.4°C, except during week 7, which was marginally non-significant ( $t = 3.96$ ;  $P_{(\text{MC})} = 0.0562$ ) (Table 3.3.21). The same was true for the 26.9°C treatment, except for week 3. In the 28.8°C treatment, the photosynthetic efficiency of hard coral was significantly higher than that of live rock during weeks 4 ( $t = 6.23$ ;  $P_{(\text{MC})} = 0.0263$ ), 5 ( $t = 5.09$ ;  $P_{(\text{MC})} = 0.0355$ ) and 6 ( $t = 14.99$ ;  $P_{(\text{MC})} = 0.0048$ ) of the middle phase. Results for week 7 of the middle phase were marginally non-significant ( $t = 4.3630$ ;  $P_{(\text{MC})} = 0.0502$ ). The *post hoc* pairwise permDISP analyses of dispersion revealed no further significant differences (Table 3.3.21).

**Table 3.3.21** *Post hoc* pairwise permutational ANOVA (permANOVA) and permutational analysis of dispersion (permDISP) comparisons investigating variation in photosynthetic efficiency between hard coral and live rock for each temperature treatment during the different experimental phases and their corresponding weeks. Significant differences are indicated in bold ( $\alpha \leq 0.05$ ).

Source of variation	permANOVA pairwise comparisons		permDISP pairwise comparisons	
	t	$P_{(\text{MC})}$	t	$P_{(\text{perm})}$
<b>Hard Coral vs Live Rock</b>				
<i>24.4°C (Control)</i>				
<i>Initial Phase</i>				
Week 2	5.8334	<b>0.0301</b>	0.97794	0.5937
Week 3	5.6266	<b>0.0305</b>	1.28150	0.3010
Week 4	5.9589	<b>0.0274</b>	0.35607	0.7096
<i>Middle Phase</i>				
Week 5	4.6257	<b>0.0481</b>	2.4451	0.1000
Week 6	6.0149	<b>0.0277</b>	1.1476	0.4011
Week 7	3.9643	0.0562	1.6223	0.1914
Week 8	6.0344	<b>0.0282</b>	1.7710	0.2912
<i>26.9°C (RCP 4.5)</i>				
<i>Initial Phase</i>				
Week 2	5.3818	<b>0.0347</b>	2.1537	0.1982
Week 3	2.2863	0.1499	1.7998	0.2011
Week 4	6.6843	<b>0.0239</b>	0.3616	0.7972
<i>Middle Phase</i>				
Week 5	3.5869	0.0668	2.1557	0.0982
Week 6	5.8845	<b>0.0276</b>	2.2766	0.1042
Week 7	10.728	<b>0.0080</b>	1.9773	0.2004
Week 8	8.0452	<b>0.0152</b>	0.4615	0.5994

### 28.8°C (Bleaching-threshold)

<i>Initial Phase</i>				
Week 2	26.540	<b>0.0016</b>	0.20769	0.7955
Week 3	3.7038	0.0634	0.58072	0.7995
Week 4	6.2327	<b>0.0263</b>	2.01870	0.1936
<i>Middle Phase</i>				
Week 5	5.0890	<b>0.0355</b>	0.84663	0.3956
Week 6	14.989	<b>0.0048</b>	1.12650	0.6009
Week 7	4.3630	0.0502	1.34920	0.5952
Week 8	1.5569	0.2620	0.88926	0.6116

### 3.3.3 Net community calcification according to the concentration of calcium carbonate

Net community calcification of reef communities fluctuated throughout a diel period and indicated changes in accretion and dissolution (Fig. 3.3.8). Coral communities exposed to the control treatment of 24.4°C showed a consistent decline in the concentration of CaCO<sub>3</sub> over a diel period, regardless of daytime or night-time conditions (Fig. 3.3.8). At 26.9°C, CaCO<sub>3</sub> concentrations initially increased after 6 hours of darkness, then stabilised for the following 12 hours before declining back to their initial values. During the 28.8°C treatment, a similar pattern in CaCO<sub>3</sub> concentration was found to that at 26.9°C, except that, after an initial increase, CaCO<sub>3</sub> concentrations stabilised after only 6 hours, and then proceeded to decline for the remaining 12 hours to levels lower than their initial concentrations (Fig. 3.3.8). The overall average  $\pm$  standard error (SE) in the concentration of CaCO<sub>3</sub> in the 24.4°C control treatment and the 26.9°C treatment was  $2786.22 \pm 12.64 \mu\text{mol CaCO}_3 \text{ kg}^{-1}$  and  $2793.57 \pm 13.37 \mu\text{mol CaCO}_3 \text{ kg}^{-1}$ , respectively. At 28.8°C, an overall average  $\pm$  SE concentration of  $2804.62 \pm 10.22 \mu\text{mol CaCO}_3 \text{ kg}^{-1}$  was measured, this being the highest concentration of CaCO<sub>3</sub> in all of the three treatments (Fig. 3.3.8).

*Post hoc* pairwise permANOVA analyses revealed significant differences in the concentrations of CaCO<sub>3</sub> between all three diel periods (Table 3.3.23). When temperatures within the relevant treatments were raised, the concentration of CaCO<sub>3</sub> was significantly higher for diel period 1 (end of week 4) compared to diel period 2 (end of week 6) ( $t = 3.97$ ;  $P_{(\text{MC})} = 0.0078$ ). The treatment temperatures were held stable for two weeks during diel period 2. The concentration of CaCO<sub>3</sub> was also significantly higher at the end of diel period 1 (week 4) compared to diel period 3 (end of week 8) ( $t = 10.00$ ;  $P_{(\text{MC})} = 0.0003$ ). Similarly, the concentration of CaCO<sub>3</sub> at diel period 2 (week 6) was also significantly higher than at diel period 3 (week 8) ( $t = 19.60$ ;  $P_{(\text{MC})} = 0.0001$ ). Significant dispersion was detected between diel periods 1 and 3 and between diel periods 2 and 3 ( $P_{(\text{perm})} < 0.05$ ) (Table 3.3.23).

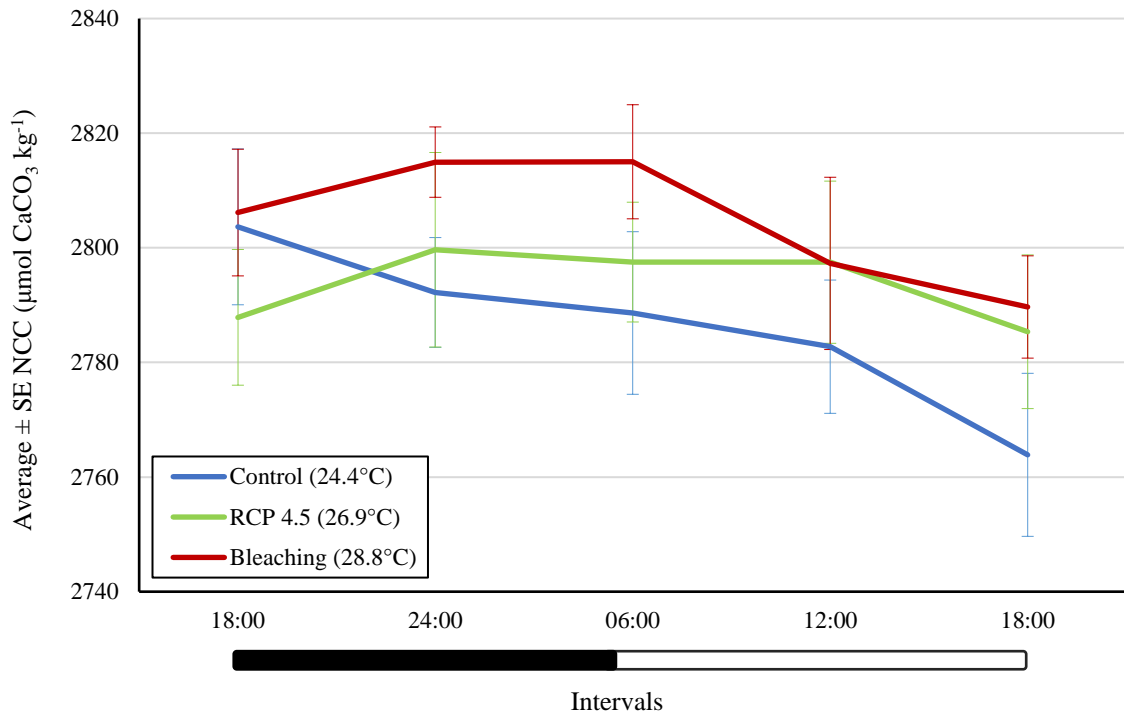


**Figure 3.3.8** Average  $\pm$  standard error (SE) net community calcification (NCC) according to the calcium carbonate concentration ( $\mu\text{mol CaCO}_3 \text{ kg}^{-1}$ ) averaged across the three diel periods at the end of the fourth, sixth and eighth week of the experiment, for each temperature treatment. The bar at the bottom indicates night-time (black) and daytime (white) measurements.

The *a priori* permANOVA investigating variation in the concentration of  $\text{CaCO}_3$  detected significant differences according to the diel period ( $F_{(\text{Pseudo})} = 95.73$ ;  $P_{(\text{MC})} = 0.0001$ ), 6-hour sampling interval nested in diel period ( $F_{(\text{Pseudo})} = 2.24$ ;  $P_{(\text{MC})} = 0.0181$ ), and the interaction of treatment and diel period ( $F_{(\text{Pseudo})} = 10.58$ ;  $P_{(\text{MC})} = 0.0007$ ) (Table 3.3.22). The effect of treatment on  $\text{CaCO}_3$  concentrations was marginally non-significant ( $F_{(\text{Pseudo})} = 3.67$ ;  $P_{(\text{MC})} = 0.0857$ ). *A priori* permDISP analyses revealed differences in dispersion according to diel period ( $F = 3.23$ ;  $P_{(\text{perm})} = 0.0428$ ) and the interaction between treatment and diel period ( $F = 2.23$ ;  $P_{(\text{perm})} = 0.0392$ ) (Table 3.3.22).

**Table 3.3.22** Permutational ANOVA (permANOVA) and permutational analysis of dispersion (permDISP) investigating variation in net community calcification (NCC) according to the concentration of calcium carbonate (CaCO<sub>3</sub>) in water containing reef communities exposed to different temperature treatments based on total alkalinity concentrations measured at 6-hour intervals within a diel period at the end of weeks 4, 6 and 8 of the experiment. Significant differences are indicated in bold ( $\alpha \leq 0.05$ ).

Source of variation	permANOVA				permDISP	
	df	MS	$F_{(Pseudo)}$	$P_{(MC)}$	$F$	$P_{(perm)}$
Treatment	2	3856.7	3.6739	0.0857	2.1803	0.1377
Diel period	2	33176	95.728	<b>0.0001</b>	3.2317	<b>0.0428</b>
Mesocosm (Treatment)	6	1049.8	1.4938	0.1876	0.0094	0.9893
Interval (Diel period)	12	1575.0	2.2412	<b>0.0181</b>	0.3498	0.8669
Treatment x Diel period	4	3665.0	10.575	<b>0.0007</b>	2.2268	<b>0.0392</b>
Treatment x Interval (Diel period)	24	755.59	1.0752	0.3983	1.7595	0.1336
Mesocosm (Treatment) x Diel period	12	346.57	0.49315	0.9089	2.5266	<b>0.0165</b>
Res	72	702.76				
Total	134					

**Table 3.3.23** *Post hoc* pairwise permutational ANOVA (permANOVA) and permutational analysis of dispersion (permDISP) comparisons investigating variation in net community calcification (NCC) according to the concentration of CaCO<sub>3</sub>, in water containing reef communities, between different diel periods during the experiment. Significant differences are indicated in bold ( $\alpha \leq 0.05$ ).

Source of variation	permANOVA		permDISP	
	pairwise comparisons		pairwise comparisons	
	$t$	$P_{(MC)}$	$t$	$P_{(perm)}$
Diel period 1 vs Diel period 2	3.9658	<b>0.0078</b>	0.3041	0.7626
Diel period 1 vs Diel period 3	10.001	<b>0.0003</b>	2.1782	<b>0.0324</b>
Diel period 2 vs Diel period 3	19.600	<b>0.0001</b>	2.4226	<b>0.0154</b>

When considering each of the three diel periods independently, the concentration of CaCO<sub>3</sub> decreased over time during diel period 1 (week 4) in all treatments (Fig. 3.3.9). The control treatment had an overall average  $\pm$  SD concentration of  $2809.34 \pm 27.50 \mu\text{mol CaCO}_3 \text{ kg}^{-1}$ , the 26.9°C treatment  $2786.72 \pm 27.49 \mu\text{mol CaCO}_3 \text{ kg}^{-1}$  and the 28.8°C treatment  $2800.38 \pm 24.27 \mu\text{mol CaCO}_3 \text{ kg}^{-1}$ .

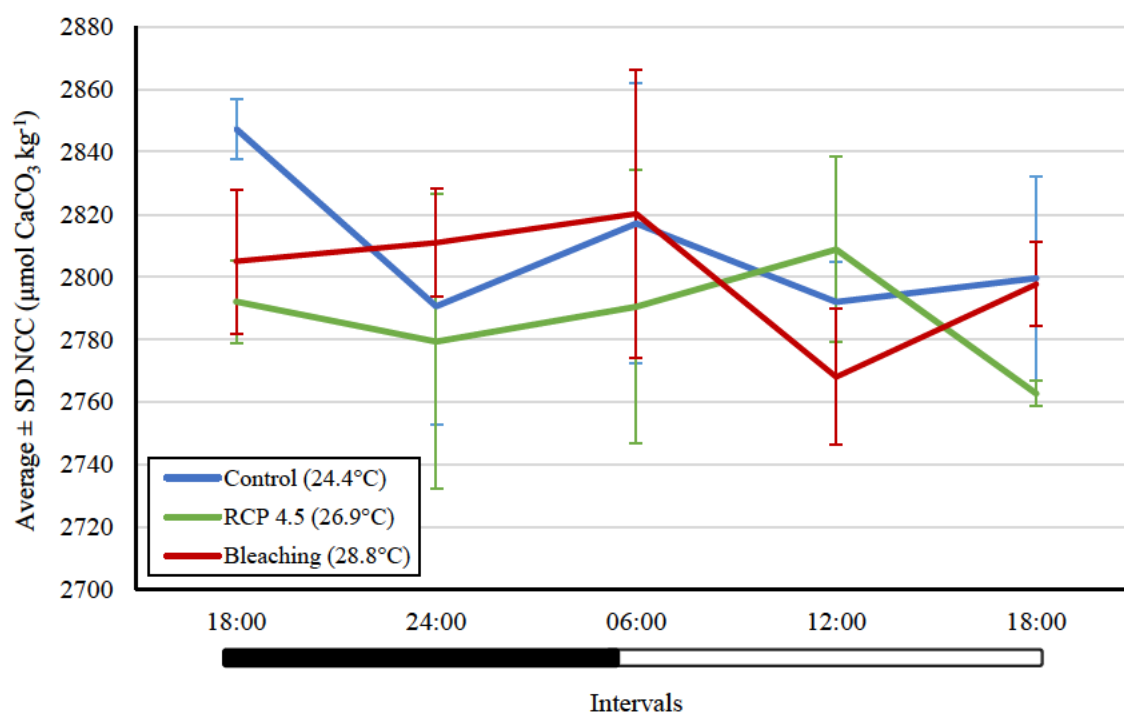


**Figure 3.3.9** Average  $\pm$  standard deviation (SD) net community calcification (NCC) according to the calcium carbonate concentration ( $\mu\text{mol CaCO}_3 \text{ kg}^{-1}$ ) during diel period 1 at the end of the initial phase (week 4) of the experiment according to each temperature treatment. The bar at the bottom indicates nighttime (black) and daytime (white) measurements.

During diel period 2, variable responses were detected between the different temperature treatments over time (Fig. 3.3.10). The 24.4°C and 28.8°C treatments manifested no peaks in  $\text{CaCO}_3$  concentration during the dark phase, whilst the 26.9°C treatment did. However, peaks in  $\text{CaCO}_3$  concentration were evident during the light phase in all temperature treatments with the highest overall  $\text{CaCO}_3$  concentration observed in water containing coral communities at 28.8°C ( $2831.89 \pm 22.09 \mu\text{mol CaCO}_3 \text{ kg}^{-1}$ ), compared to 24.4°C ( $2796.53 \pm 30.18 \mu\text{mol CaCO}_3 \text{ kg}^{-1}$ ) and 26.9°C treatments ( $2830.76 \pm 26.47 \mu\text{mol CaCO}_3 \text{ kg}^{-1}$ ). During diel period 3, lower average  $\pm$  SD  $\text{CaCO}_3$  concentrations were evident in all temperature treatments (Fig. 3.3.11) compared to diel periods 1 and 2 (Figs. 3.3.9, 3.3.10). However, the 28.8°C treatment still manifested the highest average  $\pm$  SD  $\text{CaCO}_3$  concentrations throughout, of  $2781.57 \pm 12.54 \mu\text{mol CaCO}_3 \text{ kg}^{-1}$ , compared to the 24.4°C ( $2752.80 \pm 18.15 \mu\text{mol CaCO}_3 \text{ kg}^{-1}$ ) and 26.9°C treatments ( $2763.24 \pm 11.81 \mu\text{mol CaCO}_3 \text{ kg}^{-1}$ ).

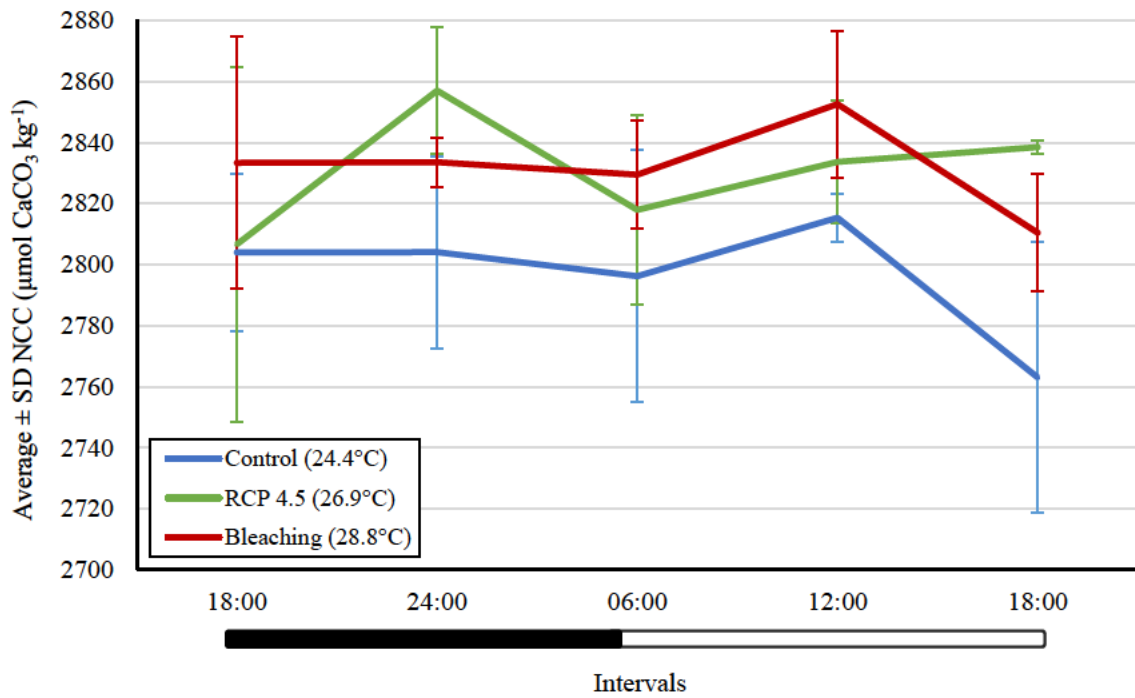


**Figure 3.3.10** Average  $\pm$  standard deviation (SD) net community calcification (NCC) according to the calcium carbonate concentration ( $\mu\text{mol CaCO}_3 \text{ kg}^{-1}$ ) at diel period 2 (week 6) during the middle phase of the experiment according to each temperature treatment. The bar at the bottom indicates night-time (black) and daytime (white) measurements.

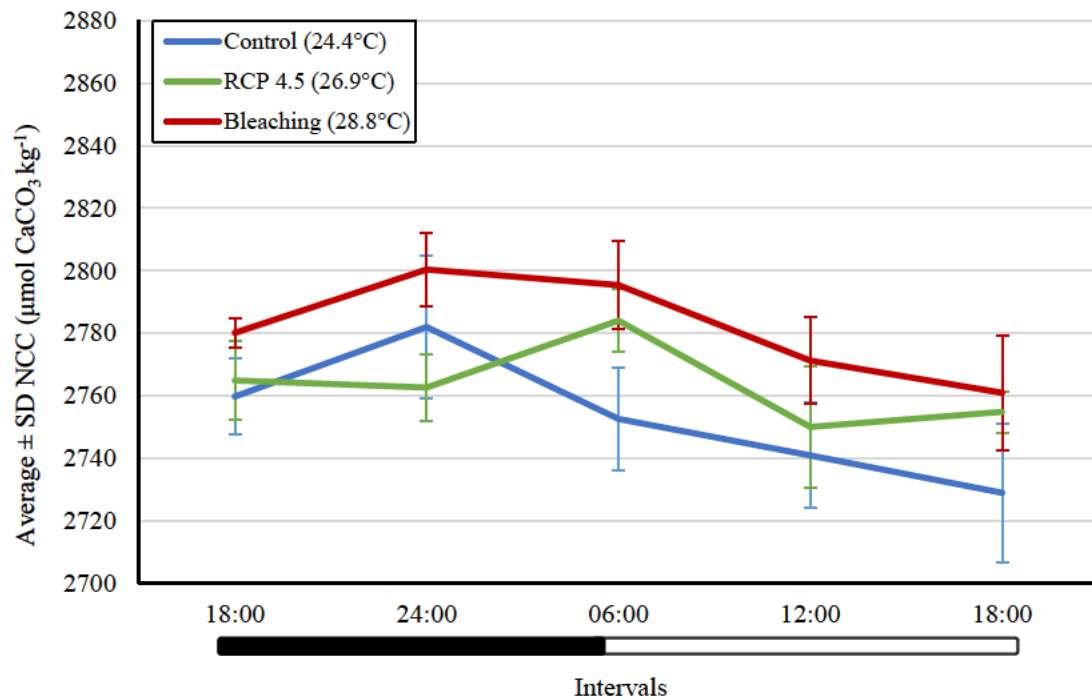


**Figure 3.3.11** Average  $\pm$  standard deviation (SD) net community calcification (NCC) according to the calcium carbonate concentration ( $\mu\text{mol CaCO}_3 \text{ kg}^{-1}$ ) during diel period 3 (week 8) at the end of the middle phase of the experiment according to each temperature treatment. The bar at the bottom indicates night-time (black) and daytime (white) measurements.

*Post hoc* permANOVA analyses of CaCO<sub>3</sub> concentrations between 6-hour sampling intervals nested within each diel period revealed significant differences (Table 3.3.24). During diel period 1 (week 4), CaCO<sub>3</sub> concentrations at interval 1 were significantly higher compared to concentrations at intervals 4 ( $t = 2.71$ ;  $P_{(MC)} = 0.0351$ ) and 5 ( $t = 2.63$ ;  $P_{(MC)} = 0.0403$ ) (Fig. 3.3.9; Table 3.3.24). During diel period 2 (week 6), CaCO<sub>3</sub> concentrations were higher at intervals 2 and 4 compared to interval 5 ( $t = 4.06$ ;  $P_{(MC)} = 0.0062$  and  $t = 2.83$ ;  $P_{(MC)} = 0.0278$ , respectively) (Fig. 3.3.10). During diel period 3 (week 8), CaCO<sub>3</sub> concentrations were significantly higher at earlier intervals relative to later intervals for intervals 1 and 5 ( $t = 4.20$ ;  $P_{(MC)} = 0.0042$ ), 2 and 4 ( $t = 2.74$ ;  $P_{(MC)} = 0.0350$ ), 2 and 5 ( $t = 4.15$ ;  $P_{(MC)} = 0.0071$ ), 3 and 4 ( $t = 2.99$ ;  $P_{(MC)} = 0.0253$ ), and 3 and 5 ( $t = 3.98$ ;  $P_{(MC)} = 0.0063$ ) (Fig. 3.3.11; Table 3.3.24). Marginally non-significant differences were detected between intervals 1 and 2 ( $t = 2.27$ ;  $P_{(MC)} = 0.0642$ ), 1 and 3 ( $t = 1.97$ ;  $P_{(MC)} = 0.0969$ ), and 1 and 4 ( $t = 2.27$ ;  $P_{(MC)} = 0.0637$ ). *Post hoc* analyses of dispersion revealed no significant differences between any interactions (Table 3.3.24).

**Table 3.3.24** *Post hoc* pairwise permutational ANOVA (permANOVA) and permutational analyses of dispersion (permDISP) investigating variation in net community calcification (NCC) according to the CaCO<sub>3</sub> concentration, in water containing reef communities, between different 6-hour intervals (1-5) measured within a diel period during weeks 4, 6 and 8 of the experiment. Intervals, when samples were taken at night-time, are given in bold. Significant differences are indicated in bold ( $\alpha \leq 0.05$ ).

Source of variation	permANOVA pairwise comparisons		permDISP pairwise comparisons	
	<i>t</i>	$P_{(MC)}$	<i>t</i>	$P_{(perm)}$
<i>Diel period 1 (Week 4)</i>				
<b>Interval 1 vs Interval 2</b>	1.48350	0.1911	0.48139	0.6164
<b>Interval 1 vs Interval 3</b>	0.32761	0.7485	0.87887	0.4191
<b>Interval 1 vs Interval 4</b>	2.70940	<b>0.0351</b>	0.84764	0.4085
<b>Interval 1 vs Interval 5</b>	2.63070	<b>0.0403</b>	0.83748	0.4083
<b>Interval 2 vs Interval 3</b>	0.72975	0.4964	0.44944	0.6441
<b>Interval 2 vs Interval 4</b>	0.22222	0.8320	1.10490	0.2790
<b>Interval 2 vs Interval 5</b>	0.53692	0.5964	1.10130	0.2749
<b>Interval 3 vs Interval 4</b>	1.28330	0.2452	1.36340	0.2038
<b>Interval 3 vs Interval 5</b>	1.20560	0.2709	1.35980	0.1989
Interval 4 vs Interval 5	0.27866	0.7846	0.13429	0.8935
<i>Diel period 2 (Week 6)</i>				
<b>Interval 1 vs Interval 2</b>	1.27400	0.2498	1.07260	0.3030
<b>Interval 1 vs Interval 3</b>	0.00587	0.9952	0.56748	0.5876
<b>Interval 1 vs Interval 4</b>	0.95879	0.3656	1.49080	0.1976
<b>Interval 1 vs Interval 5</b>	0.62378	0.5557	0.01428	0.9903
<b>Interval 2 vs Interval 3</b>	1.41720	0.2095	0.73158	0.4842

<b>Interval 2</b> vs Interval 4	0.22576	0.8204	0.20348	0.8497
<b>Interval 2</b> vs Interval 5	4.05520	<b>0.0062</b>	1.02820	0.3982
<b>Interval 3</b> vs Interval 4	1.42700	0.2044	1.30880	0.1948
<b>Interval 3</b> vs Interval 5	1.07400	0.3232	0.52930	0.6501
Interval 4 vs Interval 5	2.83430	<b>0.0278</b>	1.41370	0.2068
<i>Diel period 3 (Week 8)</i>				
<b>Interval 1</b> vs <b>Interval 2</b>	2.2743	0.0642	1.93650	0.0657
<b>Interval 1</b> vs <b>Interval 3</b>	1.9678	0.0969	1.35080	0.2455
<b>Interval 1</b> vs Interval 4	2.2687	0.0637	1.25470	0.2391
<b>Interval 1</b> vs Interval 5	4.1950	<b>0.0042</b>	0.92247	0.4691
<b>Interval 2</b> vs <b>Interval 3</b>	0.7077	0.5077	0.14452	0.8880
<b>Interval 2</b> vs Interval 4	2.7356	<b>0.0350</b>	0.46334	0.6377
<b>Interval 2</b> vs Interval 5	4.1516	<b>0.0071</b>	0.52875	0.6052
<b>Interval 3</b> vs Interval 4	2.9934	<b>0.0253</b>	0.25287	0.8124
<b>Interval 3</b> vs Interval 5	3.9843	<b>0.0063</b>	0.33575	0.7631
Interval 4 vs Interval 5	1.1509	0.2981	0.11646	0.9205

When testing the interaction of diel period with treatment, *post hoc* pairwise permANOVA revealed that concentrations of CaCO<sub>3</sub> during diel period 1 (week 4) were significantly higher at 24.4°C compared to 26.9°C ( $t = 3.66$ ;  $P_{(MC)} = 0.0240$ ), and marginally non-significant between 26.9°C and 28.8°C ( $t = 2.45$ ;  $P_{(MC)} = 0.0631$ ) (Fig. 3.3.9; Table 3.3.25). During diel period 2 (week 6), marginally non-significant differences in the concentrations of CaCO<sub>3</sub> were found between 24.4°C and 26.9°C ( $t = 2.29$ ;  $P_{(MC)} = 0.0854$ ), and 24.4°C and 28.8°C ( $t = 2.42$ ;  $P_{(MC)} = 0.0714$ ) (Fig 3.3.10; Table 3.3.25). During diel period 3 (week 8), concentrations of CaCO<sub>3</sub> were significantly lower at 24.4°C relative to 28.8°C ( $t = 3.72$ ;  $P_{(MC)} = 0.0203$ ), and significantly lower at 26.9°C compared to 28.8°C ( $t = 14.56$ ;  $P_{(MC)} = 0.0001$ ) (Fig 3.3.11; Table 3.3.25). *Post hoc* analyses of dispersion revealed no significant differences (Table 3.3.25).

**Table 3.3.25** *Post hoc* pairwise permutational ANOVA (permANOVA) and permutational analysis of dispersion (permDISP) investigating variation in net community calcification (NCC) according to CaCO<sub>3</sub> concentration, in water containing reef communities, between different temperature treatments during each diel period. Significant differences are indicated in bold ( $\alpha \leq 0.05$ ).

Source of variation	permANOVA pairwise comparisons		permDISP pairwise comparisons	
	<i>t</i>	<i>P</i> <sub>(MC)</sub>	<i>t</i>	<i>P</i> <sub>(perm)</sub>
<i>Diel period 1 (Week 4)</i>				
24.4°C vs 26.9°C	3.6610	<b>0.0240</b>	0.07399	0.9471
24.4°C vs 28.8°C	1.2729	0.2658	0.78177	0.4744
26.9°C vs 28.8°C	2.4488	0.0631	0.80863	0.4503
<i>Diel period 2 (Week 6)</i>				
24.4°C vs 26.9°C	2.2948	0.0854	0.31933	0.7964
24.4°C vs 28.8°C	2.4215	0.0714	1.60810	0.1327
26.9°C vs 28.8°C	0.2378	0.8248	1.18930	0.2693
<i>Diel period 3 (Week 8)</i>				
24.4°C vs 26.9°C	1.3585	0.2475	1.29440	0.2115
24.4°C vs 28.8°C	3.7247	<b>0.0203</b>	0.87424	0.3876
26.9°C vs 28.8°C	14.556	<b>0.0001</b>	0.40585	0.6827

Lastly, *post hoc* permANOVA analyses yielded significant differences in the interaction of diel period with treatment for each treatment (Table 3.3.26). At 24.4°C, the concentration of CaCO<sub>3</sub> was significantly higher during diel periods 1 and 2 compared to diel period 3 ( $t = 7.21$ ;  $P_{(MC)} = 0.0172$  and  $t = 6.46$ ;  $P_{(MC)} = 0.0226$ , respectively). At 26.9°C, CaCO<sub>3</sub> concentrations were significantly lower during diel period 1 compared to diel period 2 ( $t = 9.13$ ;  $P_{(MC)} = 0.0102$ ), and significantly higher during diel period 2 compared to diel period 3 ( $t = 16.10$ ;  $P_{(MC)} = 0.0023$ ), as well as during diel period 1 compared to diel period 3 ( $t = 9.38$ ;  $P_{(MC)} = 0.0116$ ). When coral communities were exposed to 28.8°C, CaCO<sub>3</sub> concentrations were significantly lower between diel periods 1 and 2 ( $t = 4.45$ ;  $P_{(MC)} = 0.0478$ ), but significantly higher during diel period 2 compared to diel period 3 ( $t = 23.46$ ;  $P_{(MC)} = 0.0016$ ). Concentrations of CaCO<sub>3</sub> were marginally non-significant between diel periods 1 and 3 ( $P_{(MC)} = 0.0715$ ) at 28.8°C. *Post hoc* analyses of dispersion revealed significant differences between only diel periods 1 and 3 ( $t = 3.32$ ;  $P_{(perm)} = 0.0036$ ), and diel periods 2 and 3 ( $t = 2.56$ ;  $P_{(perm)} = 0.0177$ ) within the 26.9°C treatment (Table 3.3.26).

**Table 3.3.26** *Post hoc* pairwise permutational ANOVA (permANOVA) and permutational analysis of dispersion (permDISP) investigating variation in net community calcification (NCC) according to CaCO<sub>3</sub> concentration, in water containing reef communities, between different diel periods during the experiment for each temperature treatment. Significant differences are indicated in bold ( $\alpha \leq 0.05$ ).

Source of variation	permANOVA pairwise comparisons		permDISP pairwise comparisons	
	<i>t</i>	<i>P</i> <sub>(MC)</sub>	<i>t</i>	<i>P</i> <sub>(perm)</sub>
<i>24.4°C (Control)</i>				
Diel period 1 vs Diel period 2	0.9633	0.4411	0.08515	0.9289
Diel period 1 vs Diel period 3	7.2104	<b>0.0172</b>	1.47580	0.1584
Diel period 2 vs Diel period 3	6.4649	<b>0.0226</b>	1.68770	0.1166
<i>26.9°C (RCP 4.5)</i>				
Diel period 1 vs Diel period 2	9.1258	<b>0.0102</b>	0.17193	0.8663
Diel period 1 vs Diel period 3	9.3839	<b>0.0116</b>	3.32180	<b>0.0036</b>
Diel period 2 vs Diel period 3	16.101	<b>0.0023</b>	2.56170	<b>0.0177</b>
<i>28.8°C (Bleaching-threshold)</i>				
Diel period 1 vs Diel period 2	4.4451	<b>0.0478</b>	0.60217	0.5797
Diel period 1 vs Diel period 3	3.4398	0.0715	1.49410	0.1587
Diel period 2 vs Diel period 3	23.462	<b>0.0016</b>	0.88827	0.3791

# CHAPTER 4 | DISCUSSION

## 4.1 Overview

Globally, coral reefs are highly susceptible to adverse environmental conditions, particularly increasing temperatures due to anthropogenic climate change (Hoegh-Guldberg *et al.* 2007). Coral health is threatened when temperatures exceed optimal conditions relative to average monthly temperature ranges, especially for prolonged periods (Winter *et al.* 1998; Brown *et al.* 1999; Celliers & Schleyer 2002; Schleyer & Celliers 2003a). Coral growth, photosynthetic efficiency, zooxanthellate densities, and calcification rates reflect various metabolic and physiological properties in corals (Rodrigues & Grottoli 2006). This study investigated the effects of global warming on the physiological responses of high-latitude coral reef communities and how these ecosystems may be affected in the future.

Consequently, three climate warming scenarios were simulated: i) the historical-average temperature quantified at Sodwana Bay used as the control temperature for the experiment; ii) the average temperature for the year 2100 projected for Sodwana Bay by the Representative Concentration Pathway 4.5 (RCP 4.5) climate scenario; and iii) the bleaching-threshold temperature previously determined at Sodwana Bay by Celliers & Schleyer (2002). The effects of three different rates of temperature increase on coral physiology were also tested during the initial phase of the experiment by gradually increasing temperatures to their setpoint values for each warming scenario (see Table 3.1). Additionally, an ‘extreme’ temperature scenario was simulated during the final phase of the experiment, by increasing the temperature in the warmest treatment (bleaching-threshold scenario) by a further degree, for two more weeks.

*Acropora appressa*, *Sinularia brassica* and live rock, each representing a particular functional group that collectively constituted a typical high-latitude coral community in South Africa, were exposed to three different temperature regimes for 10 weeks. The temperature regimes were 24.4°C (the control), 26.9°C (RCP 4.5) and 28.8°C (bleaching threshold), with a further final temperature increase to 29.8°C (extreme) in the bleaching-threshold treatment during the two-week final phase of the experiment (see Fig. 2.3.3). In terms of each functional group, *A. appressa* represented scleractinian hard corals, *S. brassica* alcyonacean soft corals and live rock the reef substratum. Throughout the experiment, various metrics of each functional component’s physiological responses were quantified individually and collectively. These metrics included

coral growth (linear and dimensional size, and buoyant weight), photosynthetic efficiency of coral and live rock, and net community calcification of all functional components collectively.

The experimental setup was a pseudo-replicated system instead of a true-replicated system (i.e. one header tank per treatment, instead of a header tank per mesocosm) (Fig. 2.3.1) due to temperature being the only variable and ease of managing a single temperature treatment. Though a true-replicated system would have allowed for more rigorous manipulation of multiple environmental parameters and data collection, the experimental setup throughout the study operated successfully for a pseudo-replicated system as designed. Additionally, use was made of *Acropora appressa* clones per mesocosm for each treatment (i.e. clones from one colony per mesocosm) (Fig. 2.3.3), effectively functioning as technical replicates in each mesocosm. *Sinularia brassica* was also cloned and allocated per mesocosm, though no technical replicates were necessary based on the size ratios to that of *A. appressa*. Instead of combining a clone from each colony in one mesocosm, the mesocosm functioned as a representative coral community found on various parts of Two-mile reef at Sodwana Bay. The data collection of the biological material based on the mesocosm setup allowed for better comparison of genetically distinct clones per mesocosm to be able to make population level conclusions. Simultaneously, the setup controlled for different genotypical interactions of colonies that could have potentially alter the reactions per clone in a single mesocosm setup. However, variation among a combination of clones from each colony in one mesocosm can potentially investigate higher-level interaction terms and factors of interest, considering the experimental design in terms of the data analyses performed throughout the study.

Aside from the experimental manipulation of temperature to hypothesised unfavourable levels in two of the treatments, it was evident that specimens were maintained in suitable conditions throughout the 10-week experiment based on their state in the control treatment. All functional groups in the control treatment, where temperatures were kept stable and at a long-term historical average derived from Sodwana Bay, responded neutrally or positively (Figs. 3.1, 3.3.1–3.3.3, 3.3.5–3.3.11, 4.1). In contrast, temperatures simulating the RCP 4.5 and local bleaching-threshold scenarios, including the two-week extreme scenario, generally affected the physiological responses of corals negatively as was hypothesised (Fig. 4.1). The implications of these findings for high-latitude coral reefs in Sodwana Bay concerning global warming in the next 80 years and at other marginal locations for reef development around the world are discussed in further detail in the following sections.

## 4.2 Water temperatures simulated in experiments

Global warming has severe and widespread implications for corals and reef communities (Hoegh-Guldberg 1999; Wilkinson 1999). On Sodwana Bay reefs, an average temperature of 24.4°C has been recorded over 25 years (Porter *et al.* 2017a; Porter & Schleyer 2017) with observed bleaching in some corals at seawater temperatures of approximately 28.8°C (Celliers & Schleyer 2002). Hence, temperatures of 24.4 and 28.8°C were used for the control and bleaching-threshold treatments, respectively (Fig. 3.1). The bleaching-threshold temperature simulated in my experiment also corresponded with the average monthly RCP 8.5 temperature of 28.6°C, projected at Sodwana Bay for the year 2100. Furthermore, the bleaching-threshold temperature of 28.8°C is on par with or exceeds monthly temperatures projected to occur at Sodwana Bay under the RCP 4.5 scenario for three separate months in the year 2100. The third temperature used in experiments of 26.9°C was based on the average monthly temperature projected for the year 2100 by the RCP 4.5 scenario, which also closely corresponded to Sodwana Bay's mid-point temperature of 26.6°C – the temperature between the historical-average and bleaching-threshold temperatures.

Factor	Comparison relative to the control treatment	Size		Buoyant weight		Photosynthetic efficiency			Net Community Calcification
		Hard coral	Soft coral	Hard coral	Soft coral	Hard coral	Soft coral	Live rock	Community
Treatment	Bleaching-threshold treatment	↓		↓		↓			↓
	RCP 4.5 (Year-2100) treatment								
Treatment x Phase	Bleaching-threshold x Initial phase	↓		↓		↓	↓	↓	NA
	Bleaching-threshold x Middle phase					↓	↓	↓	
	Bleaching-threshold x Final phase					NA	↓	↓	
	RCP 4.5 x Initial phase					↓	↓	↓	
	RCP 4.5 x Middle phase					↓	↓	↓	
	RCP 4.5 x Final phase					NA	↓	↓	
Treatment x Diel Period	Bleaching-threshold x Diel period 1	NA		NA		NA	NA	NA	↑
	Bleaching-threshold x Diel period 2								↓
	Bleaching-threshold x Diel period 3								↓
	RCP 4.5 x Diel period 1								↑
	RCP 4.5 x Diel period 2								↓
	RCP 4.5 x Diel period 3								↓

Key for symbols	
↑	Statistically significant increase
↑	Non-significant increase
↓	Marginally non-significant (0.05 ≤ 0.10) decrease
↓	Non-significant decrease
↓	Statistically significant decrease

**Figure 4.1** Summary of the results of the experiments based on permANOVA analyses conducted on each physiological parameter including coral size, buoyant weight, photosynthetic efficiency and net community calcification for the three functional groups (hard coral, soft coral and live rock) and the coral community. The summary indicates the status of statistical significance and the direction of change in each physiological parameter relative to the control treatment for the various factors (fixed effects) and their interactions. This was achieved by comparing the different physiological responses derived from the year-2100 (RCP 4.5) and bleaching-threshold scenarios with the historical-average scenario or control treatment. The cells were merged when the *a priori* tests on each physiological parameter indicated a non-significant difference ( $\alpha = 0.05$ ), obviating the need for *post hoc* comparisons, but the direction of the non-significant change was still indicated. NA = not applicable.

With the current local and global policies in force, a warming of approximately 2.9°C above pre-industrial levels are projected by the end of the century (Climate Action Tracker 2020; UNEP 2020). The projected temperature closely corresponds to the RCP 4.5 climate scenario's average range of temperature increase of 2.5 to 3.0°C. Accordingly, the RCP 4.5 scenario is possibly the most likely scenario projected for the year 2100 (Collins *et al.* 2013; Gattuso *et al.* 2014) and the remaining temperature used in the experiment. Hence, the 26.9°C treatment was referred to as the RCP 4.5 scenario (Fig. 3.1). Within the bleaching-threshold treatment, a further 1°C temperature increase was made for the last two weeks of the experiment to simulate an extreme temperature scenario (Fig. 3.1).

Overall, the three different temperature scenarios simulated in the mesocosms, as well as the extended two-week extreme scenario, approximated their setpoints with acceptable standard deviations (SDs) for the duration of the experiment (Fig. 3.1; Table 3.1). With SDs of approximately 0.5°C for all temperature treatments during the middle and final phases of the experiment, all three scenarios adequately simulated the effects that global warming may have on coral reef communities at Sodwana Bay (Fig. 2.3.3). Similar studies have achieved SDs of 0.1 and 1.0°C (Barkley *et al.* 2017; Anderson *et al.* 2019). The control treatment most closely corresponded to the setpoint value of 24.4°C. As increases were employed during the initial phase for both the RCP 4.5 and bleaching-threshold scenarios, this is where the highest deviation occurred, as expected. However, during the middle phase when temperatures were kept stable, the RCP 4.5 scenario only deviated by 0.16°C and most closely corresponded to the setpoint value during the final phase. The bleaching-threshold scenario deviated by 0.23°C during the middle phase, and after a further 1°C increase to 29.8°C the temperature closely corresponded to the setpoint value in the final phase. The variability in temperature around the setpoint derived by other studies (Barkley *et al.* 2017; Anderson *et al.* 2019) mentioned above and this experiment further indicated that the experimental design successfully achieved the desired temperature control and allowed for the testing of multiple interactions based on several climate change scenarios that could be replicated.

Several studies have quantified temperatures on Sodwana Bay's marginal reefs and assessed how these temperatures might influence reef communities (e.g. Schleyer & Celliers 2003b; Porter *et al.* 2017a). No experimental information could be found in the literature on how future warming will affect high-latitude coral reefs, such as those found in Sodwana Bay, at both an individual coral-colony level and at the level of a coral reef community. The thermal exposure time implemented in this study posed an additional challenge when comparing the results with other studies, as few experiments of this nature have lasted for 10 weeks or more. However, similar experiments to mine with temperature-controlled systems have been conducted on scleractinian (Bellworthy & Fine 2017, 2018; Krueger *et al.* 2017) and alcyonacean corals (Lieberman *et al.* 2018) for at least 4 weeks of exposure. In contrast to most previous research, such as the studies mentioned above (Bellworthy & Fine 2017, 2018; Krueger *et al.* 2017;

Lieberman *et al.* 2018), which have focused on the effects of either individual-level coral responses or community-level responses, this study focused on both individual- and community-level responses.

### **4.3 Buoyant weights of marbles at different temperatures**

The weighing of marbles in different temperatures was performed to assess possible variability due to water density as a confounding factor, and thus determine if buoyant weights measured for corals across the different temperature treatments required a correction factor to account for the dissimilar water densities prior to statistical analysis. Similar approaches have been applied in other experimental studies using a control as a reference (Oliver & Palumbi 2011; Schubert & Wilke 2017). The study conducted by Schubert and Wilke (2017) referred to such experimental controls as ‘devices’ that assisted with accurate measurements.

All buoyant weight measurements of each marble in the different temperature treatments employed in this study resulted in negligible maximum ranges and minimal standard deviations (Fig. 3.2). The results indicated that the range of water temperatures used in the experiment did not materially affect the buoyant weight measurements of the corals and their respective control mounts. Therefore, subsequent buoyant weights measured during the experiment reflected true changes in the growth of corals regardless of water density due to the different temperature treatments. No correction factor was necessary to be applied before performing data analyses.

Additionally, control mounts were employed for both hard and soft corals, similar to Schubert and Wilke (2017), that functioned as standards within the replicate mesocosms to further ensure rigorous interpretation of the data. These coral mounts ensured minimising the effects of the variables and increasing the reliability of the analysed data. After buoyant weighing of the control mounts in all the treatments, the results revealed that only minor weight changes occurred (Figs. 3.3.3, 3.3.4).

### **4.4 Physiological responses**

Different treatments had varying effects on the physiological responses of individual coral and live rock functional groups as well as these components assessed together, functioning as a reef community, during each phase (initial, middle, final) of my experiment. One of the effects included the paling and bleaching observed in corals (predominantly in the hard coral *Acropora appressa*) during the end of the middle phase and throughout the final phase in the RCP 4.5 and the bleaching-threshold scenarios (Fig. 2.3.3). It was evident from the study that the change in temperature had a noticeable positive influence on net community calcification (NCC) of reef communities, specifically for the RCP 4.5 scenario (further information in subsection 4.4.3; Fig. 4.1). Further, under the RCP 4.5 scenario, the NCC

significantly increased relative to historical-average conditions during diel period 1 (Fig. 4.1; Tables 3.3.22, 3.3.23).

The study thus identified two critical time periods of physiological change in the corals and coral communities relative to the control treatment: at the end of the initial phase when setpoint temperatures were reached in the RCP 4.5 and bleaching-threshold scenarios; and during the final phase as thermal stress increased in corals and coral communities due to persistent warm temperatures in the two warmest treatments. A study conducted by Roth *et al.* (2012) found similar results for both decreasing and increasing temperature experiments showing distinct physiological responses per treatment at different phases of the experiment. Roth *et al.* (2012) further concluded that prolonged increases in seawater temperatures would eventually become harmful and cause irreversible damage to coral reefs, more so than for cold-induced stress experienced by corals.

#### **4.4.1 Coral growth according to size and buoyant weight**

Coral growth, which refers to both a change in size (linear extension or diameter increase) and weight, is a major indicator of coral fitness and ecological success (Anderson *et al.* 2015, 2019). An increase in temperature may influence a coral's ability to compete successfully for space and light, as well as its ability to repair structural damage caused by anthropogenic disturbances, storms and bioeroders. Initially, the growth trend for the change in size of both *Acropora appressa* and *Sinularia brassica* increased until week 5 of the experiment in all temperature treatments. An overall, continuous increase in size was evident in the control and RCP 4.5 scenarios for both species (Figs. 3.3.1, 3.3.2). As the experiment reached the end of the middle phase, *A. appressa* showed a decrease in linear extension in the bleaching-threshold scenario. For *S. brassica*, a similar reduction in diameter was evident towards the end of the middle phase and throughout the final phase in the bleaching-threshold scenario (Figs. 3.3.1, 3.3.2). The results also indicated probable further decreases in the size of *S. brassica* over time in the bleaching-threshold scenario if experiments were to continue.

Additionally, *A. appressa* showed a slower linear growth rate under the RCP 4.5 scenario compared to the control treatment and bleaching-threshold scenario (Fig. 3.3.1). Suppressed or slower growth under conditions such as an RCP 4.5 scenario could be due to the rate at which temperature was increased. However, the heat-stress response of *A. appressa* may have manifested as a lag effect only in the subsequent phase of my experiment, as the *a priori* permutational analysis of variance (permANOVA) showed no significant differences among treatments (Fig. 4.1). The overall treatment term also resulted in non-significant dispersions after further investigation with a permutational analyses of dispersion (permDISP). Distinct structural and functional traits in scleractinian corals are elicited by heat stress, allowing scleractinian corals to acclimatise for at least a short period (Scheufen *et al.* 2017).

*Sinularia brassica* showed a faster dimensional growth rate in both the RCP 4.5 and bleaching-threshold scenarios relative to the cooler control treatment (Fig. 3.3.2). A study conducted by Mohamed *et al.* (2017) on a *Sinularia* species from the Red Sea recorded the highest growth rates during warmer conditions compared to cooler conditions. As the optimum range in seawater temperature for *Sinularia* species in the Indo-West Pacific Ocean is between 20 and 28°C, bleaching-threshold and extreme-temperature conditions such as those simulated in my study will likely negatively influence coral growth, as was evident in the last dimensional growth measurements of *S. brassica* (Figs. 3.3.1, 3.3.2).

Growth in terms of dimensional changes of high-latitude corals will be constrained if temperatures like those of the bleaching-threshold scenario become more frequent, which will cause corals to struggle to grow and survive in unfavourable environmental conditions (van Hooidonk *et al.* 2014). High-latitude reefs might initially serve as refugia from thermal stress. Still, these reefs are also being affected by increasing ocean temperatures, leading to a further reduction in general growth rates (Anderson *et al.* 2015). The decrease in coral growth was evident in a study done on high-latitude reefs of the southern Great Barrier Reef (De'ath *et al.* 2009) and was also apparent in the warmest treatment during the last three weeks of this study.

It is crucial to understand how increasing ocean temperatures will affect the growth and survival of corals. Such knowledge will be imperative to make accurate predictions about the possible persistence of reef communities at Sodwana Bay and other more typical tropical coral reefs. Although this study did not find any significant treatment effects based on linear or diameter growth in both coral species (Fig. 4.1), significant differences were evident between phase, week nested in phase and the interaction between species and week nested in phase (Fig. 4.1; Table 3.3.1). The significant results found can be related to previous studies that yielded similar results on decreasing growth in Hawaiian (Jokiel & Coles 1977) and Californian (Roth *et al.* 2012) corals under warmer seawater conditions. As the corals are trying to grow within temperature conditions outside their optimal range, their symbiotic relationship is disrupted which causes a decrease in zooxanthellar activity (Iglesias-Prieto *et al.* 1992). An impaired availability of zooxanthellar results in less energy available to corals and could ultimately influence skeletal and tissue growth in *A. appressa* and *S. brassica*. Hence, it is possible that coral growth is constrained by persistent and increasing heat waves, as well as a continued rise in average ocean temperatures.

The rate of coral growth and calcification worldwide is much lower than it has been prior to 1940 (Cantin *et al.* 2010). The rates at which corals grow according to their specific morphologies differ, depending on the environmental conditions and stresses that they are found in (Lough & Barnes 2000). The growth of corals may thus differ based on varying environmental parameters such as temperature (Matsumoto 2007; Silverman *et al.* 2007), light (Reynaud-Vaganay *et al.* 2001) and seawater carbonate chemistry (Langdon *et al.* 2000; Form & Riebesell 2012). The growth differences became evident

across the different temperature treatments as the experiment progressed. Corals could potentially adapt if environmental pressures such as climate change cease to increase at such a rate, which can be measured in physiological changes such as coral growth (Fisher *et al.* 2019). As thermal stress persisted in the middle phase of this experiment, including throughout the further increase within the warmest treatment, no positive response or acclimation was apparent in the linear extension data of both coral species in the bleaching-threshold scenario. The results were further confirmed after performing *a priori* permDISP, where significant dispersions were found between all the terms analysed in the *a priori* permANOVA model (Fig. 4.1). After conducting *post hoc* pairwise permDISP, only significant-dispersion effects were found in growth between all the phases of the experiment but no location effects.

The loss in coral weight is a better indicator of physiological stress than skeletal linear growth of scleractinian corals, partly due to the skeleton being less dense as it becomes more brittle with increasing climate-change effects. Nevertheless, both parameters are still complementary and used in conjunction (Anthony *et al.* 2002), as performed in this study. The coral growth results based on the dimensional changes and buoyant weight measurements detected in the study are representative of the above statement made by Anthony *et al.* (2002), as well as results found in a recent study conducted by Nielsen *et al.* (2020). An increase in weight of a coral along with the absence of an increase in linear extension can explain an increase in density (Lohr & Patterson 2017). However, this was not the case in my study where both a decline in coral weight and linear extension was apparent in the warmer treatments relative to the control group.

A comparative study tested the effects of both heat- and cold-stress treatments (i.e. 23.0°C, 27.0°C and 29.5°C) on *Acropora millepora* from the central Great Barrier Reef and found coral mass to decline with increasing temperatures (Nielsen *et al.* 2020). The lower skeletal weight recorded in the bleaching-threshold scenario in *A. appressa* could indicate increasing skeletal porosity. The more porous the skeleton, the greater the reduction in the quality of the coral skeleton becomes (Rippe *et al.* 2018). If skeletal weight and the density of that skeleton continues to decline due to thermal stress, coral skeletons will be more porous and become more susceptible to chemical and biological erosion (Enochs *et al.* 2016; Webb *et al.* 2017).

The trajectory of the coral growth trends (i.e. linear extension, dimension and weight) in both *A. appressa* and *S. brassica* towards the end of the experiment in the bleaching-threshold scenario (Figs. 3.3.1–3.3.4) indicated further decreases in growth should such temperatures persist. The results suggest that, if bleaching-threshold and extreme temperature conditions were to characterise local conditions on South African coral reefs in the future, growth of both *A. appressa* and *S. brassica* would probably be suppressed. Consequently, as these two species were chosen to represent two specific functional groups (hard corals and soft corals), the results may also indicate that general declines in the growth of both these groups are to be expected on South African coral reefs in the future.

The change in buoyant weight of *A. appressa* during the experiment increased gradually across all treatments and all experimental phases (Fig. 3.3.3). Both the *a priori* permANOVA and permDISP results found significant differences for the treatment crossed with phase interaction, however, the *post hoc* pairwise analyses revealed no differences (Fig. 4.1). In the bleaching-threshold scenario, the growth rate in weight of *A. appressa* slowed down by week 6. The coral then started losing weight, indicating a trend of attrition as bleaching-threshold conditions and extreme temperatures continued (Fig. 3.3.3). The buoyant weight results of *A. appressa* suggest that the species, along with its geographical location, may be important factors to consider in the future to comprehend coral responses to temperature changes better. The significant differences found for the interaction of treatment and phase in *A. appressa* (Fig. 4.1), as well as for the random effect of colony nested in species and its interaction with most fixed effects (Table 3.3.6), further support the former statement.

*Acropora appressa* experienced thermal stress in the warmest treatment, as bleaching started to occur between weeks 7 and 8. As tissue sampling was required for future work beyond the scope of the thesis, the experiment was concluded for the hard coral fragments at the end of week 8. The marginally non-significant results that were evident after conducting a *post hoc* pairwise permANOVA analysis between the middle and final phase of the bleaching-threshold treatment, may be indicative of the observed bleaching while the growth of *A. appressa* persisted until week 6 (Fig. 4.1). If *A. appressa* were kept in thermally-stressed conditions, including a further increase of 1°C during the final phase, the growth trend projected eventual death of the hard corals before termination of the experimental trial.

*Sinularia brassica* only started increasing in weight towards the end of the initial phase in the control treatment and maintained a positive growth rate until the experiment was terminated (Fig. 3.3.4). The RCP 4.5 scenario had a negative growth effect on *S. brassica* up until week 5 and only started having a positive growth influence on *S. brassica* thereafter, where an increasing trend in weight was measured up until the end of the experiment. The increase in buoyant weight of *S. brassica* only after week 5 may have indicated that it was acclimatising to the conditions of the control and RCP 4.5 scenarios (Fig. 3.3.4), and why most of the terms resulted in non-significance after conducting the *a priori* permANOVA analysis (Fig. 4.1). Another probable reason for the negative growth trend in both the control and RCP 4.5 scenarios could be that the general conditions the species were exposed to were not optimal from the start. Hence, the negative responses in both the treatments suggest that the trend was not related to temperature as such.

Contrarily, the bleaching-threshold scenario negatively influenced soft coral growth, more so than for the control and RCP 4.5 scenarios and continued to do so, especially during weeks 7 and 9 until the experiment was terminated after 10 weeks (Fig. 3.3.4). The suppressed growth of *S. brassica* evident in the final phase of the RCP 4.5 (from week 9) and bleaching-threshold scenarios may be because these corals experienced acute thermal stress indicated by observations of the paling of their tissues (Harrison

*et al.* 2011; Fig. 2.3.3). However, many of the factors resulted in non-significant differences after *a priori* permANOVA analysis, which may be due to the duration of the experiment being too short to detect statistically significant growth changes in the corals. Another reason may be attributed to the relatively high variability in the change of buoyant weight of replicates measured in the bleaching threshold treatment.

As community structure on coral reefs is likely to change if many of the climate change projections manifest, as indicated by this study's coral growth results, such changes are predicted to influence the southward migration of high-latitude reef communities due to increasing climate-change pressures (Beger *et al.* 2014; Cacciapaglia & van Woesik 2015). Examples of local distributional changes in coral species due to seawater temperature increases have previously been suggested by Floros *et al.* (2012) and Schleyer (unpublished data) on South African reefs. Because of global warming, corals are likely to experience more temperature anomalies that will increase physiological stress and, resultantly, cause long-term repercussions on coral growth and fitness (Hoegh-Guldberg *et al.* 2007).

Additionally, a visible increase of coenosteum for *A. appressa* and coenenchyme for *S. brassica* was noted in the control treatment, which was not surprising, considering this treatment simulated average temperature conditions throughout the experiment based on those recorded on reefs at Sodwana Bay. In the RCP 4.5 scenario, there was also a visible increase of coenenchyme for both species. However, a loss in coenenchyme was visible in the bleaching-threshold scenario for both *A. appressa* and *S. brassica*, especially by weeks 7 and 8 of the experiment (Fig. 2.3.3). When temperatures were increased in the final phase of the warmest treatment to simulate an extreme-temperature scenario for *S. brassica*, the loss of coenenchyme and consequent presence of sclerites was obvious. The loss of coenenchyme may reduce the ability of corals to produce a three-dimensional framework (Hennige *et al.* 2015). Tissue loss can also indicate a change in how corals allocate their energy to maintain optimal health, such as diverting the energy into maintaining other metabolic requirements (e.g. sclerite production, respiration and calcification) instead of energy input into tissue maintenance.

Furthermore, *S. brassica* showed continuous reduction in diameter under the bleaching-threshold scenario (Fig. 2.3.3). A decrease in tissue thickness is a negative response by corals to thermal and other environmental stresses (Ainsworth *et al.* 2008). Accordingly, energetic demands on corals are increased, which ultimately affects the overall health and productivity of corals negatively (Crossland *et al.* 1980; Ainsworth *et al.* 2008). With coral growth decreasing and *S. brassica* losing weight because of exposure to bleaching-threshold temperatures, less energy is available to maintain optimal coral health, which is likely to increase the chance of mortality. When the frequency and intensity of warming are anomalous, it is more than likely that maximum temperatures will exceed optimum levels for many corals in a given area, with the potential to lead to net negative effects on coral growth (Cantin & Lough 2014; Foster *et al.* 2014).

Variations in growth occur annually and depend on cooler winters and warmer summer ocean temperatures, particularly on high-latitude reefs (Pratchett *et al.* 2015; Scheufen *et al.* 2017). Recent studies have found that coral growth and calcification rates are declining in several species due to global warming (Cooper *et al.* 2008; De'ath *et al.* 2009, 2013; Cantin *et al.* 2010; Carricart-Ganivet *et al.* 2012; Tanzil *et al.* 2013). Lasting adverse effects of global warming on the rate of coral growth are likely to be exacerbated by increasing frequencies of coral-bleaching episodes because the energetic costs of corals surviving the bleaching result in a period of stunted growth (Goreau & Macfarlane 1990; Carilli *et al.* 2010). The environmental conditions associated with coral bleaching may further prolong the recovery time of the affected reefs for several years or even decades should corals survive the bleaching event.

#### 4.4.2 Photosynthetic Efficiency

When zooxanthellate corals are stressed due to either increasing or decreasing temperatures, reduced values of  $F_v/F_M$  reflect declines in the photosynthetic efficiency of zooxanthellae (Jones *et al.* 1999). In the historical-average temperature scenario of 24.4°C employed as the control, both *Acropora appressa* and *Sinularia brassica* continued to photosynthesise without a decline in photosynthetic efficiency until experimentation ceased (Figs. 3.3.5, 3.3.6). However, in the RCP 4.5 scenario of 26.9°C, both species showed an overall decline in photosynthetic efficiency from week 5 onwards. *Sinularia brassica* showed possible acclimation during weeks 7 to 9 in the RCP 4.5 scenario but did not sustain the increase in photosynthetic efficiency (Fig. 3.3.6). Both *A. appressa* and *S. brassica* experienced noticeable declines in photosynthetic efficiency throughout the bleaching-threshold scenario, which persisted in *S. brassica* when temperatures were further increased to simulate an extreme-warming scenario during weeks 9 and 10. The observed decrease in photosynthetic efficiency in the warmest treatments for both coral species corresponded with the reduction in linear and dimensional extensions recorded.

Additionally, the permANOVA revealed significant differences for the terms species (*A. appressa* more so than for *S. brassica* in the bleaching-threshold scenario), phase (initial phase compared to the middle and final phases) and week nested in phase (weeks 1 and 4, 2 and 3, 3 and 4 during the initial phase; weeks 5 and 6, 5 and 7, 5 and 8 during the middle phase; and week 9 compared to week 10 during the final phase) (Fig. 4.1). The interactions of treatment and week nested in phase, species and week nested in phase, as well as the three-way interaction of treatment-species-phase were also significantly different (Fig. 4.1; Table 3.3.11). A decline in photosynthetic efficiency was likely due to reduced enzymatic activities as they are temperature dependant. Photosynthetic reactions decrease in continuous heat stressed conditions, such as those simulated in the RCP 4.5 and bleaching-threshold scenarios, which further cause an increased need for photoprotection in corals (Somero 1995).

A temperature of 28.8°C, simulated by the local bleaching-threshold scenario (Celliers & Schleyer 2002), seems to be a critical threshold from a photobiological standpoint. Hence, the bleaching-threshold temperature potentially represents an inherent limit to photosynthetic efficiency, which is supported by the *post hoc* pairwise permANOVA and supplementary permDISP results. Both the analyses resulted in significant differences (Fig. 4.1), which might indicate dispersion existed within the warmest treatments. Furthermore, an inherent limit to photosynthetic efficiency suggests that photodamage accumulated in both species of coral in the warmest treatment. Once temperatures had reached 28.8°C, the photosynthetic systems of the individual corals could no longer efficiently process light energy during the middle phase (week 4 to 8) of the experiment and onwards (Figs. 3.3.5, 3.3.6). Less light energy was also absorbed due to probable loss of zooxanthellae during heat-stress conditions, but zooxanthellate density was beyond the scope of this investigation. The decline in  $F_v/F_M$  values for *A. appressa* and *S. brassica* during the middle phase of the experiment suggests that the bleaching-threshold scenario caused an immediate imbalance between the light energy absorbed and what was processed through the photosynthetic efficiency of photosystem II. The imbalance may be due to the temperature-dependent reduction of enzyme activities (Pandolfi *et al.* 2003). Consequently, photosynthetic reaction rates decrease, and corals develop a need for increased photoprotection (Gorbunov *et al.* 2001).

In the final phase (week 9 to 10) of the bleaching-threshold treatment that simulated an extreme-warming scenario of 29.8°C, *S. brassica* experienced a relatively fast decline in photosynthetic efficiency. The thermal stress resulted in *S. brassica* corals expelling their photosynthetic symbionts as indicated by the paling of their tissues (Figs. 2.3.3, 3.3.5, 3.3.6). These results suggest that zooxanthellae in both corals exposed to the warmest treatment became a source of oxidative stress as temperatures increased (Lesser 1997; Yakovleva *et al.* 2009) and were under immense photosynthetic stress, causing rapid disruption of the coral-zooxanthellae symbiosis. Therefore, corals exposed to bleaching conditions are not able to acclimate and are thus under severe strain if such conditions persist (Roth *et al.* 2010).

If temperatures projected by climate models such as the RCP 4.5 and bleaching-threshold scenarios (equivalent to an RCP 8.5 scenario) prevail, corals will unlikely be able to recover and re-establish themselves, especially on reefs that experience local anthropogenic pressures as well. Similar trends and results were found in studies measuring photosynthetic efficiency of coral species under climate-change scenarios such as the RCP 4.5 and RCP 8.5 by Langdon and Atkinson (2005) and Biscéré *et al.* (2019). A declining trend of photosynthetic efficiency was evident for both *A. appressa* and *S. brassica* in my study in the warmer treatment, as was found in the coral species tested in the above-mentioned studies. A substantial decrease in photosynthetic efficiency corresponded with observations of mainly paling of the soft coral sections and mostly bleaching of the hard coral fragments in the bleaching-threshold scenario, which is further supported by the *post hoc* pairwise permANOVA and permDISP

results. The permDISP analysis found significant dispersion effects for *A. appressa* during the middle phase between 24.4°C and 28.8°C and for *S. brassica* during the final phase between 24.4°C and 29.8°C.

Bleaching and mortality of corals will likely lead to a decline in herbivore abundance, decreasing the number of grazers available to control the overgrowth of algae (Grottoli *et al.* 2006; Hughes *et al.* 2007). Contrastingly, despite multiple pressures, the Keppel Islands' corals have recovered rapidly even after experiencing three bleaching events (1998, 2002 and 2006) (Berkelmans *et al.* 2003). Some studies have observed varying susceptibility of corals to thermal stress at Sodwana Bay (Gudka *et al.* 2018). For example, Ruiz Sebastián *et al.* (2009) found that *Stylophora pistillata* and *Montipora* species were the most susceptible taxa in southern Mozambique and Maputaland, South Africa. They also found significantly different bleaching responses in common branching corals such as *Acropora* and *Pocillopora*. Another study conducted by Harikishun (2013) on Two-mile Reef and Nine-mile Reef at Sodwana Bay found standardised taxon-specific bleaching responses with large variability over time. *Montipora* species were, again, the most susceptible taxon whereas *Galaxea* and *Platygyra*, were the least susceptible to bleaching (Harikishun 2013).

Field and laboratory observations were conducted on *Acropora* corals on the Great Barrier Reef during the 2016 bleaching event, which showed clear evidence that *Acropora* was the most severely impacted by heat stress (Hughes *et al.* 2017). *Acropora* species are highly susceptible to disturbances such as anomalously warm temperatures and they may decline in abundance with global warming (Marshall & Baird 2000; McClanahan *et al.* 2007). Contrastingly, taxa like *Favia*, *Pocillopora* and *Sinularia* are more resistant to increasing temperatures and may become more dominant in the future as found in the study conducted by Shu *et al.* (2011) at the Nansha Islands, South China Sea. As the genus *Sinularia* is more resilient to increasing temperatures (Shu *et al.* 2011), their tolerance may explain their higher percentage cover found on Sodwana Bay reefs (Porter & Schleyer 2019).

The photosynthetic efficiency of live rock remained relatively unchanged across all climate change scenarios during all experimental phases (Fig. 3.3.7). Only a statistically insignificant decrease of 0.03  $\mu\text{mol m}^{-2} \text{s}^{-1}$  was evident during the final phase of the warmest treatment. Nevertheless, no overall changes in photosynthetic efficiency were evident among treatments and similar trends were found throughout the experiment (Fig. 3.3.7), which was further confirmed by the *post hoc* permANOVA analysis that resulted in no significant differences (Fig. 4.1). As live rock consists predominantly of calcium carbonate and crustose coralline algae, which seems to be more resilient than zooxanthellate corals, it experiences and shows little to no heat-stress response compared to that of the coral species this study investigated based on photosynthetic efficiency measurements.

While corals effectively grow on live rock substrata, foliose algal growth could potentially overgrow stressed coral colonies and lead to coral mortality (McCook *et al.* 2001; Jompa & McCook 2002).

Hence, the results of this study have important implications for coral recruitment in that the health of the crustose coralline algae did not appear to be compromised. As nutrient concentrations at Sodwana Bay are oligotrophic, little nutritional sources are available (Porter *et al.* 2017a). However, the region's low nutrient levels and the fact that these reefs are protected from fishing (Porter & Schleyer 2017) may help suppress algal growth at Sodwana Bay. Still, Bridge *et al.* (2014) found that algae such as turf algae were well-adapted to flourish when temperature-induced disturbances occurred on coral-dominated high-latitude reefs at Houtman Abrolhos Islands, Western Australia.

Overall, measuring photosynthetic efficiency can be an efficient way to gain insight into the metabolism of corals found in oligotrophic environments (Gattuso *et al.* 1999). Furthermore, competitive dynamics between foliose algae and coral may change on marginal reefs based on my results if warmer conditions become more prevalent. However, live rock which maintained levels of photosynthetic efficiency across treatments demonstrated that it is likely to persist under future global warming conditions.

#### **4.4.3 Net community calcification**

While temperature is a vital environmental parameter that controls the physiology and calcification of coral species, an increase in seawater temperature only significantly affected the rates of calcification in the bleaching-threshold treatment during diel period 3. A consistent increasing trend in net community calcification (NCC) was evident after averaging across the three diel periods (i.e. weeks 4, 6 and 8) within the control treatment at 24.4°C, as indicated by a decline in the concentration of CaCO<sub>3</sub> with time (Fig. 3.3.8). Similar increasing trends in NCC over a diel period were seen in the control treatment after studying the diel periods independently with increases in calcification especially evident during the light phase of diel periods 1 (week 4), 2 (week 6) and 3 (week 8) (Figs. 3.3.9–3.3.11). The increasing trends in NCC during the light phase indicated favourable responses over a diel period for reef communities under historical-average temperature conditions derived from Sodwana Bay that were used as a control. Contrariwise, coral communities that experience persistent heat stress conditions such as bleaching-threshold or extreme scenarios, will endure adverse effects on their calcification processes and overall survivorship (Hughes *et al.* 2017; Anderson *et al.* 2019).

My study demonstrated that net community calcification decreased in both the RCP 4.5 and bleaching-threshold scenarios compared to the control treatment based on the concentration of calcium carbonate (Fig. 3.3.8). The results corroborate the findings of Dove *et al.* (2013), where higher dissolution rates were also evident under the bleaching-threshold scenario and significantly higher for diel period 1 compared to diel period 2, even though the treatment term was marginally non-significant after running a permANOVA test (Fig. 4.1; Table 3.3.22). However, the permANOVA revealed a significant treatment crossed with diel period effect. NCC in the control treatment of 24.4°C was significantly lower than the RCP 4.5 treatment of 26.9°C during diel period 1 (week 4). Contrastingly, during diel

period 3 (week 8), significantly higher levels of NCC were evident at 24.4°C relative to 28.8°C and 26.9°C compared to 28.8°C (Fig. 4.1). Similar NCC results tested for equivalent RCP 4.5 and 8.5 temperature scenarios were found in the studies done by Meissner *et al.* (2011) and Dove *et al.* (2013).

After investigating three IPCC representative pathways (RCP 2.6, RCP 4.5 and RCP 8.5), Meissner *et al.* (2011) concluded that changes in temperatures resulted in changes to the seawater aragonite saturation state, especially in RCP 4.5 and 8.5 simulations. Virtually all the reefs they considered in their study would experience thermal stress by the year 2050. Conversely, Dove *et al.* (2013) found calcification decreased during daylight and increased during night-time in the future warming scenarios compared to the control conditions. Their results demonstrated that reef calcification processes might not have been capable of adjusting and coping with the environmental changes that have arisen over the last century, which was also evident in the present NCC results, especially for diel periods 2 and 3 (Figs. 3.3.9–3.3.11) in the warmest treatment.

The increasing evidence for calcification processes in reef communities being disrupted suggests that projected climate-change scenarios of global warming will result in increasing net dissolution of reef carbonate substrates. A similar trend was observed for the dissolution of coralline algae under increased temperature scenarios (Diaz-Pulido *et al.* 2011). Hence, the NCC results revealed in this study that with increasing temperatures the concentration of calcium carbonate was consistently higher in the bleaching-threshold scenario (Fig. 3.3.8), indicating suppressed NCC, which corresponds with similar NCC trends found in related coral studies (Marshall & Clode 2004; Reynaud *et al.* 2007; Cooper *et al.* 2008). Contrastingly, Marshall and Clode (2004) found calcification rates to be at a maximum in much warmer seawater conditions compared to the norm. Reynaud *et al.* (2007) concluded that the change in water temperatures during future heat-stress conditions had a significant effect on coral accretion, more so than light. Similarly, Anderson *et al.* (2019) found calcification rates intensifies when treatment temperatures were much warmer than the control temperature, at temperatures close to or surpassing 30°C. Cooper *et al.* (2008) also found that temperatures from 26.7°C and above started disrupting typical coral calcification rates as was evident in the results of this study (Fig. 4.1; Table 3.3.22).

Furthermore, when comparing each diel period of the experiment, diel period 1 during the initial phase yielded greater overall concentrations of calcium carbonate ( $\mu\text{mol CaCO}_3 \text{ kg}^{-1}$ ) in the bleaching-threshold scenario (Fig. 3.3.9), compared to the concentrations found during diel period 3 at the end of the middle phase in the same treatment (Fig. 3.3.11). These results are comparable to other studies that considered calcification processes at different phases of an experiment (Meissner *et al.* 2012; Dove *et al.* 2013; Anderson *et al.* 2019). The lower NCC for diel period 3 in the bleaching-threshold scenario relative to the other two scenarios can be attributed to warmer conditions than those required for optimal calcification. The results of this study demonstrated that calcification might have ceased for some specimens comprising the coral communities in the heat-stressed bleaching-threshold treatment. As reef

communities become more stressed, certain physiological functions in corals are inhibited that require substantial energy demands such as calcification (Rodrigues & Grottoli 2007; Tambutté *et al.* 2011). Such impairment in physiological response is likely as increasing temperatures break down the *Symbiodinium* photosystem. In return, energy availability is diminished for calcification processes (Tambutté *et al.* 2011; DeCarlo *et al.* 2018), which suffices as a survival technique in reef communities, facilitating energy distribution in corals and may result in more resilient reef frameworks (Rodrigues & Grottoli 2007).

After further *post hoc* statistical analysis, significant differences in dispersion in replicates among diel periods were evident, especially between diel period 2 (week 6) and diel period 3 (week 8). A further significant difference was found in diel period 3 between the control and bleaching-threshold treatment and between the year-2100 and bleaching-threshold treatment (Fig. 4.1). Variations in NCC during a diel cycle have been recorded in other coral reef studies where nocturnal sediment dissolution was found to be related to increasing sea temperatures and carbon dioxide (CO<sub>2</sub>) levels, associated with high rates of aerobic respiration (Yates & Halley 2006). Similarly, increases in dissolution have also been recorded in experimental mesocosms where the overlying seawater was either naturally or artificially acidified (Andersson *et al.* 2007). Another study done by McNeil *et al.* (2004), which solely focused on the influence of temperature on coral calcification rates, found that overall concentrations of calcium carbonate will increase with future ocean warming. The results found in my study suggest that a bleaching-threshold scenario will likely have severe impacts on overall coral reef calcification, especially because *p*CO<sub>2</sub> levels increase with temperature (Dove *et al.* 2013; Anderson *et al.* 2019). Surprisingly, the *post hoc* pairwise permANOVA analyses revealed no further dispersion effects between any of the interaction terms (Fig. 4.1), which possibly suggests that a longer experimental period and more NCC diel period measurements may have been necessary.

As per the recommendations given in the study conducted by Schoepf *et al.* (2016), my study successfully measured NCC over three diel periods using a similar alkalinity anomaly technique to Schoepf *et al.* (2016). The recommendations suggested using the alkalinity anomaly technique to investigate NCC while also using the buoyant weight technique. Both methods present practical limitations, hence their combined results provide more sound analyses and conclusions. Accordingly, the buoyant weight technique was also utilised in my study, but no formal comparisons between the NCC and buoyant weight results were made. The results from the NCC experiments measured community-level responses, whereas the buoyant weight results applied only to individual component responses. Complementary NCC measurements were therefore undertaken across different temperature scenarios to indicate coral reef community responses (Figs. 3.3.8–3.3.11; Table 3.3.25). Due to the marginality and high-latitude location of the reef communities that this study focused on, calcification is one of the main physiological responses that will probably be negatively affected by global warming (Kleypas *et al.* 1999).

## 4.5 Conclusions

### 4.5.1 Concluding Remarks

The results presented in my study found that the physiological responses of coral individuals and coral communities were influenced differently by the three temperature scenarios at different phases of the experiment. The influence on the corals was especially evident within the bleaching-threshold (28.8°C) scenario. Changes in the dimensions of *Acropora appressa* and *Sinularia brassica* indicated growth throughout the historical-average (24.4°C) and year-2100 RCP 4.5 (26.9°C) scenarios. Significant differences in the size of both coral species were found between phase, week nested in phase, and the interaction between species and week nested in phase. Both *A. appressa* and *S. brassica* underwent adverse change in growth at the end of the middle phase in the bleaching-threshold scenario, which continued in the case of *S. brassica* during the final phase of the experiment. *Acropora appressa* had bleached entirely by the end of the middle phase and was removed from the experiment for subsequent analyses beyond the scope of this work. Therefore, the null hypothesis was rejected and the first hypothesis was accepted as the growth of both coral species were negatively influenced by heat-stress conditions.

Similar growth trends were evident for the buoyant weight measurements. However, *A. appressa* showed continuous growth across all treatments, only levelling off to some extent in the warmest treatment during the middle phase. Contrastingly, *S. brassica* in the bleaching-threshold scenario manifested notable thermal stress based on growth from the middle phase until the experiment was terminated. The absence of significant declines in both coral growth parameters for *A. appressa* in the RCP 4.5 and bleaching-threshold scenarios and for *S. brassica* in the RCP 4.5 scenario suggests that inherent spatial variation in thermal-stress susceptibility and impact may impede reliable correlation of acute stress events with long-term growth records. However, when and if extreme climate-change conditions persist and become more frequent, repeated exposure to coral communities may lead to future reductions in coral growth rates.

Photosynthetic efficiency measured in all three individual functional groups indicated varying responses to the different climate-change scenarios. Both coral species started showing a decline in photosynthetic efficiency towards the end of the experiment in the RCP 4.5 scenario. A substantial decrease in photosynthetic efficiency was also evident in the bleaching-threshold scenario for both corals. However, the zooxanthellae seemed to be more affected in *A. appressa* than in *S. brassica*, as *A. appressa* started paling by the end of the middle phase under the bleaching-threshold scenario. Contrastingly, live rock maintained its photosynthetic efficiency across all treatments throughout each phase of the experiment. *Sinularia brassica* was able to avoid bleaching in the warmest treatment and only started paling during the extended two-week extreme-temperature scenario of 29.8°C. *Acropora appressa*, however, bleached in the middle phase of the bleaching-threshold scenario. Accordingly, the

second hypothesis was also accepted based on the negative responses and significant results found in the middle phase of the experiment for *A. appressa* and during the final phase for *S. brassica*. As the photosynthetic efficiency of live rock persisted throughout all the experimental phases, the rest of the hypothesis was rejected for live rock.

The differing stress responses indicate higher resistance in many soft corals to anomalously warm temperatures. The aragonite saturation state at higher latitudes favours corals with less calcifying abilities, as noted at Sodwana Bay (Celliers & Schleyer 2008). My findings suggest that soft corals are more resilient to increasing temperatures (see McClanahan *et al.* 2009). Even though physiological acclimation and adaptive mechanisms by corals could delay the extreme effects of some climate scenarios, evidence indicates that corals and their symbionts will struggle to adapt rapidly enough to global warming (Hoegh-Guldberg *et al.* 2007). Even corals with more robust adaptive mechanisms to increasing temperatures will only sustain increases of between 2 and 4°C above their long-term threshold for short periods (Hoegh-Guldberg 1999; Loya *et al.* 2001). With increasing bleaching events occurring in shorter timeframes, the capacity of reefs to recover diminishes along with it (Done 1999).

Net community calcification (NCC) followed a diel cycle throughout all the total alkalinity measurements. The reef communities within the warmest treatment had the lowest levels of NCC, indicated by the highest concentrations of dissolved calcium carbonate, for all diel periods. Accordingly, significant differences were found for the diel period, and the interaction term of treatment and diel period. Collectively, the results suggest depletion in reef calcification under bleaching-threshold conditions, allowing for the third hypothesis of this study to be accepted. With warmer summers projected in the future, reef communities are likely to be seriously impacted by such conditions, with winter seasons offering insufficient recovery time for the damage caused (Baker *et al.* 2008). Under consistent bleaching-threshold temperatures, coral reefs are unlikely to bear much resemblance to coral-dominated reefs at present (Dove *et al.* 2013).

Species with higher thermal stress tolerances may survive and adapt to climate change, whereas the opposite will be true for those species with lower stress tolerances. The results from this study suggest that high-latitude coral reefs will most likely experience a shift in community composition, considering the stressed physiological responses measured in *Acropora appressa* relative to the responses of *Sinularia brassica* and live rock. Although some subtropical locations, such as the South African high-latitude reefs, may provide refuges for biodiversity during increased heatwaves and prolonged global-warming events, this study suggests that high-latitude coral communities will be adversely affected by climate change.

As global warming persists and its related effects become more apparent, the oceanographic processes and properties change, which pose severe challenges to the future health and maintenance of marine ecosystems such as coral reefs. This is especially so for corals that are already found close to their upper

thermal threshold (Hoffmann & Sgrò 2011). The effects of the year-2100 RCP 4.5 and bleaching-threshold temperature scenarios on coral communities tested in this study are likely to have serious consequences for subsistence-dependent societies, along with broader regional economies by influencing coastal protection, fisheries and tourism. Consequently, the effects become successively worse as ocean temperatures increase with rising CO<sub>2</sub> levels. Reef ecosystem services will decline significantly under these persistent heat-stressed conditions (Hoegh-Guldberg *et al.* 2007). Furthermore, when an understanding of how environmental factors such as increasing temperatures influence coral physiology is gained, clarity will be provided when one considers multi-trait responses in the same individuals and reef communities. This means that differential bleaching susceptibility among coral genera may be present, regardless of the same individuals hosting similar *Symbiodinium* clades or symbiont types (Loya *et al.* 2001; Baird *et al.* 2009).

The study concludes that temperatures projected to occur according to the climate change models simulated are likely to be deleterious to high-latitude coral reef communities, inducing stress through different physiological mechanisms. Therefore, the null hypothesis was rejected according to the results obtained throughout the study.

#### **4.5.2 Future recommendations**

The overlapping processes of anthropogenic pressures, correlating with the adaptability of certain corals, will play a vital role in the future of each reef system as they face climate change over the following century. Anthropogenically-induced change in marine environments is multifaceted. Changes in temperature, pH, nutrient composition and concentrations, dissolved oxygen, pollution, and salinity are likely to co-occur to varying degrees of magnitude. The need to conduct factorial, multi-stressor experiments require large-scale, high-precision experimental systems that incorporate natural environmental variability into controlled manipulations (Gunderson *et al.* 2016). Consequently, such experiments can more accurately advance our understanding of the consequences of projected global changes. Therefore, it is recommended that more in-depth and integrated empirical models for different health parameters of corals should continue to be investigated and developed, explicitly focusing on non-steady-state processes such as global warming and climate change and how it affects diverse reef ecosystems.

When local stressors are better managed, the resilience of coral reefs can be increased to counteract the effects of climate change (Scheffer *et al.* 2015). Some local stressors that can be managed better include point-source pollution and run-off, overfishing and coastal development. Accordingly, future experiments should consider the interactive effects of warmer waters with chemical run-off, solar radiation and to a lesser extent, ocean acidification. By monitoring various aspects of coral physiology based on time scales relevant to metabolic and environmental cycles, scientists and local communities

can more effectively develop comprehensive coral-health tools and create better awareness of these intricate reef systems. Further research should also focus on the phenotypic plasticity of individual coral and how corals respond to different temperature regimes, assisting in reef restoration projects on a local and global scale. The scientific knowledge gained through completing this study can better advise and guide the requisite decision-making processes. Such efforts will further help attain the United Nations Sustainable Development Goals and the 2°C Paris Climate Agreement (UN Environment *et al.* 2018) within the United Nations Framework Convention on Climate Change.

## References

- Abram NJ, Gagan MK, Cole JE, Hantoro WS, Mudelsee M. 2003. Recent intensification of tropical climate variability in the Indian Ocean. *Nature Geoscience* 1: 849–853.
- Adey WH, Halfar J, Williams B. 2013. Biological, physiological and ecological factors controlling carbonate production in an Arctic-Subarctic Climate Archive: The calcified coralline genus *Clathromorphum* Foslíe. *Smithsonian Institution Contribution to the Marine Sciences*. Washington, DC.
- Ainsworth TD, Hoegh-Guldberg O, Heron SF, Skirving WJ, Leggat W. 2008. Early cellular changes are indicators of pre-bleaching thermal stress in the coral host. *Journal of Experimental Marine Biology and Ecology* 364: 63–71.
- Al-Footy KO, Alarif WM, Asiri F, Aly MM, Ayyad S-EN. 2015. Rare pyrane-based cembranoids from the Red Sea soft coral *Sarcophyton trocheliophorum* as potential antimicrobial-antitumor agents. *Medicinal Chemistry Research* 24: 505–512.
- Allemand D, Tambutté É, Zoccola D, Tambutté S. 2011. Coral calcification, cells to reefs. *Coral Reefs: An Ecosystem in Transition*, Dordrecht, Springer Netherlands, pp 119–150.
- Allen GR. 2008. Conservation hotspots of biodiversity and endemism for Indo-Pacific coral reef fishes. *Aquatic Conservation: Marine and Freshwater Ecosystems* 18(5): 541–556.
- Amman C, Boehnert J, Wilhemi O. 2018. World climate data CMIP5 multi model ensemble. *Research Applications Laboratory, National Center for Atmospheric Research, Boulder, Colorado*. <https://learn.arcgis.com/en/projects/explore-future-climate-projections/>. Downloaded on 21 August 2018.
- Anderson KD, Heron SF, Pratchett MS. 2014. Species-specific declines in the linear extension of branching corals at a sub-tropical reef, Lord Howe Island. *Coral Reefs* 34(2): 479–490.
- Anderson KD, Cantin NE, Casey JM, Pratchett MS. 2019. Independent effects of ocean warming versus acidification on the growth, survivorship and physiology of two *Acropora* corals. *Coral Reefs* 38(1): 1–16.
- Anderson KD, Cantin NE, Heron SF, Pisapia C, Pratchett MS. 2017. Variation in growth rates of branching corals along Australia's Great Barrier Reef. *Scientific Reports* 7(2920): 1–13.
- Anderson KD, Heron SF, Pratchett M. 2015. Species-specific declines in the linear extension of branching corals at a subtropical reef, Lord Howe Island. *Coral Reefs* 34: 479–490.

- Anderson MJ, Gorley RN, Clarke KR. 2008. PERMANOVA+ for PRIMER: Guide to software and statistical methods. *PRIMER-E*, Plymouth, UK.
- Andersson AJ, Kuffner IB, Mackenzie FT, Jokiel PL, Rodgers KS, Tan A. 2009. Net loss of CaCO<sub>3</sub> from a subtropical calcifying community due to seawater acidification: Mesocosm-scale experimental evidence. *Biogeosciences* 6: 1811–1823.
- Andersson AJ, Mackenzie FT, Ver LM. 2007. Dissolution of carbonate sediments under rising pCO<sub>2</sub> and ocean acidification: Observations from Devil’s Hole, Bermuda. *Aquatic Geochemistry* 13(3): 237–264.
- Anthony KRN, Connolly SR, Willis BL. 2002. Comparative analysis of energy allocation to tissue and skeletal growth in corals. *Limnology and Oceanography* 47: 1417–1429.
- Anthony KRN, Hoogenboom MO, Maynard JA, Grottoli AG, Middlebrook R. 2009. Energetics approach to predicting mortality risk from environmental stress: a case study of coral bleaching. *Functional Ecology* 23(3): 539–550.
- Anthony KRN, Kline DI, Diaz-Pulido G, Dove S, Hoegh-Guldberg O. 2008. Ocean acidification causes bleaching and productivity loss in coral reef builders. *Proceedings of the National Academy of Sciences* 105: 17442–17446.
- ARC Reef. 2016. Live Rock – The Ultimate Guide. *Atlantic Reef Conservation*. <https://arcreef.com/live-rock/live-rock-guide/>. Accessed on 21 December 2020.
- Atweberhan M, McClanahan TR, Graham NAJ, Sheppard CRC. 2011. Episodic heterogeneous decline and recovery of coral cover in the Indian Ocean. *Coral Reefs* 30: 739–752.
- Baird AH, Bhagooli R, Ralph PJ, Takahashi S. 2009. Coral bleaching: The role of the host. *Trends in Ecology and Evolution* 24(1): 16–20.
- Bak RPM, Nieuwland G, Meesters EH. 2009. Coral growth rates revisited after 31 years: What is causing lower extension rates in *Acropora palmata*? *Bulletin of Marine Science* 84: 287–294.
- Bak RPM. 1973. Coral weight increment in situ. A new method to determine coral growth. *Marine Biology* 20: 45–49.
- Baker A, Glynn PW, Riegl B. 2008. Climate change and coral reef bleaching: An ecological assessment of long-term impacts, recovery trends and future outlook. *Estuarine, Coastal and Shelf Science* 80(4): 435–471.
- Bakun A. 1990. Global climate change and intensification of coastal ocean upwelling. *Science* 247: 198–201.

- Barkley HC, Cohen AL, McCorkle DC, Golbuu Y. 2017. Mechanisms and thresholds for pH tolerance in Palau corals. *Journal of Experimental Marine Biology and Ecology* 489: 7–14.
- Beal LM, de Ruijter WPM, Biastoch A, Zahn R, SCOR/WCRP/IAPSO Working Group 136. On the role of the Agulhas system in ocean circulation and climate. *Nature* 472: 429–436.
- Beer S, Bjork M. 2000. A comparison of photosynthetic rates measured by pulse amplitude modulated (PAM) fluorometry and O<sub>2</sub> evolution in two tropical seagrasses. *Aquatic Botany* 66: 69–73.
- Beer S, Larsson C, Poryan O, Axelsson L. 2000. Measuring photosynthetic rates of the marine macroalga *Ulva* by pulse amplitude modulated (PAM) fluorometry. *European Journal of Phycology* 35: 69–74.
- Beer S, Vilenkin B, Weil A, Veste M, Susel L, Eshel A. 1998. Measuring photosynthetic rates in seagrasses by pulse amplitude modulated (PAM) fluorometry. *Marine Ecology Progress Series* 164: 293–300.
- Beger M, Sommer B, Harrison PL, Smith SDA, Pandolfi JM *et al.* 2014. Conserving potential coral reef refuges at high latitudes. *Diversity and Distributions* 20: 245–257.
- Bellwood DR, Hughes TP, Folke C, Nystrom M. 2004. Confronting the coral reef crisis. *Nature* 429: 827–833.
- Bellworthy J, Fine M. 2017. Beyond peak summer temperatures, branching corals in the Gulf of Aqaba are resilient to thermal stress but sensitive to high light. *Coral Reefs* 36: 1071–1082.
- Bellworthy J, Fine M. 2018. The red sea simulator: A high-precision climate change mesocosm with automated monitoring for the long-term study of coral reef organisms. *Limnology and Oceanography: Methods* 16(6): 367–375.
- Berkelmans R, De'ath G, Kininmonth S, Skirving WJ. 2003. A comparison of the 1998 and 2002 coral bleaching events on the Great Barrier Reef: spatial correlation, patterns, and predictions. *Coral Reefs* 23: 74–83.
- Bessell-Browne P, Negri AP, Fisher R, Clode PL, Jones R. 2017. Impacts of light on corals and crustose coralline algae. *Scientific Reports* 7: 11553.
- Bestion E, Teyssier A, Richard M, Clobert J, Cote J. 2015. Live fast, die young: Experimental evidence of population extinction risk due to climate change. *PLoS Biology* 13(10): e1002281.
- Biscéré T, Zampighi M, Lorrain A, Jurriaans S, Foggo A *et al.* 2019. High pCO<sub>2</sub> promotes coral primary production. *Biology Letters* 15(7): 1–15.

- Blackall LL, Wilson B, van Oppen MJ. 2015. Coral – The world’s most diverse symbiotic ecosystem. *Molecular Ecology* 24: 5330–5347.
- Bopp L, Resplandy L, Orr JC, Doney SC, Dunne JP *et al.* 2013. Multiple stressors of ecosystems in the 21<sup>st</sup> century: Projections with CMIP5 models. *Biogeosciences* 10: 6225–6245.
- Borneman EH, Lowrie J. 2001. Advances in captive husbandry and propagation: An easily utilized reef replenishment means from the private sector? *Bulletin of Marine Science* 69(2): 897–913.
- Bridge TCL, Ferrari R, Bryson M, Hovey R, Figueira WF *et al.* 2014. Variable responses of benthic communities to anomalously warm sea temperatures on a high-latitude coral reef. *PLoS ONE* 9(11): e113079.
- Broecker WS. 1975. Climatic change: Are we on the brink of pronounced global warming? *Science* 189(4201): 460–463.
- Brown BE, Dunne RP, Ambarsari I, Le Tissier MDA, Satapoomin U. 1999. Seasonal fluctuations in environmental factors and variations in symbiotic algae and chlorophyll pigments in four Indo-Pacific coral species. *Marine Ecology Progress Series* 191: 53–69.
- Brown BE. 1997. Coral bleaching: Causes and consequences. *Coral Reefs* 16: S129–S138.
- Bruckner AW. 2002. Life-saving products from coral reefs. *Issues in Science and Technology* 18(3).
- Burke L, Reytar K, Spalding M, Perry A. 2011. Chapter 3: Threats to the world’s reefs. In: Cooper E, Kushner B, Selig E, Starkhouse B, Teleki K *et al.* (eds), *Reefs At Risk Revisited*. World Resources Institute, pp 21–37.
- Burrows K, Kinney P. 2016. Exploring the climate change, migration and conflict nexus. *International Journal of Environmental Research and Public Health* 13(4): 443.
- Cacciapaglia, C, van Woesik R. 2015. Reef-coral refugia in a rapidly changing ocean. *Global Change Biology* 21(6): 2272–2282.
- Camp EF, Schoepf V, Mumby PJ, Hardtke LA, Rodolfo-Metalpa R *et al.* 2018. The future of coral reefs subject to rapid climate change: Lessons from natural extreme environments. *Frontiers in Marine Science* 5: 4.
- Cantin NE, Cohen AL, Karnauskas KB, Tarrant AM, McCorkle DC. 2010. Ocean warming slows coral growth in the central Red Sea. *Science* 329: 322–325.
- Cantin NE, Lough JM. 2014. Surviving coral bleaching events: *Porites* growth anomalies on the Great Barrier Reef. *PLoS ONE* 9: e88720.

- Carilli JE, Norris RD, Black B, Walsh SM, McField M. 2010. Century-scale records of coral growth rates indicate that local stressors reduce coral thermal tolerance threshold. *Global Change Biology* 16: 1247–1257.
- Caroselli E, Falini G, Goffredo S, Dubinsky Z, Levy O. 2015. Negative response of photosynthesis to natural and projected high seawater temperatures estimated by pulse amplitude modulation fluorometry in a temperate coral. *Frontiers in Physiology* 6(317): 1–11.
- Caroselli E, Prada F, Pasquini L, Marzano FN, Zaccanti F *et al.* 2011. Environmental implications of skeletal micro-density and porosity variation in two scleractinian corals. *Zoology* 114: 255–264.
- Carpenter KE, Abrar M, Aeby G, Aronson RB, Banks S *et al.* 2008. One-third of reef-building corals face elevated extinction risk from climate change and local impacts. *Science* 321: 560–563.
- Carricart-Ganivet JP, Cabanillas-Teran N, Cruz-Ortega I, Blanchon P. 2012. Sensitivity of calcification to thermal stress varies among genera of massive reef-building corals. *PLoS ONE* 7: e32859.
- Cawthra HC, Neumann FH, Uken R, Smith AM, Guastella LA *et al.* 2012. Sedimentation on the narrow (8 km wide), oceanic current-influenced continental shelf off Durban, KwaZulu-Natal, South Africa. *Marine Geology* 323-325: 107–122.
- Celliers L, Schleyer MH. 2002. Coral bleaching on high-latitude marginal reefs at Sodwana Bay, South Africa. *Marine Pollution Bulletin* 44: 1380–1387.
- Celliers L, Schleyer MH. 2008. Coral community structure and risk assessment of high-latitude reefs at Sodwana Bay, South Africa. *Biodiversity and Conservation* 17: 3097–3117.
- Cesar H, Burke L, Per-Soede L. 2003. The economics of worldwide coral reef degradation. *Cesar Environmental Economics Consulting*, Arnhem, The Netherlands, 24 pp.
- Chan NCS, Connolly SR. 2013. Sensitivity of coral calcification to ocean acidification: A meta-analysis. *Global Change Biology* 19: 282–290.
- Chevin L-M, Lande R, Mace GM. 2010. Adaptation, plasticity, and extinction in a changing environment: towards a predictive theory. *PLoS Biology* 8: e1000357.
- Chisholm JRM, Gattuso J-P. 1991. Validation of the alkalinity anomaly technique for investigating calcification of photosynthesis in coral reef communities. *Limnology and Oceanography* 36(6): 1232–1239.
- Cinner JE, McClanahan TR, Graham NAJ, Pratchett MS, Wilson SK *et al.* 2009. Gear-based fisheries management as a potential adaptive response to climate change and coral mortality. *Journal of Applied Ecology* 46(3): 724–732.

- Clayton S, Dutkiewicz S, Jahn O, Follows MJ. 2013. Dispersal, eddies, and the diversity of marine phytoplankton. *Limnology and Oceanography: Fluids Environment* 3: 182–197.
- Climate Action Tracker. 2020. Pandemic recovery: Positive intentions vs policy rollbacks, with just a hint of green. *Climate Action Tracker – Warming Projections Global Update*. <https://climateactiontracker.org/publications/global-update-pandemic-recovery-with-just-a-hint-of-green/>. Accessed on 06 May 2021.
- Cohen AL, Hart SR. 1997. The effect of colony topography on climate signals in coral skeleton. *Geochimica et Cosmochimica Acta* 61(18): 3905–3912.
- Cohen AL, Holcomb M. 2009. Why corals care about ocean acidification: Uncovering the mechanism. *Oceanography* 22: 118–127.
- Cohen S, Krueger T, Fine M. 2017. Measuring coral calcification under ocean acidification: Methodological considerations for the <sup>45</sup>Ca-uptake and total alkalinity anomaly technique. *PeerJ* 5: e3749.
- Cole AJ, Pratchett MS, Jones GP. 2008. Diversity and functional importance of coral-feeding fishes on tropical coral reefs. *Fish and Fisheries* 9(3): 286–307.
- Collins M, Knutti R, Arblaster J, Dufresne J-L, Fichetef T *et al.* 2013. Long-term climate change: Projections, commitments and irreversibility. In: Stocker TF, Qin D, Plattner G-K, Tignor M, Allen SK *et al.* (eds), *Climate Change 2013: The Physical Science Basis. Contribution of Working Group I to the Fifth Assessment Report of the Intergovernmental Panel on Climate Change*, Cambridge University Press, Cambridge, United Kingdom and New York, pp 1029–1136.
- Colombo-Pallota MF, Rodriguez-Román A, Iglesias-Prieto R. 2010. Calcification in bleached and unbleached *Monastraea faveolata*: Evaluating the role of oxygen and glycerol. *Coral Reefs* 29(4): 899–907.
- Comeau S, Carpenter RC, Lantz CA, Edmunds PJ. 2015. Ocean acidification accelerates dissolution of experimental coral reef communities. *Biogeosciences* 12: 365–372.
- Connell SD, Russell B. 2010. The direct effects of increasing CO<sub>2</sub> and temperature on non-calcifying organisms: Increasing the potential for phase shifts in kelp forest. *Proceedings of the Royal Society: Biology* 277: 1409–1415.
- Cooper TF, Berkelmans R, Ulstrup KE, Weeks S, Radford B *et al.* 2011. Environmental factors controlling the distribution of *Symbiodinium* harboured by the coral *Acropora millepora* on the Great Barrier Reef. *PLoS ONE* 6(10): e25536.

- Cooper TF, De'ath G, Fabricius KE, Lough JM. 2008. Declining coral calcification in massive *Porites* in two nearshore regions of the northern Great Barrier Reef. *Global Change Biology* 14: 529–538.
- Cornwall CE, Comeau S, Mcculloch MT. 2017. Coralline algae elevate pH at the site of calcification under ocean acidification. *Global Change Biology* 23: 4245–4256.
- Cornwall CE, Diaz-Pulido G, Comeau S. 2019. Impacts of ocean warming on coralline algal calcification: Meta-analysis, knowledge gaps, and key recommendations for future research. *Frontiers in Marine Science* 6: 186.
- Courtney TA, Lebrato M, Bates NR, Collins A, de Putron SJ *et al.* 2017. Environmental controls on modern scleractinian coral and reef-scale calcification. *Science Advances* 3: e1701356.
- Crabbe MJC, Smith DJ. 2005. Sediment impacts on growth rates of *Acropora* and *Porites* corals from fringing reefs of Sulawesi, Indonesia. *Coral Reefs* 24: 437–441.
- Cronin TM. 1999. Principles of paleoclimatology. Perspectives in paleobiology and Earth history series. *Geological Magazine*. New York, Columbia University Press, 137(4): 463–479.
- Crossland CJ, Barnes DJ, Borowitzka MA. 1980. Diurnal lipid and mucus production in the staghorn coral *Acropora acuminata*. *Marine Biology* 60: 81–90.
- Cunning R, Bay RA, Gillette P, Baker AC, Traylor-Knowles N. 2018. Comparative analysis of the *Pocillopora damicornis* genome highlights role of immune system in coral evolution. *Scientific Reports* 8: 16134.
- Darling ES, Alvarez-Filip L, Oliver TA, McClanahan TR, Côté IM. 2012. Evaluating life-history strategies of reef corals from species traits. *Ecology Letters* 15(12): 1378–1386.
- Davies GM, Gray A. 2015. Don't let spurious accusations of pseudoreplication limit our ability to learn from natural experiments (and other messy kinds of ecological monitoring). *Ecology and Evolution* 5(22): 5295–5304.
- Davies PS. 1989. Short-term growth measurements of corals using an accurate buoyant weighing technique. *Marine Biology* 101(3): 389–395.
- de Ruijter WPM, Beal L, Biastoch A, Zahn R. 2013. The role of the Agulhas system in regional and global climate. *American Geophysical Union Chapman Conference: The Agulhas system and its role in changing ocean circulation, climate, and marine ecosystems*, Stellenbosch, South Africa, 94(10): 100–103.
- De'ath G, Fabricius KE, Lough JM. 2013. Yes – Coral calcification rates have decreased in the last twenty-five years! *Marine Geology* 346: 400–402.

- De'ath G, Fabricius KE, Sweatman H, Puotinen M. 2012. The 27-year decline of coral cover on the Great Barrier Reef and its causes. *Proceedings of the National Academy of Sciences* 109: 17995–17999.
- De'ath G, Lough JM, Fabricius KE. 2009. Declining coral calcification on the Great Barrier Reef. *Science* 323: 116–119.
- DeCarlo TM, Comeau S, Cornwall CE, McCulloch MT. 2018. Coral resistance to ocean acidification linked to increase calcium at the site of calcification. *Proceedings of the Royal Society B: Biological Sciences* 285: 20180564.
- Demunshi Y, Chugh A. 2010. Role of traditional knowledge in marine bioprospecting. *Biodiversity and Conservation* 19: 3015–3033.
- Diaz-Pulido G, Anthony KRN, Kline DI, Dove S, Hoegh-Guldberg O. 2011. Interactions between ocean acidification and warming on the mortality and dissolution of coralline algae. *Journal of Phycology* 48: 32–39.
- Dickson AG, Millero FJ. 1987. A comparison of the equilibrium constants for the dissociation of carbonic acid in seawater media. *Deep Sea Research: Part A. Oceanographic Research Papers* 34(10): 1733–1743.
- Dickson AG. 1981. An exact definition of total alkalinity and a procedure for the estimation of alkalinity and total CO<sub>2</sub> from titration data. *Deep-Sea Research Part A: Oceanographic Research Papers* 28: 609–623.
- Done TJ, Whetton P, Jones RN, Berkelmans R, Lough JM *et al.* 2003. Global climate change and coral bleaching on the Great Barrier Reef. Final report to the State of Queensland Greenhouse Taskforce through the Department of Natural Resources and Mining, Townsville.
- Doney SC, Fabry VJ, Feely RA, Kleypas JA. 2009. Ocean acidification: The other CO<sub>2</sub> problem. *Annual Review of Marine Science* 1: 169–192.
- Dove SG, Kline DI, Pantos O, Angly FE, Tyson GW *et al.* 2013. Future reef decalcification under a business-as-usual CO<sub>2</sub> emission scenario. *Proceedings of the National Academy of Sciences* 110(38): 15342–15347.
- Eakin CM, Donner S, Logan C, Gledhill D, Liu G *et al.* 2010. Thresholds for coral bleaching: Are synergistic factors and shifting thresholds changing the landscape for management? *Fall Meeting 2010*, San Francisco, CA, American Geophysical Union.
- Eakin CM, Liu G, Gomez AM, De la Couri JL, Heron SF *et al.* 2018. Unprecedented three years of global coral bleaching 2014–2017. *Bulletin of the American Meteorological Society* 99(8): S74–S75.

- Eakin CM, Sweatman HPA, Brainard RE. 2019. The 2014–2017 global-scale coral bleaching event: Insights and impacts. *Coral Reefs* 38: 539–545.
- Edmunds PJ, Leichter JJ. 2016. Spatial scale-dependent vertical zonation of coral reef community structure in French Polynesia. *Ecosphere* 7(5): e01342.
- Enochs IC, Manzello DP, Kolodziej G, Noonan SH, Valentino L *et al.* 2016. Enhanced macroboring and depressed calcification drive net dissolution at high-CO<sub>2</sub> coral reefs. *Proceedings of the Royal Society of London B: Biological Sciences* 283(1842): 20161742.
- Fabricius KE, Alderslade P. 2001. *Soft Corals and Sea Fans*. Australian Institute of Marine Science and the Museum and Art Gallery of the Northern Territory, 264 pp.
- Fabricius KE, McCorry D. 2006. Changes in octocoral communities and benthic cover along a water quality gradient in the reefs of Hong Kong. *Marine Pollution Bulletin* 52: 22–33.
- Falls WW, Enringer JN, Herndon R, Herndon T, Nicholls MS *et al.* 2003. Aquaculture of live rock: An eco-friendly alternative. *World Aquaculture*.
- Fantazzini P, Mengoli S, Pasquini L, Bortolotti V, Brizi L *et al.* 2015. Gains and losses of coral skeletal porosity changes with ocean acidification acclimation. *Nature Communications* 6: 7785.
- Farag MA, Al-Mahdy DA, Meyer A, Westphal H, Wessjohann LA. 2017. Metabolomics reveals biotic and abiotic elicitor effects on the soft coral *Sarcophyton ehrenbergi* terpenoid content. *Scientific Reports* 7(648).
- Ferse SCA, Máñez KS, Kunzmann A. 2010. Gems of the sea – Assessing the economic potential of ornamental coral reef fishes. *11<sup>th</sup> Biennial ISEE Conference*. Oldenburg, Germany. Accessed on 21 December 2020.
- Fisher R, Bessell-Browne P, Jones R. 2019. Synergistic and antagonistic impacts of suspended sediments and thermal stress on corals. *Nature Communications* 10(1): 2346.
- Fisher R, O’Leary RA, Low-Choy S, Mengersen K, Knowlton N *et al.* 2015. Species richness on coral reefs and the pursuit of convergent global estimates. *Current Biology* 25(4): 500–505.
- Floros C, Schleyer MH, Maggs JQ, Celliers L. 2012. Baseline assessment of high-latitude coral reef fish communities in southern Africa. *African Journal of Marine Science* 34: 55–69.
- Floros C. 2010. An evaluation of coral reef fish communities in South African marine protected areas. PhD thesis, University of KwaZulu-Natal, South Africa, 189 pp.
- Form AU, Riebesell U. 2012. Acclimation to ocean acidification during long-term CO<sub>2</sub> exposure in the cold-water coral *Lophelia pertusa*. *Global Change Biology* 18: 843–853.

- Foster T, Short JA, Falter JL, Ross C, McCulloch MT. 2014. Reduced calcification in Western Australian corals during anomalously high summer water temperatures. *Journal of Experimental Marine Biology and Ecology* 461: 133–143.
- Franklin LA, Badger MR. 2001. A comparison of photosynthetic electron transport rates in macroalgae measured by pulse amplitude modulated chlorophyll fluorescence. *Biochimica et Biophysica Acta* 990: 87–92.
- Freeman LA. 2015. Robust performance of marginal pacific coral reef habitats in future climate scenarios. *PLoS ONE* 10(6): e0128875.
- Freiwald A, Fosså JH, Grehan A, Koslow T, Roberts JM. 2004. *Cold-water coral reefs: Out of sight – no longer out of mind*. Cambridge, UNEP-WCMC.
- Frieler K, Meinshausen M, Golly A, Mengel M, Lebek K *et al.* 2013. Limiting global warming to 2°C is unlikely to save most coral reefs. *Nature Climate Change* 3: 165–170.
- Fujise L, Yamashita H, Suzuki G, Sasaki K, Liao LW *et al.* 2014. Moderate thermal stress causes active and immediate expulsion of photosynthetically damaged zooxanthellae (*Symbiodinium*) from corals. *PLoS ONE* 9(12): e114321.
- García Molinos J, Halpern BS, Schoeman DS, Brown CJ, Kiessling W *et al.* 2015. Climate velocity and the future global redistribution of marine biodiversity. *Nature Climate Change* 6: 83–88.
- Gattuso J-P, Allemand D, Frankignoulle M. 1999. Photosynthesis and calcification at cellular, organismal and community levels in coral reefs: A review on interactions and control by carbonate chemistry. *American Zoologist* 39(1): 160–183.
- Gattuso J-P, Brewer PG, Hoegh-Guldberg O, Kleypas JA, Pörtner H-O, Schmidt DN. 2014. Cross-chapter box on ocean acidification. In: Field CB, Barros VR, Dokken DJ, Mach KJ, Mastrandrea MD *et al.* (eds), *Climate Change 2014: Impacts, Adaptation, and Vulnerability. Part A: Global and Sectoral Aspects. Contribution of Working Group II to the Fifth Assessment Report of the Intergovernmental Panel on Climate Change*, Cambridge University Press, Cambridge, UK and NY, pp 129–131.
- Gattuso J-P, Magnan A, Billé R, Cheung WWL, Howes EL *et al.* 2015. Contrasting futures for ocean and society from different anthropogenic CO<sub>2</sub> emissions scenarios. *Science* 349(6243).
- Genty B, Briantais J-M, Baker NR. 1989. The relationship between quantum yield of photosynthetic electron transport and quenching of chlorophyll fluorescence. *Biochimica et Biophysica Acta* 990: 87–92.
- Glassom D, Celliers L, Schleyer MH. 2006. Coral recruitment patterns at Sodwana Bay, South Africa. *Coral Reefs* 25: 485–492.

- Glynn PW, D’Croz L. 1990. Experimental evidence for high temperature stress as the cause of the El Niño-co-incident coral mortality. *Coral Reefs* 8: 181–191.
- Goffredo S, Caroselli E, Mattioli G, Pignotti E, Dubinsky Z *et al.* 2009. Inferred level of calcification decreases along an increasing temperature gradient in a Mediterranean endemic coral. *Limnology and Oceanography* 54: 930–937.
- Goffredo S, Caroselli E, Mattioli G, Pignotti E, Zaccanti F. 2008. Relationships between growth, population structure and sea surface temperature in the temperate solitary coral *Balanophyllia europaea* (*Scleractinia*, *Dendrophylliidae*). *Coral Reefs* 27: 623–632.
- Goffredo S, Prada F, Caroselli E, Capaccioni B, Zaccanti F *et al.* 2014. Biomineralization control related to population density under ocean acidification. *Nature Climate Change* 4: 593–597.
- Gorbunov MY, Kolber ZS, Lesser MP, Falkowski PG. 2001. Photosynthesis and photoprotection in symbiotic corals. *Limnology and Oceanography* 46(1): 75–85.
- Goreau TF, Macfarlane A. 1990. Reduced growth rate of *Montastrea annularis* following the 1987-1988 coral-bleaching event. *Coral Reefs* 8: 211–215.
- Goreau TF. 1959. The physiology of skeleton formation in corals: A method for measuring the rate of calcium deposition by corals under different conditions. *The Biological Bulletin* 116: 59–75.
- Grottoli AG, Rodrigues LJ, Palardy JE. 2006. Heterotrophic plasticity and resilience in bleached corals. *Nature* 440: 1186–1189.
- Grottoli AG, Warner ME, Levas SJ, Aschaffenburg MD, Schoepf V *et al.* 2014. The cumulative impact of annual coral bleaching can turn some coral species winners into losers. *Global Change Biology* 20(12): 3823–3833.
- Guastella L. 2014. Ugu Lwethu – Our Coast. A profile of coastal KwaZulu-Natal. In: Goble BJ, van der Elst RP, Oellermann LK (eds), *Physical Oceanography*, KwaZulu-Natal, Department of Agriculture and Environmental Affairs and the Oceanographic Research Institute, Cedara, pp 20–26.
- Gudka M, Obura D, Mwaura J, Porter S, Yahya S *et al.* 2018. *Impact of the 3<sup>rd</sup> global coral bleaching event on the Western Indian Ocean in 2016*. Global Coral Reef Monitoring Network (GCRMN)/Indian Ocean Commission, 67 pp.
- Guinotte JM, Buddemeier RW, Kleypas JA. 2003. Future coral reef habitat marginality: Temporal and spatial effects of climate change in the Pacific basin. *Coral Reefs* 22(4): 551–558.
- Gunderson AR, Armstrong EJ, Stillman JH. 2016. Multiple stressors in a changing world: The need for an improved perspective on physiological responses to the dynamic marine environment. *Annual Review of Marine Science* 8: 357–378.

- Halo I, Raj RP. 2020. Comparative oceanographic eddy variability during climate change in the Agulhas Current and Somali Coastal Current Large Marine Ecosystems. *Environmental Development* 36: 100586.
- Harikishun A. 2013. Coral bleaching responses in Sodwana Bay, South Africa. MSc thesis, University of Cape Town, South Africa, pp 1–34.
- Harris DL, Rovere A, Casella E, Power H, Canavesio R *et al.* 2018. Coral reef structural complexity provides important coastal protection from waves under rising sea levels. *Science Advances* 4(2): eaa04350.
- Harrison P, Dalton S, Carroll A. 2011. Extensive coral bleaching on the world’s southernmost coral reef at Lord Howe Island, Australia. *Coral Reefs* 30: 775–776.
- Hart JR. 2018. The fertilisation and recruitment dynamics of scleractinian corals on South Africa’s high-latitude reefs. PhD thesis, University of KwaZulu-Natal, South Africa, pp 1–102.
- Hatcher BG. 1997. Organic production and decomposition. In: Birkeland C (ed.), *Life and Death of Coral Reefs*, Chapman and Hall, New York, pp 140–174.
- Hauter S, Hauter D. 2019. What is live rock? *The Spruce Pets*. <https://www.thesprucepets.com/purpose-of-live-rock-in-marine-aquariums-2925051>. Accessed on 21 December 2020.
- Hegazy M-EF, Eldeen AMG, Shahat AA, Abdel-Latif FF, Mohamed TA *et al.* 2012. Bioactive hydroperoxyl cembranoids from the Red Sea Soft Coral *Sarcophyton glaucum*. *Marine Drugs* 10(1): 209–222.
- Henkel TP. 2012. Coral reefs. *Nature Education Knowledge* 3: 12.
- Hennige SJ, Wicks LC, Kamenos NA, Perna G, Findlay HS *et al.* 2015. Hidden impacts of ocean acidification to live and dead coral framework. *Proceedings of the Royal Society B: Biological Sciences* 282(1813): 1–10.
- Herler J, Dirnwöber M. 2011. A simple technique for measuring buoyant weight increment of entire, transplanted coral colonies in the field. *Journal of Experimental Marine Biology and Ecology* 407: 250.
- Hoegh-Guldberg O, Bruno JF. 2010. The impact of climate change on the world’s marine ecosystems. *Science* 328(5985): 1523–1528.
- Hoegh-Guldberg O, Cai R, Poloczanska ES, Brewer PG, Sundby S *et al.* 2014. The Ocean. In: Barros VR, Field CB, Dokken DJ, Mastrandrea MD, Mach KJ *et al.* (eds), *Climate Change 2014: Impacts, Adaptation, and Vulnerability. Part B. Regional Aspects. Contribution of Working Group II to the Fifth ASSESSMENT Report of the Intergovernmental Panel on Climate Change*, Cambridge University Press, Cambridge, New York, pp 1655–1731.

- Hoegh-Guldberg O, Jacob D, Taylor M, Bindi M, Brown S *et al.* 2018. Impacts of 1.5°C global warming on natural and human systems. In: Masson-Delmotte V, Zhai P, Pörtner H-O, Roberts D, Skea J *et al.* (eds), *Global Warming of 1.5°C. An IPCC Special Report on the impacts of global warming of 1.5°C above pre-industrial levels and related global greenhouse gas emission pathways, in the context of strengthening the global response to the threat of climate change, sustainable development, and efforts to eradicate poverty.*
- Hoegh-Guldberg O, Mumby PJ, Hooten AJ, Steneck RS, Greenfield P *et al.* 2007. Coral reefs under rapid climate change and ocean acidification. *Science* 318: 1737–1742.
- Hoegh-Guldberg O, Pendleton L, Kaup A. 2019. People and the changing nature of coral reefs. *Regional Studies in Marine Science* 30: 100699.
- Hoegh-Guldberg O. 1999. Climate change, coral bleaching and the future of the world's coral reefs. *Marine and Freshwater Research* 50: 839–866.
- Hoegh-Guldberg O. 1999. Climate change, coral bleaching and the future of the world's coral reefs. *Marine and Freshwater Research* 50(8): 839–866.
- Hoegh-Guldberg O. 2011. The impact of climate change on coral reef ecosystems. In: Dubinsky Z, Stambler N (eds), *Coral Reefs*, Springer Netherlands, pp 391–403.
- Hoeke RK, Jokiel PL, Buddemeier RW, Brainard RE. 2011. Projected changes to growth and mortality of Hawaiian corals over the next 100 years. *PLoS ONE* 6(3): e18038.
- Hoffmann AA, Sgrò CM. 2011. Climate change and evolutionary adaptation. *Nature* 470: 479–485.
- Holcomb M, Cohen AL, McCorkle DC. 2013. An evaluation of staining techniques for marking daily growth in scleractinian corals. *Journal of Experimental Marine Biology and Ecology* 440: 126–131.
- Holcomb M, McCorkle DC, Cohen AL. 2010. Long-term effects of nutrient and CO<sub>2</sub> enrichment on the temperate coral *Astrangia poculata* (Ellis & Solander 1786). *Journal of Experimental Marine Biology and Ecology* 386: 27–33.
- Hönisch B, Ridgwell A, Schmidt DN, Thomas E, Gibbs SJ *et al.* 2012. The geological record of ocean acidification. *Science* 335: 1058–1063.
- Hubbard DK. 2015. Reef biology and geology – not just a matter of scale. In: Birkeland C (ed.), *Coral Reefs in the Anthropocene*, Dordrecht, Springer Netherlands, pp 43–66.
- Hughes AD, Grottoli A, Pease T, Matsui Y. 2010. Acquisition and assimilation of carbon in non-bleached and bleached corals. *Marine Ecology Progress Series* 420: 91–101.

Hughes TP, Baird AH, Bellwood DR, Card M, Connolly SR *et al.* 2003. Climate change, human impacts, and the resilience of coral reefs. *Science* 301(80): 929–933.

Hughes L. 2000. Biological consequences of global warming: Is the signal already apparent? *Trends in Ecology and Evolution* 15: 56–61.

Hughes TP, Anderson KD, Connolly SR, Heron SF, Kerry JT *et al.* 2018. Spatial and temporal patterns of mass bleaching of corals in the Anthropocene. *Science* 359: 80–83.

Hughes TP, Barnes ML, Bellwood DR, Cinner JE, Cumming GS *et al.* 2017. Coral reefs in the Anthropocene. *Nature* 546: 82–90.

Hughes TP, Jackson JBC. 1985. Population dynamics and life histories of foliaceous corals. *Ecological Monographs* 55: 141–166.

Hughes TP, Kerry JT, Álvarez-Noriega M, Álvarez-Romero JG, Anderson KD *et al.* 2017. Global warming and recurrent mass bleaching of corals. *Nature* 543(7645): 373–377.

Hughes TP, Rodrigues MJ, Bellwood DR, Ceccarelli DM, Hoegh-Guldberg O *et al.* 2007. Phase shifts, herbivory, and the resilience of coral reefs to climate change. *Current Biology* 17: 1–6.

Hughes TP. 1987. Skeletal density and growth form of corals. *Marine Ecology Progress Series* 35(3): 259–266.

Iglesias-Prieto R, Matta JL, Robins WA, Trench RK. 1992. Photosynthetic response to elevated temperature in the symbiotic dinoflagellate *Symbiodinium microadriaticum* in culture. *Proceedings of the National Academy of Sciences of the United States of America* 89: 10302–10305.

Iluz D, Vago R, Chadwick NE, Hoffman R, Dubinsky Z. 2008. Seychelles lagoon provides corals a refuge from bleaching. *Research Letters in Ecology*. doi.org/10.1155/2008/281038.

Intergovernmental Panel on Climate Change (IPCC). 2007. Summary for policymakers. In: Solomon S, Qin D, Manning M, Chen Z, Marquis M *et al.* (eds), *Climate change 2007: The Physical Science Basis. Contribution of working group I to the fourth assessment report of the Intergovernmental Panel on Climate Change*, Cambridge University Press, Cambridge, United Kingdom and New York.

IPCC. 2013. Summary for policymakers. In: Stocker TV, Qin D, Plattner G-K, Tignor M *et al.* (eds), *Climate Change 2013: The Physical Science Basis. Contribution of Working Group I to the Fifth Assessment Report of the Intergovernmental Panel on Climate Change*, Cambridge University Press, Cambridge, United Kingdom and New York, pp 33–115.

IPCC. 2014. *Climate Change 2014: Synthesis Report. Contribution of Working Groups I, II and III to the Fifth Assessment Report of the Intergovernmental Panel on Climate Change*, Geneva, Switzerland.

- IPCC. 2018. Global Warming of 1.5°C: An IPCC Special Report on the impacts of global warming of 1.5°C above pre-industrial levels and related global greenhouse gas emission pathways, in the context of strengthening the global response to the threat of climate change, sustainable development, and efforts to eradicate poverty. In: Masson-Delmotte V, Zhai P, Pörtner HO, Roberts D, Skea J *et al.* (eds), *Summary for Policy Makers*, World Meteorological Organization, Geneva, Switzerland, 32 pp.
- Jiddawi NS. 1997. The reef dependent fisheries of Zanzibar. In: Johnstone RW, Francis J, Muhando CA (eds), *Proceedings of the National Conference on Coral Reefs*, Zanzibar, pp 22–35.
- Jokiel PL, Coles SL. 1977. Effects of heated effluent on hermatypic corals at Kahe Point, Oahu. *Pacific Science* 28: 1–18.
- Jokiel PL, Maragos JE, Franzisket L. 1978. Coral growth: Buoyant weight technique. In: Stoddart DR, Johannes RE (eds), *Coral Reefs: Research Methods*, UNESCO, Paris, pp 529–541.
- Jokiel PL, Rodgers KS, Kuffner IB, Andersson AJ, Cox EF *et al.* 2008. Ocean acidification and calcifying reef organisms: A mesocosm investigation. *Coral Reefs* 27(3): 473–483.
- Jompa J, McCook LJ. 2002. Effects of competition and herbivory on interactions between a hard coral and a brown alga. *Journal of Experimental Marine Biology and Ecology* 271: 25–39.
- Jones GP, McCormick MI, Srinivasan M, Eagle JV. 2004. Coral decline threatens fish biodiversity in marine reserves. *Proceedings of the National Academy of Sciences of the United States of America* 101(21): 8251–8253.
- Jones RJ, Hoegh-Guldberg O. 2001. Diurnal changes in the photochemical efficiency of the symbiotic dinoflagellates (Dinophyceae) of corals: Photoprotection, photoinactivation and the relationship to coral bleaching. *Plant, Cell and Environment* 24: 89–99.
- Jones RJ, Kildea T, Hoegh-Guldberg O. 1999. PAM chlorophyll fluorometry: A new *in situ* technique for stress assessment in scleractinian corals, used to examine the effects of cyanide from cyanide fishing. *Marine Pollution Bulletin* 38(10): 864–874.
- Kearney M, Porter WP, Williams C, Ritchie S, Hoffmann AA. 2009. Integrating biophysical models and evolutionary theory to predict climatic impacts on species' ranges: The dengue mosquito *Aedes aegypti* in Australia. *Functional Ecology* 23: 528–538.
- Kerry J, Bellwood D. 2012. The effect of coral morphology on shelter selection by coral reef fishes. *Coral Reefs* 31: 415–424.
- Kinsey D. 1978. Alkalinity changes and coral reef calcification. *Limnology and Oceanography* 23(5): 989–991.

- Kitajima M, Butler WL. 1975. Quenching of chlorophyll fluorescence and primary photochemistry in chloroplasts by dibromothymoquinone. *Biochimica et Biophysica Acta* 376: 105–115.
- Kleypas JA, Langdon C. 2006. Coral reefs and changing seawater carbonate chemistry. In: Phinney JT, Hoegh-Guldberg O, Kleypas JA (eds), *Coastal and Estuarine Studies: Coral Reefs and Climate Change Science and Management* 61: 73–110.
- Kleypas JA, McManus JW, Menez LAB. 1999. Environmental limits to coral reef development: Where do we draw the line? *American Zoologist* 39(1): 146–159.
- Klughammer C, Schreiber U. 2008. Complementary PS II quantum yields calculated from simple fluorescence parameters measured by PAM fluorometry and the Saturation Pulse method. *PAM Application Notes* 1: 27–35.
- Koren S, Dubinsky Z, Chomsky O. 2008. Induced bleaching of *Stylophora pistillata* by darkness stress and its subsequent recovery. *Proceedings of the 11<sup>th</sup> International Coral Reef Symposium*, pp 139–143.
- Kornder NA, Riegl BM, Figueiredo J. 2018. Thresholds and drivers of coral calcification responses to climate change. *Global Change Biology* 24: 5084–5095.
- Kovacs ZP, Du Plessis DB, Bracher PR, Dunn P, Mallory GCL. 1985. Republic of South Africa Department of Water Affairs documentation of the 1984 Domoina floods. *Technical Report* 122.
- Kroeker KJ, Kordas RL, Crim R, Hendriks IE, Ramajo L *et al.* 2013. Impacts of ocean acidification on marine organisms: Quantifying sensitivities and interaction with warming. *Global Change Biology* 19: 1884–1896.
- Krueger T, Horwitz N, Bodin J, Giovani M-E, Escrig S *et al.* 2017. Common reef-building coral in the Northern Red Sea resistant to elevated temperature and acidification. *Royal Society Open Science* 4(5): 170038.
- Kuffner IB, Bartels E, Stathakopoulos A, Enochs IC, Kolodziej G *et al.* 2017. Plasticity in skeletal characteristics of nursery-raised staghorn coral, *Acropora cervicornis*. *Coral Reefs* 36: 679–684.
- Langdon C, Atkinson MJ. 2005. Effect of elevated  $p\text{CO}_2$  on photosynthesis and calcification of corals and interactions with seasonal change in temperature/irradiance and nutrient enrichment. *Journal of Geophysical Research* 110(9): 1–16.
- Langdon C, Takahashi T, Sweeney C, Chipman D, Goddard J *et al.* 2000. Effect of calcium carbonate saturation state on the calcification rate of an experimental coral reef. *Global Biogeochemical Cycles* 14(2): 639–654.

- Le Treut H, Somerville R, Cubasch U, Ding Y, Mauritzen C *et al.* 2007. Historical overview of climate change science. *Climate Change 2007: The Physical Basis. Contribution of Working Group I to the Fourth Assessment Report of the Intergovernmental Panel on Climate Change*, pp 93–127.
- Leblud J, Moulin L, Batigny A, Dubois P, Grosjean P. 2014. Technical Note: Artificial coral reef mesocosms for ocean acidification investigations. *Biogeosciences* 11: 15463–15505.
- Leclercq N, Gattuso J-P, Jaubert J. 2000. CO<sub>2</sub> partial pressure controls the calcification rate of a coral community. *Global Change Biology* 6: 329–334.
- Leclercq N, Gattuso J-P, Jaubert J. 2002. Primary production, respiration, and calcification of a coral reef mesocosm under increased CO<sub>2</sub> partial pressure. *Limnology and Oceanography* 47(2): 558–564.
- Lesser MP. 1997. Oxidative stress causes coral bleaching during exposure to elevated temperatures. *Coral Reefs* 16: 187–192.
- Lesser MP. 2011. Coral bleaching: Causes and mechanisms. In: Dubinsky Z, Stambler N (eds), *Coral Reefs: An Ecosystem in Transition*, Springer Science & Business Media, Dordrecht, pp 405–419.
- Lieberman R, Shlesinger T, Loya Y, Benayahu Y. 2018. Octocoral sexual reproduction: Temporal disparity between mesophotic and shallow-reef populations. *Frontiers in Marine Science* 5(445): 1–14.
- Lichtenberg M, Larkum AWD, Kühl M. 2016. Photosynthetic acclimation of *Symbiodinium in hospite* depends on vertical position in the tissue of the scleractinian coral *Montastrea curta*. *Frontiers in Microbiology* 7(230): 1–13.
- Lirman D, Thyberg T, Herlan J, Hill C, Young-Lahiff C *et al.* 2010. Propagation of the threatened staghorn coral *Acropora cervicornis*: Methods to minimize the impacts of fragment collection and maximize production. *Coral Reefs* 29: 729–735.
- Logue JB, Mouquet N, Peter H, Hillebrand H. 2011. Empirical approaches to metacommunities: A review and comparison with theory. *Trends in Ecology & Evolution* 26: 482–491.
- Lohr KE, Patterson JT. 2017. Intraspecific variation in phenotype among nursery-reared staghorn coral *Acropora cervicornis* (Lamarck, 1816). *Journal of Experimental Marine Biology and Ecology* 486: 87–92.
- Longstaff BJ, Kildea T, Runcie JW, Cheshire A, Dennison WC *et al.* 2002. An *in situ* study of photosynthetic oxygen exchange and electron transport rate in the marine macroalga *Ulva lactuca* (Chlorophyta). *Photosynthesis Research* 74: 281–293.
- Lough JM, Barnes DJ. 2000. Environmental controls on growth of the massive coral *Porites*. *Journal of Experimental Marine Biology and Ecology* 245(2): 225–243.

- Loya YK, Sakai K, Yamazato K, Nakano Y, Sambali H *et al.* 2001. Coral bleaching: The winners and the losers. *Ecology Letters* 4(2): 122–131.
- Lutjeharms JRE. 2004. The coastal oceans of south-eastern Africa. In: Robinson AR, Brink KH (eds), *The global coastal ocean: The Sea – Ideas and observations on the progress in the study of the seas*, Harvard University Press, Cambridge, 14(B): 783–834.
- Lutjeharms JRE. 2006. *The Agulhas Current*. Springer, Germany.
- Maier C, Schubert A, Berzunza Sánchez MM, Weinbauer MG, Watremez P, Gattuso J-P. 2013. End of the century  $p\text{CO}_2$  levels do not impact calcification in Mediterranean cold-water corals. *PLoS ONE* 8: e62655.
- Manola I, Selten FM, de Ruijter WPM, Hazeleger W. 2015. The ocean-atmosphere response to wind-induced thermocline changes in the tropical South Western Indian Ocean. *Climate Dynamics* 45: 989–1007.
- Marshall AT, Clode P. 2004. Calcification rate and the effect of temperature in a zooxanthellate and an azooxanthellate scleractinian reef coral. *Coral Reefs* 23: 218–224.
- Marshall PA, Baird AH. 2000. Coral reefs – Bleaching of corals on the Great Barrier Reef differential susceptibilities among taxa. *Coral Reefs* 19: 155–163.
- Martin S, Gattuso J-P. 2009. Response of Mediterranean coralline algae to ocean acidification and elevated temperature. *Global Change Biology* 15: 2089–2100.
- Martone PT, Alyono M, Stites S. 2010. Bleaching of an intertidal coralline alga: Untangling the effects of light, temperature, and desiccation. *Marine Ecology Progress Series* 416: 57–67.
- Masui T, Matsumoto K, Hijioka Y, Kinoshita T, Nozawa T *et al.* 2011. An emission pathway for stabilization at  $6 \text{ Wm}^{-2}$  radiative forcing. *Climatic Change* 109: 59.
- Matsumoto AK. 2007. Effects of low water temperature on growth and magnesium carbonate concentrations in the cold-water gorgonian *Primnoa pacifica*. *Bulletin of Marine Science* 81: 423–435.
- McClanahan TR, Ateweberhan M, Graham NAJ, Wilson SK, Ruiz Sebastian C *et al.* 2007. Western Indian Ocean coral communities: Bleaching responses and susceptibility to extinction. *Marine Ecology Progress Series* 337: 1–13.
- McClanahan TR, Graham NAJ, Maina J, Chabanet P, Bruggemann JH *et al.* 2007. Influence of instantaneous variation on estimates of coral reef fish populations and communities. *Marine Ecology Progress Series* 340: 221–234.

- McClanahan TR, Obura D. 1997. Sedimentation effects on shallow coral communities in Kenya. *Journal of Experimental Marine Biology and Ecology* 209(1–2): 103–122.
- McClanahan TR, Weil E, Maina J. 2009. Strong relationship between coral bleaching and growth anomalies in massive *Porites*. *Global Change Biology* 15: 1804–1816.
- McClanahan TR. 2004. The relationship between bleaching and mortality of common corals. *Marine Biology* 144(6): 1239–1245.
- McCook LJ, Jompa J, Diaz-Pulido G. 2001. Competition between corals and algae on coral reefs: a review of evidence and mechanisms. *Coral Reefs* 19: 400–417.
- McIntosh F. 2010. Atlas of dive sites of South Africa and Mozambique, Map Studio, Cape Town.
- McLachlan RH, Price JT, Solomon SL, Grottoli AG. 2020. Thirty years of coral heat-stress experiments: A review of methods. *Coral Reefs* 1–18 pp.
- McNeil BI, Matear RJ, Barnes DJ. 2004. Coral reef calcification and climate change: The effect of ocean warming. *Geophysical Research Letters* 31(22): L22309.
- Mehrbach C, Culberso CH, Hawley JE, Pytkowic RM. 1973. Measurement of apparent dissociation constants of carbonic acid in seawater at atmospheric pressure. *Limnology and Oceanography* 18: 897–907.
- Meinshausen M, Smith SJ, Calvin K, Daniel JS, Kainuma MLT *et al.* 2011. The RCP greenhouse gas concentrations and their extensions from 1765 to 2300. *Climatic Change* 109: 213–241.
- Meissner KJ, Lippmann T, Sen Gupta A. 2011. Large-scale stress factors affecting coral reefs: Open ocean sea surface temperature and surface seawater aragonite saturation over the next 400 years. *Coral Reefs* 31: 309–319.
- Moberg F, Folke C. 1999. Ecological goods and services of coral reef ecosystems. *Ecological Economics* 29: 215–233.
- Moffat D, Ngoile MN, Linden O, Francis J. 1998. The reality of the stomach: Coastal management at the local level in eastern Africa. *AMBIO* 26: 590–598.
- Mograbi J, Rogerson CM. 2007. Maximising the local pro-poor impacts of dive tourism: Sodwana Bay, South Africa. *Urban Forum* 18: 85–104.
- Mohamed TAA, El-Komi MM, Shoukr FM, El-Arab ME. 2017. Growth rate evaluation of the alcyonacean soft coral *Sinularia polydactyla* (Ehrenberg, 1834) at Hurghada, Northern Red Sea, Egypt. *Journal of Biology, Agriculture and Healthcare* 7(22): 42–50.

- Moritz C, Vii J, Lee Long W, Tamelander J, Thomassin A *et al.* 2018. Status and trends of coral reefs of the Pacific. *Global Coral Reef Monitoring Network (GCRMN)*, pp 16–99.
- Morris T, Lamont T, Roberts MJ. 2013. Effects of deep-sea eddies on the northern KwaZulu-Natal shelf, South Africa. *African Journal of Marine Science* 35: 343–350.
- Morris T. 2009. Physical oceanography of Sodwana Bay and its effects on larval transport and coral bleaching. MTech thesis, Cape Peninsula University of Technology, Cape Town, 73 pp.
- Moss RH, Edmonds JA, Hibbard KA, Manning MR, Rose SK *et al.* 2010. The next generation of scenarios for climate change research and assessment. *Nature* 463: 747–756.
- Murillo LJA, Jokiel PL, Atkinson MJ. 2014. Alkalinity to calcium flux ratios for corals and coral reef communities: Variances between isolated and community conditions. *PeerJ* 2: e249.
- Muscatine L, Cernichiari E. 1969. Assimilation of photosynthetic products of zooxanthellae by a reef coral. *Biology Bulletin* 137: 506–523.
- Muscatine L, McCloskey LR, Marian RE. 1981. Estimating the daily contribution of carbon from zooxanthellae to coral animal respiration. *Limnology and Oceanography* 26: 601–611.
- Muscatine L, Porter JW. 1977. Reef corals: Mutualistic symbioses adapted to nutrient-poor environments. *Bioscience* 27(7): 454–460.
- Nakicenovic N, Alcamo J, Davis G, Vries BD, Fenhann J *et al.* 2000. IPCC Special Report on Emissions Scenarios. In: Nakicenovic N, Swart R (eds), Cambridge University Press, Cambridge.
- Nielsen JJV, Kenkel CD, Bourne DG, Despringhere L, Mocellin VJL *et al.* 2020. Physiological effects of heat and cold exposure in the common reef coral *Acropora millepora*. *Coral Reefs* 39: 259–269.
- National Research Council (NRC). 2011. Climate stabilization targets: Emissions, concentrations, and impacts over decades to millennia. National Research Council, The National Academies Press, Washington, 298 pp.
- Obura DO, Gudka M, Rabi F, Gian S, Bijoux J *et al.* 2017. Coral reef status report for the Western Indian Ocean. *Global Coral Reef Monitoring Network (GCRMN)/International Coral Reef Initiative (ICRI)*.
- Obura DO, Wells S, Church J, Horrill C. 2002. Monitoring of fish and fish catches by local fishermen in Kenya and Tanzania. *Marine and Freshwater Research* 53(2): 215–222.
- Obura DO. 2005. Resilience and climate change: Lessons from coral reefs and bleaching in the Western Indian Ocean. *Estuarine, Coastal and Shelf Science* 63: 353–372.
- Odum E. 1984. The mesocosm. *BioScience* 34: 558–562.

- Oliver ECJ, Burrows MT, Donat MG, Sen Gupta A, Alexander LV *et al.* 2019. Projected marine heatwaves in the 21<sup>st</sup> century and the potential for ecological impact. *Frontiers in Marine Science* 6: 734.
- Oliver ECJ, Donat MG, Burrows MT, Moore PJ, Smale DA *et al.* 2018. Longer and more frequent marine heatwaves over the past century. *Nature Communications* 9(1): 1324.
- Oliver TA, Palumbi SR. 2011. Do fluctuating temperature environments elevate coral thermal tolerance? *Coral Reefs* 30: 429–440.
- Orr JC, Fabry VJ, Aumont O, Bopp L, Doney SC *et al.* 2005. Anthropogenic ocean acidification over the twenty-first century and its impact on calcifying organisms. *Nature* 437(7059): 681–686.
- Osinga R, Schutter M, Wijgerde T, Rinkevich B, Shafir S *et al.* 2012. The CORALZOO project: A synopsis of four years of public aquarium science. *Journal of the Marine Biological Association of the UK* 92: 753–768.
- Pandolfi JM, Connolly SR, Marshall DJ, Cohen AL. 2011. Projecting coral reef futures under global warming and ocean acidification. *Science* 333: 418–422.
- Parks JE, Pomeroy RS, Balboa CM. 2003. The economics of live rock and live coral aquaculture. In: Cato JC, Brown C (eds), *Marine Ornamental Species: Collection, Culture and Conservation*, Blackwell Science, Gainesville, pp 185–206.
- Pearson RG, Stanton JC, Shoemaker KT, Aiello-Lammens ME, Ersts PJ *et al.* 2014. Life history and spatial traits predict extinction risk due to climate change. *Nature Climate Change* 4: 217–221.
- Porter SN, Branch GM, Sink KJ. 2013. Biogeographic patterns on shallow subtidal reefs in the western Indian Ocean. *Marine Biology* 160: 1271–1283.
- Porter SN, Branch GM, Sink KJ. 2017a. Changes in shallow-reef community composition along environmental gradients on the East African coast. *Marine Biology* 164(101).
- Porter SN, Branch GM, Sink KJ. 2017b. Sand-mediated divergences between shallow reef communities on horizontal and vertical substrata in the western Indian Ocean. *African Journal of Marine Science* 39: 121–127.
- Porter SN, Kaehler S, Branch GM, Sink KJ. 2014. Riverine subsidies for inshore filter-feeder communities: Potential influences on trophic patterns among bioregions. *Marine Ecology Progress Series* 498: 13–26.
- Porter SN, Schleyer MH. 2017. Long-term dynamics of a high-latitude coral reef community at Sodwana Bay, South Africa. *Coral Reefs* 36: 369–382.

- Porter SN, Schleyer MH. 2019. Environmental variation and how its spatial structure influences the cross-shelf distribution of high-latitude coral communities in South Africa. *Diversity* 11(4): 57.
- Pörtner, HO, Karl D, Boyd PW, Cheung W, Lluich-Cota SE *et al.* 2014. Ocean systems. In: Field CB, Barros VR, Dokken DJ, Mach KJ, Mastrandrea MD *et al.* (eds), *Climate Change 2014: Impacts, Adaptation, and Vulnerability Part A: Global and Sectoral Aspects Contribution of Working Group II to the Fifth Assessment Report of the Intergovernmental Panel for Climate Change*, Cambridge, New York, Cambridge University Press, pp 411–484.
- Pratchett MS, Anderson KD, Hoogenboom MO, Windman E, Baird AH *et al.* 2015. Spatial, temporal and taxonomic variation in coral growth – Implications for the structure and function of coral reef ecosystems. In: Hughes RN, Hughes DJ, Smith IP, Dale AC (eds), *Oceanography and Marine Biology: An Annual Review* 53: 215–295.
- Pratchett MS, Munday PL, Wilson SK, Graham NA, Cinner J *et al.* 2008. Effects of climate-induced coral bleaching on coral reef fishes: A review of ecological and economic consequences. *Oceanography and Marine Biology: An Annual Review* 46: 251–296.
- Ralph PJ, Gademann R, Larkum AWD, Kühl M. 2002. Spatial heterogeneity in active chlorophyll fluorescence and PS II activity of coral tissues. *Marine Biology* 141(4): 639–646.
- Ralph PJ, Gademann R. 2005. Rapid light curves: A powerful tool to assess photosynthetic activity. *Aquatic Botany* 82: 222–237.
- Ramsay PJ. 1991. Sedimentology, coral reef zonation, and late Pleistocene coastline models of the Sodwana Bay continental shelf, northern Zululand. PhD thesis, University of KwaZulu-Natal, 202 pp.
- Ramsay PJ. 1994. Marine geology of the Sodwana Bay shelf, South Africa. *Marine Geology* 120: 225–247.
- Ramsay PJ. 1996. Quaternary marine geology of the Sodwana Bay continental shelf, northern KwaZulu-Natal. *Bulletin of the Geological Society of South Africa* 117: 1–85.
- Reaka-Kulda MI. 1997. The global biodiversity of coral reefs: A comparison with rainforests. In: Reaka-Kulda MI, Wilson DE, Wilson OE (eds), *Biodiversity II: Understanding and Protecting our Natural Resources*. Joseph Henry/National Academy Press, Washington, DC, pp 83–108.
- Reason CJC, Keibel A. 2004. Tropical cyclone Eline and its unusual penetration and impacts over the southern African mainland. *Weather and Forecasting* 19: 789–805.
- Reid EC, DeCarlo TM, Cohen AL, Wong GTF, Lentz SJ *et al.* 2019. Internal waves influence the thermal and nutrient environment on a shallow coral reef. *Limnology and Oceanography* 64(5): 1949–1965.

- Reynaud S, Ferrier-Pagès C, Meibom A, Mostefaoui S, Mortlock R *et al.* 2007. Light and temperature effects on Sr/Ca and Mg/Ca ratios in the scleractinian coral *Acropora* species. *Geochimica et Cosmochimica Acta* 71: 354–362.
- Reynaud-Vaganay S, Juillet-Leclerc A, Jaubert J, Gattuso J-P. 2001. Effect of light on skeletal  $\delta^{13}\text{C}$  and  $\delta^{18}\text{O}$ , and interaction with photosynthesis, respiration and calcification in two zooxanthellate scleractinian corals. *Palaeogeography, Palaeoclimatology, Palaeoecology* 175: 393–404.
- Riahi K, Rao S, Krey V, Cho C, Chirkov V *et al.* 2011. RCP 8.5 – A scenario of comparatively high greenhouse gas emissions. *Climatic Change* 109: 33–57.
- Richard Y, Trzaska S, Roucou P, Rouault M. 2000. Modification of the Southern African rainfall variability/ ENSO relationship since the late 1960s. *Climate Dynamics* 16(12): 883–895.
- Richards Z, Kirkendale L, Moore G, Hosie A, Huisman J *et al.* 2016. Marine biodiversity in temperate western Australia: Multi-taxon surveys of Minden and Roe Reefs. *Diversity* 8(2): 7.
- Richmond RH. 1993. Coral reefs: Present problems and future concerns resulting from anthropogenic disturbance. *Coral Reefs* 33: 524–536.
- Riegl B, Pillar WE. 2003. Possible refugia for reefs in times of environmental stress. *International Journal of Earth Science* 92: 520–531.
- Riegl B, Riegl A. 1996. How episodic coral breakage can determine community structure: A South African coral reef example. *Marine Ecology Progress Series* 17: 399–410.
- Riegl B, Schleyer MH, Cook PJ, Branch GM. 1995. Structure of Africa's southernmost coral communities. *Bulletin of Marine Science* 56: 676–691.
- Riegl B. 1995. Effects of sand deposition on scleractinian and alcyonacean corals. *Marine Biology* 121: 517–526.
- Riegl B. 2001. Inhibition of reef framework by frequent disturbance: examples from the Arabian Gulf, South Africa, and the Cayman Islands. *Palaeogeography, Palaeoclimatology, Palaeoecology* 175: 79–101.
- Ries JB, Cohen AL, McCorkle DC. 2009. Marine calcifiers exhibit mixed responses to CO<sub>2</sub>-induced ocean acidification. *Geology* 37: 1131–1134.
- Rippe JP, Baumann JH, De Leener DN, Aichelman HE, Friedlander EB *et al.* 2018. Corals sustain growth but not skeletal density across the Florida Keys Reef Tract despite ongoing warming. *Global Change Biology* 24(11): 5205–5217.

- Robert C. 2001. Marine bioprospecting – trawling for treasure and pleasure. *MicroReview* 1434: 633–645.
- Roberts JM, Wheeler AJ, Freiwald A. 2006. Reefs of the deep: The biology and geology of cold-water coral ecosystems. *Science* 312 (5773): 543–547.
- Roberts MJ, van der Lingen CD, Whittle C, van den Berg M. 2010. Shelf currents, lee-trapped and transient eddies on the inshore boundary of the Agulhas Current, South Africa: Their relevance to the KwaZulu-Natal sardine run. *African Journal of Marine Science* 32(2): 423–447.
- Rocha RJM, Serôdio J, Leal MC, Cartaxana P, Calado R. 2013. Effect of light intensity on post-fragmentation photobiological performance of the soft coral *Sinularia flexibilis*. *Aquaculture* 388: 24–29.
- Roche RC, Abel RA, Johnson KG, Perry CT. 2010. Quantification of porosity in *Acropora pulchra* (Brook 1891) using X-ray micro-computed tomography techniques. *Journal of Experimental Marine Biology and Ecology* 396: 1–9.
- Rodolfo-Metalpa R, Martin S, Ferrier-Pagès C, Gattuso J-P. 2010. Response of the temperate coral *Cladocora caespitosa* to mid- and long-term exposure to  $p\text{CO}_2$  and temperature levels projected for the year 2100 AD. *Biogeosciences* 7: 289–300.
- Rodrigues LJ, Grottoli AG. 2006. Calcification rate and the stable carbon, oxygen, and nitrogen isotopes in the skeleton, host tissue, and zooxanthellae of bleached and recovering Hawaiian corals. *Geochimica et Cosmochimica Acta* 70(11): 2781–2789.
- Rodrigues LJ, Grottoli AG. 2007. Energy reserves and metabolism as indicators of coral recovery from bleaching. *Limnology and Oceanography* 52: 1874–1882.
- Rosenberg NA, VanLiere JM. 2009. Replication of genetic associations as pseudoreplication due to shared genealogy. *Genetic Epidemiology* 33(6): 479–487.
- Rosenzweig C, Karoly D, Vicarelli M, Neofotis P, Wu Q *et al.* 2008. Attributing physical and biological impacts to anthropogenic climate change. *Nature* 453: 353–357.
- Roth MS, Goericke R, Deheyn DD. 2012. Cold induces acute stress but heat is ultimately more deleterious for the reef-building coral *Acropora yongei*. *Scientific Reports* 2(240): 1–5.
- Rouault M, White SA, Reason CJC, Lutjeharms JRE, Jobard I. 2002. Ocean–atmosphere interaction in the Agulhas Current region and a South African extreme weather event. *Weather Forecasting* 17: 655–669.
- Roxy M, Ritika K, Terray P, Masson S. 2014. The curious case of Indian Ocean warming. *Journal of Climate* 27(22): 8501–8509.

- Ruiz Sebastián C, Sink KJ, McClanahan TR, Cowan DA. 2009. Bleaching response of corals and their *Symbiodinium* communities in southern Africa. *Marine Biology* 156: 2049–2062.
- Saji NH, Goswami BN, Vinayachandran PN, Yamagata T. 1999. A dipole model in the tropical Indian Ocean. *Nature* 401: 360–393.
- Sarmiento JL, Gruber N. 2006. *Ocean Biogeochemical Dynamics*, Princeton University Press, Princeton, 503 pp.
- Scheffer M, Barrett S, Carpenter SR, Folke C, Green AJ *et al.* 2015. Creating a safe operating space for iconic ecosystems. *Science* 347: 1317–1319.
- Scheufen T, Krämer WE, Iglesias-Prieto R, Enríquez S. 2017. Seasonal variation modulates coral sensibility to heat-stress and explains annual changes in coral productivity. *Scientific Reports* 7(1): 4937.
- Schleyer MH, Celliers L. 2003a. Biodiversity on the marginal coral reefs of South Africa: What does the future hold? *Zoologische Verhandelingen* 345: 387–400.
- Schleyer MH, Celliers L. 2003b. Coral dominance at the reef-sediment interface in marginal coral communities at Sodwana Bay, South Africa. *Marine and Freshwater Research* 54: 967–972.
- Schleyer MH, Celliers L. 2005. Modelling reef zonation in the Greater St Lucia Wetland Park, South Africa. *Estuarine, Coastal and Shelf Science* 63: 373–384.
- Schleyer MH, Floros C, Laing SCS, Macdonald AHH, Montoya-Maya PH *et al.* 2018. What can South African reefs tell us about the future of high-latitude coral systems? *Marine Pollution Bulletin* 136: 491–507.
- Schleyer MH, Heikoop JM, Risk MJ. 2006. A benthic survey of Aliwal Shoal and assessment of the effects of a wood pulp effluent on the reef. *Marine Pollution Bulletin* 52(5): 503–514.
- Schleyer MH, Kruger A, Celliers L. 2008. Long-term community changes on a high-latitude coral reef in the Greater St Lucia Wetland Park, South Africa. *Marine Pollution Bulletin* 56(3): 493–502.
- Schleyer MH, Porter SN. 2018. Drivers of soft and stony coral community distribution on the high-latitude coral reefs of South Africa. *Advances in Marine Biology* 80: 1–55.
- Schleyer MH, Reinicke GB, Van Ofwegen L. 2003. A field guide to the soft corals of the Western Indian Ocean and Red Sea. Sida, Kalmar, Sweden.
- Schleyer MH. 1995. South African coral reef communities. *Wetlands of South Africa*, Department of Environmental Affairs and Tourism, Pretoria.

- Schleyer MH. 1999. A synthesis of KwaZulu-Natal coral research. South African Association for Marine Biological Research. *Special Publication 5*: 36.
- Schleyer MH. 2000. South African coral communities. In: McClanahan T, Sheppard C, Obura DO (eds), *Coral reefs of the Indian Ocean: Their ecology and conservation*, Oxford University Press, New York, pp 83–105.
- Schoepf V, Hu X, Holcomb M, Cai W-J, Li Q *et al.* 2016. Coral calcification under environmental change: A direct comparison of the alkalinity anomaly and buoyant weight techniques. *Coral Reefs* 36(1): 13–25.
- Schoepf V, Stat M, Falter JL, McCulloch MT. 2015. Limits to the thermal tolerance of corals adapted to a highly fluctuating, naturally extreme temperature environment. *Scientific Reports* 5(17639): 1–14.
- Schott AF, Xie S-P, McCreary JP. 2009. Indian ocean circulation and climate variability. *Reviews of Geophysics* 47: 1–46.
- Schreiber U, Bilger W. 1993. Progress in chlorophyll fluorescence research: Major developments during the past years in retrospect. In: Dietmar B-H, Heidelberg UL, Darmstadt KE, Kadereit JW (eds), *Progress in Botany*, Springer-Verlag, Berlin, pp 151–173.
- Schreiber U, Schliwa U, Bilger W. 1986. Continuous recording of photochemical and non-photochemical chlorophyll quenching with a new type of modulation fluorometer. *Photosynthesis Research* 10: 51–62.
- Schubert P, Wilke T. 2017. Coral microcosms: Challenges and opportunities for global change biology. In: Duque C, Camacho ET (eds). *Corals in a Changing World*. IntechOpen, pp 143–175.
- Schumann EH. 1988. Physical oceanography off Natal. In: Schumann E (ed.), *Lecture notes on coastal and estuarine studies: Coastal ocean studies off Natal, South Africa*, Springer-Verlag, New York, pp 101–130.
- Shafir S, Rinkevich B. 2013. Mariculture of coral colonies for the public aquarium sector. In: Leewis RJ, Janse M (eds), *Advances in Coral Husbandry in Public Aquariums 2*: 315–318.
- Sheppard CRC, Wilson SC, Salm RV, Dixon D. 2000. Reefs and coral communities of the Arabian Gulf and Arabian Sea. In: McClanahan TR, Sheppard CRC, Obura DO (eds), *Coral reefs of the Indian Ocean: Their ecology and conservation*. Oxford University Press, Oxford, pp 257–293.
- Sheppard CRC. 2003. Predicted recurrences of mass coral mortality in the Indian Ocean. *Nature* 425: 294–297.

- Shi T, Wang Y, Zhao Y, Loucaides S. 2019. Detecting the calcium carbonate saturation state under the stress of ocean acidification using saturometry technique. *IOP Conference Series: Earth and Environmental Science* 227: 062027.
- Shu L, KeFu Y, TianRan C, Qi S, HuiLing Z. 2011. Assessment of coral bleaching using symbiotic zooxanthellae density and satellite remote sensing data in the Nansha Islands, South China Sea. *Chinese Science Bulletin* 56: 1031–1037.
- Silverman J, Lazar B, Erez J. 2007. The effect of aragonite saturation, temperature and nutrients on the community calcification rate of a coral reef. *Journal of Geophysical Research* 112: C05004.
- Smith SV, Key GS. 1975. Carbon dioxide and metabolism in marine environments. *Limnology and Oceanography* 20: 493–495.
- Smith SV, Kinsey DW. 1978. Calcification and organic carbon metabolism as indicated by carbon dioxide. In: Stoddart DR, Johannes RE (eds), *Coral Reefs: Research Methods*, pp 469–484.
- Somero GN. 1995. Protein and temperature. *Annual Review of Physiology* 57: 43–68.
- Spalding MD, Fox HE, Allen GR, Davidson N, Ferdaña ZA *et al.* 2007. Marine ecoregions of the world: A bioregionalization of coastal and shelf areas. *Bioscience* 57(7): 573–583.
- Spalding MD, Ravilious C, Green EP. 2001. *World Atlas of Coral Reefs*. University of California Press, California.
- Spurgeon JPG. 1992. The economic valuation of coral reefs. *Marine Pollution Bulletin* 24: 529–536.
- Stanley GD. 2003. The evolution of modern corals and their early history. *Earth-Science Reviews* 60(4): 195–225.
- Stat M, Carter D, Hoegh-Guldberg O. 2006. The evolutionary history of *Symbiodinium* and scleractinian hosts – Symbiosis, diversity, and the effect of climate change. *Perspectives in Plant Ecology, Evolution and Systematics* 8: 23–24.
- Stewart RIA, Dossena M, Bohan DA, Jeppesen E, Kordas RL *et al.* 2013. Mesocosm experiments as a tool for ecological climate-change research. In: Woodward G, Ogorman EJ (eds), *Advances in Ecological Research: Global Change in Multispecies Systems* 48(3): 71–181.
- Storz D, Gischler E. 2011. Coral extension rates in the NW Indian Ocean I: Reconstruction of 20<sup>th</sup> century SST variability and monsoon current strength. *Geo-Marine Letters* 31: 141–154.
- Studivan MS, Hatch WI, Mitchelmore CL. 2015. Responses of the soft coral *Xenia elongata* following acute exposure to a chemical dispersant. *SpringerPlus* 4: 80.

- Tambutté S, Holcomb M, Ferrier-Pagès C, Reynaud S, Tambutté É *et al.* 2011. Coral biomineralization: From the gene to the environment. *Journal of Experimental Marine Biology and Ecology* 408: 58–78.
- Tanzil JT, Brown BE, Dunne RP, Lee JN, Kaandorp JA *et al.* 2013. Regional decline in growth rate of massive *Porites* corals in Southeast Asia. *Global Change Biology* 19: 3011–3023.
- Taylor KE, Stouffer RJ, Meehl GA. 2012. An overview of CMIP5 and the experiment design. *Bulletin of the American Meteorological Society* 93(4): 485–498.
- Thomson AM, Calvin KV, Smith SJ, Kyle GP, Volke A *et al.* 2011. RCP 4.5: A pathway for stabilization of radiative forcing by 2100. *Climatic Change* 109: 77–94.
- Turley C, Gattuso J-P. 2012. Future biological and ecosystem impacts of ocean acidification and their socioeconomic-policy implications. *Current Opinion in Environmental Sustainability* 4: 278–286.
- UN Environment, ISU (International Sustainability Unit), ICRI (International Coral Reef Initiative), Trucost. 2018. The coral reef economy: The business case for investment in the protection, preservation, and enhancement of coral reef health, 36 pp.
- UNESCO (United Nations Educational, Scientific and Cultural Organisation). 2000. Convention concerning the protection of the world cultural and natural heritage. *World Heritage Committee: Twenty-third session, 29 November–4 December 1999, Marrakesh, Morocco*, UNESCO, Paris.
- UNEP (United Nations Environment Programme). 2020. Projections of future coral bleaching conditions using IPCC CMIP6 models: Climate policy implications, management applications, and Regional Seas summaries. *United Nations Environment Programme*, Nairobi, Kenya.
- van Hooidonk R, Maynard JA, Tamelander J, Gove J, Ahmadi G *et al.* 2016. Local-scale projections of coral reef futures and implications of the Paris Agreement. *Scientific Report* 6(39666).
- van Hooidonk R, Maynard JA, Manzello D, Planes S. 2014. Opposite latitudinal gradients in projected ocean acidification and bleaching impacts on coral reefs. *Global Change Biology* 20: 103–112.
- van Vuuren DP, Deetman S, den Elzen MGJ, Hof A, Isaac M *et al.* 2011. RCP 2.6: Exploring the possibility to keep global mean temperature increase below 2°C. *Climatic Change* 109: 95–116.
- Vasseur DA, DeLong JP, Gilbert B, Greig HS, Harley CDG *et al.* 2014. Increased temperature variation poses a greater risk to species than climate warming. *Proceedings of the Royal Society B: Biological Sciences* 281, 20132612.
- Veron JEN, Hoegh-Guldberg O, Lenton TM, Lough JM, Obura DO *et al.* 2009. The coral reef crisis: The critical importance of <350 ppm CO<sub>2</sub>. *Marine Pollution Bulletin* 58: 1428–1436.

- Veron JEN. 2000. *Corals of the World*, Vol 1, Australian Institute of Marine Science and CRR, Australia, 463 pp.
- Warner ME, Lesser MP, Ralph PJ. 2010. Chlorophyll fluorescence in reef building corals. In: Suggett DJ, Prasil O, Borowitzka MA (eds), *Chlorophyll fluorescence in aquatic sciences: Methods and applications*, Springer, Berlin, pp 209–222.
- Watanabe TK, Watanabe T, Yamazaki A, Pfeiffer M, Claereboudt MR. 2019. Oman coral  $\delta^{18}\text{O}$  seawater record suggests that Western Indian Ocean upwelling uncouples from the Indian Ocean Dipole during the global-warming hiatus. *Scientific Reports* 9(1887): 1–9.
- Weart SR. 2008. Timeline (Milestones). *The Discovery of Global Warming*. Harvard University Press, Cambridge, United States, 240 pp.
- Webb AE, van Heuven SM, de Bakker DM, van Duyl FC, Reichart G-J *et al.* 2017. Combined effects of experimental acidification and eutrophication on reef sponge bioerosion rates. *Frontiers in Marine Science* 4: 311.
- Webster MS, Hixon MA. 2000. Mechanisms and individual consequences of intraspecific competition in a coral-reef fish. *Marine Ecology Progress Series* 196: 187–194.
- Webster PJ, Holland GJ, Curry JA, Chang H-R. 2005. Changes in tropical cyclone number, duration, and intensity in a warming environment. *Science* 309: 1844–1846.
- Webster PJ, Magana VO, Palmer TN, Shukla J, Tomas RA *et al.* 1998. Monsoons: Processes, predictability, and the prospect for prediction. *Journal of Geophysical Research* 103: 14451–14510.
- Wild C, Huettel M, Kleuter A, Kremb SG, Rasheed MYM *et al.* 2004. Coral mucus functions as an energy carrier and particle trap in the reef ecosystem. *Nature* 428 (6978): 66–70.
- Wilkinson C. 2008. *Status of Coral Reefs of the World: 2008*. Global Coral Reef Monitoring Network and Reef and Rainforest Research Centre, Townsville, Australia, 296 pp.
- Winter A, Appeldoorn RS, Bruckner A, Williams EH, Goenaga C. 1998. Sea surface temperatures and coral reef bleaching off La Parguera, Puerto Rico (northeastern Caribbean Sea). *Coral Reefs* 17: 377–382.
- Winters G, Loya Y, Röttgers R, Beer S. 2003. Photoinhibition in shallow-water colonies of the coral *Stylophora pistillata* as measured *in situ*. *Limnology and Oceanography* 48(4): 1388–1393.
- Wolf-Gladrow DA, Zeebe RE, Klaas C, Körtzinger A, Dickson AG. 2007. Total alkalinity: The explicit conservative expression and its application to biogeochemical processes. *Marine Chemistry* 106: 287–300.

Woolsey ES, Keith SA, Byrne M, Schmidt-Roach S, Baird AH. 2015. Latitudinal variation in thermal tolerance thresholds of early life stages of corals. *Coral Reefs* 34: 471–478.

WWF (World Wide Fund). 2004. The future of Fiji's live rock. *World Wide Fund for Nature*. <https://wwf.panda.org/?10626>. Accessed on 21 December 2020.

Yates KK, Halley RB. 2006. Diurnal variation in rates of calcification and carbonate sediment dissolution in Florida Bay. *Estuaries and Coasts* 29(1): 24–39.

Zartler Z. 2012. Aquarium corals: Applying PAM fluorometry for the advancement of coral aquaculture. *Advanced Aquarist* 11: 1–11.

Zinke J, Pfeiffer M, Timm O, Dullo WC, Brummer GJA. 2009. Western Indian Ocean marine and terrestrial records of climate variability: A review and new concepts on land-ocean interactions since AD 1660. *International Journal of Earth Sciences* 98: 115–133.